Challenges, Successes, and Opportunities in Investigating Novel Strategies for Polymer Synthesis

By

Brock Elliott Lynde

A dissertation submitted in partial fulfillment of
the requirements for the degree of

Doctor of Philosophy
(Chemistry)

at the

UNIVERSITY OF WISCONSIN-MADISON

2021

Date of final oral examination: 04/23/2021

The dissertation is approved by the following members of the Final Oral Committee:
Andrew J. Boydston, Professor, Chemistry
Padma Gopalan, Professor, Materials Science and Engineering and Chemistry
Tehshik Yoon, Professor, Chemistry
Clark Landis, Professor, Chemistry

Challenges, Successes, and Opportunities in Investigating Novel Strategies for Polymer Synthesis

Brock Elliott Lynde

Under the supervision or Professor Andrew J. Boydston

At the University of Washington, Seattle
and
The University of Wisconsin – Madison

Abstract

Much of the work that is done in polymer chemistry are performed through the creative use of well understood polymers and reactions. With the introduction of novel methods for polymer synthesis being few and far between. This thesis discusses the investigation of introducing new strategies for the synthesis of novel polymers and the attempts to understand their behavior. In Chapter 2, the synthesis and ring-opening metathesis polymerization (ROMP) of a unique macrocyclic stilbene-based monomer. Ultimately, we found that high initiation efficiency was achieved, and that the rate of chain transfer was competitive with propagation during polymerization. We discuss the modular synthesis of the monomer, ROMP kinetics, attempts to limit the rate of chain transfer, and potential applications of this new system. Chapter 3 and 4 investigated the synthesis of monomers that utilize the hetero-Diels-Alder reaction in a step-growth polymerization. The targeted monomers can facilitate the synthesis of both linear polymers and covalent adaptable networks. Ultimately, we found that the solubility of the monomers inhibits the synthesis of the of the polymer networks. We will also discuss the synthesis and its complications as well as potential solutions for these limitations. In Chapter 5, the mechanochemical reactivity of 1,2-oxazines is explored and how different isomers impact the

rate of mechanical activation. Finally in Chapter 6, we explore methods for the synthesis of amphiphilic block copolymers to act as polyelectrolytes for the development of moisture resistant super gas barriers.

Acknowledgements

Thank you, AJ Boydston, for being a great mentor. I appreciate that you allowed me to pursue projects that I found the most interesting despite the many setbacks that I encountered and pushed me to find new and creative ways to solve my problems. Over the past 5 years I have always like I was working with you and not just for you. I also appreciate that you were supportive of my travels back and forth between Wisconsin and Washington to see Andrea.

Thank you, the many iterations of the Boydston group, everybody that has been part of this group, no matter how long, has helped me grow as a scientist. You each helped me learn my weaknesses and pushed me to overcome them. I am the scientist I am now because of you and I cannot thank you enough.

Thank you, Dan Seidenkranz, your support after moving to Wisconsin was extremely appreciated. Not only were you a great mentor, but you were an awesome friend helping me become comfortable so far from home.

Thank you, Troy Becker, Cody Schilling, and Chang-Uk Lee, you guys were awesome friends during our time together in graduate school. You both really made graduate school fun and helped make the absurd hours we worked each and every day easier to deal with.

Thank you, Tom Kolibaba, you have been a great friend during our times in graduate school, even though you were down in Texas. I have always enjoyed coming up with crazy ideas with you, and talking about science endlessly, until Ciani wanting to duct tape our mouths shut.

Thank you, Daniel Lee, we started this crazy adventure of graduate school together. Our late nights and weekends stuck in the same fume, while nobody else was around, calling each other names for getting in the way are some of my fondest memories from graduate school.

Thank you, to my family and future in-laws, you have supported me during my time in graduate school, in more ways than you know. Having some place to go were everything did not revolve around science helped save my sanity. And when we did talk about it you pushed me to think creatively about learning to explain what I do in less jargon filled ways.

Thank you, mon (mom) and dad, you both have always been so supportive of me and I could not have done this without you. I could probably write an entire book on all the things you have done that I appreciate but I cannot handle writing another one after this. I could not have asked for better and more supportive parents, so thank you and I love you.

Lastly, thank you, Andrea Westling, when I started graduate school, we thought our biggest barrier to seeing each other would be waiting for the weekend free parking at the University of Washington. We never imagined that I would end up 1800 miles away in Wisconsin. You have always been there for me when I need somebody to complain to about work. Even after starting medical school, you were still there for me even with your limited amount of time away from studying. Words cannot describe how much I appreciate you for that. So hopefully for the last time via text, I love you, you are my favorite, and have an excellent day.

Table of Contents

Abstract i

Acknowledgements iii

Table of Contents v

List of Abbreviations ix

List of Figures xii

List of Tables xv

List of Equations xvi

Chapter 1. The Need for Expanding Available Methods for Polymer Synthesis 1

Notes and references for Chapter 1 3

Chapter 2. Ring Opening Metathesis Polymerization of a Macrocyclic Stilbene-Based Monomer 6

2.1 Abstract 6

2.2 Introduction 6

2.3 Results and discussion 11

2.3.a. Synthesis and characterization of stilbene-based polymer 11

2.3.b. Mechanistic investigations into the polymerization of **2.1**. 14

2.3.c. Inhibition of chain transfer during the polymerization 16

2.4 Conclusions 17

2.5 Experimental 17

2.5.a General Considerations. 17

2.5.b. Monomer Synthesis 19

2.5.c. Polymerization Studies 29

Notes and References for Chapter 2 40

Chapter 3. Using 1,2-Oxazines to synthesize Covalent Adaptable Networks 43

3.1 Abstract 43

3.2 Introduction 43

3.3 Results and Discussion 48

3.4 Conclusions 52

3.5 Future Directions 53

3.6 Experimental 53

3.6.a General Considerations 53

3.6.b Synthetic Procedures 54

3.6.c ^{1}H and ^{13}C NMR Spectra 60

Notes and references for Chapter 3 66

Chapter 4. Synthesis of a Dynamic Linear Step-Growth Polymer Using 1,2-oxazines 68

4.1 Abstract 68

4.2 Introduction 68

4.2 Results and Discussion 74

4.2.a Synthesis of CP*-oxazine monomer 74

4.2.b. Synthesis of Anthracene-oxazine monomer 75

4.3 Conclusion 76

4.4 Future Work 77

4.5 Experimental 77

4.5.a General considerations 77

4.5.b Synthetic procedures 78

4.5.c Spectral Data 81

Notes and References for Chapter 4 86

Chapter 5. Mechanochemical Reactivity of 1,2-Oxazine Hetero Diels-Alder Adducts 88

5.1 Abstract 88

5.2 Introduction 88

5.3 Results and Discussion 92

5.4 Conclusions 95

5.5 Experimental 96

5.5.a. General Considerations 96

5.5.b. Synthetic Procedures 97

Notes and References for Chapter 5 133

Chapter 6. Using Amphiphilic Block Co-Polymers for Moisture Resistant Ultra Gas-Barriers 138

6.1 Abstract 138

6.2 Introduction 138

6.3. Results and Discussion 140

6.3.a. Anionic Block Co-Polymer Synthesis and Characterization 140

6.3.b. Cationic Block Co-Polymer Synthesis..... 143

6.3.c. LbL assembly of block copolymers 145

6.4. Conclusions..... 146

6.5 Future Directions 146

6.6 Experimental..... 147

6.6.a General Considerations 147

6.6.b. Polymer Synthesis..... 148

6.6.c. Polymer Characterization Data 152

Notes and References for Chapter 6 156

List of Abbreviations

AABB – a two–monomer step–growth polymerization

AB – single monomer step–growth polymerization

AcBr – acetyl bromide

ARGET–ATRP – Activator ReGenerated by Electron Transfer atom transfer radical polymerization

ATR–FTIR – attenuated total reflectance Fourier transformed inferred spectroscopy

ATRP – atom transfer radical polymerization

CANs – Covalent adaptable networks

CDI – carbonyl diimidazole

CP* – 1,2,3,4,5–pentamethylcyclopenta–1,3–diene

$Đ$ – molecular weight dispersity

DMAP – 4–dimethylaminopyridine

DMF – dimethylformamide

DSC – differential scanning calorimetry

ED–ROMPs – entropy–driven ring–opening metathesis polymerizations

Fmoc – fluorenylmethoxycarbonyl

GPC – Gel permeation chromatography

k – Rate constants

LbL – layer–by–layer

MALDI–TOF/MS – matrix–assisted laser desorption ionization time of flight mass spectrometry

MALS – multi–angle laser light scattering

MeOH – methanol

M_n – number average molecular weight

M_p – peak molecular weight

M_w – weight average molecular weight

p – conversion

PAA – poly(acrylic acid)

PDMAEMA – poly(2–dimethylaminoethyl methacrylate)

PEC – polyelectrolyte complexes

PET – polyethylene terephthalate

PS – poly(styrene)

PS–b–PAA – poly(styrene–block–acrylic acid)

PS–b–PDMAEMA – poly(styrene–block–2–dimethylaminoethyl methacrylate)

P*t*BA – poly(tert–butyl acrylate)

r – stoichiometric ratio

RAFT – reversable addition fragmentation chain–transfer polymerization

RI – refractive index

ROMP – ring–opening metathesis polymerization

SEC – size exclusion chromatography

T_d – decomposition temperature

TFA – trifluoracetic acid

T_g – glass transition temperature

TGA – thermogravimetric analysis

THF – tetrahydrofuran

TLC – Thin Layer Chromatography

$\bar{X}_n$ – degree of polymerization

List of Figures

Figure 2.1 Examples of both small molecule and macrocyclic monomers for ROMP and ED-ROMP. 7
Figure 2.2 Proposed polymerization of macrocycle (**2.1**). 11
Figure 2.3 Synthetic scheme for **2.1**. 12
Figure 2.4 MALDI-TOF/MS spectrum for poly(**2.1**). The molecular weight between repeat units was measured to be 558.9 amu, consistent with the molecular weight of the monomer. 14
Figure 2.5 Mn vs conversion plot for the polymerization of **2.1** follows a linear progression consistent with a chain growth mechanism, *Đ* for each time point in parenthesis. 15
Figure 2.6 a) GPC traces for polymer-polymer chain transfer experiment for the two starting polymers (black solid, Mn = 71 kDa; blue dash, M_n = 15.2 kDa) and the final polymer (red dot, M_n = 24 kDa). b) GPC traces for polymer-stilbene chain transfer experiment for the starting polymer (black solid, M_n: 41.5 kDa) and the final polymer (blue dash, M_n: 16.9 kDa). 16
Figure 2.7 ^{13}C NMR spectrum of **2.2** in $CDCl_3$. 24
Figure 2.8 ^{1}H NMR spectrum of **2.2** in $CDCl_3$. 24
Figure 2.9 ^{13}C NMR spectrum of **2.3** in $CDCl_3$. 25
Figure 2.10 ^{1}H NMR spectrum of **2.3** in $CDCl_3$. 25
Figure 2.11 ^{13}C NMR spectrum of **2.4** in $CDCl_3$. 26
Figure 2.12 ^{1}H NMR spectrum of **2.4** in $CDCl_3$. 26
Figure 2.13 ^{13}C NMR spectrum of **2.1** in $CDCl_3$. 27
Figure 2.14 ^{1}H NMR spectrum of **2.1** in $CDCl_3$. 27
Figure 2.15 ^{1}H NMR comparing trans isomer and a mixture of *cis* and *trans* isomers for the benzylether of **2.1** 28
Figure 2.16 ^{13}C NMR comparing trans isomer and a mixture of *cis* and *trans* isomers for the benzylether of **2.1** 28
Figure 2.17 ^{1}H NMR spectrum for **poly(2.1)** in $CDCl_3$. 30
Figure 2.18 ^{13}C NMR spectrum for **poly(2.1)** in $CDCl_3$. 31
Figure 2.19 TGA trace for **poly(2.1)** under N_2 atmosphere. 31
Figure 2.20 First order kinetics plot for the consumption of **2.1** over the course of the polymerization. 32
Figure 2.21 DSC trace for **poly(2.1)** showing the first cooling cycle (dashed blue) and second heating cycle (solid black). 32
Figure 2.22 ^{1}H NMR spectra showing the progression of the polymerization. Conversion was determined following the transformation of the benzylic ether hydrogen from monomer (blue star) to polymer (red star). 33
Figure 2.23 Arrhenius plot for the polymerization of **2.1** using **2.5b** 33
Figure 2.24 Homodesmotic reactions to estimate strain energy of model stilbene-based macrocycle (DFT at the B3LYP/6-31G* level of theory) 34
Figure 3.1 A) Furan-maleimide Diels-Alder reaction used in the synthesis of a covalent adaptable network by Wudl et. al. B) Hetero-Diels-Alder reaction between thiocarbonyl and

cyclopentadiene terminated poly(methyl methacrylate). C) General scheme for the synthesis of a CAN using 1,2-oxazines. 44
Figure 3.2 Proposed monomers for the CAN. 47
Figure 3.3 Synthetic scheme CAN monomers. i) $POCl_3$, N-methylformanalide, 100 °C. ii) $NaBH_4$, EtOH. iii) 1,3,5-benzenetricarbonyl trichloride, 4-dimethylaminopyridine. iv) NH_2OH•HCl, Na_2CO_3. v) NH_2OH•HCl, K_2CO_3. vi) Et_3N, CH_2Cl_2. 47
Figure 3.4 ^{1}H NMR spectrum for the conversion for the synthesis of **3.19** using 0.2 eq. pyridine (bottom) and 2.0 eq. pyridine (top). 48
Figure 3.5 Synthesis of bis-oxazine **3.12** from phenyl N-hydroxycarbamate and bis-oxazines **3.13** and **3.14** from their corresponding hydroxamic acids. 50
Figure 3.6 Cartoon depiction for the synthesis of the CAN using **3.2** and **3.1**. 51
Figure 3.7 A) Unsuccessful synthesis of **3.18**. B)Synthesis of less rigid dienes **3.16** and **3.17** via reductive amination. i) 1) CH_2Cl_2 2) $NaBH_4$ 51
Figure 3.8 1,3-dienes of interest for future studies. 53
Figure 3.9 ^{1}H NMR spectrum of **3.5** in $CDCl_3$. 60
Figure 3.10 ^{1}H NMR spectrum of **3.6** in $CDCl_3$. 61
Figure 3.11 ^{13}C NMR spectrum of **3.6** in $CDCl_3$. 61
Figure 3.12 ^{1}H NMR spectrum of **3.1** in $CDCl_3$. 62
Figure 3.13 ^{1}H NMR spectrum of **3.2** in DMSO-d_6 62
Figure 3.14 ^{1}H NMR spectrum of **3.7** in DMSO-d_6 63
Figure 3.15 ^{1}H NMR spectrum of **3.11** in $CDCl_3$. 63
Figure 3.16 ^{1}H NMR spectrum of **3.14** in $CDCl_3$. 64
Figure 3.17 ^{1}H NMR spectrum of **3.3** in DMSO-d_6 64
Figure 3.18 ^{1}H NMR spectrum of **3.12** in $CDCl_3$. 65
Figure 3.19 ^{1}H NMR spectrum of **3.16** in $CDCl_3$. 65
Figure 3.20 ^{1}H NMR spectrum of the decomposition of **3.13** (top) and **3.14** (bottom) in DMSO-d_6. In both experiments the top spectrum is t=0 and the bottom is t=24 hours. 66
Figure 4.1 Examples of linear step-growth polymers synthesized using the Diels-Alder reaction. 70
Figure 4.2 Cartoon depiction of a dynamic linear polymer synthesized via a step-growth polymerization (top). Monomers (**4.1** and **4.2**) used in the synthesis of the dynamic polymer (bottom) 73
Figure 4.3. A) Synthesis for CP*-hydroxamic acid. i) *n*BuLi, paraformaldehyde. ii) **4.3**, CDI, DMAP. iii) AcBr, *i*PrOH. iv) **3.11**, Et_3N. B) Proposed synthesis for anthracene-hydroxamic acid. v) **3.6**, CDI, Gly-a/b. vi) a) AcBr, *i*PrOH. b) piperidine. vii) **3.11**, Et_3N. 74
Figure 4.4 ^{1}H NMR spectra from the attempts at the Boc deprotection of **4.7a**. The ^{1}H signals for the benzylic ester (red) are no longer present in the crude reaction mixtures after the different deprotection attempts. 76
Figure 4.5 ^{1}H NMR spectrum of **4.3** in $CDCl_3$. 82
Figure 4.6 ^{1}H NMR spectrum of **4.4** in $CDCl_3$. 82
Figure 4.7 ^{13}C NMR spectrum of **4.4** in $CDCl_3$. 83
Figure 4.8 ^{1}H NMR spectrum of **4.5** in DMSO-d_6 83
Figure 4.9 ^{1}H NMR spectrum of **4.7a** in $CDCl_3$. 84

Figure 4.10 ^{13}C NMR spectrum of **4.7a** in $CDCl_3$. 84
Figure 4.11 ^{1}H NMR spectrum of **4.8** in $CDCl_3$. 85
Figure 4.12 ^{1}H NMR spectrum of **4.7b** in $CDCl_3$. 85
Figure 5.1 Reversibility of 1,2-oxazines. 89
Figure 5.2 Precedence and current work on stimuli-responsive 1,2-oxazine-containing polymers. 89
Figure 5.3 Synthesis of **Ox1**, **Ox2** and **Ox3**. 90
Figure 5.4 Structures of 1,2-oxazine containing polymers and control polymers. 91
Figure 5.5 A) Reaction scheme for in situ oxidation and tagging of liberated diene with **5.20**. B) Photoluminescent spectra of sonicated solutions of **polyOx1** and **polyOx4** in THF. 94
Figure 6.1 Synthetic scheme for poly(styrene-*block*-acrylic acid). i) *tert*-butyl acrylate, $CuBr_2$, Me_6Tren, Ascorbic acid, DMF. ii) styrene, $CuBr_2$, Me_6Tren, Ascorbic acid, anisole. iii) conc. HCl, 1,4-dioxane. 140
Figure 6.2 GPC trace for the P*t*BA macroinitiator (solid black line) and the product of the chain extension(blue dash). 141
Figure 6.3 Comparison of the TGA for P*t*BA-b-PS (solid black) and PAA-b-PS (blue dash).. 142
Figure 6.4 Synthetic scheme for poly(styrene-*block*-2-dimethylaminoethyl methacrylate). i) styrene, V-501. ii) 2-dimethylaminoethyl methacrylate, AIBN, toluene. 143
Figure 6.5 Attempted chain extension of PS (solid black) via RAFT (blue dash). 143
Figure 6.6 ^{1}H NMR spectrum comparing PS-b-PDMAEMA that was not triturated with methanol (blue) and one that was triturated with methanol. 144
Figure 6.7 ATR-FTIR spectrum of PAA-b-PS. 152
Figure 6.8 ^{1}H NMR spectrum of P*t*BA macroinitiator. 153
Figure 6.9 ^{1}H NMR spectrum of PS-b-P*t*BA. 153
Figure 6.10 ^{1}H NMR spectrum of PS macroinitiator. 154
Figure 6.11 ^{1}H NMR spectrum of PS-b-PDMAEMA. 154
Figure 6.12 ^{1}H NMR spectrum of PDMAEMA macroinitiator. 155
Figure 6.13 ^{1}H NMR spectrum of PDMAEMA-b-PS. 155
Figure 6.14 ATR-FTIR of failed deprotection of P*t*BA-b-PS. Red spectrum is the starting polymer and the blue spectrum is the polymer post deprotection. 156
Figure 6.15 Results for the LbL deposition of PS-b-PAA and PS-b-PDMAEMA using THF (Blue) and 3:1 THF:H_2O (orange). 156

List of Tables

Table 2.1 Summary of ROMP experiments performed. 13
Table 3.1 Reaction Optimization for hydroxamic acid synthesis 49
Table 5.1 Summary of k_{RI} for mechanochemical chain scission of control and oxazine-containing polymers. 93

List of Equations

Equation 2.1. Average end to end distance from polymer chain ends.....8

Equation 4.1. Degree of polymerization for a step-growth polymerization using the ratio between two bifunctional monomers and polymerization conversion.....70

Equation 4.2. Degree of polymerization for the step-growth polymerization using the ratio between two bifunctional monomers assuming 100% conversion 70

Equation 4.3. Carothers equation 71

Equation 6.1. Ratio of PS and PtBA.....142

Chapter 1.The Need for Expanding Available Methods for Polymer Synthesis

Polymer chemistry has changed dramatically since first defined in 1920, becoming a necessity in our day to day lives.[1] In 2018 alone, the global production of plastics was 360 megatons, with nearly half of that production going into packaging alone.[2,3] Over the past 100 years our understanding of polymers has greatly increased. Allowing for the development of polymers and materials with unique properties such as healable materials, high performance polymers, biodegradable/recyclable materials, and conductive polymers.[4–10]

Many unique reactions have been utilized by polymer chemists to synthesize these materials. For example click-reactions are one class that have enabled this growth due to their versitility.[11] Two common examples of click-reactions are the Cu(I)-catalyzed azide-alkyne click reaction and the Diels-Alder reaction, the latter of these being more readily reversible allowing for applications beyond coupling reactions. Taking advantage of this reversibility, the Diels-Alder reaction has enabled the synthesis of many novel dynamic materials.

The Diels-Alder adduct has been used as both a reversible crosslink for linear polymers, as well as a reactive functional group for both linear and branched step-growth polymers.[12–18] When utilized as a crosslink, one of the Diels-Alder components (diene or dienophile) is incorporated into the polymer chain as a monomer while a dimer of the second component is added to the polymer matrix after polymerization to enable the crosslinking.[6,19–24] It has also been shown that you can synthesize two separate polymers that each contain a component of the Diels-Alder adduct and when mixed results in a crosslinked material.[25–27]

Monomers used in step-growth polymerization can have a variety of linking segments between the reactive functional groups. Using the Diels-Alder reaction, has enabled the synthesis

of materials that are 3D printable and healable materials, as well as linear and branched polymers that can be fully depolymerized.[28–33] The Diels-Alder reaction and other reversible cycloadditions have the potential to be applied to many issues such as preventing delamination within extrusion 3D-printing, further increasing the capabilities for chemically recycling polymers, and extended or delayed drug delivery using drug-polymer conjugates. However, one major limitation to expanding into some of these applications is the lack of diversity amongst the Diels-Alder adducts used.

When looking at the extent of work done using the Diels-Alder reaction on Scifinder, nearly 30% of the published work uses a single reaction, furan-maleimide Diels-Alder. To further belabor this point, during this discussion on Diels-Alder chemistry every citation has been for a paper using this reaction. While this reaction is well understood and can be easily synthesized from commercially available components, it does have limitations.[34] The thermal reversibility is limited to a temperature range of 80-110 °C. This can greatly limit its use in areas such as medicine (body temperature ~37 °C) and other low temperature applications. Furthermore, when a furan-maleimide Diels-Alder adduct is heated above 200 °C, the adduct will aromatize by eliminating water, removing its reversible characteristic. This limited thermal stability prevents this chemistry from being applicable in high temperature environments, such as those needed for high performance polymers.[7] There are a few other examples of different Diels-Alder adducts that have been used polymer chemistry, but none to the extent that the furan-maleimide Diels-Alder adduct.[35]

Other limitations within the lack of diversity amongst the chemistries used can be found in different forms throughout polymer chemistry. Another such example can be found in the monomers used for ring-opening metathesis polymerization (ROMP). Using ROMP we have been

able to synthesize many functional and complex polymers including conductive, and sequence controlled polymers, as well as tapered bottle brush polymers.[36–39] As a testament to the ingenuity of the polymer community, much of this work was accomplished using very few monomer architectures, mainly cyclopropenes, cyclobutenes, and [2.2.1] bicycles.[40–46] The lack of diversity amongst the base monomer structures used in ROMP leads to a lack of novel polymer backbones, and limits the properties of the polymers synthesized. Two possible avenues for expanding the monomers available for ROMP could be achieved by synthesizing strained macrocycles, or by using relay metathesis.[47,48]

To keep polymer chemistry growing at the pace it has been for the next 100 years, the types of chemistries used in polymer and monomer design needs to expand. A lot of work goes into finding applications for already well studied reactions and not to introducing new reactions into the field to solve current problems. In the work presented here, I will discuss my progress towards accomplishing both tasks, by introducing a new class of strained macrocycle that can undergo ROMP, using 1,2-oxazines for the synthesis of linear and branched polymer networks as well as, my attempts to understand how 1,2-oxazines behave as mechanophores.

Notes and references for Chapter 1

(1) Staudinger, H. *J. Chem. Inf. Model.* **1920**, *53* (6), 1073–1085.

(2) GmbH, C. M. & S. Market and Strategy GmbH Global Plastics Flow 2018 https://www.carboliq.com/pdf/19_conversio_global_plastics_flow_2018_summary.pdf (accessed Dec 4, 2021).

(3) Billiet, S.; Trenor, S. R. *ACS Macro Lett.* **2020**, *9* (9), 1376–1390.

(4) Wang, S.; Urban, M. W. *Nat. Rev. Mater.* **2020**, *5* (8), 562–583.

(5) Burattini, S.; Greenland, B. W.; Chappell, D.; Colquhoun, H. M.; Hayes, W. *Chem. Soc. Rev.* **2010**, *39* (6), 1973–1985.

(6) Wei, Y.; Ma, X. *Adv Polym Technol* **2018**, *37*, 1987–1993.

(7) Boydston, A. J.; Cui, J.; Lee, C.-U.; Lynde, B. E.; Schilling, C. A. *ACS Macro Lett.* **2020**, *9* (8).

(8) Lee, C. U.; Vandenbrande, J.; Goetz, A. E.; Ganter, M. A.; Storti, D. W.; Boydston, A. J. *Addit. Manuf.* **2019**, *28* (May), 430–438.

(9) Gross, R. A.; Kalra, B. *Science* **2002**, *297* (5582), 803–807.

(10) Nezakati, T.; Seifalian, A.; Tan, A.; Seifalian, A. M. *Chem. Rev.* **2018**, *118* (14), 6766–6843.

(11) Moses, J. E.; Moorhouse, A. D. *Chem. Soc. Rev.* **2007**, *36* (8), 1249–1262.

(12) Motoki, S.; Nakano, T.; Tokiwa, Y.; Saruwatari, K.; Tomita, I.; Iwamura, T. *Polymer (Guildf).* **2016**, *101*, 98–106.

(13) Defize, T.; Thomassin, J. M.; Alexandre, M.; Gilbert, B.; Riva, R.; Jérôme, C. *Polym. (United Kingdom)* **2016**, *84*, 234–242.

(14) Sugane, K.; Kumai, N.; Yoshioka, Y.; Shibita, A.; Shibata, M. *Polymer (Guildf).* **2017**, *124*, 20–29.

(15) Vilela, C.; Cruciani, L.; Silvestre, A. J. D.; Gandini, A. *Macromol. Rapid Commun.* **2011**, *32* (17), 1319–1323.

(16) Nasresfahani, A.; Zelisko, P. M. *Polym. Chem* **2017**, *8*, 2942.

(17) Adzima, B. J.; Aguirre, H. A.; Kloxin, C. J.; Scott, T. F.; Bowman, C. N. *Macromolecules* **2008**, *41* (23), 9112–9117.

(18) Zhang, Y.; Yang, Y.; Tang, K. *Polym. Polym. Compos.* **2007**, *21* (7), 449–456.

(19) Le, C. M. Q.; Thi, H. H. P.; Cao, X. T.; Kim, G. Do; Oh, C. W.; Lim, K. T. *J. Polym. Sci. Part A Polym. Chem.* **2016**, *54* (23), 3741–3750.

(20) Gu, L.; Wu, Q.-Y. *J. Appl. Polym. Sci* **2018**, *135*, 46272.

(21) Padhan, A. K.; Mandal, D. *Polym. Chem.* **2018**, *9*, 3248.

(22) Kuang, X.; Liu, G.; Dong, X.; Wang, D. *Polymer (Guildf).* **2016**, *84*, 1–9.

(23) Fan, M.; Liu, J.; Li, X.; Zhang, J.; Cheng, J. *Ind. Eng. Chem. Res.* **2014**, *53*, 16156–16163.

(24) Patil, S. S.; Torris, A.; Wadgaonkar, P. P. *J. Polym. Sci., Part A Polym. Chem* **2017**, *55*, 2700–2712.

(25) Peng, Y. J.; He, X.; Wu, Q.; Sun, P. C.; Wang, C. J.; Liu, X. Z. *Polymer (Guildf).* **2018**, *149*, 154–163.

(26) Hager, M. D.; Schubert, U. S.; Kötteritzsch, J.; Hager, M. D.; Schubert, U. S. *Polymer (Guildf).* **2015**, *69*, 321–329.

(27) Engel, T.; Kickelbick, G. *Polym. Int.* **2014**, *63*, 915–923.

(28) Davidson, J. R.; Appuhamillage, G. A.; Thompson, C. M.; Voit, W.; Smaldone, R. A. *ACS Appl. Mater. Interfaces* **2016**, *8* (26), 16961–16966.

(29) Lacerda, T. M.; Carvalho, A. J. F. F.; Gandini, A. *RSC Adv.* **2016**, *6* (51), 45696–45700.

(30) Berto, P.; Pointet, A.; Le Coz, C. C.; Grelier, S. S.; Peruch, F. F. *Macromolecules* **2018**, *51* (3), 651–659.

(31) Diaz, M. M. M.; Brancart, J.; Van Assche, G.; Van Mele, B.; Assche, G. Van; Van Mele, B. *Polymer (Guildf).* **2018**, *153*, 453–463.

(32) Sugane, K.; Yoshioka, Y.; Shimasaki, T.; Teramoto, N.; Shibata, M. *Polymer (Guildf).* **2018**, *144*, 92–102.

(33) Brancart, J.; Scheltjens, G.; Muselle, T.; Van Mele, B.; Terryn, H.; Van Assche, G.; Assche, G. Van. *J. Intell. Mater. Syst. Struct.* **2014**, *25* (1), 40–46.

(34) Cuvellier, A.; Verhelle, R.; Brancart, J.; Vanderborght, B.; Van Assche, G.; Rahier, H. *Chem. A Eur. J.* **2019**, *10* (4), 473–485.

(35) Zhou, J.; Guimard, N. K.; Inglis, A. J.; Namazian, M.; Lin, C. Y.; Coote, M. L.; Spyrou, E.; Hilf, S.; Schmidt, F. G.; Barner-Kowollik, C. *Polym. Chem.* **2011**, *3* (3), 628–639.

(36) Lee, D. C.; Sellers, D. L.; Liu, F.; Boydston, A. J.; Pun, S. H. *Angew. Chem. Int. Ed* **2020**, *59* (32), 13430–13436.

(37) Kawamoto, K.; Zhong, M.; Gadelrab, K. R.; Cheng, L. C.; Ross, C. A.; Alexander-Katz, A.; Johnson, J. A. *J. Am. Chem. Soc.* **2016**, *138* (36), 11501–11504.

(38) Gutekunst, W. R.; Hawker, C. J. *J. Am. Chem. Soc.* **2015**, *137*, 8038–8041.

(39) Weiss, R. M.; Short, A. L.; Meyer, T. Y. *ACS Macro Lett.* **2015**, *4* (9), 1039–1043.

(40) Bielawski, C. W.; Grubbs, R. H. *Prog. Polym. Sci.* **2007**, *32*, 1–29.

(41) Elling, B. R.; Su, J. K.; Xia, Y. *ACS Macro Lett.* **2020**, 9, 180–184.

(42) Su, J. K.; Lee, S. Y.; Elling, B. R.; Xia, Y. *Macromolecules* **2020**, 53, 5833–5838.

(43) Elling, B. R.; Su, J. K.; Xia, Y. *Acc. Chem. Res.* **2021**, *54* (2), 356–365.

(44) Yang, J.; Horst, M.; Werby, S. H.; Cegelski, L.; Burns, N. Z.; Xia, Y. *J. Am. Chem. Soc.* **2020**, *142* (34), 14619–14626.

(45) Varlas, S.; Lawrenson, S. B.; Arkinstall, L. A.; O'Reilly, R. K.; Foster, J. C. *Prog. Polym. Sci.* **2020**, *107*, 101278.

(46) Lu, P.; Kensy, V. K.; Tritt, R. L.; Seidenkranz, D. T.; Boydston, A. J. *Acc. Chem. Res.* **2020**, *53* (10), 2325–2335.

(47) Fu, L.; Sui, X.; Crolais, A. E.; Gutekunst, W. R. *Angew. Chem. Int. Ed* **2019**, *58* (44), 15726–15730.

(48) Maker, D.; Maier, C.; Brodner, K.; Bunz, U.; Mäker, D.; Maier, C.; Brödner, K.; Bunz, U. *ACS Macro Lett.* **2014**, *3*, 415–418.

Chapter 2. Ring Opening Metathesis Polymerization of a Macrocyclic Stilbene-Based Monomer

Reproduced from Lynde, B. E.; Maust, R. L.; Penghao, L.; Lee, D. C.; Jasti, R.; Boydston, A. J. "Ring Opening Metathesis Polymerization of a Macrocyclic Stilbene-Based Monomer." *Mater. Chem. Front.* **2020**, 4, 252-256. with permission from the Chinese Chemical Society (CCS), Institute of Chemistry of Chinese Academy of Sciences (IC), and the Royal Society of Chemistry.

2.1 Abstract

We report the synthesis of a new class of strained macrocycle that performs well in ring-opening metathesis polymerization (ROMP). The polymerization displays chain growth characteristics with evidence of secondary metathesis in the form of chain transfer. The unique structure enables access to stilbene- based polymers that are traditionally prepared via uncontrolled polymerizations.

2.2 Introduction

Ring-opening metathesis polymerization (ROMP) has become an indispensable synthetic tool in modern polymer chemistry and materials science.[40,49–53] One of the greatest advantages to ROMP unlike traditional radical polymerizations is the retention of the reactive sp2 bonds from the monomer to the polymer. This however also introduces the greatest limitation to monomers used in ROMP which is the loss of the enthalpic driving force for the polymerization. To regain this driving force the typical monomers that are used for ROMP have a high amount of ring strain that is released upon ring opening. As such the monomer landscape for ROMP is dominated largely by four motifs: norbornenes, cyclobutenes, cyclopropenes, and cyclooctenes (Figure 2.1) that have ring strains of 66.9, 129.7-142.3, 228.0, and 69.9 kJ/mol respectively.[40,54–62] From these

frameworks, functional groups within the polymer are limited to being introduced via side chains resulting in little diversity within the polymer backbone itself. This limitation has been partially overcome through the use of macrocycles (ring size >14 atoms) as monomers for ROMP, but introduces a new problem because most macrocyclic monomers have little or no ring strain.[63] Therefore, a trade off exists between selection of monomers with high ring strain versus macrocyclic systems of greater diversity albeit without an enthalpic driving force.

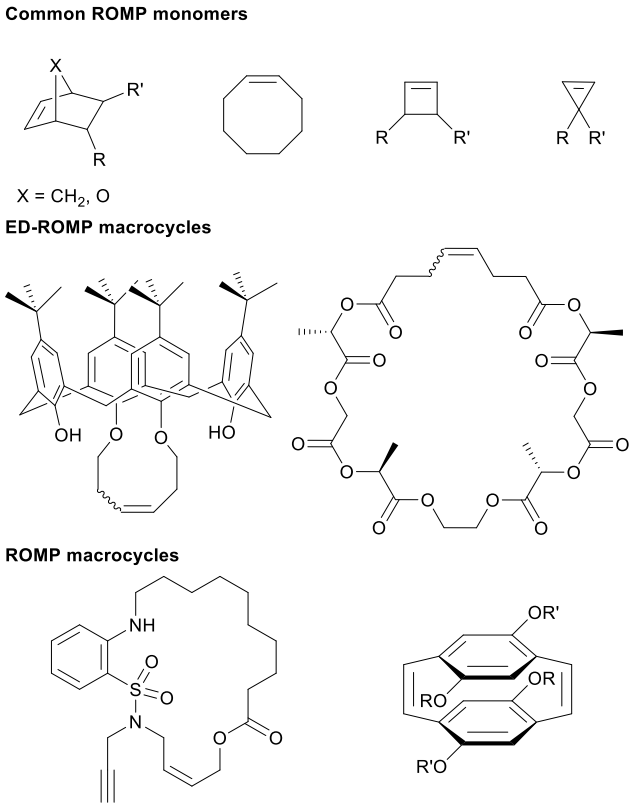

Figure 2.1 Examples of both small molecule and macrocyclic monomers for ROMP and ED-ROMP.

These macrocyclic monomers use entropy to circumvent the need for ring strain to drive the polymerization and as such are categorized as entropy-driven ring-opening metathesis polymerizations (ED-ROMPs).[63–65] ED-ROMPs exist in an equilibrium between linear polymer and macrocyclic oligomer, and the thermodynamic drive is provided by the increase in conformational entropy as the macrocyclic oligomers become linear polymer chains.[63] In a typical polymerization with smaller rings very few degrees are freedom are gained upon ring opening but as the size of the ring increases so does the number of degrees of freedom gained via ring opening. This can be visualized via comparing the average distance between chain ends of a random coil polymer and the corresponding macrocycle. For any size macrocycle the average distance for the

potential chain ends is always 1 bond length. However, after the ring opening occurs this number increases, and this value can be predicted for a random coil using the following equation:

$$< r^2 > = 2Nb^2 \quad (2.1)$$

where r is the average end to end distance, N is the number of bonds within the polymer backbone, and b is the length of a bond. This means for example that a macrocycle of ring size 18 will have an average end to end distance of 6 bond lengths, which clearly is going to increase the number of possible confirmations. Furthermore, this result increases as the size of the ring increase.

Taking advantage of this characteristic of ED-ROMP many different macrocyclic platforms have been developed, that have created a diverse and complex polymer landscape. One common strategy adopted is to attach long alkyl chains with a terminal olefin. After which under dilute conditions undergo ring closing metathesis to synthesize the desired monomer. This has enabled the synthesis of some exciting polymers including liquid crystalline polymers,[66] poly(catenates),[67] poly(calixarenes),[68] as well as sequence-controlled polymers (**Figure 2.1**).[39,69,70]

There are also a few disadvantages of using ED-ROMP that can limit the scope of monomers available. In most traditional polymerizations there is an entropic penalty from the decrease in translational entropy that arises from the conjoining of multiple monomers into a single polymer chain. To limit this loss of translational entropy ED-ROMPs must be performed at high concentrations, ideally bulk polymerizations must be carried out. This limits the monomers that can be used in these polymerizations to those that along with the resulting polymer are highly soluble in organic solvents or to those that have low melting temperatures. Furthermore, polymers synthesized via ED-ROMP in many cases will have high molecular weight dispersity (*Đ*), often the *Đ* for these polymerizations fall between 1.5 - 2.0, and can have a mixture of linear and cyclic polymers in the final material. [39,63,65,69]

These limitations have been overcome using a few different techniques. The first that I will discuss is SEED-ROMP or selectively enhanced entropy-driven ring opening metathesis polymerization. SEED-ROMP was able to synthesize simple sequence-controlled polymers utilizing the same mechanism as ED-ROMP taking advantage of how quickly the monomer polymerizes and the fact that ED-ROMPs are an equilibrium. In their previous work the authors demonstrated ED-ROMP with a monomer that had a high rate of polymerization to produce polymers with $Đ$ of 1.3. They increased the living characteristics of the polymerization by selectively synthesizing the *cis* isomer of the monomer, which has a much higher rate of polymerization. When the polymerization is carried out it reaches 90% conversion ($Đ$ = 1.1) in just 2 minutes, when the polymerization was stopped and not allowed to equilibrate thus limiting the amount of secondary metathesis that can occur.

The second method that has been demonstrated to overcome the issues of polymerizing strain free monomers is to incorporate a step into the polymerization that is effectively irreversible. This has been accomplished using enyne metathesis as this irreversible step within the polymerization. Ruthenium carbenes are known to react rapidly with terminal alkynes to make a less reactive intermediate, however, by incorporating an olefin near the reactive alkyne intramolecular metathesis can be promoted.[71] By synthesizing monomers with both a terminal alkyne and a nearby olefin that is located within a ring this process can be used polymerize monomers with many different ring sizes. The Hawker group used this method to polymerize a sequence-controlled polymer.

The last method that will be discussed and probably the most common approach is to design the monomers that have ring strain in them. This is typically done through the incorporation of aromatic rings as well as areas with an extended pi-system. For instance, Miao et al. utilized

[2.2]paracyclophan-1-ene, a highly strained macrocycle, to synthesize a homopolymer as well as block and random co-polymers with norbornene initiated by a Schrock-type catalyst.[72] 15 years after this initial demonstration Turner et al. was able to synthesize polyphenylenevinylene through microwave assisted ROMP of a [2.2]paracyclphane-1,9-diene derivatives.[73] The authors were able to synthesize polymers with relatively low *Đ* (1.18-1.28) across a range of molecular weights from 10-35 kDa. Using this method, the authors were able to synthesize polymers that had a higher absorption maximum when compared to the same polymer synthesized via traditional methods, suggesting that the polymer had greater conjugator and/or fewer defects within the polymer backbone than the traditionally prepared polymers. Later the same year the authors synthesized a diblock copolymer of two different [2.2]paracyclophane-1,9-dienes that had the same extended conjugation system but due to the differences in the monomers would phase separate when thin films were made.[74]

To demonstrate the capabilities for using these paracyclopanenes as strained macrocyclic monomers Bunz. et al. synthesized a [2.2.2]paracyclophane-triene derivative.[48] The monomer was still highly strained but they were able to synthesize it in 4 steps with moderate yields. By modulating the side chains on the [2.2.2]paracychlphanenes they were able to control the absorption and emission spectra of the polymers. In 2019 Turner et al. and Gregor et al. simultaneously expanded the selection of paracyclophanene monomers available by synthesizing several benzothiadiazole paracyclophane-1,9-diene derivatives.

Since this initial demonstration, several other cyclophanenes and cyclophanedienes have been used in ROMP to synthesize homo- and co-polymers.[73–75] In addition, a series of donor-acceptor block co-polymers have been synthesized via ROMP of macrocycles based on

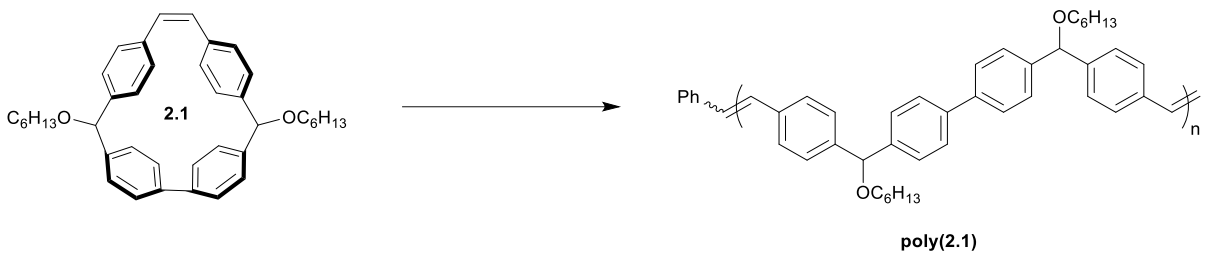

Figure 2.2 Proposed polymerization of macrocycle (**2.1**).

arylenevinylenes.[75–77] Inspired by this work, we set out to investigate methods to synthesize a new class of strained macrocycles capable of undergoing ROMP.

2.3 Results and discussion

2.3.a. Synthesis and characterization of stilbene-based polymer

We conceived of *cis*-stilbene-based macrocycle **2.1**, which we predicted would possess a high degree of ring strain and would enable predefined control of the structure of the resulting polymer backbone (**Figure 2.2**).[78] By synthesizing a polymer through chain growth polymerization instead of intensive step growth condensation polymerization, we envisioned that we could readily obtain polymers with low *Đ* and controlled molecular weight. Additionally, the polymer resulting from macrocycle **2.1** would be similar in structure to high-performance polymers, such as poly(phenylene)s, poly(phenylenevinylene)s, and poly(aryletherketone)s, that with a few exceptions have traditionally been synthesized through uncontrolled polymerizations.[79–86] The potential to synthesize high-performance polymers through readily accessible chain growth polymerizations instead of step growth polymerizations could be an exciting advancement toward complex polymer structures that were previously unachievable.

Despite the broad utility of strained macrocycles for ROMP, there are few efficient synthetic routes to obtain macrocyclic monomers with enough ring strain to drive ring-opening polymerization. We therefore employed oxidative bisboronate homocoupling—a

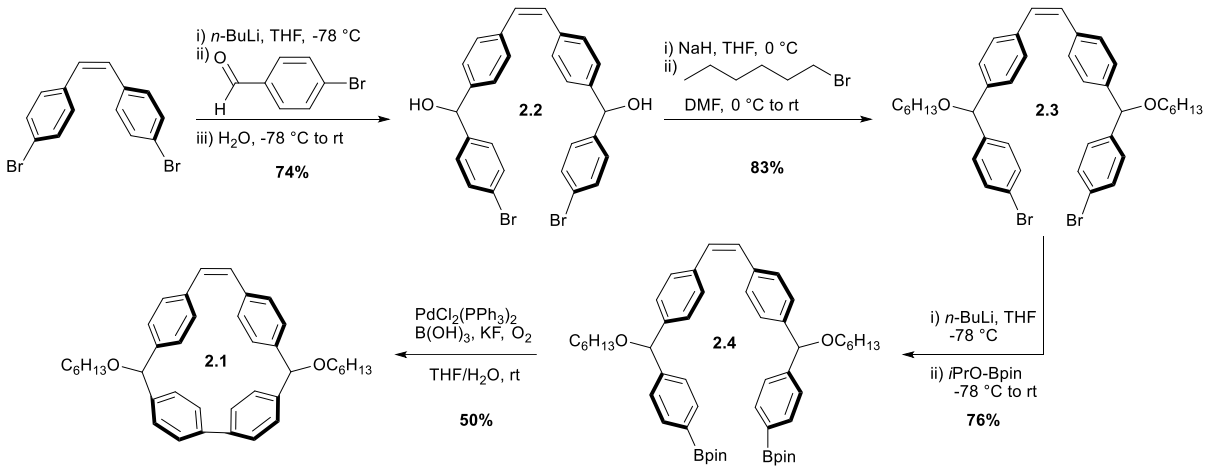

Figure 2.3 Synthetic scheme for **2.1**.

simple, scalable, and efficient strain-building reaction—for the preparation of macrocycle **2.1** (**Figure 2.3**).[87] First, curved diol intermediate **2.2** was obtained by double lithiation of 4,4'-dibromostilbene and subsequent nucleophilic addition to 4-bromobenzaldehyde. Deprotonation of the free alcohols with sodium hydride and treatment with 1-bromohexane yielded **2.3**. Lithium-halogen exchange followed by treatment with 2-isopropoxy-4,4,5,5-tetramethyl-1,3,2-dioxaborolane yielded bisboronate **2.4**. Finally, **2.4** was subjected to mild Pd-catalyzed oxidative homocoupling conditions to yield final macrocyclic monomer **2.1** on a multigram scale. The key cyclization reaction is 50% yielding with the remaining mass balance primarily attributed to oligomeric byproducts. In principle, other sized macrocycles could form as well, but we did not observe these products to any appreciable extent.

With monomer **2.1** in hand, we proceeded to investigate the polymerization of **2.1**. To this end we chose two different third generation Grubbs catalysts, both known to be highly active in traditional and ED-ROMP.[40,63] These initial experiments were carried out on NMR scale in tetrahydrofuran-d_8 ([**2.1**]$_0$ = 1 M) with a monomer to initiator ratio of 100:1 (Table 2.1, entries 1&2). Within 12 hours at 60 °C each initiator reached conversions ≥ 99% as determined by ^{1}H NMR spectroscopy. From these experiments, it was found that the molecular weight distribution

of **poly(2.1)** was monomodal with a M_w = 107 kDa and $Đ$ of 1.7, based upon SEC analysis using multi-angle laser light scattering and refractive index detection. It should be noted that in both cases the resulting solution formed a viscous gel, to circumvent this in future trials the polymerization was performed at a lower concentration ([**2.1**]$_0$ = 0.1 M).

The structure of **poly(2.1)** was confirmed by ^{1}H NMR spectroscopy and matrix-assisted laser desorption ionization time of flight mass spectrometry (MALDI-TOF/MS). In the case of **poly(2.1)** only a single vinylic signal at δ = 7.24 ppm was observed, while no other vinylic signals were present above the detection limit for ^{1}H NMR spectroscopy. This observation is consistent with the backbone of **poly(2.1)** being primarily *trans*-stilbene isomers (**Figure 2.17**).[48,88,89] MALDI-TOF/MS then was used to better understand the structural speciation within samples of

Table 2.1 Summary of ROMP experiments performed.

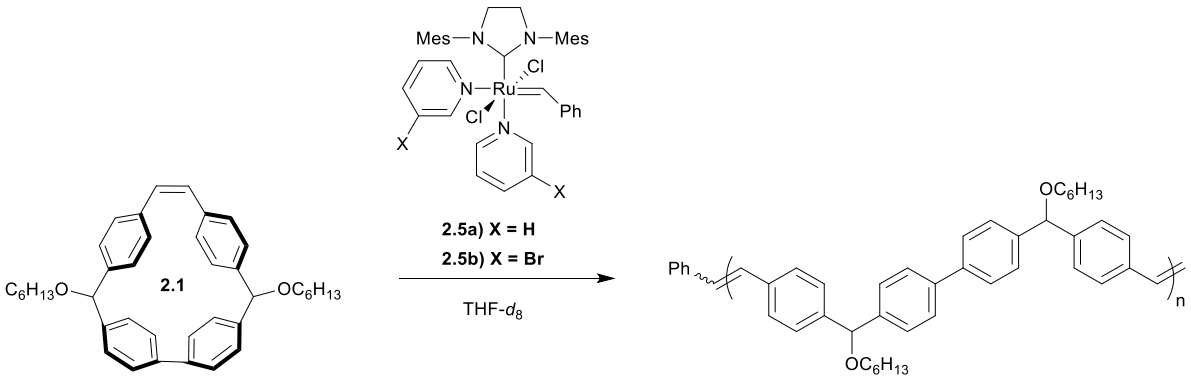

Entry	[**2.1**]:[**2.5**]	Conc.	Temp (°C)	Conv. (%)	$M_{n,\,theo}$ (kg/mol)	M_n (kg/mol)	M_w (kg/mol)	$Đ$	k^d (sec^{-1})
1[a]	100:1	1 M	60	>99	55.9	62.1	107.0	1.7	--
2[b]	100:1	1 M	60	99	55.9	55.4	102.2	1.7	--
3[a]	75:1	0.1 M	40	>99	42.4	53.4	79.7	1.5	--
4[ac]	35:1	1 M	20	45	8.6	8.0	8.7	1.1	$9.97 \times 10^{-6} \pm 0.02$
5[ac]	35:1	1 M	30	>99	20.1	18.3	27.8	1.5	$5.1 \times 10^{-5} \pm 0.4$
6[ac]	35:1	1 M	40	>99	18.4	23.9	36.0	1.5	$2.2 \times 10^{-4} \pm 0.3$

[a] Initiator **2.5b** [b] Initiator **2.5a** [c] Average of 3 experiments [d] Error represents the standard deviation

poly(2.1). The repeat unit for **poly(2.1)** has an experimental mass of 558.9 amu, which is consistent with the predicted molecular weight of **2.1** (**Figure 2.4**). Notably, we did not see evidence of cyclic polymer structures from any of the analyses.

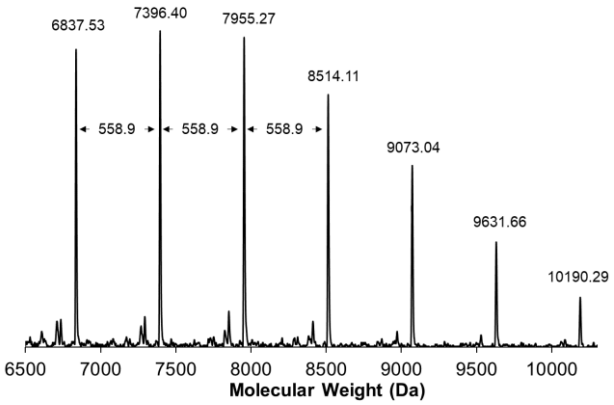

Figure 2.4 MALDI-TOF/MS spectrum for poly(**2.1**). The molecular weight between repeat units was measured to be 558.9 amu, consistent with the molecular weight of the monomer.

We also evaluated the thermal properties of **poly(2.1)** using differential scanning calorimetry (DSC) and thermogravimetric analysis (TGA). The decomposition temperature (T_d) for **poly(2.1)** was found to be 281 °C under N_2, determined by the onset of weight loss using TGA (**Figure 2.19**), a close comparison to **poly(2.1)** would be poly(phenylenevinylenes) which have T_d >300 °C.[48] A glass transition temperature (T_g) for **poly(2.1)** was found to be 94 °C determined by DSC, and no other thermal transitions were observed (**Figure 2.20**).

*2.3.b. Mechanistic investigations into the polymerization of **2.1**.*

Given the ring strain and addition of an enthalpic driving force for the ROMP of **2.1**, we expected the polymerization to demonstrate chain growth characteristics, and a high degree of molecular weight control. To better understand the polymerization mechanism of **poly(2.1)**, monomer conversion was monitored by ^{1}H NMR spectroscopy using the benzylic ether hydrogen of the monomer and polymer at δ = 5.39 and 5.48 ppm, respectively (**Figure 2.21**). The polymerization displayed first order kinetics with respect

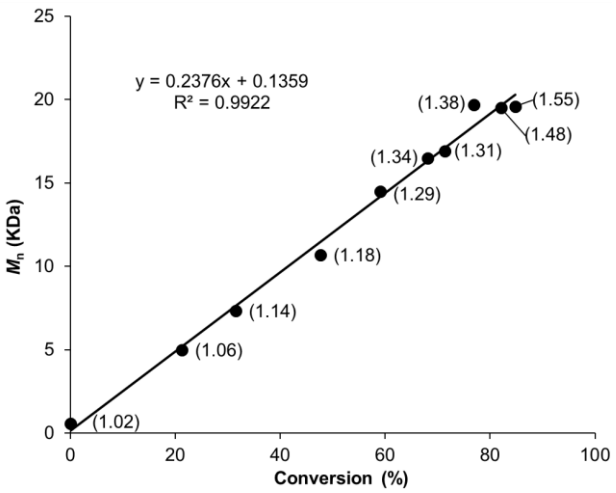

Figure 2.5 Mn vs conversion plot for the polymerization of **2.1** follows a linear progression consistent with a chain growth mechanism, *Đ* for each time point in parenthesis.

to consumption of **1** (**Figure 2.22**) and a linear correlation between M_n and conversion (**Figure 2.5**). Collectively, these results are consistent with a chain growth polymerization mechanism that does not exhibit slow initiation or early irreversible termination. Rate constants (k) for propagation were measured at 20, 30, and 40 °C (Table 2.1 entries 4-6), in all experiments the polymerization was stopped after 16 hours. Using this information an activation energy was determined to be 28.2 kcal/mol (**Figure 2.23**). We next turned our attention toward understanding the underlying reason for the high *Đ*.

Chain transfer has been observed during ROMP, typically facilitating an equilibration of chain lengths via intermolecular cross metathesis reactions. We investigated the occurrence of chain transfer by combining two different molecular weight polymers (M_n = 71.5 kDa and 15.2 kDa) in the presence of **2.5b** in THF. After 4 hours, the resulting polymer had an intermediate molecular weight (M_n = 24 kDa) that was consistent with the weighted average of the feed polymers (**Figure 2.6a**) and a higher *Đ* of 2.0. Chain transfer with *trans*-stilbene was also found to be efficient under our polymerization conditions. Specifically, 1 equivalent of *trans*-stilbene (relative to repeat unit) was combined with a sample of **poly(2.1)** (M_n = 41.5 kDa, *Đ* = 1.6) and **2.5b** in THF. After 3.5 hours, the molecular weight of **poly(2.1)** decreased (M_n = 16.9 kDa) (**Figure 2.6b**). These results are consistent with chain transfer occurring during

the polymerization of **2.1**. It should be noted in the latter experiment no change in *Đ* was observed contrary to what is expected, this result could be due to a change in column resolution between the molecular weights.

Taken together, our results suggested to us that, likely due to the ring strain of **2.1**, the polymerization proceeds through a chain growth mechanism and is not an entropy-driven polymerization. Over the course of the polymerization of **2.1** the *Đ* of **poly(2.1)** increased from 1.0 to 1.5 further corroborating the presence of chain transfer during the polymerization (**Figure 2.5**).

2.3.c. Inhibition of chain transfer during the polymerization

The presence of chain transfer during the polymerization can inhibit the ability to accurately target a desired molecular weight for a polymer. For this reason, we set out to inhibit chain transfer from occurring over the course of the polymerization. It has been shown that one way to inhibit chain transfer is to have a sterically bulky alkene in the polymer backbone. To this end we designed two monomers **2.5** and **2.6** that had varying levels of sterics introduced around the backbone olefin (Figure **2.7a**). Initial

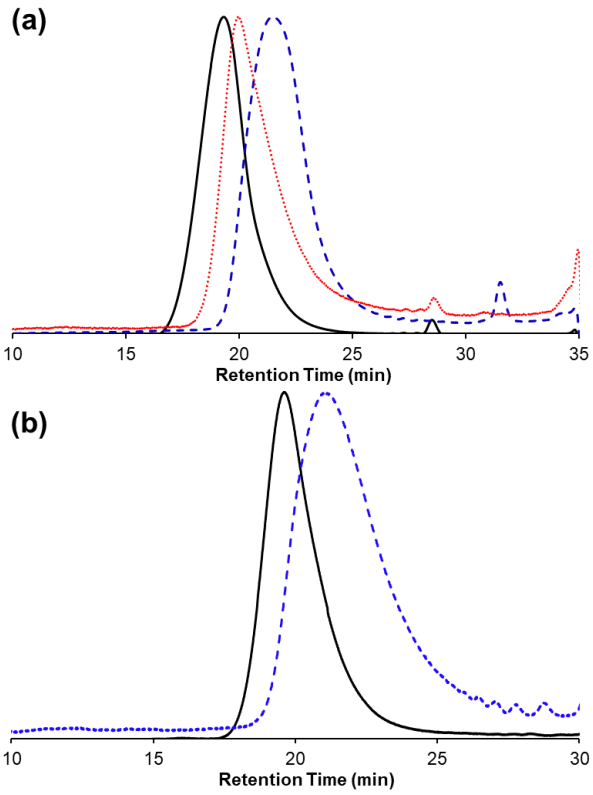

Figure 2.6 a) GPC traces for polymer-polymer chain transfer experiment for the two starting polymers (black solid, Mn = 71 kDa; blue dash, M_n = 15.2 kDa) and the final polymer (red dot, M_n = 24 kDa). b) GPC traces for polymer-stilbene chain transfer experiment for the starting polymer (black solid, M_n: 41.5 kDa) and the final polymer (blue dash, M_n: 16.9 kDa).

attempts to polymerize **2.5** were carried out under the same conditions as the polymerization of **2.1** ($[\mathbf{2.5}]_0$ = 0.1 M, M:I = 35:1), but to our dismay no polymer was observed by ^{1}H NMR spectroscopy nor GPC (Figure **2.7b**). To decrease the steric bulk around the olefin of the monomer we then synthesized **2.6**, which only had 1 ortho-methyl substitution, but similar results were obtained. Further attempts to polymerize **2.6** were carried out using Grubbs' 2nd generation catalyst (**C**) at an elevated temperature (40 °C) but to no avail (Figure **2.7b**).

2.4 Conclusions

In summary, we have reported the synthesis and subsequent polymerization of a new class of strained macrocycle. The polymerization of **2.1** demonstrated first order kinetics and a linear correlation between M_n and conversion, consistent with chain growth polymerization. The resulting linear polymer obtained through this method had a T_g of 94 °C and a T_d of 281 °C. Further work is being done to use variations of **2.1** to make more complex polymeric materials that cannot be achieved using traditional small molecule-based poly(olefins). In this way, we hope to be able to control and modify the thermal and physical properties of these modular polymers. Ultimately, ROMP of highly strained macrocyclic monomers provides an exciting avenue to create and develop new polymeric materials from efficient synthetic methods.

2.5 Experimental

2.5.a General Considerations.

Deuterated solvents were purchased from Cambridge Isotopes. Anhydrous tetrahydrofuran (THF), dimethylformamide (DMF), and pyridine were obtained from a solvent purification system. All other reagents were obtained from commercial sources and used as received. Moisture- and oxygen-sensitive reactions during monomer synthesis were carried out in

flame-dried glassware and under an inert atmosphere of purified nitrogen using syringe/septa technique. Thin Layer Chromatography (TLC) was performed using Sorbent Technologies Silica Gel XHT TLC plates. Developed plates were visualized using UV light at wavelengths of 254 and 365 nm. Silica column chromatography was conducted with Zeochem Zeoprep 60 Eco 40-63 μm silica gel. ^{1}H and ^{13}C NMR spectroscopy was performed on a 300, 500, or 600 MHz Bruker NMR spectrometer. Spectra taken in $CDCl_3$ are reported in parts per million (ppm) referenced to TMS (δ 0.00 ppm) for ^{1}H NMR and residual $CHCl_3$ (δ 77.16 ppm) for ^{13}C NMR. Spectra taken in THF-d_8 are reported in parts per million (ppm) referenced to residual protio-solvent (^{1}H: 3.58, 1.72).

MALDI-TOF/MS was performed using a Bruker Daltonics AutoFlex II MALDI-TOF Mass spectrometer. The polymer matrix used was 1,8,9-anthracenetriol in THF, and data was obtained in linear (positive) mode.

Gel permeation chromatography (GPC) was performed using an Agilent Technologies Infinity Series II pump, 3 in line columns (MZ Gel), Wyatt Technology light scattering and refractive index detectors with tetrahydrofuran (THF) as the mobile phase with an flow rate of 1 mL/min. Number average molecular weights (M_n) and weight-average molecular weights (M_w) were calculated from light scattering and refractive index data using Astra software from Wyatt Technology The absolute weight-average molecular weights were determined by a dn/dc value which was measured by assuming 100% mass recovery of the polymers after passing the columns. The dn/dc of **poly(2.1)** was found to be 0.246 (mL/g).

Thermogravimetric analysis was performed on a TA TGA Q50 under nitrogen from room temperature to 600 °C at 5 °C/min. Differential Scanning Calorimetry (DSC) was performed on a TA DSC Q250 calorimeter at a heating rate of 10 °C/min and cooling rate of 5 °C/min. The

decomposition temperature of the polymer was determined at 2% weight loss. Heatflow in units of watts was recorded and is reported after normalizing by the mass of the sample (W/g).

Cis-4,4'-dibromostilbene[90] and initiators **2.5a** and **2.5b**[91] were synthesized using previously reported procedures.

2.5.b. Monomer Synthesis

(Z)-(ethene-1,2-diylbis(4,1-phenylene))bis((4-bromophenyl)methanol) **2.2**

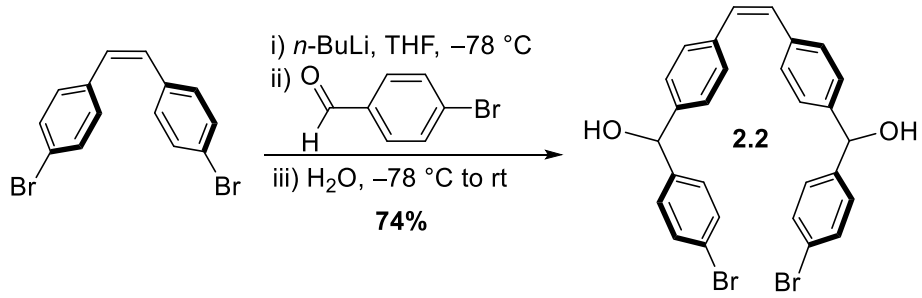

4,4'-dibromostilbene (12.0 g, 35.5 mmol, 1.00 equiv.) and THF (200 mL) were added to a 500 mL round bottom flask with a magnetic stir bar. The solution was cooled to -78 °C, then n-butyllithium (31.6 mL, 2.3 M in hexane, 2.05 equiv.) was added over the course of 20 min. After stirring at -78 °C for 3 min, 4 bromobenzaldehyde (13.1 g, 71.0 mmol, 2.00 equiv.) in THF (40 mL) was added in stream via cannula, during which the solution gradually became viscous with solid crashed out. The cold bath was removed, and the mixture was kept stirring at room temperature for 2 hours. The reaction mixture was quenched with water (20 mL). The THF was removed under reduced pressure, then DCM (200 mL) was added to the mixture, which was washed with water (100 mL) and brine (100 mL) and dried over Na_2SO_4. Concentration under reduced pressure resulted in a yellow gel. The material was dissolved in DCM (80 mL) and stored in the freezer (-20 °C) overnight, resulting in powdered precipitate. The precipitate was collected by filtration and washed with DCM (10 mL) to give the product as a white powder (7.55 g). The filtrate was concentrated, and the residue was purified by column chromatography (silica, 0% to

3% ethyl acetate in DCM) to yield more product (6.58 g). Overall, the product was obtained in a yield of 74%. ^{1}H NMR (600 MHz, $CDCl_3$): δ 7.46 (d, J = 8.4 Hz, 4H, Ar-H), 7.25 (d, J = 8.4 Hz, 4H, Ar-H), 7.22 (d, J = 8.4 Hz, 4H, Ar-H), 7.19 (d, J = 8.4 Hz, 4H, Ar-H), 6.55 (s, 2H, C=C-H), 5.76 (d, J = 3.4 Hz, 2H, CH), 2.18 (d, J = 3.4 Hz, 2H, OH); ^{13}C NMR (150 MHz, $CDCl_3$): δ 142.74, 142.34, 136.90, 131.73, 130.11, 129.25, 128.34, 126.59, 121.63, 75.62. IR (neat): 3264.5, 1484.0, 1404.3, 1172.5, 1067.9, 1027.3, 1008.0, 819.5, 799.7 cm^{-1}. HRMS (TOF MS ASAP+) (m/z): $[M+H]^+$ calculated for $C_{28}H_{23}Br_2O_2$: 549.0065; found 549.0039.

(Z)-1,2-bis(4-((4-bromophenyl)(n-hexyloxy)methyl)phenyl)ethene **2.3**

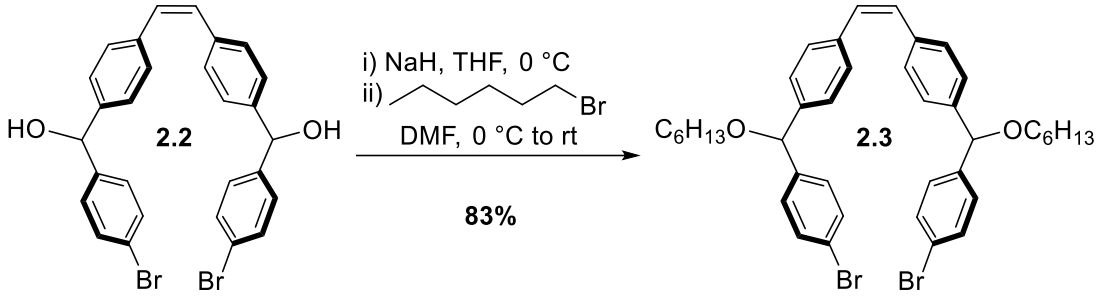

NaH (4.10 g, 60 wt% in mineral oil, 102.5 mmol, 4.00 equiv.) and THF (150 mL) were added to a 500 mL round bottom flask. The slurry was cooled to 0 °C at which point **2.2** (14.1 g, 25.6 mmol, 1.00 equiv.) in THF (30 mL) was added in stream. The mixture was stirred at 0 °C for 1 hour. Then 1-bromohexane (28.8 mL, 205 mmol, 8.00 equiv.) and DMF (30 mL) were added, and the reaction was stirred at room temperature overnight. The reaction was carefully quenched with water. After THF was removed under vacuum, DCM (150 mL) was added. The solution was washed with water (100 mL), 5 wt% aqueous LiCl solution (3×100 mL), and brine (100 mL) and dried over Na_2SO_4. After concentration under reduced pressure, the crude solid was purified via column chromatography (silica, 0% to 8% ethyl acetate in hexanes) to yield a colorless oil (15.0 g, 83%). ^{1}H NMR (600 MHz, $CDCl_3$): δ 7.44 (d, J = 8.4 Hz, 4H, Ar-H), 7.22 (d, J = 8.4 Hz, 4H,

Ar-H), 7.20 (d, J = 8.1 Hz, 4H, Ar-H), 7.15 (d, J = 8.1 Hz, 4H, Ar-H), 6.52 (s, 2H, C=C-H), 5.24 (s, 2H, CH), 3.42 (td, J = 6.6, 3.1 Hz, 4H, OCH_2), 1.62 (dt, J = 15.0, 6.6 Hz, 4H, CH_2), 1.37 (p, J = 7.0 Hz, 4H, CH_2), 1.33-1.22 (overlap, 8H, CH_2), 0.88 (t, J = 7.0 Hz, 6H, CH_3); ^{13}C NMR (150 MHz, $CDCl_3$): δ 141.75, 141.14, 136.61, 131.58, 130.01, 129.03, 128.82, 126.89, 121.36, 82.87, 69.46, 31.79, 29.94, 26.04, 22.75, 14.21. IR (neat): 2927.3, 2855.3, 1484.3, 1395.0, 1088.7, 1069.8, 1009.8, 816.0, 799.2 cm^{-1}. HRMS (TOF MS ASAP+) (m/z): $[M+H]^+$ calculated for $C_{40}H_{47}Br_2O_2$: 717.1943; found 717.1893.

(Z)-1,2-bis(4-((n-hexyloxy)(4-(4,4,5,5-tetramethyl-1,3,2-dioxaborolan-2-yl)phenyl)-methyl)phenyl)ethene **2.4**

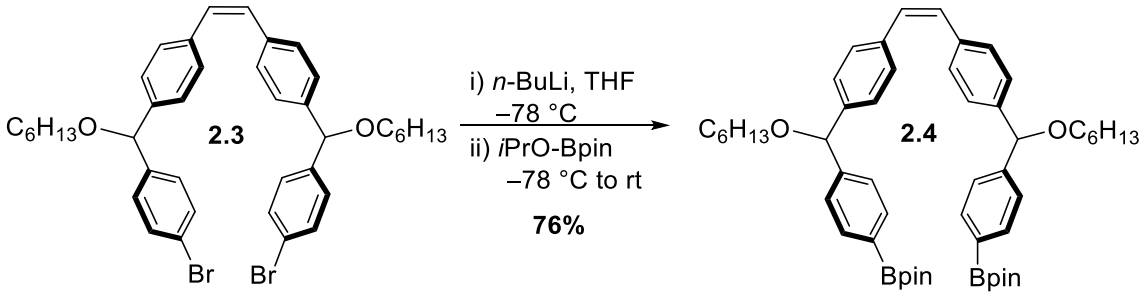

Compound **2.3** (14.7 g, 20.5 mmol, 1.00 equiv.) was dissolved in THF and cooled to -78 °C. Then n-butyllithium (21.5 mL, 2.3 M in hexane, 2.40 equiv.) was added slowly via syringe. Isopropyl pinacol borate (16.7 mL, 81.8 mmol, 4.00 equiv.) was quickly added in stream. The mixture was stirred at -78 °C for 5 min. and allowed to warm to room temperature. After 2 hours, the reaction was carefully quenched with water. The mixture was extracted with dichloromethane (3×), and the combined organic layers were washed with brine and dried over Na_2SO_4. The material was purified by column chromatography (silica, 0% to 8% ethyl acetate in hexanes), yielding a colorless oil (12.4 g, 76%). ^1H NMR (600 MHz, $CDCl_3$): δ 7.77 (d, J = 8.0 Hz, 4H, Ar-

H), 7.36 (d, J = 8.0 Hz, 4H, Ar-H), 7.22-7.13 (m, 8H, Ar-H), 6.48 (s, 2H, C=C-H), 5.29 (s, 2H, CH), 3.42 (t, J = 6.7 Hz, 4H, OCH_2), 1.63 (dt, J = 15.0, 6.7 Hz, 4H, CH_2), 1.42-1.20 (overlap, 36H, CH_2 and CH_3), 0.88 (t, J = 6.9 Hz, 6H, CH_3); ^{13}C NMR (150 MHz, $CDCl_3$): δ 145.76, 141.52, 136.38, 135.01, 129.91, 128.92, 126.94, 126.48, 83.86, 83.53, 69.43, 31.82, 29.97, 26.05, 25.01, 22.76, 14.22, 13C-B signal not observed. IR (neat): 2929.0, 2856.5, 1610.9, 1511.2, 1397.2, 1357.4, 1319.2, 1270.6, 1142.6, 1085.9, 1019.6, 961.8, 858.2, 824.7, 798.9, 656.7 cm^{-1}. HRMS (TOF MS ASAP+) (m/z): $[M+H]^+$ calculated for $C_{52}H_{71}B_2O_6$: 813.5437; found 813.5327.

(Z)-3,8-bis(n-hexyloxy)-1,2,4,7(1,4)-tetrabenzenacyclooctanophan-5-ene **2.1**

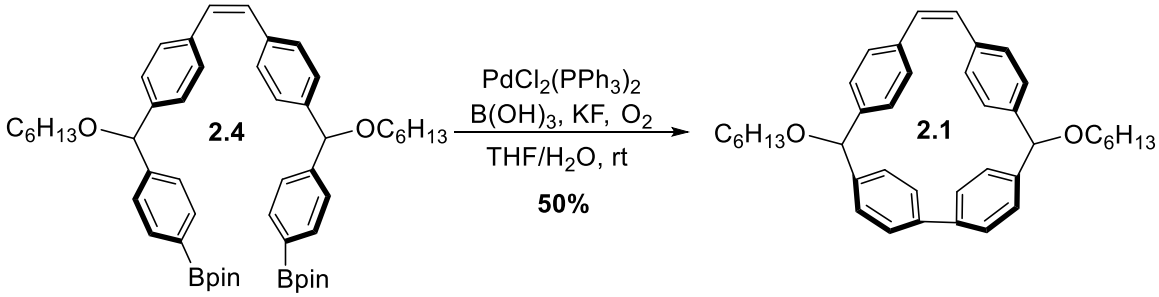

Bisboronate **2.4** (3.00 g, 3.76 mmol, 1.00 equiv.), PdCl2(PPh3)2 (0.26 g, 0.38 mmol, 0.10 equiv.), and B(OH)3 (1.16 g, 18.8 mmol, 5.00 equiv.) were dissolved in THF (450 mL) in a 500 mL round bottom flask equipped with a stir bar. The mixture was stirred open to air at room temperature for 10 min. until a clear yellow solution was achieved. Then KF (0.44 g, 7.52 mmol, 2.00 equiv.) was dissolved in water (45 mL) and added. The mixture was sonicated until orange color appeared, after which it was stirred overnight at room temperature. After THF was removed under vacuum, DCM was added. The solution was washed with water and brine and dried over Na_2SO_4. The material was purified by column chromatography (silica, 0% to 50% DCM in hexanes), yielding a colorless oil which solidified upon standing (1.05 g, 50%). ^1H NMR (600

MHz, $CDCl_3$): δ *trans* 7.45 (dd, J = 8.5, 2.0 Hz, 2H, Ar-H), 7.39 (dd, J = 8.5, 2.0 Hz, 2H, Ar-H), 7.35 (dd, J = 8.3, 2.0 Hz, 2H, Ar-H), 7.02 (dd, J = 8.3, 2.0 Hz, 2H, Ar-H), 6.65 (d, J = 8.3 Hz, 4H, Ar-H), 6.52 (d, J = 8.3 Hz, 4H, Ar-H), 6.45 (s, 2H, C=C-H), 5.28 (s, 2H, CH), 3.77 (dt, J = 9.0, 6.7 Hz, 2H, OCH_2), 3.61 (dt, J = 9.0, 6.7 Hz, 2H, OCH_2), 1.78-1.69 (m, 4H, CH_2), 1.50-1.41 (m, 4H, CH_2), 1.37-1.26 (overlap, 8H, CH_2), 0.90 (t, J = 6.9 Hz, 6H, CH_3); *cis* 7.46 (dd, J = 8.5, 2.0 Hz, 2H, Ar-H), 7.39 (dd, J = 8.5, 2.0 Hz, 2H, Ar-H), 7.34 (dd, J = 8.3, 2.0 Hz, 2H, Ar-H), 7.03 (dd, J = 8.3, 2.0 Hz, 2H, Ar-H), 6.65 (d, J = 8.3 Hz, 4H, Ar-H), 6.53 (d, J = 8.3 Hz, 4H, Ar-H), 6.46 (s, 2H, C=C-H), 5.27 (s, 2H, CH), 3.77 (dt, J = 9.0, 6.7 Hz, 2H, OCH_2), 3.61(dt, J = 9.0, 6.7 Hz, 2H, OCH_2), 1.78-1.69 (m, 4H, CH_2), 1.50-1.41 (m, 4H, CH_2), 1.37-1.26 (overlap, 8H, CH_2), 0.90 (t, J = 6.9 Hz, 6H, CH_3); ^{13}C NMR (150 MHz, $CDCl_3$): δ trans 144.48, 142.46, 140.92, 135.90, 130.71, 128.30, 128.03, 127.94, 127.36, 126.43, 125.87, 82.65, 69.59, 31.88, 30.06, 26.15, 22.81, 14.23; cis 144.50, 142.51, 140.96, 135.87, 130.70, 128.28, 127.91, 127.14, 126.58, 125.78, 82.60, 69.56, 31.89, 30.06, 25.15, 22.81, 14.24. IR (neat): 2950.6, 2925.6, 2851.0, 1450.0, 1414.2, 1332.9, 1186.3, 1094.1, 1015.2, 836.8, 805.2, 751.0, 735.1, 705.9 cm^{-1}. HRMS (TOF MS ASAP+) (m/z): $[M+H]^+$ calculated for $C_{40}H_{47}O_2$: 559.3576; found 559.3565.

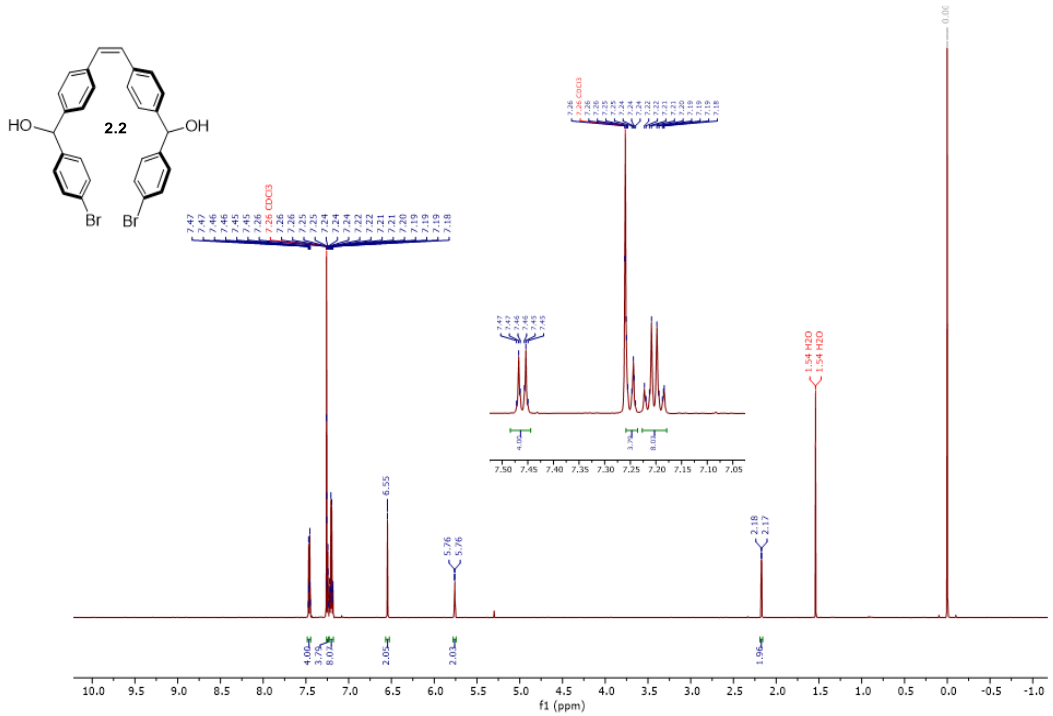

Figure 2.8 ^{1}H NMR spectrum of **2.2** in $CDCl_3$.

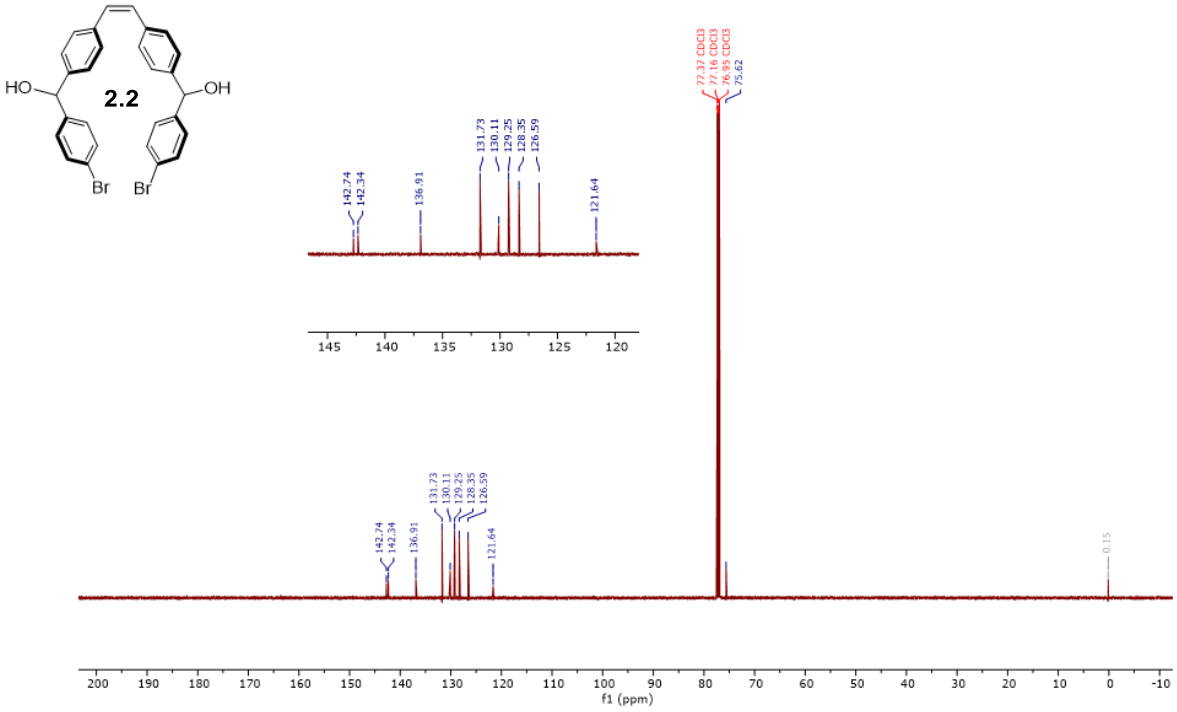

Figure 2.7 ^{13}C NMR spectrum of **2.2** in $CDCl_3$.

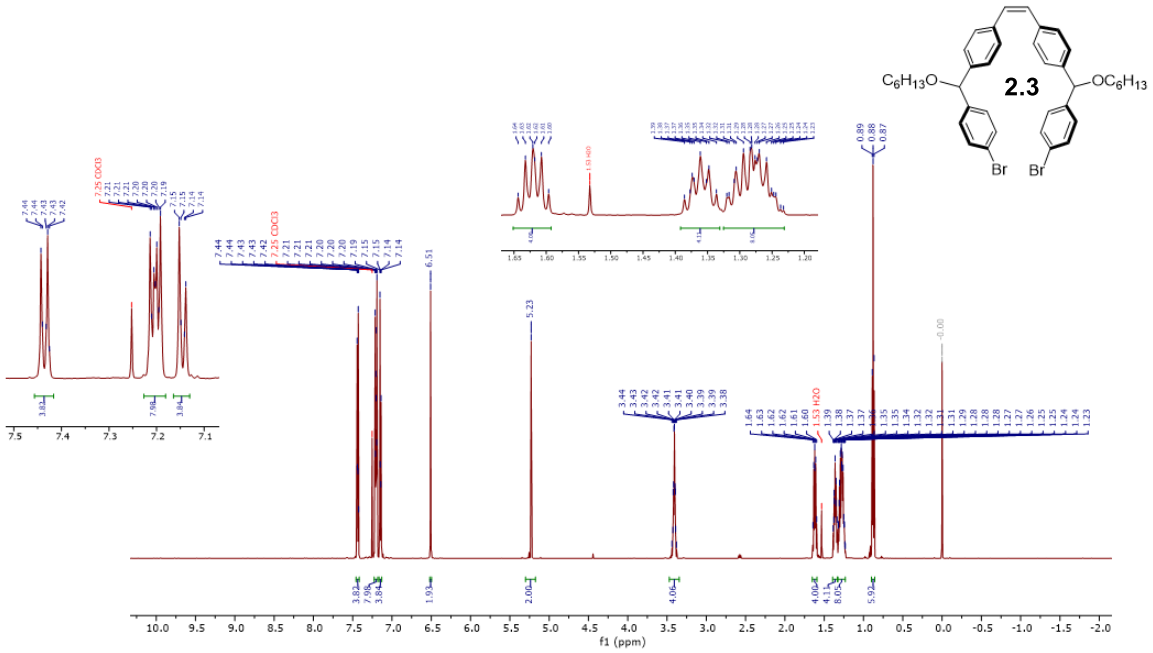

Figure 2.10 ^{1}H NMR spectrum of **2.3** in $CDCl_3$.

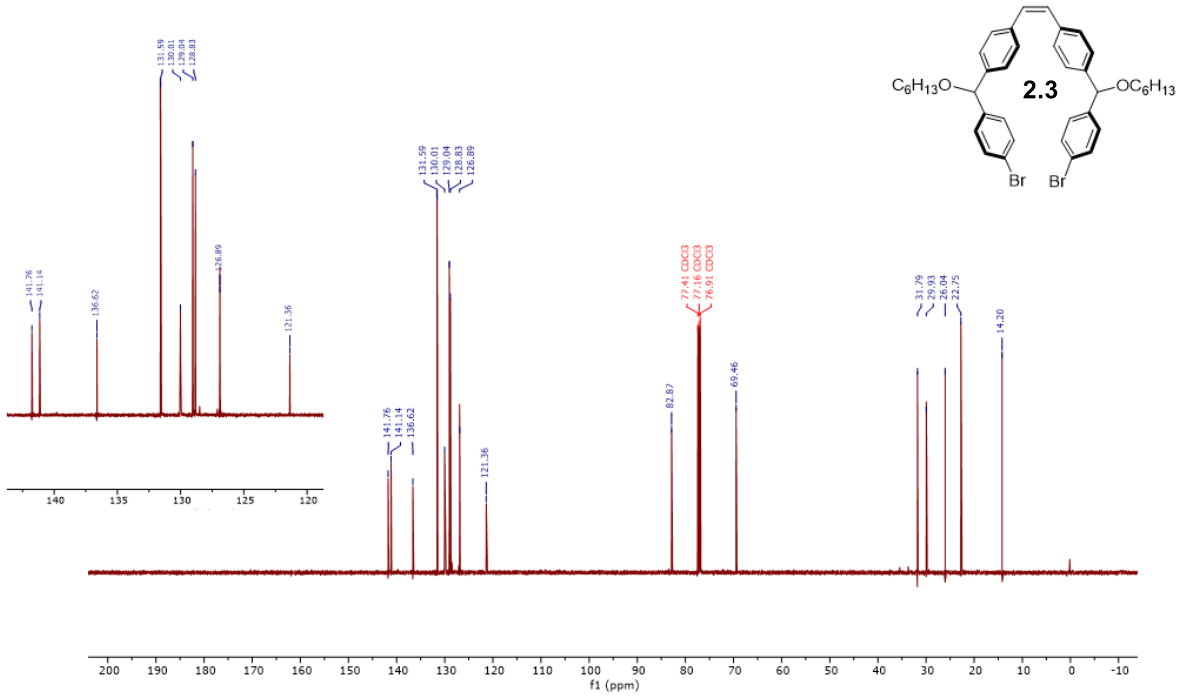

Figure 2.9 ^{13}C NMR spectrum of **2.3** in $CDCl_3$.

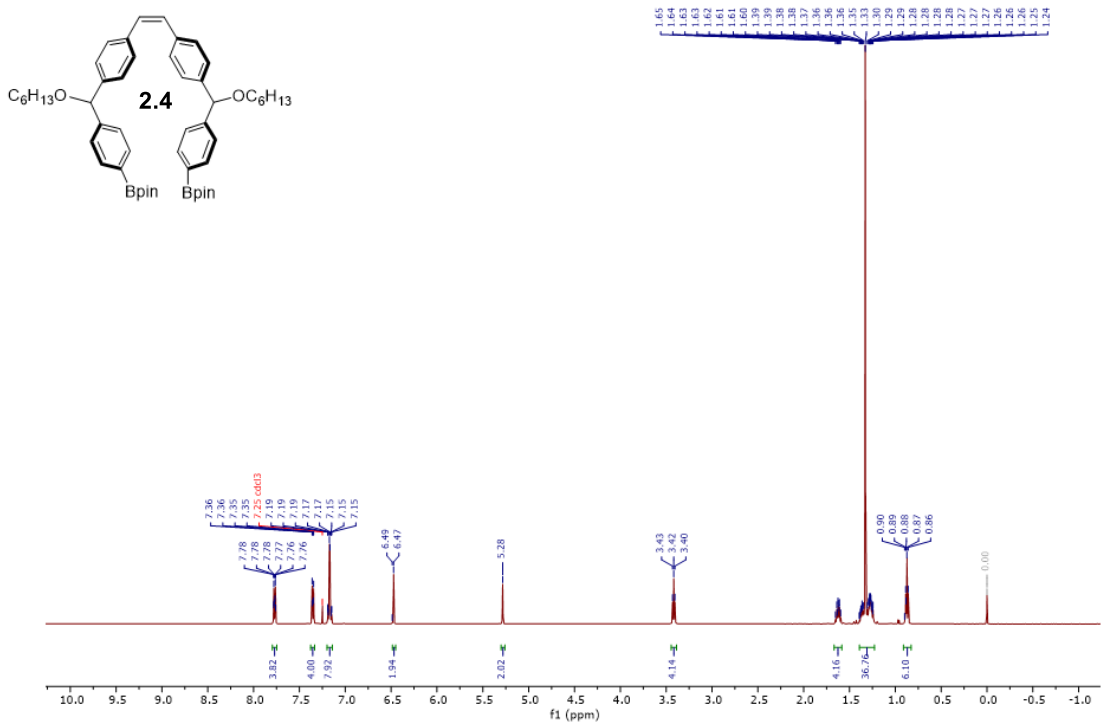

Figure 2.12 ^{1}H NMR spectrum of **2.4** in $CDCl_3$.

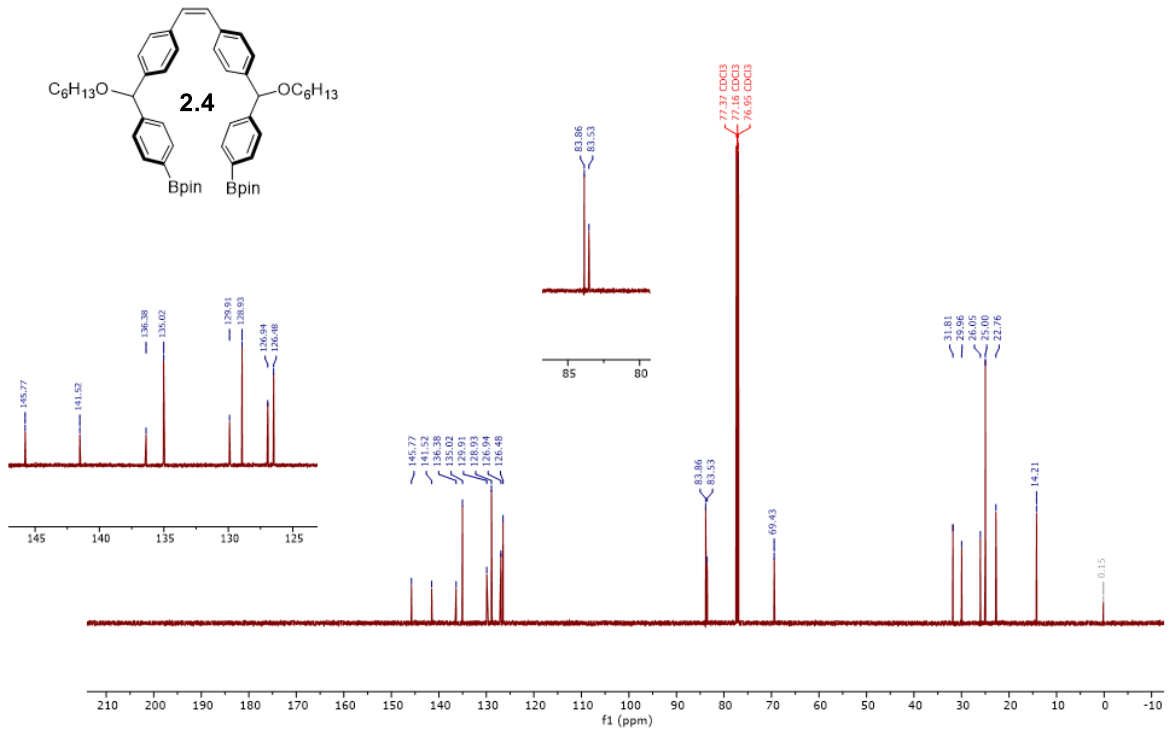

Figure 2.11 ^{13}C NMR spectrum of **2.4** in $CDCl_3$.

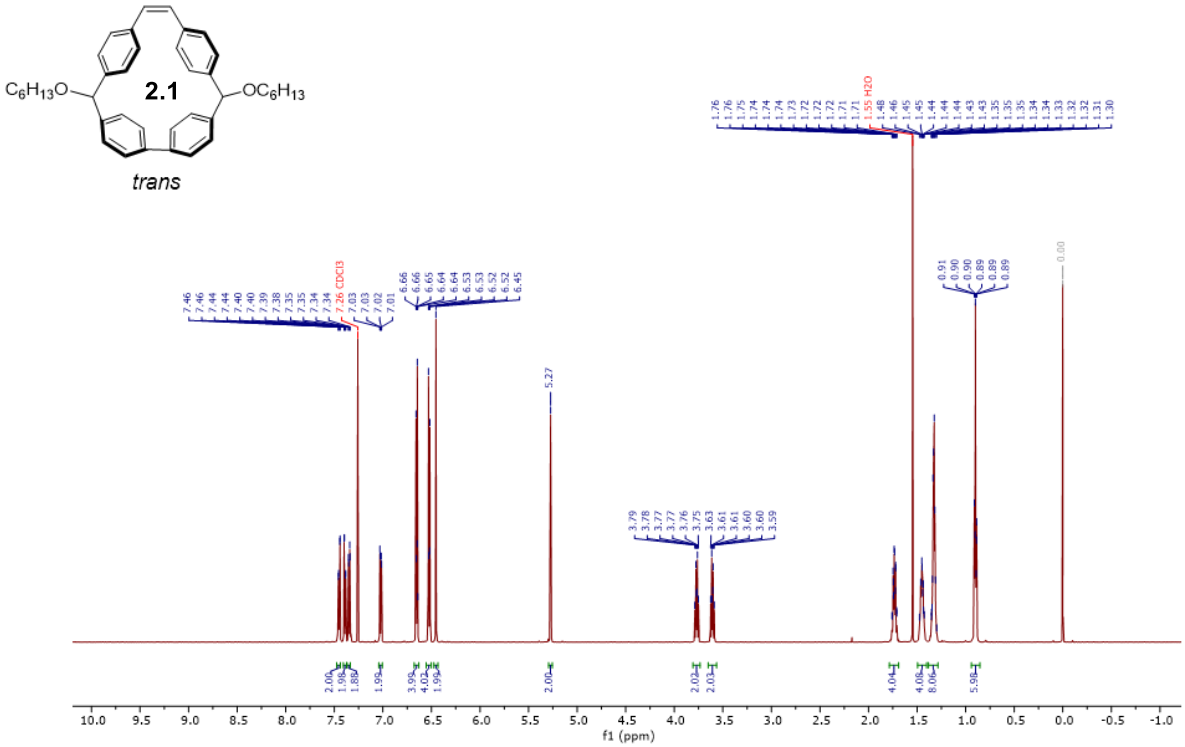

Figure 2.14 ^{1}H NMR spectrum of **2.1** in $CDCl_3$.

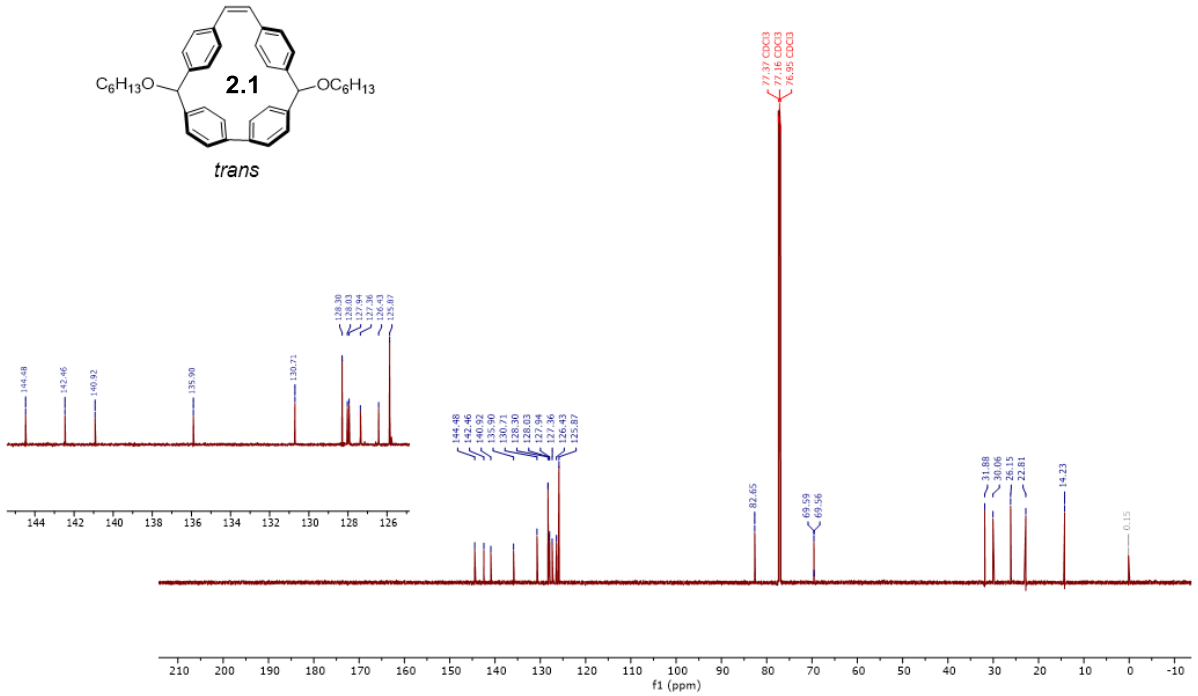

Figure 2.13 ^{13}C NMR spectrum of **2.1** in $CDCl_3$.

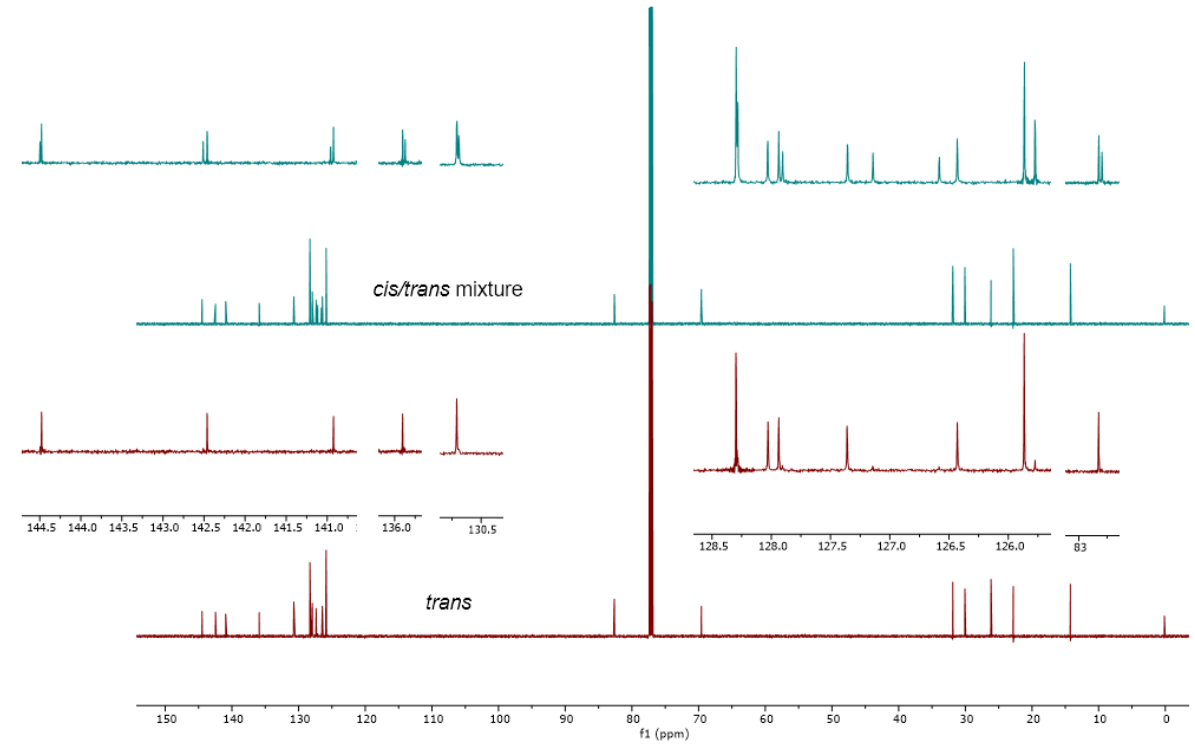

Figure 2.16 ^{13}C NMR comparing trans isomer and a mixture of *cis* and *trans* isomers for the benzylether of **2.1**.

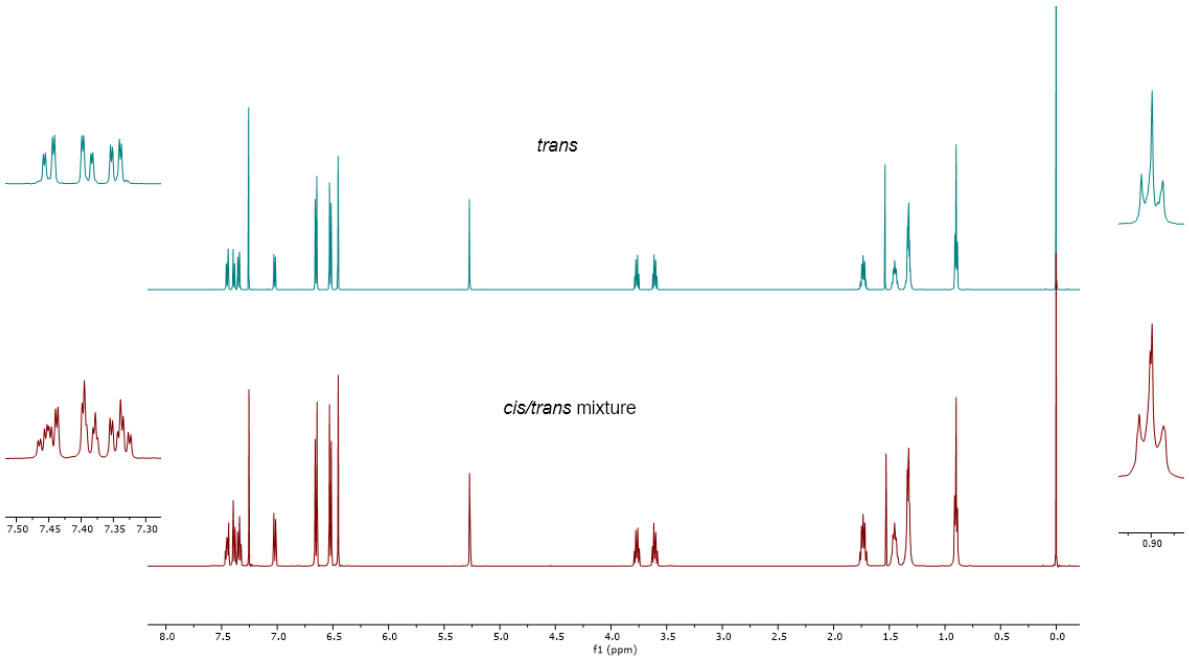

Figure 2.15 ^{1}H NMR comparing trans isomer and a mixture of *cis* and *trans* isomers for the benzylether of **2.1**.

2.5.c. Polymerization Studies

General Kinetics Procedure

In a dry box, **2.1** (0.110 g, 0.2 mmol) was added to a 7 mL vial. To the 7 ml vial **2.5b** (0.005 g, 0.002 mmol) in 0.2 mL of THF-d_8 was added, before being transferred and sealed in a screwcap NMR tube. After 10 minutes of equilibration time at room temperature the NMR tube was placed in a preheated NMR spectrometer. After 16 hours the polymerization was quenched via the addition 0.1 mL of ethyl vinyl ether in 1 mL of THF. Crude GPC was obtained before precipitation of the polymer into cold methanol. The polymer was isolated via vacuum filtration to provide **poly(2.1)** as a white solid (0.0825 g, 75% yield, M_n:15.2 kDa, M_w: 23.4 kDa, $Đ$: 1.5).

Molecular Weight vs. Conversion

In a dry box, **2.1** (0.4965 g, 0.89 mmol) was charged into a flame-dried and N_2-purged 25 mL 3-neck flask with 7.9 mL of anhydrous THF and sealed, before being removed from the glovebox and being placed in a 34˚ °C oil bath. An oven-dried 7 mL vial was charged with **2.5b** (0.0228 g, 0.026 mmol) and 1 mL of anhydrous THF before being sealed and removed from the glovebox. The solution of **2.5b** was added to the 3-neck flask, followed by the immediate removal of a 0.2 mL aliquot of the reaction mixture which was quenched with 1 mL ethyl vinyl ether. The sample was split into 2 equal portions. GPC data was gathered on one portion and conversion was determined with the remaining.

Polymer-Polymer Molecular Weight Equilibrium

In a dry box, 71.5 kDa **poly(2.1)** (0.0788 g, 0.0011 mmol) and 15.2 kDa **poly(2.1)** (0.0167 g, 0.0011 mmol) were charged into a 2-dram vial followed by 0.512 mL of anhydrous THF. **2.5b** (0.00973 g, 0.0011 mmol) was added and the vial was removed from the dry box and placed into

40 °C oil bath. After 3.5 hours, the reaction was quenched with ethyl vinyl ether and diluted with THF before obtaining a crude GPC.

Polymer-trans-stilbene Molecular Weight Equilibrium

In a dry box, 41.5 kDa **poly(2.1)** (0.0748 g, 0.0018 mmol) was added to a 7 mL vial, followed by **2.5b** (0.0012 g, 0.002 mmol), *trans*-stilbene (0.024 g, 0.133 mmol) and 0.3 mL of anhydrous THF. The vial was placed in a 40 °C oil bath. After 3.5 hours the reaction was quenched with ethyl vinyl ether and diluted with THF before obtaining a crude GPC.

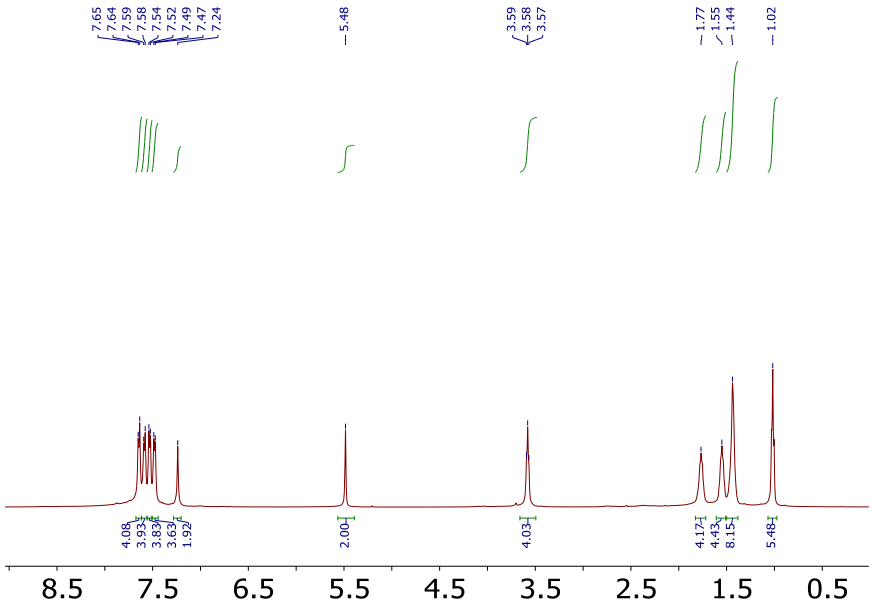

Figure 2.17 ^{1}H NMR spectrum for **poly(2.1)** in $CDCl_3$.

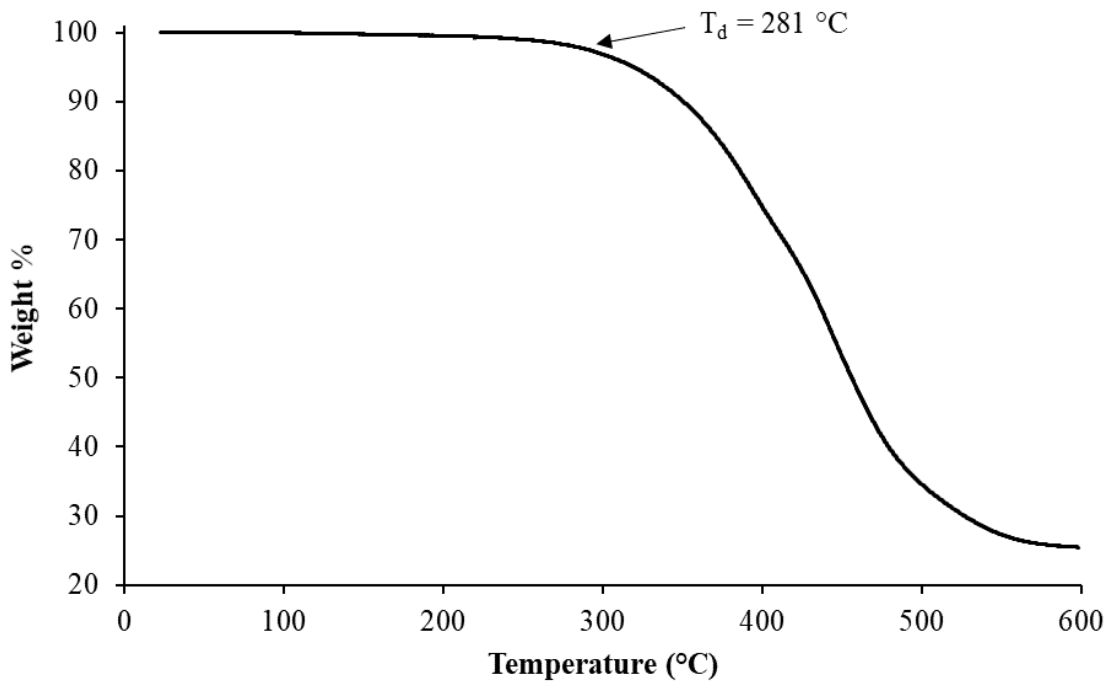

Figure 2.19 TGA trace for **poly(2.1)** under N_2 atmosphere.

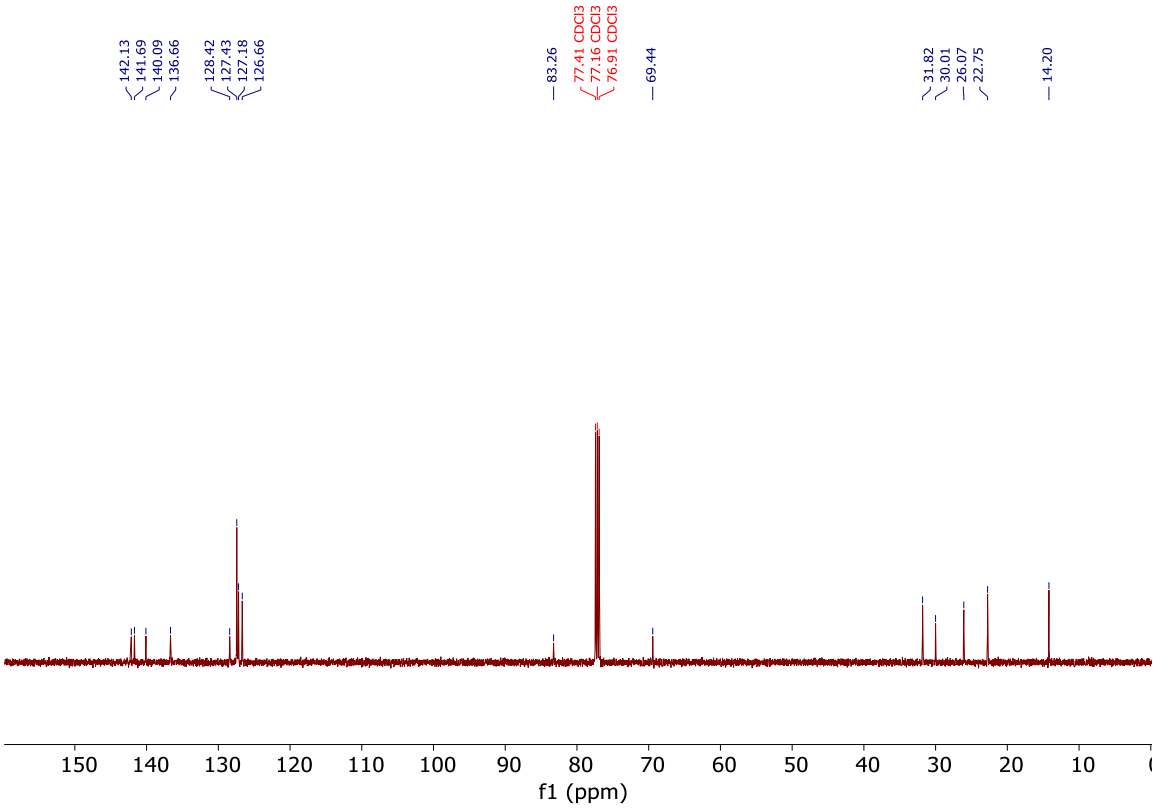

Figure 2.18 ^{13}C NMR spectrum for **poly(2.1)** in $CDCl_3$.

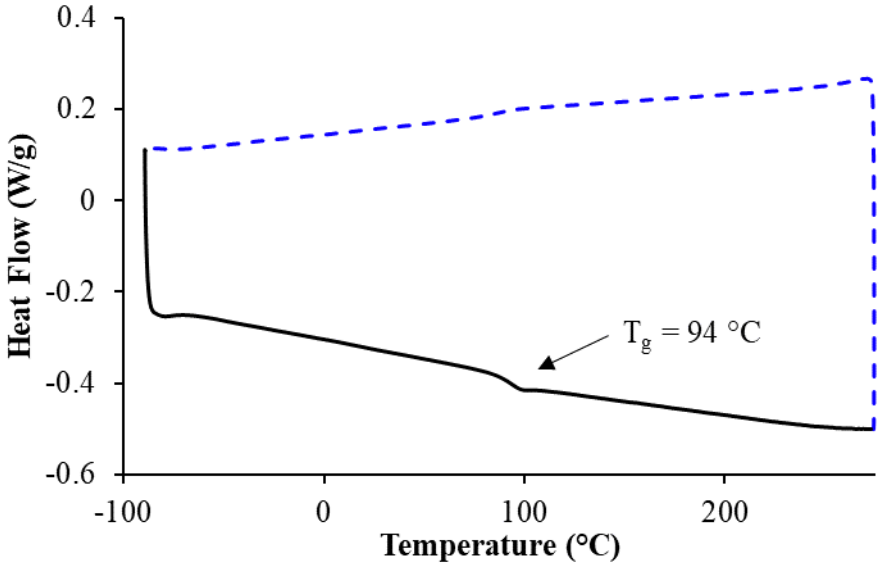

Figure 2.21 DSC trace for **poly(2.1)** showing the first cooling cycle (dashed blue) and second heating cycle (solid black).

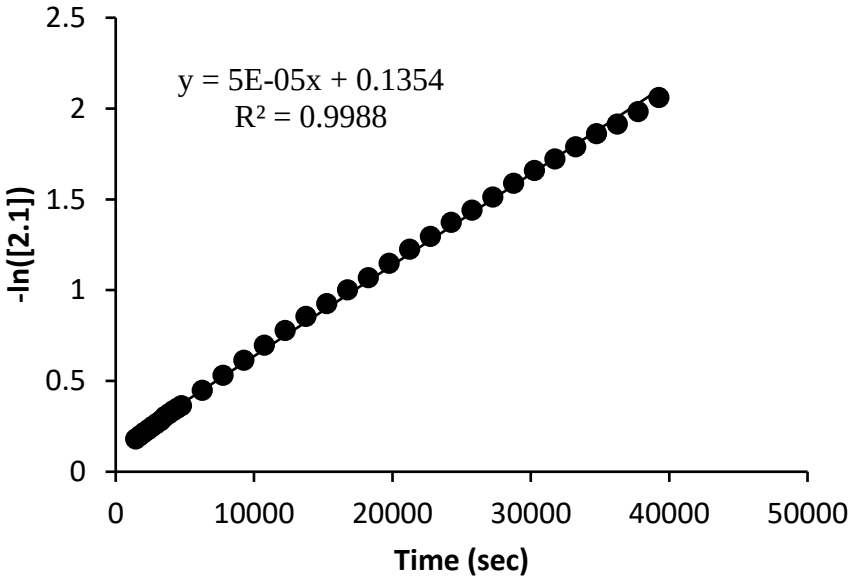

Figure 2.20 First order kinetics plot for the consumption of **2.1** over the course of the polymerization.

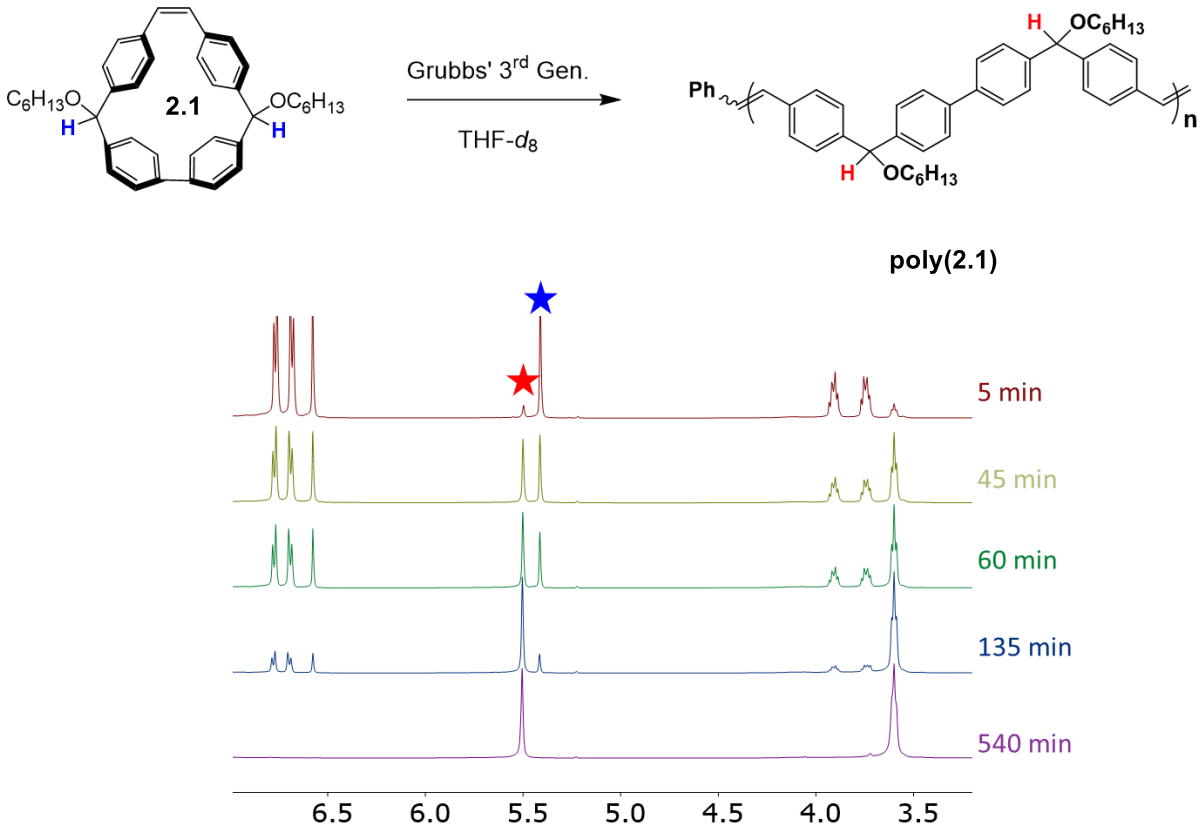

Figure 2.22 ^{1}H NMR spectra showing the progression of the polymerization. Conversion was determined following the transformation of the benzylic ether hydrogen from monomer (blue star) to polymer (red star).

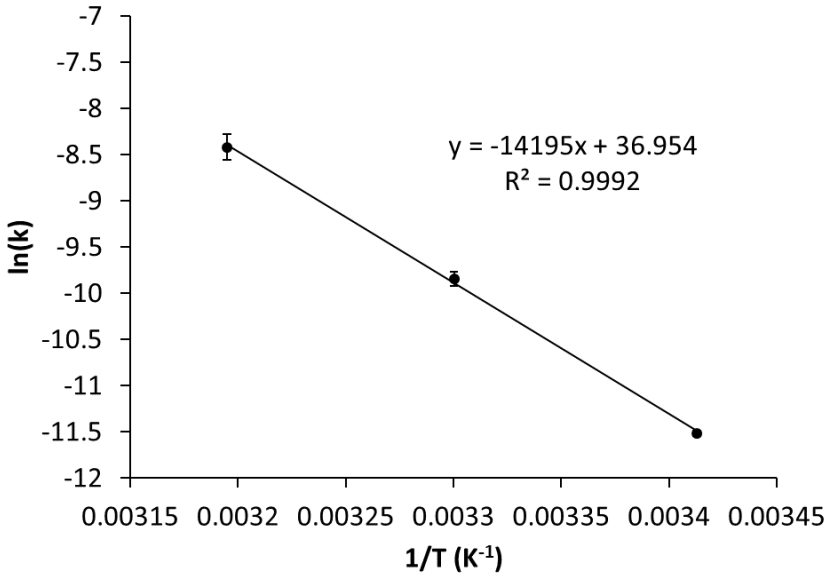

Figure 2.23 Arrhenius plot for the polymerization of **2.1** using **2.5b**

2.5.c. Strain Energy Analysis

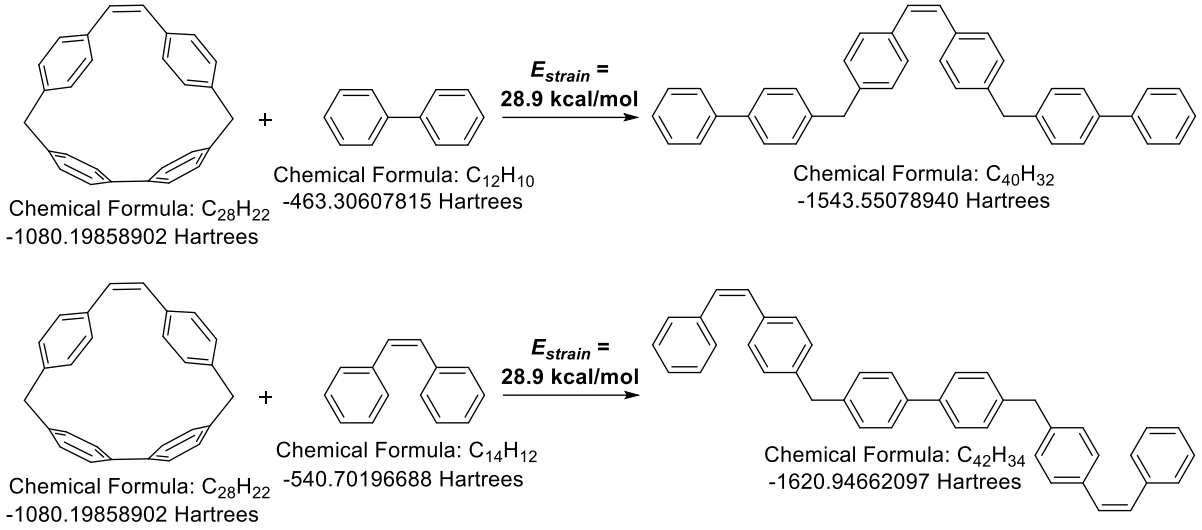

Figure 2.24 Homodesmotic reactions to estimate strain energy of model stilbene-based macrocycle (DFT at the B3LYP/6-31G* level of theory)

Cartesian Coordinates of Selected Compounds

Model macrocycle, *B3LYP/6-31G** (Energy = -1080.19858902 Hartrees)

C 0.674124 4.084744 -0.022638
H 1.158173 5.060458 -0.081984
C -0.674138 4.084744 0.022674
H -1.158187 5.060457 0.082025
C -1.602165 2.932470 -0.044895
C -2.727402 2.850887 0.791136
C -1.427702 1.911694 -0.996191
C -3.593280 1.754108 0.735773
H -2.910445 3.637928 1.519504
C -2.305813 0.837367 -1.065855
H -0.588822 1.965508 -1.683239
C -3.388489 0.715678 -0.179790
H -4.429524 1.701635 1.430103
H -2.119246 0.053528 -1.794066
C 1.602152 2.932470 0.044906
C 2.727386 2.850907 -0.791131
C 1.427697 1.911675 0.996183
C 3.593271 1.754131 -0.735790
H 2.910424 3.637962 -1.519485
C 2.305814 0.837353 1.065826
H 0.588820 1.965473 1.683236
C 3.388489 0.715685 0.179757

H 4.429513 1.701676 -1.430124
H 2.119256 0.053499 1.794024
C 4.224271 -0.571312 0.154792
H 4.800790 -0.680054 1.082553
H 4.945468 -0.519954 -0.669832
C -4.224263 -0.571326 -0.154844
H -4.800757 -0.680079 -1.082621
H -4.945483 -0.519966 0.669759
C 3.260491 -1.735722 -0.006945
C 2.551442 -1.875186 -1.207237
C 2.816292 -2.476528 1.095733
C 1.313984 -2.505415 -1.229694
H 2.896286 -1.354709 -2.097999
C 1.578953 -3.122991 1.072869
H 3.388242 -2.458264 2.021464
C 0.742391 -3.026196 -0.052213
H 0.716192 -2.444596 -2.133843
H 1.216383 -3.602969 1.978265
C -3.260484 -1.735730 0.006935
C -2.551440 -1.875156 1.207233
C -2.816280 -2.476572 -1.095718
C -1.313979 -2.505379 1.229714
H -2.896288 -1.354650 2.097978
C -1.578941 -3.123032 -1.072829
H -3.388228 -2.458339 -2.021451
C -0.742381 -3.026197 0.052252
H -0.716189 -2.444528 2.133863
H -1.216367 -3.603038 -1.978209

Biphenyl, *B3LYP/6-31G** (Energy = -463.30607815 Hartrees)

C 2.859818 -1.138669 0.396129
C 1.465728 -1.138008 0.396512
C 0.742860 -0.000022 -0.000011
C 1.465705 1.137995 -0.396510
C 2.859788 1.138687 -0.396130
C 3.563714 0.000011 -0.000008
H 3.397098 -2.028241 0.714723
H 0.928274 -2.020474 0.732601
H 0.928222 2.020452 -0.732577
H 3.397058 2.028268 -0.714715
H 4.650390 0.000030 -0.000010
C -0.742860 -0.000022 0.000008
C -1.465704 1.137995 0.396508
C -1.465729 -1.138010 -0.396508

C -2.859787 1.138685 0.396135
H -0.928220 2.020453 0.732574
C -2.859819 -1.138668 -0.396130
H -0.928276 -2.020476 -0.732597
C -3.563713 0.000013 0.000005
H -3.397056 2.028268 0.714719
H -3.397099 -2.028240 -0.714726
H -4.650389 0.000034 0.000004

Cis-stilbene, *B3LYP/6-31G** (Energy = -540.70196688 Hartrees)

C 0.674910 1.824300 0.000588
C -0.674824 1.824402 -0.000276
C 1.646718 0.716745 -0.066921
C -1.646726 0.716889 0.066986
C -1.416888 -0.466736 0.792638
C -2.390029 -1.460780 0.863310
C -3.617421 -1.297825 0.215155
C -3.868259 -0.122302 -0.494226
C -2.897418 0.875936 -0.557095
C 1.416519 -0.467196 -0.791951
C 2.389648 -1.461241 -0.862731
C 3.617389 -1.298005 -0.215307
C 3.868596 -0.122171 0.493427
C 2.897768 0.876067 0.556393
H 1.142026 2.808617 0.042497
H -1.141815 2.808792 -0.041880
H -0.474145 -0.598368 1.313119
H -2.192613 -2.364109 1.434794
H -4.374418 -2.075379 0.272520
H -4.823000 0.021390 -0.993474
H -3.102906 1.793942 -1.103222
H 0.473525 -0.599085 -1.311901
H 2.191935 -2.364813 -1.433730
H 4.374359 -2.075579 -0.272747
H 4.823610 0.021762 0.992083
H 3.103544 1.794314 1.102007

Open adduct 1, *B3LYP/6-31G** (Energy = -1543.55078940 Hartrees)

C 0.653514 2.520168 -0.168802
H 1.093602 3.505364 -0.325722
C -0.653697 2.520207 0.169602
H -1.093747 3.505422 0.326507
C 1.614377 1.416684 -0.346839
C 2.682354 1.586056 -1.248807

C 1.576513 0.225023 0.396407
C 3.643737 0.597443 -1.428629
H 2.750858 2.509378 -1.819852
C 2.544647 -0.761171 0.217093
H 0.790317 0.075732 1.129004
C 3.589118 -0.599961 -0.701612
H 4.456057 0.759891 -2.133149
H 2.489670 -1.673229 0.807843
C -1.614570 1.416725 0.347682
C -1.576919 0.225273 -0.395894
C -2.682279 1.585880 1.250007
C -2.545013 -0.760969 -0.216576
H -0.790900 0.076180 -1.128724
C -3.643616 0.597225 1.429828
H -2.750586 2.509038 1.821340
C -3.589222 -0.599981 0.702455
H -2.490193 -1.672888 -0.807557
H -4.455725 0.759471 2.134638
C 4.631576 -1.686378 -0.906839
H 4.572817 -2.058306 -1.938380
H 4.380151 -2.540257 -0.263664
C -4.631729 -1.686348 0.907647
H -4.573269 -2.058039 1.939283
H -4.380169 -2.540373 0.264719
C -6.061361 -1.249927 0.629650
C -6.425779 -0.728875 -0.620030
C -7.057740 -1.369504 1.604111
C -7.737717 -0.349842 -0.884893
H -5.671009 -0.621994 -1.395533
C -8.373466 -0.987263 1.343160
H -6.801880 -1.762788 2.585770
C -8.742105 -0.470239 0.092161
H -7.995843 0.023245 -1.872213
H -9.118080 -1.066791 2.130497
C 6.061281 -1.249966 -0.629295
C 6.426064 -0.728986 0.620309
C 7.057367 -1.369434 -1.604069
C 7.738070 -0.349936 0.884811
H 5.671518 -0.622184 1.396044
C 8.373162 -0.987181 -1.343481
H 6.801220 -1.762644 -2.585683
C 8.742168 -0.470254 -0.092550
H 7.996474 0.023099 1.872078
H 9.117544 -1.066634 -2.131047
C -10.141882 -0.063247 -0.191117
C -11.226020 -0.799633 0.316345

C -10.421189 1.069364 -0.975010
C -12.540271 -0.418038 0.050574
H -11.034752 -1.694100 0.902834
C -11.735124 1.450667 -1.242767
H -9.599869 1.669921 -1.356231
C -12.801342 0.708936 -0.730991
H -13.362124 -1.008300 0.447681
H -11.925867 2.334934 -1.845449
H -13.825633 1.006131 -0.939211
C 10.142023 -0.063263 0.190352
C 11.226022 -0.799622 -0.317444
C 10.421536 1.069304 0.974232
C 12.540345 -0.418039 -0.052004
H 11.034593 -1.694054 -0.903932
C 11.735543 1.450595 1.241657
H 9.600315 1.669832 1.355713
C 12.801623 0.708892 0.729551
H 13.362090 -1.008281 -0.449363
H 11.926446 2.334828 1.844338
H 13.825970 1.006076 0.937514

Open adduct 2, *B3LYP/6-31G** (Energy = -1620.94662097 Hartrees)

C 1.842009 -1.149871 1.346883
C 0.613058 -0.553376 1.065627
C 0.386371 0.095444 -0.157695
C 1.442754 0.122751 -1.086016
C 2.666952 -0.473750 -0.802326
C 2.889130 -1.124487 0.419804
H 1.983383 -1.655123 2.300061
H -0.189055 -0.615118 1.795963
H 1.309277 0.641889 -2.031173
H 3.470380 -0.420920 -1.533218
C -0.921161 0.728585 -0.462192
C -1.465468 0.687828 -1.754740
C -1.661747 1.387329 0.535861
C -2.695970 1.280936 -2.036260
H -0.933957 0.162772 -2.543640
C -2.890675 1.974124 0.252386
H -1.255927 1.459534 1.541222
C -3.430400 1.934376 -1.041196
H -3.094059 1.228230 -3.047452
H -3.440951 2.474133 1.046011
C 4.220217 -1.795637 0.717128
H 4.361955 -2.643369 0.033582
H 4.177429 -2.226605 1.726407

C -4.763476 2.594554 -1.352488
H -4.676348 3.679553 -1.206889
H -4.984835 2.450882 -2.418687
C 5.428609 -0.880173 0.610093
C 5.510774 0.298489 1.364528
C 6.496304 -1.187719 -0.242315
C 6.622868 1.128500 1.272420
H 4.687434 0.574346 2.019072
C 7.615144 -0.362144 -0.332417
H 6.449591 -2.087352 -0.852588
C 7.710335 0.810010 0.436549
H 6.658513 2.042490 1.861258
H 8.416459 -0.621490 -1.016143
C -5.931176 2.086319 -0.522947
C -6.721362 2.962917 0.227433
C -6.254199 0.720513 -0.491438
C -7.800658 2.494913 0.975881
H -6.488558 4.025687 0.230666
C -7.336022 0.251635 0.244438
H -5.636471 0.014014 -1.040765
C -8.146159 1.133468 0.986128
H -8.391872 3.196970 1.559727
H -7.551026 -0.811639 0.260177
C 8.838100 1.754636 0.347413
H 8.546888 2.791741 0.516236
C -9.270276 0.690783 1.830394
H -9.410016 1.304949 2.720422
C -10.129743 -0.342496 1.702104
H -10.808597 -0.491618 2.542182
C 10.145764 1.560072 0.073998
H 10.741583 2.467550 -0.027636
C 10.929562 0.321779 -0.094898
C 12.032890 0.332049 -0.967518
C 10.677832 -0.853463 0.636859
C 12.832309 -0.797505 -1.134734
H 12.257452 1.238878 -1.524672
C 11.482018 -1.979571 0.477324
H 9.854291 -0.875195 1.342942
C 12.558536 -1.960785 -0.413611
H 13.673121 -0.766354 -1.822850
H 11.272530 -2.874263 1.058094
H 13.183859 -2.841149 -0.535503
C -10.334360 -1.307436 0.605663
C -10.793275 -2.599887 0.919155
C -10.171006 -0.976823 -0.752398
C -11.042794 -3.539993 -0.079152

H -10.948052 -2.867170 1.962131
C -10.428478 -1.913175 -1.751022
H -9.853434 0.024845 -1.022363
C -10.858731 -3.201040 -1.420582
H -11.387376 -4.534954 0.190581
H -10.301136 -1.633277 -2.793644
H -11.058890 -3.928937 -2.202263

Notes and References for Chapter 2

(49) Nuyken, O.; Pask, S. D. *Polymers (Basel).* **2013**, *5* (2), 361–403.

(50) Unsal, H.; Onbulak, S.; Calik, F.; Er-Rafik, M.; Schmutz, M.; Sanyal, A.; Rzayev, J. *Macromolecules* **2017**, *50* (4), 1342–1352.

(51) Johnson, J. A.; Lu, Y. Y.; Burts, A. O.; Xia, Y.; Durrell, A. C.; Tirrell, D. A.; Grubbs, R. H. *Macromolecules* **2010**, *43* (24), 10326–10335.

(52) Hu, Y.; Li, X.; Lang, A. W.; Zhang, Y.; Nutt, S. R. *Polym. Degrad. Stab.* **2016**, *124*, 35–42.

(53) Wang, Y.; Zhang, L.; Sun, J.; Bao, J. B.; Wang, Z.; Ni, L. *Ind. Eng. Chem. Res.* **2017**, *56* (16), 4750–4757.

(54) Martinez, H.; Ren, N.; Matta, M. E.; Hillmyer, M. A. *Polym. Chem.* **2014**, *5* (11), 3507–3532.

(55) Chen, Z.; Mercer, J. A. M.; Zhu, X.; Romaniuk, J. A. H.; Pfattner, R.; Cegelski, L.; Martinez, T. J.; Burns, N. Z.; Xia, Y. *Science* **2017**, *357* (6350), 475–479.

(56) Elling, B. R.; Su, J. K.; Xia, Y. *Chem. Commun.* **2016**, *52* (58), 9097–9100.

(57) Binder, W. H.; Kurzhals, S.; Pulamagatta, B.; Decker, U.; Pawar, G. M.; Wang, D.; Kühnel, C.; Buchmeiser, M. R. *Macromolecules* **2008**, *41* (22), 8405–8412.

(58) Singh, R.; Czekelius, C.; Schrock, R. R. *Macromolecules* **2006**, *39*, 1316–1317.

(59) Wu, Z.; Grubbs, R. H. *Macromolecules* **1994**, *27* (23), 6700–6703.

(60) Lin, N. T.; Ke, Y. Z.; Satyanarayana, K.; Huang, S. L.; Lan, Y. K.; Yang, H. C.; Luh, T. Y. *Macromolecules* **2013**, *46* (18), 7173–7179.

(61) Leroux, F.; Pascual, S.; Montembault, V.; Fontaine, L. *Macromolecules* **2015**, *48* (12), 3843–3852.

(62) Yang, J.; Horst, M.; Romaniuk, J. A. H.; Jin, Z.; Cegelski, L.; Xia, Y. *J. Am. Chem. Soc.* **2019**, *141* (16), 6479–6483.

(63) Hodge, P. *Chem. Rev.* **2014**, *114*, 2278–2312.

(64) Tastard, C. Y.; Hodge, P.; Ben-Haida, A.; Dobinson, M. *React. Funct. Polym.* **2006**, *66*,

93–107.

(65) Xue, Z.; Mayer, M. F. *Soft Matter* **2009**, *5* (23), 4600–4611.

(66) Deng, L.-L.; Guo, L.-X.; Lin, B.-P.; Zhang, X.-Q.; Sun, Y.; Yang, H. *Polym. Chem.* **2016**, *7*, 5265–5272.

(67) Berrocal, J. A.; Pitet, L. M.; Nieuwenhuizen, M. M. L.; Mandolini, L.; Meijer, E. W.; Di Stefano, S. *Macromolecules* **2015**, *48* (5), 1358–1363.

(68) Yang, Y.; Swager, T. M. *Macromolecules* **2007**, *40* (21), 7437–7440.

(69) Short, A. L.; Fang, C.; Nowalk, J. A.; Weiss, R. M.; Liu, P.; Meyer, T. Y. *ACS Macro Lett.* **2018**, *7* (7), 858–862.

(70) Swisher, J. H.; Nowalk, J. A.; Meyer, T. Y. *Polym. Chem.* **2019**, *10* (2), 244–252.

(71) Hoye, T. R.; Jeffrey, C. S.; Tennakoon, M. A.; Wang, J.; Zhao, H. *J. Am. Chem. Soc.* **2004**, *126* (33), 10210–10211.

(72) Miao, Y.-J.; Bazan, G. C. *Macromolecules* **1994**, *27*, 1063–1064.

(73) Spring, A. M.; Yu, C.-Y.; Horie, M.; Turner, M. L. *Chem. Commun.* **2009**, No. 19, 2676–2678.

(74) Yu, C.-Y.; Kingsley, J. W.; Lidzey, D. G.; Turner, M. L. *Macromol. Rapid Commun.* **2009**, *30* (22), 1889–1892.

(75) Elacqua, E.; Gregor, M. *Angew. Chem. Int. Ed* **2019**, *58* (28), 9527–9532.

(76) Chang, S.-W.; Horie, M. *Chem. Commun.* **2015**, *51* (44), 9113–9116.

(77) Komanduri, V.; Tate, D. J.; Marcial-Hernandez, R.; Kumar, D. R.; Turner, M. L. *Macromolecules* **2019**, *52* (18), 7137–7144.

(78) Ring strain calculated to be 28.9 Kcal/mol.

(79) Schönbein, A. K.; Wagner, M.; Blom, P. W. M.; Michels, J. J. *Macromolecules* **2017**, *50* (13), 4952–4961.

(80) Burroughes, J. H.; Bradley, D. D. C.; Brown, A. R.; Marks, R. N.; Mackay, K.; Friend, R. H.; Burns, P. L.; Holmes, A. B. *Nature* **1990**, *347*, 539–541.

(81) Ballard, D. G. H.; Courtis, A.; Shirley, I. M.; Taylor, S. C. *Macromolecules* **1988**, *21* (2), 294–304.

(82) Abdulkarim, A.; Strunk, K. P.; Bäuerle, R.; Beck, S.; Makowska, H.; Marszalek, T.; Pucci, A.; Melzer, C.; Jänsch, D.; Freudenberg, J.; et al. *Macromolecules* **2019**, *52* (12), 4458–4463.

(83) Attwood, T. . E. E.; Dawson, P. C.; Freeman, J. L.; Hoy, L. R. J. . J.; Rose, J. B.; Staniland, P. A. *Polymer (Guildf).* **1981**, *22* (8), 1096–1103.

(84) Papadimitrakopoulos, F.; Konstadinidis, K.; Miller, T. M.; Opila, R.; Chandross, E. A.; Galvin, M. E. *Chem. Mater.* **1994**, *6* (9), 1563–1568.

(85) Louwet, F.; Vanderzande, D.; Gelan, J.; Mullens, J. A New Synthetic Route to a Soluble High Molecular Weight Precursor for Poly(p-Phenylenevinylene) Derivatives. *Macromolecules*. UTC 1995, pp 1330–1331.

(86) Junkers, T.; Vandenbergh, J.; Adriaensens, P.; Lutsen, L.; Vanderzande, D. *Polym. Chem.* **2012**, *3* (2), 275–285.

(87) Darzi, E. R.; White, B. M.; Loventhal, L. K.; Zakharov, L. N.; Jasti, R. *J . Am. Chem. Soc.* **2017**, *139*, 3106–3114.

(88) Xu, Y.; Xu, W. L.; Smith, M. D.; Shimizu, L. S. *RSC Adv.* **2014**, *4*, 1675–1682.

(89) Adhikary, R.; Barnes, C. A.; Trampel, R. L.; Wallace, S. J.; Kee, T. W.; Petrich, J. W. *J. Phys. Chem. B* **2011**, *115*, 10707–10714.

(90) Linseis, M.; Záliš, S.; Zabel, M.; Winter, R. F. *J. Am. Chem. Soc.* **2012**, *134*, 16671–16692.

(91) Love, J. A.; Morgan, J. P.; Trnka, T. M.; Grubbs, R. H. *Angew. Chem. Int. Ed* **2002**, *41* (21), 4035–4037.

Chapter 3. Using 1,2-Oxazines to synthesize Covalent Adaptable Networks

3.1 Abstract

We report the synthesis of monomers for use in covalent adaptable networks using 1,2-oxazeines. Initial attempts at synthesizing the monomers consisted of a tris-anthracene species conjugated to both an aromatic core and branched alkyl chain as the 1,3-diene. We also report the synthesis of bis-amide, bis-carbonate, and bis-carbamate hydroxamic acid and 1,2-oxazine derivatives. Initial attempts at synthesizing the network with the aromatic diene has proven to be challenging due to the incompatible solubilities of the monomers.

3.2 Introduction

The consumption of polymer based materials has increased dramatically over the past few years and will continue to do so, it is expected that by 2039 the annual plastic production will be over 1000 million tons.[92] The increase in production over time will also result in an increase in plastic waste that will be produced. Recycling of these plastic materials is typically achieved in one of three routes; reusing, mechanical recycling, or chemical recycling.[93,94] Many of the plastics used in our day to day lives are thermosets, which consist covalently crosslink polymer chains, that lose the ability to flow once thermally crosslinked. Covalent adaptable networks (CANs) have the potential to maintain these covalent crosslinks between polymer chains while being more amenable to chemical recycling. CANs are formed through covalent crosslinks that are reversible when the correct stimulus is applied.[95] Thus, enabling the networks to have materials properties and chemical stability similar to those of thermosets while also being chemically recyclable.

Pericyclic reactions have shown promise for use in CANs. One advantage of pericyclic reactions is that they are click-reactions or reactions that are high yielding and produce no biproducts, of particular interest is the Diels-Alder reaction. The first example of a CAN using the Diels-Alder reaction was demonstrated by Wudl et. al. in 2002. In their report they used the Diels-Alder reaction between furan and maleimide (**Figure 3.1A**).[96] The material they synthesized was able to recover after being damaged by heating the network to 145 °C under an inert atmosphere. Since this initial demonstration furan-maleimide Diels-Alder has been used to synthesize many different networks, and has utilized linkers such as poly(ethylene glycol), poly(lactic acid), long chain hydrocarbons, and unsaturated hydrocarbons in applications such as 3D-printed materials, healable and shape memory materials.[14,17,18,28,97–99]

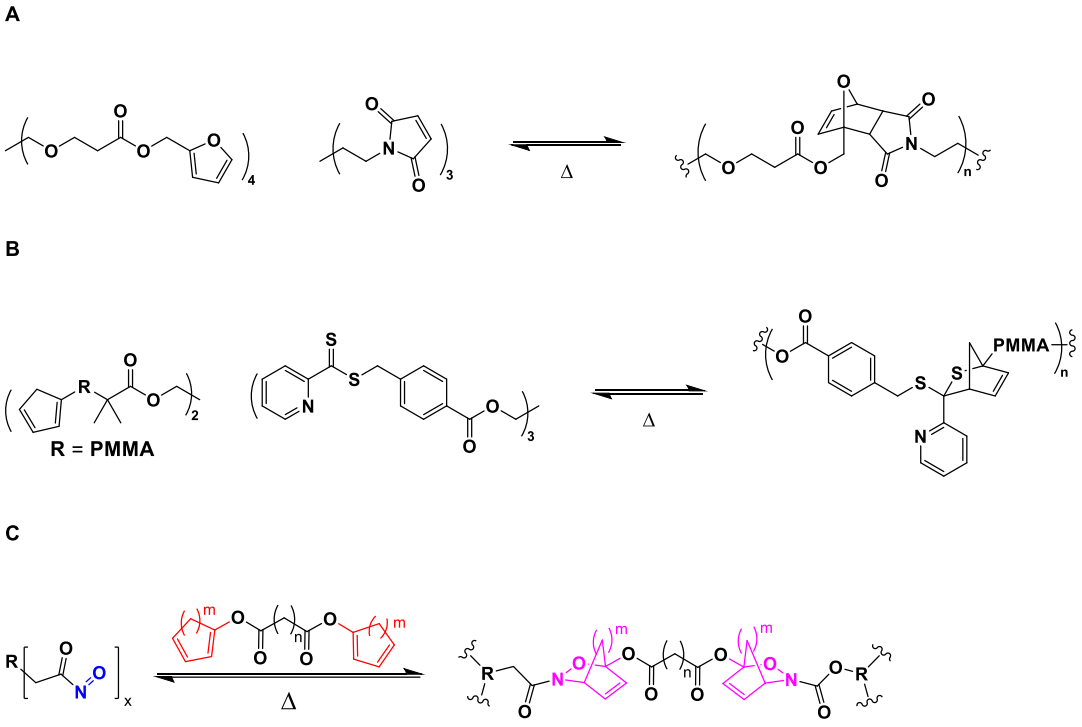

Figure 3.1 A) Furan-maleimide Diels-Alder reaction used in the synthesis of a covalent adaptable network by Wudl et. al. B) Hetero-Diels-Alder reaction between thiocarbonyl and cyclopentadiene terminated poly(methyl methacrylate). C) General scheme for the synthesis of a CAN using 1,2-oxazines.

Two other examples of Diels-Alder adducts have been used to make polymer networks. The first being the hetero-Diels-Alder reaction between a thiocarbonyl and a 1,3-diene (**Figure 3.1B**). In these publications the authors synthesized networks using linkers such as carbonates and poly(acrylates), to achieve materials that could be depolymerized when heated to 80-120 °C.[100,101] The only other Diels-Alder adduct that has been used in the synthesis of polymer networks is anthracene and maleimide.[102] However, unlike the previous two examples, this adduct is not thermally reversible but mechanochemically reversible, but the network can reform by thermally inducing the Diels-Alder reaction

1,2-oxazines can expand the capabilities for pericyclic reactions in CANs (**Figure 3.1C**). 1,2-oxazines have been shown to be readily reversible at temperatures ranging from 27 °C to over 80 °C.[103] This temperature range is enabled by changing the 1,3-diene and the dienophile used to synthesize 1,2-oxazines. In early examples using substituted nitrosobenzene derivatives authors would have to perform reactions and purifications at very low temperatures (-70 °C) to prevent decomposition.[104] When the aryl-nitroso is replaced with acyl and cyano-nitroso compounds the stability of the 1,2-oxazines increases allowing them to be synthesized closer to ambient temperature. Kirby et. al. demonstrated this characteristic using 1,3-dienes such as 9,10-dimethylanthracene, thebaine, ergosterol acetate, 1,3-cyclohexadiene and 1,3-cyclopentadiene.[105–107]

Two groups have investigated how the structure of the nitroso dienophile impacts the rates of the retro-Diels-Alder reaction. The first study was done by King et. al. in 2000, they investigated the impact of changing both the electronics and sterics around a nitroso carbamide has on the rate of diene exchange between 9,10-dimethylanthracene and 1,3-cyclohexadiene.[108] In their work they showed that by changing from a hydroxyurea to an N-phenyl-N’-nitrosocarbamide, the half-life of

the diene exchange at 40 °C decreases from 2.6 hours to 0.26 hours. They also hypothesized that altering the electronics of the aryl substituent could further impact the half-life of the diene exchange, however both *para*-OMe, and *para*-NO_2 substitutions decreased the rate of the retro-Diels-Alder reaction compared to *para*-H, suggesting that electronics alone do not control the rate of the retro-Diels-Alder reaction; and the increase in decomposition rate is related to the increase in steric bulk from the aryl substituents.

The influence of dienophile on the rate of the retro-Diels-Alder reaction was further studied in 2016 by the Boydston group.[103] In their work they compared the rate of isomerization of a carbamate, an amide, and two carbamide nitroso dienophiles with a 1,2,3,4,5-pentmethylcyclopenta-1,3-diene derivative. Again, no obvious trend based on electronics was observed, however there was a distinct change in the rates of isomerization for the different dienophiles. The slowest of the dienophile was the amide derivative, which did not reach equilibrium at 37 °C after 11 days. While the unsubstituted carbamide derivative reached full equilibrium in less than 10 days. This rate difference was even more pronounced at 80 °C, where the unsubstituted carbamide reached full conversion within 3 hours while the amide derivative was still approaching equilibrium after 4 hours.

Unlike the extensive studies performed on how dienophiles impact the retro-Diels-Alder reaction of 1,2-oxazines, information about the impact of 1,3-dienes is limited. Work has been published performing diene exchange reactions between two or three dienes, or investigations into the stability of a small number (2 or 3) Diels-Alder adducts with different dienes, but the work ends there. For example comparing the stabilities of 1,2-oxazines synthesized from aryl-nitroso species synthesized using both 1,3-cyclopentadiene and 1,3-cyclohexadiene, the former could be isolated and stored at room temperature while the latter readily underwent the retro-Diels-Alder

reaction at the same temperature.[104] Furthermore, there have been several examples using 1,2-oxazine adducts synthesized with 9,10-dimethyl anthracene and performing a diene exchange reaction with a 1,3-cyclohexadinene, thebaine, *trans,trans*-1,4-phenyl-1,3-butadiene, cyclopentadiene, and 1,3-cyclohexadiene.[105,106,109,110]

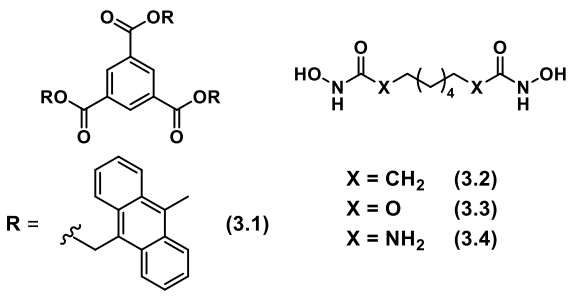

Figure 3.2 Proposed monomers for the CAN.

The diversity of the thermal reversibility of inspired us to use 1,2-oxazines for the synthesis of CANs enabling CANs to have much broader range of accessible temperatures. To investigate the use of 1,2-oxazines we proposed synthesizing these networks via a step-growth polymerization using two separate monomer classes (dienes/dienophiles) (**Figure 3.2**). We chose to work with anthracene as the diene because it is the most reactive diene for the retro-Diels-Alder reaction at the low temperatures . While carbamide, carbamate, and amide hydroxamic acid derivatives were

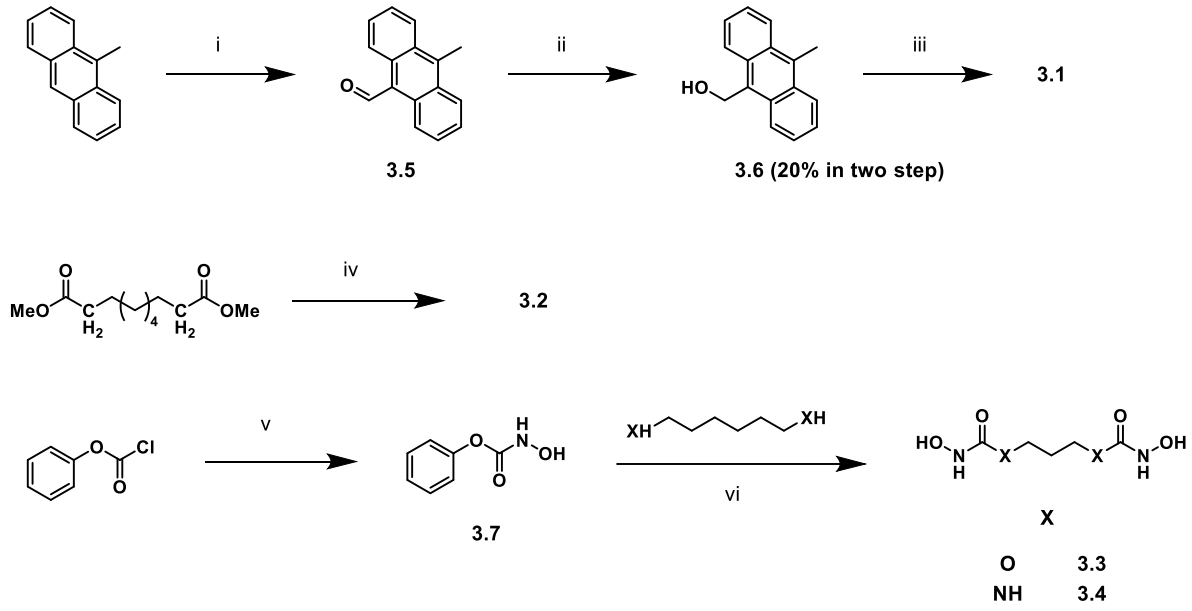

Figure 3.3 Synthetic scheme CAN monomers. i) $POCl_3$, N-methylformanalide, 100 °C. ii) $NaBH_4$, EtOH. iii) 1,3,5-benzenetricarbonyl trichloride, 4-dimethylaminopyridine. iv) NH_2OH•HCl, Na_2CO_3. v) NH_2OH•HCl, K_2CO_3. vi) Et_3N, CH_2Cl_2.

chosen as dienophiles in this system to form the Diels-Alder adducts; we chose these adducts because their impact on the retro-Diels-Alder reaction has been previously studied and can help us understand how changing the stability of the adduct impact the CAN.

3.3 Results and Discussion

Initially we proposed the synthesis of trimeric anthracene species **3.1** (**Figure 3.3**). We chose 1,3,5-benzenetricarbonyl trichloride as our core as it should be more electrophilic compared to acyl derivatives, allowing for poorer nucleophiles to be used, such as **3.3**, to be used. To synthesize **3.3** we modified a previously reported procedure, briefly 9-methylanthracene was oxidize to the aldehyde using $POCl_3$, and N-methyformanalide to yield **3.5**.[111] Which was then reduced using $NaBH_4$ to produce **3.6** in moderate yields (20% over two steps). A test reaction was

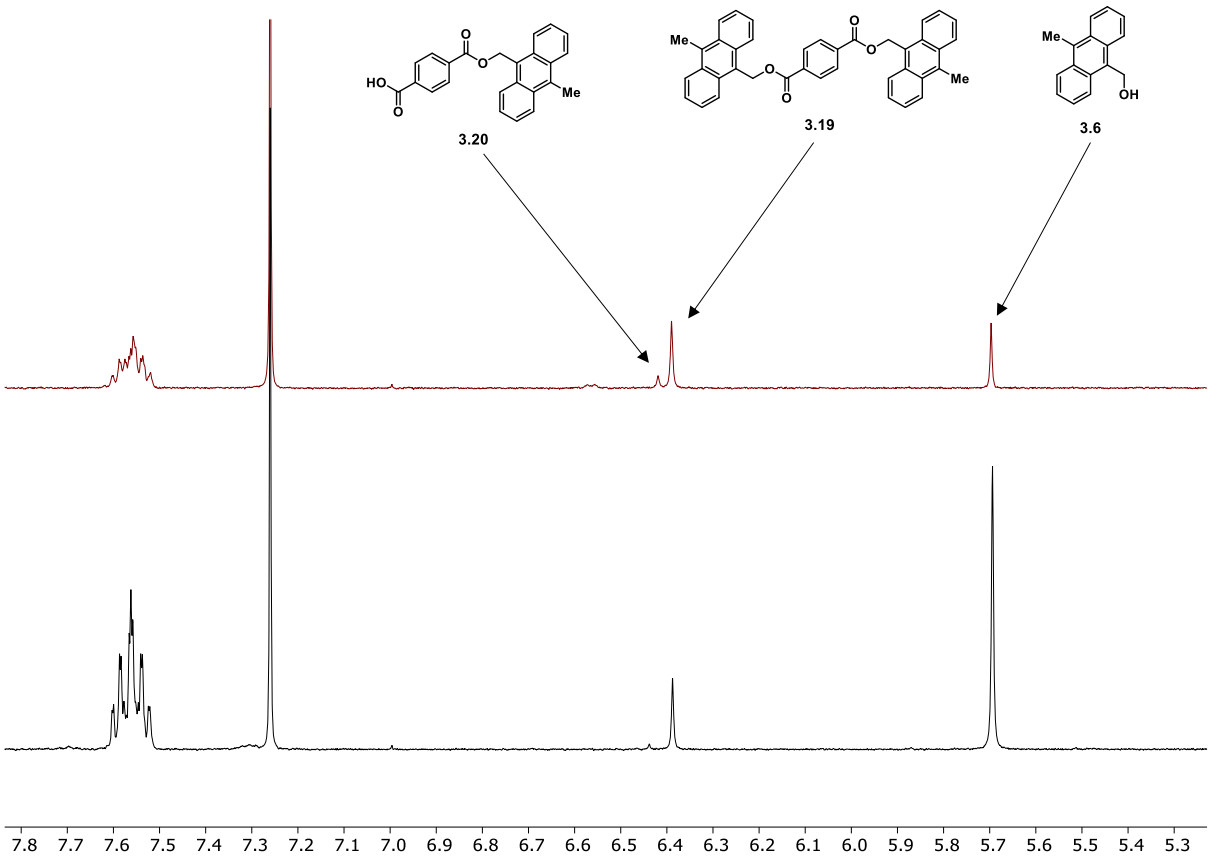

Figure 3.4 ^{1}H NMR spectrum for the conversion for the synthesis of **3.19** using 0.2 eq. pyridine (bottom) and 2.0 eq. pyridine (top).

Table 3.1 Reaction Optimization for hydroxamic acid synthesis

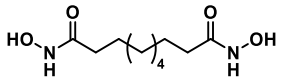

3.2

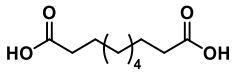

3.10

entry	solvent	base	SM[a]:3.2:3.10
1	MeOH	NaOH	0.08:1:0.08
2	MeOH	Na_2CO_3	0.09:1:0
3	MeOH:H_2O	NaOMe	0.09:1:0.41
4	MeOH:H_2O	NaOH	0.05:1:0.54
5	MeOH:H_2O	Na_2CO_3	0.09:1:0.12

[a] Remaining dimethyl ester

done using 1,4-benzenedicarboynyl dichloride to synthesize **3.19** using **3.6** triethylamine and catalytic 4-dimethylaminopyridine (DMAP) resulted in low conversion by ^{1}H NMR spectroscopy (20%). We noticed that as we increased the amount of DMAP relative to 1,4-benzenedicarboynyl dichloride there was a noticeable increase in the conversion to **3.19** from 20% to 61% (**Figure 3.4**). When the conditions were applied to the synthesis of **3.1** increasing the amount of DMAP to 3 times that of 1,3,5-benzenetricarbonyl trichloride we achieved high conversion of **3.1** (>99%).

The first targeted dienophile was the amide derived hydroxamic acid **3.2**. Initial attempts involved the reaction with adipoyl chloride and hydroxylamine hydrochloride. However, the reaction was messy, resulting in a mixture of the hydroxamic acid, carboxylic acid, and the cyclized N-hydroxy adduct. Switching the condition from adipoyl chloride to dimethyl sebacate and using aqueous hydroxylamine gave **3.2** in a yield of 120%, the high yield is due to excess NaCl that could not be separated from the product. However, a substantial amount of carboxylic acid (**3.10**, 10%) was also present in the product, and separation of the two products was difficult due to similarities in polarity. We next attempted to optimize the reaction using 3 different bases (Na_2CO_3, NaOH, NaOMe), in methanol with varying amounts of H_2O as a cosolvent, the results for this screening can be seen in **Table 3.1**. When using anhydrous methanol and Na_2CO_3, we were able to achieve 90% conversion of the ester to the hydroxamic acid and no conversion of the carboxylic acid (**3.10**). Similar results were also achieved by using NaOH as the base, however

these results were not repeatable and the amount of carboxylic acid (**3.10**) and hydroxamic acid (**3.2**) changed on subsequent runs.

With the difficulty to obtain pure **3.2**, we next attempted the synthesis of the carbamate and carbamide hydroxamic acid derivatives (**3.3** and **3.4** as shown in **Figure 3.3**). To achieve this, we first synthesized phenyl N-hydroxycarbamate (**3.7**) from phenyl chloroformate and hydroxylamine. The synthesis of the carbamate **3.3** was carried out using NaH in THF. However, when the same conditions were applied to 1,6-hexanediamine no conversion was achieved. This is potentially due to the poor solubility of the urea adducts, as there was a large amount of precipitate forming over the course of the reaction. To help with the solubility we synthesized 1,2-oxazine (**3.11**) from **3.7** with dicyclopentadiene and tetrabutylammonium periodate (**Figure 3.5**). The resulting oxazine (**3.11**) was reacted with 1,6-diaminohexane and triethylamine to yield bis-oxazine (**3.12**). Using **3.2** and **3.3** along with 1,3-cyclopentadiene and tetrabutylammonium periodate we were also able so synthesize their 1,2-oxazine counterparts (**3.13** and **3.14**) using the same conditions.

Having synthesized both the dienes and dienophiles for the polymer network we next attempted to synthesize the networks (**Figure 3.6**). Initial attempts to synthesize the network

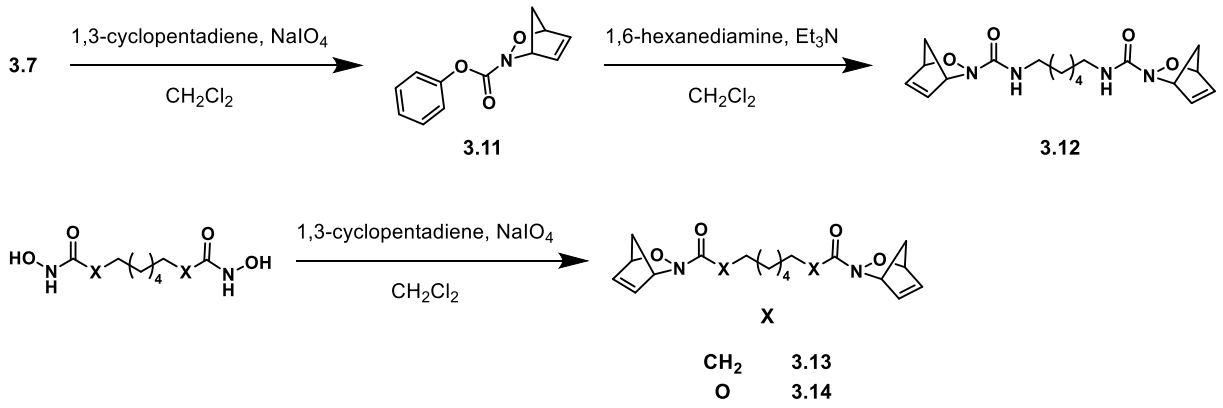

Figure 3.5 Synthesis of bis-oxazine **3.12** from phenyl N-hydroxycarbamate and bis-oxazines **3.13** and **3.14** from their corresponding hydroxamic acids.

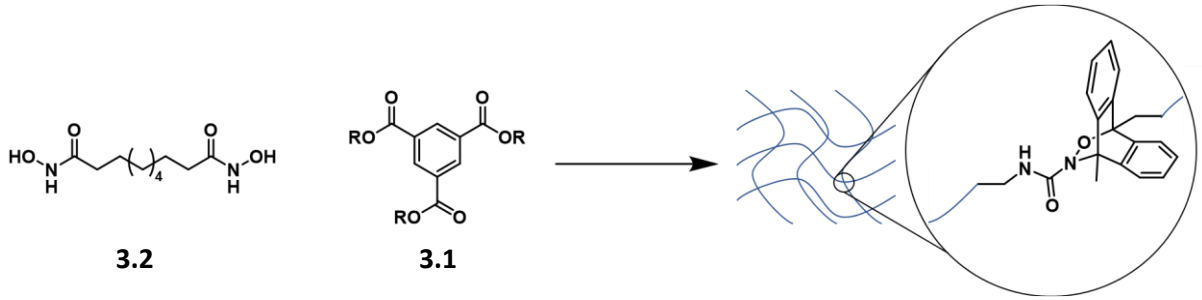

Figure 3.6 Cartoon depiction for the synthesis of the CAN using **3.2** and **3.1**.

utilized compounds **3.1** and **3.2** as the amide derivatives should form the most stable of the networks. However, after trying several different oxidants ($NaIO_4$, tBu_4NIO_4, iodobenzene diacetate) and solvents (CH_2Cl_2, MeOH, THF, 1,2-dichloroethane, chlorobenzene) as well as different combinations of these solvents, along with elevated temperatures for extended periods of time ultimately, we were unsuccessful. It is possible that small quantities of the network were formed, however due to the extremely poor solubilities of the starting materials we were unable to discern starting material from any new network if any had formed. Tris-anthracene **3.1** was very insoluble in most solvents, with halogenated solvents working best (CH_2Cl_2, 1,2-dichloroethane). While hydroxamic acid **3.2** was only soluble in solvents that could undergo hydrogen bonding (MeOH, THF).

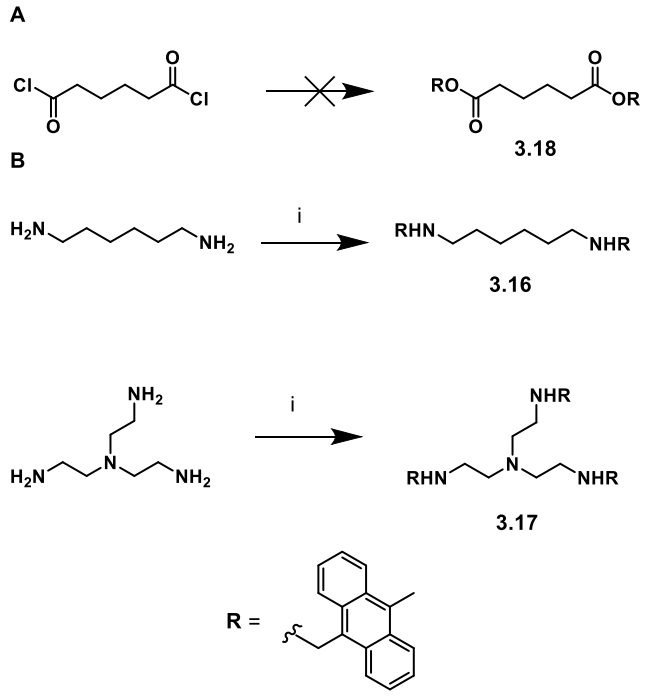

Figure 3.7 A) Unsuccessful synthesis of **3.18**. B)Synthesis of less rigid dienes **3.16** and **3.17** via reductive amination. i) 1) CH_2Cl_2 2) $NaBH_4$

To overcome this problem, we pursued using the bis-oxazine species to synthesize the networks by forming the

nitroso intermediate in situ via the retro-Diels-Alder reaction. To this end we first wanted to investigate the decomposition of various 1,2-oxazines. By ^{1}H NMR we saw significant decomposition of both oxazines **3.13** and **3.14** in 24 hours at 100 °C (**Figure 3.20**). As it should be the least stable of the derivatives, we did not investigate the decomposition of **3.12**. When attempting to synthesize the networks from these bis-oxazine species however we still ran into solubility issues. While **3.13** and **3.14** were readily soluble in halogenated solvents we were unable to find conditions to fully solubilize **3.1** and were unable to determine if any network formed after heating the materials to 100 °C for 24 hours and allowing them to cool for 5 days.

The next route we tried was to change the structure of the 1,3-diene. The aromatic core for **3.1** can inhibit the solubility of the anthracene species, as such we hypothesized that by changing to a longer alkyl chain linking the anthracene species, we would be able to increase its solubility. We first targeted bis-anthracene (**3.18**) that could be synthesized from adipoyl chloride and **3.6** however no ester was formed during the reaction even after refluxing in pyridine for several days (**Figure 3.7A**). As such we decided to pursue using the anthracene species as an electrophile rather than a nucleophile for synthesizing the dienes. To this end we targeted compounds **3.16** and **3.17** that could be synthesized via reductive amination (**Figure 3.7B**). We found that high conversion of dimeric anthracene species **3.16** could be achieved using 2 equivalencies of anthracene to 1,6-hexanediamine. However, for similar results to be achieved with **3.17**, 3 Å molecular sieves needed to be added. No attempts have been made to use these dienes to synthesize the networks yet.

3.4 Conclusions

1,2-oxazines have the potential to greatly increase the capabilities of covalent adaptable networks. Unlike many of the current examples of reversable networks 1,2-oxazines have the potential to create a diverse selection of networks that respond differently across a range of

temperatures. We demonstrated the synthesis of three different bis-1,2-oxazines and their corresponding hydroxamic acids. Furthermore, we demonstrated the synthesis of two different anthracene containing diene compounds for the synthesis of CANs. Due to solubility limitations the aromatic centered anthracene species did not form any detectable networks, and no attempts have been yet made to use the aliphatic cores.

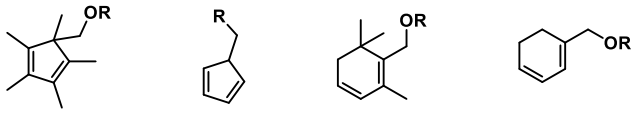

Figure 3.8 1,3-dienes of interest for future studies.

3.5 Future Directions

Overcoming the issues with competing solubilities is going to be the major hurdle to working with the anthracene dienes. Going forward there are two pathways that could be used to overcome this. The first possibility is to drastically alter the linking component of both the diene and dienophile. By incorporating branched alkanes onto the 1,3-diene could help increase its solubility. The approach could be moving away from 9-methylanthracene as the 1,3-diene, and towards more soluble anthracene derivatives or to other 1,3-dienes completely.[112] Some examples of these dienes can be easily synthesized from commercially available starting materials in a single step, such as 1,2,3,4,5-pentamethyl-5-methanolcyclopentadiene or safranol (**Figure 3.8**).

Eventually both changes will have to be made to show reach the full capabilities of 1,2-oxazines. Furan-maleimide Diels-Alder is used in many applications all of which are done in materials that must operate within a specific temperature profile. Construction of 1,2-oxazines could allow the synthesis of polymer networks that were previously thought to be impossible because of their thermal limitations, both at much lower and higher temperatures.

3.6 Experimental

3.6.a General Considerations

^{1}H and ^{13}C NMR spectral data were recorded on Bruker Avance III 500 and Bruker Avance III 400 spectrometers. ^{1}H NMR chemical shifts for spectra collected in $CDCl_3$ or DMSO-d_6 are referenced to TMS (d = 0.00 ppm) or residual solvent peaks DMSO (d = 2.50 ppm), and $CDCl_3$ (d 7.26 ppm). ^{13}C NMR chemical shifts of spectra collected in $CDCl_3$ or DMSO-d_6 are referenced to the shifts of the carbon in $CDCl_3$ (d = 77.16 ppm) or DMSO-d_6 (d = 39.52 ppm). ^{1}H resonance data are reported as the following format: chemical shift in ppm [multiplicity, coupling constant(s) (J in Hz), and integration].

Reactions requiring anhydrous or air-free conditions were performed in the flame-dried glassware under a nitrogen or argon atmosphere. Reported reaction temperatures are the temperature of the external heating bath. Triethylamine was distilled from CaH_2 and stored in a Schlenk flask. Anhydrous solvents were collected from a solvent purification system prior to use. All other reagents were purchased from commercial sources and used as received unless otherwise specified.

3.6.b Synthetic Procedures

10-methylanthracene-9-carbaldehyde (**3.5**)

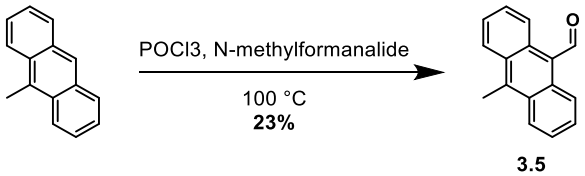

3.5

To a flame-dried N_2 purged 200 mL round bottom flask 9-methylanthracene (6.0 g, 31.2 mmol, 1.0 eq.) was added with a magnetic stir bar. Then N-methyl-N-phenylformamide (7.7 mL, 62.4 mmol, 2.0 eq.) and $POCl_3$ (5.1 mL, 54.6 mmol, 1.75 eq.) were added before being placed in a preheated 100 °C oil bath. After 60 minutes, 100 mL of 2 M sodium acetate was added. And the reaction was allowed to stir for an additional 30 minutes. The resulting slurry was filtered and

washed with DI H_2O. The crude solid was purified by recrystallization from acetic acid to yield an orange solid (1.6 g, 25 %). ^{1}H NMR (400 MHz, $CDCl_3$) δ 11.51 (s, 1H), 9.00 (dt, J = 9.0, 1.0 Hz, 2H), 8.41 (dt, J = 8.8, 1.0 Hz, 2H), 7.68 (ddd, J = 8.9, 6.5, 1.3 Hz, 2H), 7.59 (ddd, J = 8.9, 6.5, 1.3 Hz, 2H), 3.20 (s, 3H).

(10-methylanthracen-9-yl)methanol (**3.6**)

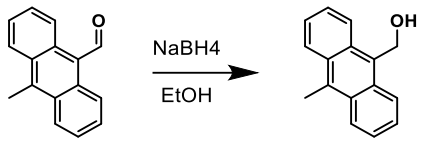

3.5 **3.6**

To a 200 mL round bottom flask was added **3.5** (1.8 g, 8.17 mmol, 1.0 eq.) and ethanol (73 mL). Then sodium borohydride (0.613 g, 16.3 mmol, 2.0 eq.) was added portion wise. The reaction was monitored by TLC (80:20 hexanes : ethyl acetate) until no starting material remained. The reaction color would change from orange to yellow when the reduction completed. The resulting yellow slurry was poured into 200 mL DI H_2O before being filtered and washed with water. The crude solids were recrystallized from toluene to yield **3.6** (1.48 g, 81%) as thin yellow crystals. ^{1}H NMR (400 MHz, $CDCl_3$) δ 8.47 (dd, J = 8.0, 1.6 Hz, 2H), 8.39 – 8.34 (m, 2H), 7.57 (dtt, J = 13.4, 6.5, 3.2 Hz, 4H), 5.69 (d, J = 5.5 Hz, 2H), 3.14 (s, 3H), 1.68 (t, J = 5.6 Hz, 1H). ^{13}C NMR (126 MHz, $CDCl_3$) δ 132.22, 130.16, 130.14, 129.64, 126.11, 125.60, 125.17, 124.64, 57.78, 14.59.

tris((10-methylanthracen-9-yl)methyl) benzene-1,3,5-tricarboxylate (**3.1**)

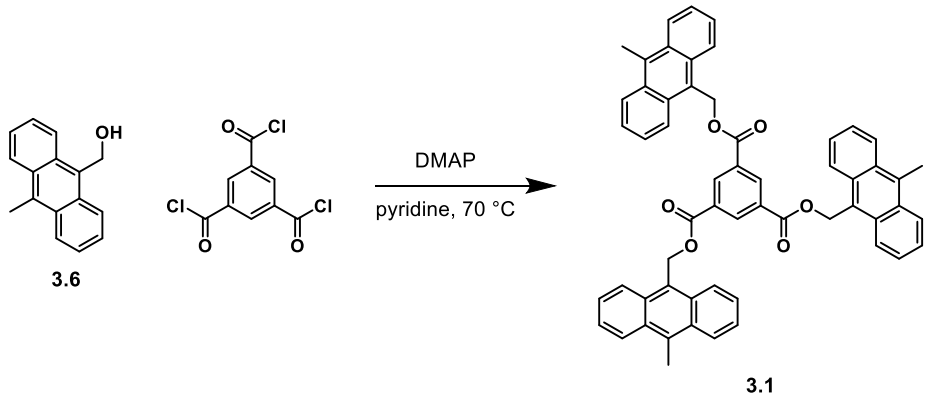

3.6 **3.1**

A flame-dried 25 mL round bottom flask equipped with a reflux condenser was added purged **3.6** (0.600 g, 2.70 mmol, 3.1 eq.), DMAP (0.351 g, 2.87 mmol, 3.3 eq.), and pyridine (10.8 mL) under N_2. Then 1,3,5-benzenetricarbonyl trichloride was added and the flask was placed into a preheat 70 °C oil bath. After 18 hours, the reaction mixture was diluted with ethyl acetate and washed 3 times with 1 M HCl and brine, and then dried over Na_2SO_4. The resulting material was purified by column chromatography to yield **3.1** (0.500 g, 70%) as yellow solids. ^{1}H NMR (500 MHz, $CDCl_3$) δ 8.63 (s, 3H), 8.31 (dd, J = 8.8, 2.9 Hz, 12H), 7.46 (dd, J = 8.9, 6.4 Hz, 6H), 7.38 (dd, J = 9.0, 6.4 Hz, 6H), 6.29 (s, 6H), 3.11 (s, 9H).

N^1,N^{10}-dihydroxydecanediamide (**3.2**)

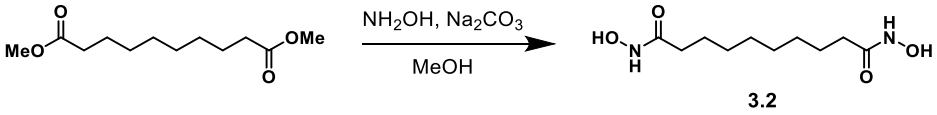

3.2

A 250 mL round bottom flask was charged with a stir bar and MeOH (168 mL). After which dimethyl sebacate (10 mL, 42 mmol, 1.0 eq.), NH_2OH (11.2 mL, 50 wt%, 4 eq.), and Na_2CO_3 (9.92 g, 93.0 mmol, 2.2 eq.) were added. After 30 minutes the resulting solution was acidified using 1 M HCl to pH = 7 before being concentrated under reduced pressure. The resulting white solids were triturated with methanol. The resulting organic solution was concentrated under reduced pressure to yield **3.2** as white solids. ^{1}H NMR (400 MHz, DMSO) δ 1.92 (t, J = 7.4 Hz, 4H), 1.52 – 1.41 (m, 5H), 1.28 – 1.14 (m, 12H).

phenyl hydroxycarbamate (**3.7**)[113]

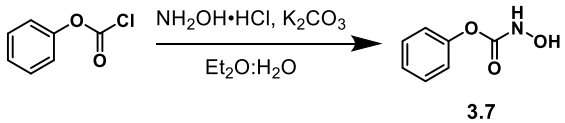

3.7

To 50 mL round bottom flask NH_2OH•HCl (5.24 g, 75.4 mmol, 1.05 eq.), K_2CO_3 (11.9 g, 86.2 mmol, 1.2 eq.), H_2O (7.5 mL), and Et_2O (72 mL) were added. The flask was then placed in an ice

bath before adding phenyl chloroformate (9 mL, 71.9 mmol, 1.0 eq.) in Et_2O (72 mL) dropwise over 30 minutes. The reaction mixture was then removed from the ice bath and allowed to stir continuously at room temperature. After 4 hours, the phases were separated, and the organic layer was dried with $MgSO_4$ and concentrated under reduced pressure to yield **3.7** as pink solids. ^1H NMR (400 MHz, DMSO) δ 10.32 (s, 1H), 9.07 (s, 1H), 7.42 – 7.36 (m, 2H), 7.25 – 7.19 (m, 1H), 7.13 – 7.07 (m, 2H).

phenyl 2-oxa-3-azabicyclo[2.2.1]hept-5-ene-3-carboxylate (**3.11**)

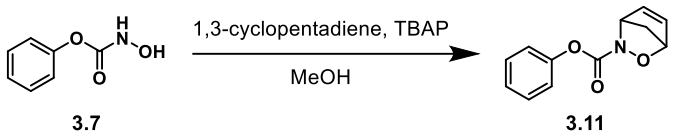

3.7 **3.11**

To a N_2 purged round bottom flask **3.7** (0.20 g, 1.3 mmol, 1.0 eq.), MeOH (14 mL) and 1,3-cyclopentadiene (0.21 mL, 2.6 mmol, 2.0 eq.) were added. After which tetrabutylammonium periodate (0.62 g, 1.4 mmol, 1.2 eq.) in MeOH (28 mL) was added. After 18 hours the reaction was diluted with EtOAc and washed with sat. NaS_2O_3 solution, sat. $NaHCO_3$ solution, and brine, then dried with Na_2SO_4. The organic layer was concentrated under reduced pressure and purified by column chromatography to yield **3.11**. ^1H NMR (400 MHz, $CDCl_3$) δ 7.39 – 7.33 (m, 2H), 7.24 – 7.19 (m, 1H), 7.13 – 7.08 (m, 2H), 6.61 (dt, J = 5.7, 2.0 Hz, 1H), 6.50 (ddd, J = 5.6, 2.4, 1.5 Hz, 1H), 5.35 (q, J = 2.0 Hz, 1H), 5.21 (p, J = 1.9 Hz, 1H), 2.12 (dt, J = 8.8, 2.0 Hz, 1H), 1.86 (dt, J = 8.8, 1.1 Hz, 1H).

hexane-1,6-diyl bis(2-oxa-3-azabicyclo[2.2.1]hept-5-ene-3-carboxylate) (**3.14**)

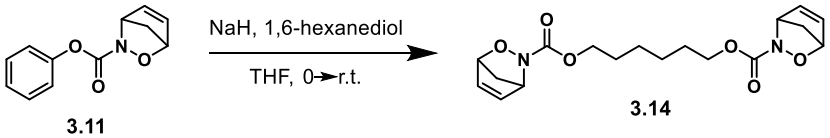

3.11 **3.14**

To a flame-dried N_2 purged 10 mL round bottom flask THF (2 mL), 1,6-hexanediol (0.0495 g, 0.419 mmol, 1.0 eq.) were added. The flask was then placed into an ice bath followed by the

addition of NaH (0.0343 g, 60 wt%, 2.05 eq.). After 30 minutes, **3.11** (0.200 g, 0.920 mmol, 2.2 eq.) in THF (2 mL) was added dropwise. After 18 hours, the reaction was diluted with EtOAc and washed with sat. NH4Cl solution and brine before drying with Na_2SO_4. The resulting solution was concentrated under reduced pressure and purified by column chromatography (50 to 74% EtOAc in hexanes) to yield **3.14**. ^{1}H NMR (400 MHz, $CDCl_3$) δ 6.57 (d, J = 5.5 Hz, 2H), 6.35 (d, J = 5.7 Hz, 2H), 5.29 (d, J = 25.2 Hz, 4H), 1.98 (d, J = 11.0 Hz, 8H), 1.84 (s, 1H), 1.82 (s, 1H), 1.70 (s, 2H).

phenyl hydroxycarbamate--1,1'-(hexane-1,6-diyl)bis(3-hydroxyurea) (**3.3**)

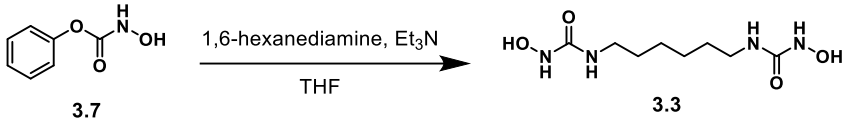

3.7 3.3

To a flame-dried 100 mL round bottom flask equipped with a reflux condenser was charged with a magnetic stir bar, 1,6-hexanediamine (0.304 g, 2.60 mmol, 1.0 eq.), **3.7** (1.00 g, 6.50 mmol, 2.5 eq.) and THF (26 mL) under N_2. After addition of Et_3N (0.93 mL, 6.5 mmol, 2.5 eq.), the flask was placed in a preheated oil bath. The reaction was refluxed for 18 hours, over the course of which an off-white precipitate formed on the sides of the flask. The organic layer was decanted, and the solids were washed with THF and filtered to yield **3.3**. ^{1}H NMR (400 MHz, DMSO) δ 8.20 (s, 2H), 6.65 (t, J = 5.9 Hz, 2H), 3.02 (q, J = 6.7 Hz, 4H), 1.39 (t, J = 6.8 Hz, 6H), 1.32 – 1.19 (m, 5H).

N,N'-(hexane-1,6-diyl)bis(2-oxa-3-azabicyclo[2.2.1]hept-5-ene-3-carboxamide) (**3.12**)

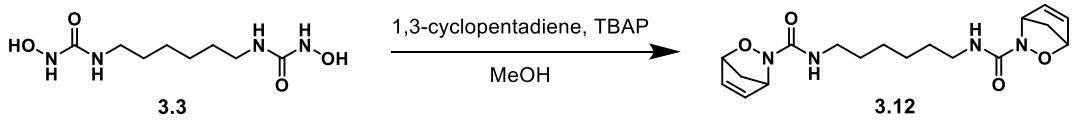

3.3 3.12

To a N_2 purged round bottom flask **3.3** (0.1233 g, 0.5263 mmol, 1.0 eq.), MeOH (3.5 mL) and 1,3-cyclopentadiene (0.18 mL, 2.1 mmol, 2.0 eq.) were added. After which tetrabutylammonium

periodate (0.50 g, 1.2 mmol, 2.2 eq.) in MeOH (7 mL) was added. After 18 hours the reaction was diluted with EtOAc and washed with sat. NaS_2O_3 solution, sat. $NaHCO_3$, and brine, then dried with Na_2SO_4. The organic layer was concentrated under reduced pressure and purified by column chromatography to yield **3.12**. ^{1}H NMR (400 MHz, $CDCl_3$) δ 6.40 (dd, J = 4.9, 2.7 Hz, 2H), 6.33 (dt, J = 5.6, 1.9 Hz, 2H), 5.62 (s, 2H), 5.19 – 5.11 (m, 4H), 3.13 (q, J = 6.7 Hz, 3H), 1.98 (dt, J = 8.7, 2.0 Hz, 2H), 1.76 (d, J = 8.9 Hz, 2H), 1.59 (s, 11H), 1.48 – 1.37 (m, 3H).

N1,N6-bis((10-methylanthracen-9-yl)methyl)hexane-1,6-diamine (**3.16**)

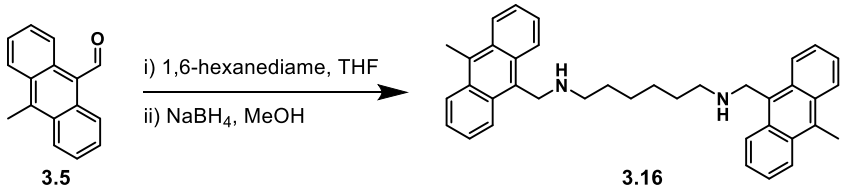

3.5 **3.16**

A flame-dried N_2 purged round bottom flask was charged with a magnetic stir bar, **3.5** (0.600 g, 2.72 mmol, 2.0 eq.), 1,6-hexanediamine (0.158 g, 1.36 mmol, 1.0 eq.), and THF (4.0 mL). After 18 hours the reaction was placed in an ice bath and $NaBH_4$ (0.114 g, 3.03 mmol, 2.2 eq.) along with MeOH (4.0 mL) was added. After 3 hours, the reaction was quenched with sat. $NaHCO_3$ solution and precipitated into water to yield **3.16** as yellow solids. ^{1}H NMR (400 MHz, $CDCl_3$) δ 8.42 – 8.30 (m, 9H), 7.58 – 7.47 (m, 9H), 4.71 (s, 4H), 3.10 (s, 6H), 2.87 (t, J = 7.2 Hz, 4H), 1.59 (d, J = 7.9 Hz, 7H), 1.44 – 1.33 (m, 4H).

N1-((10-methylanthracen-9-yl)methyl)-N2,N2-bis(2-(((10-methylanthracen-9-yl)methyl)amino)ethyl)ethane-1,2-diamine (**3.17**)

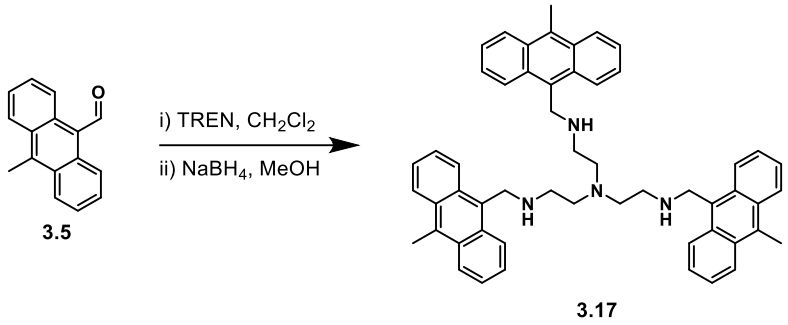

A flame-dried N_2 purged round bottom flask was charged with a magnetic stir bar, **3.5** (0.300 g, 1.36 mmol, 3.0 eq.), tris(2-aminoethyl)amine (0.066 g, 0.454 mmol, 1.0 eq.), and CH_2Cl_2 (2.0 mL). After 18 hours, the reaction was placed in an ice bath and $NaBH_4$ (0.114 g, 3.03 mmol, 2.2 eq.) along with MeOH (2.0 mL) was added. After 3 hours, the reaction was quenched with sat. $NaHCO_3$ solution and precipitated into water to yield **3.17** as yellow solids.

3.6.c ^{1}H and ^{13}C NMR Spectra

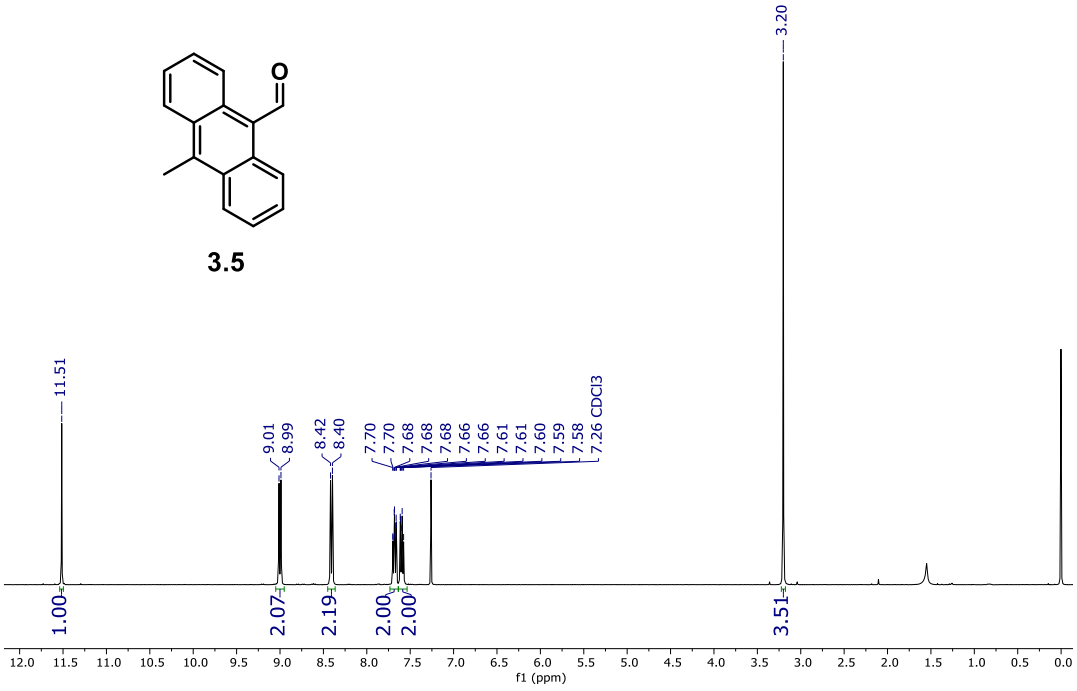

Figure 3.9 ^{1}H NMR spectrum of **3.5** in $CDCl_3$.

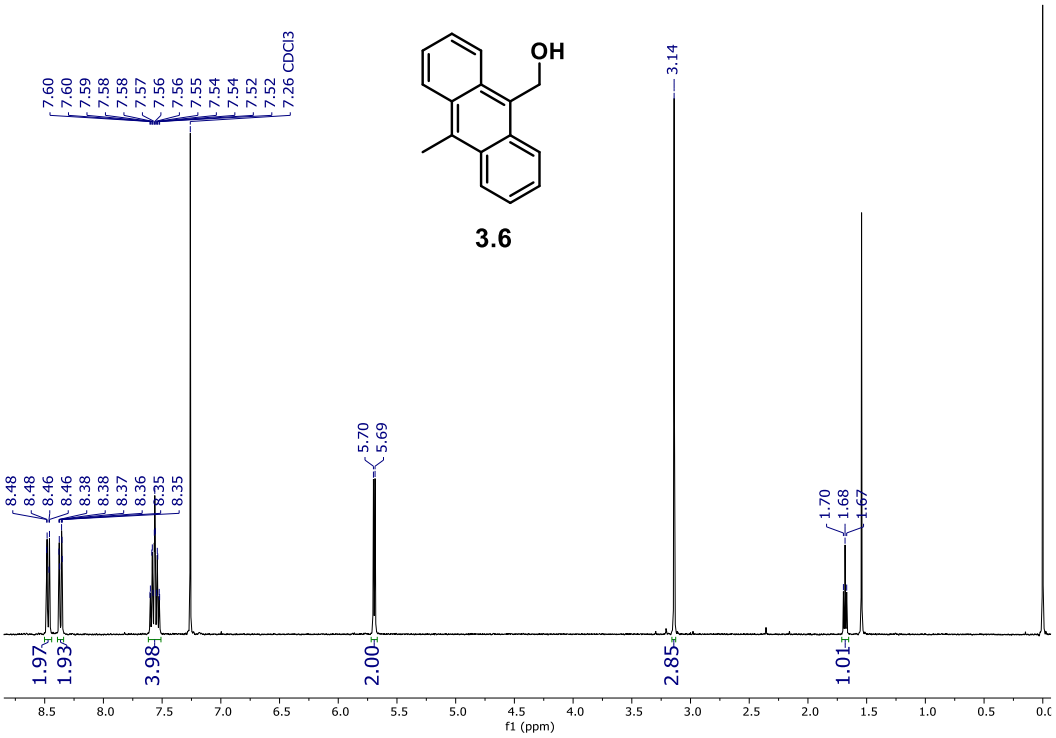

Figure 3.10 ^{1}H NMR spectrum of **3.6** in $CDCl_3$.

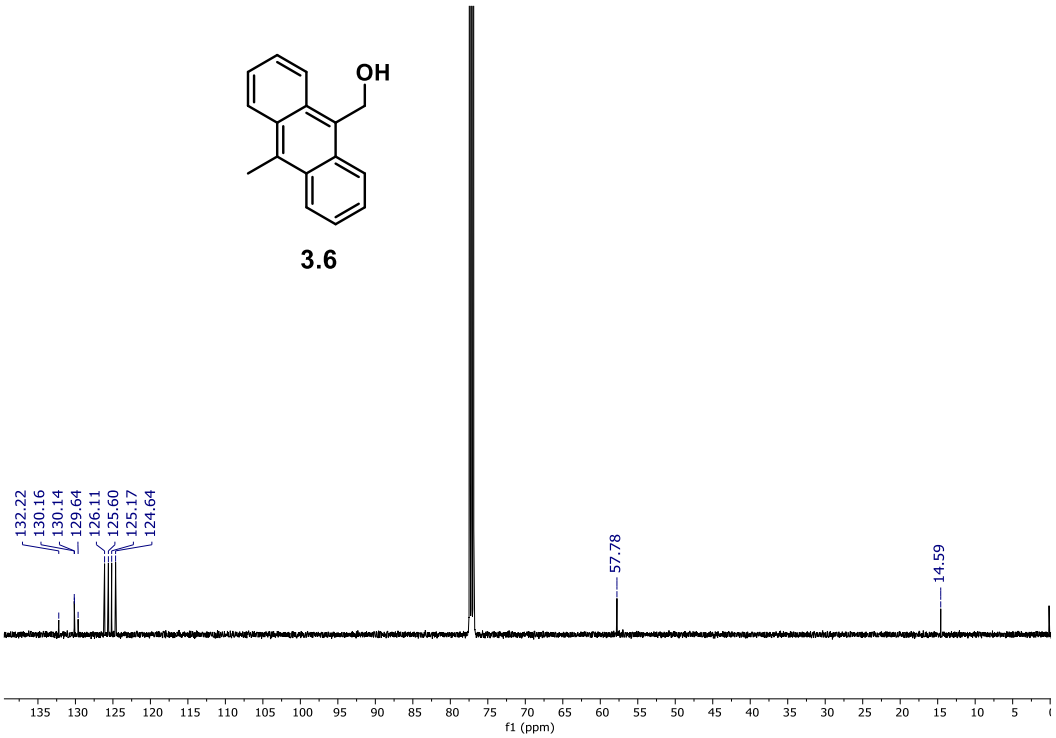

Figure 3.11 ^{13}C NMR spectrum of **3.6** in $CDCl_3$.

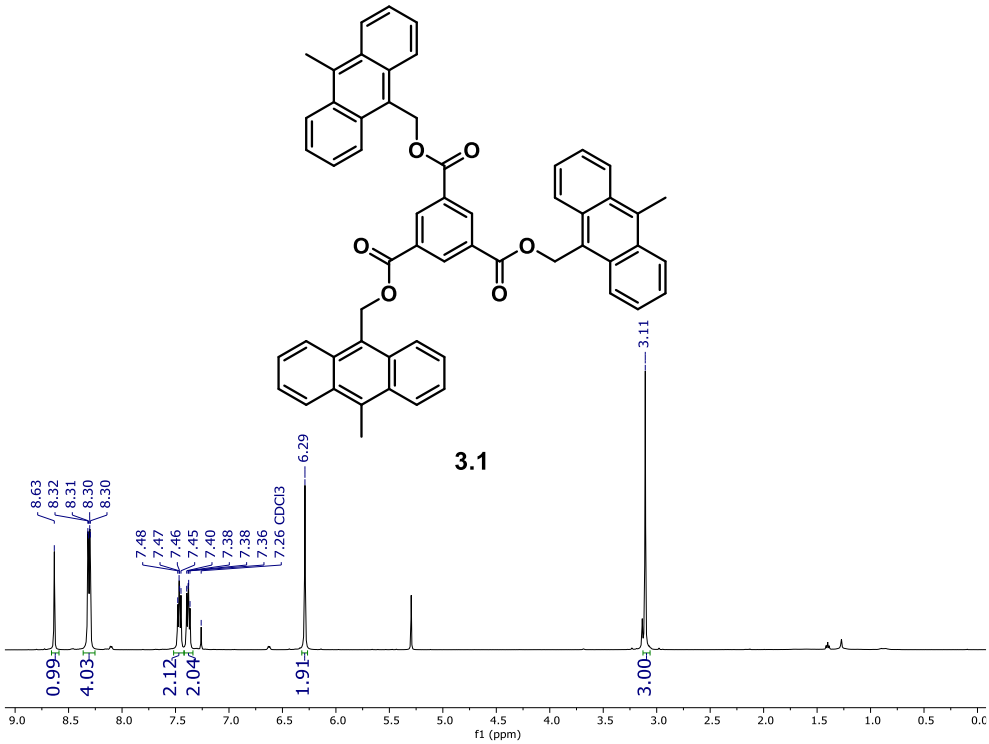

Figure 3.12 ^{1}H NMR spectrum of **3.1** in $CDCl_3$.

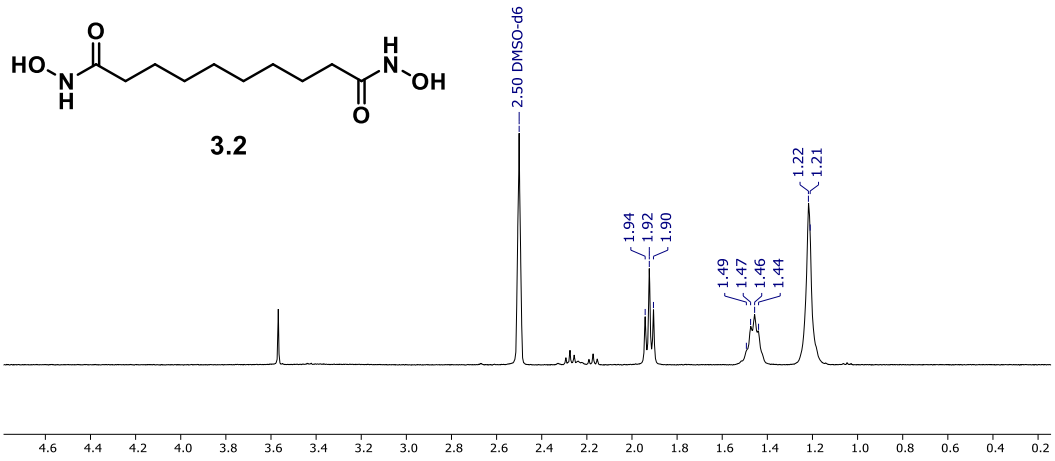

Figure 3.13 ^{1}H NMR spectrum of **3.2** in DMSO-d_6.

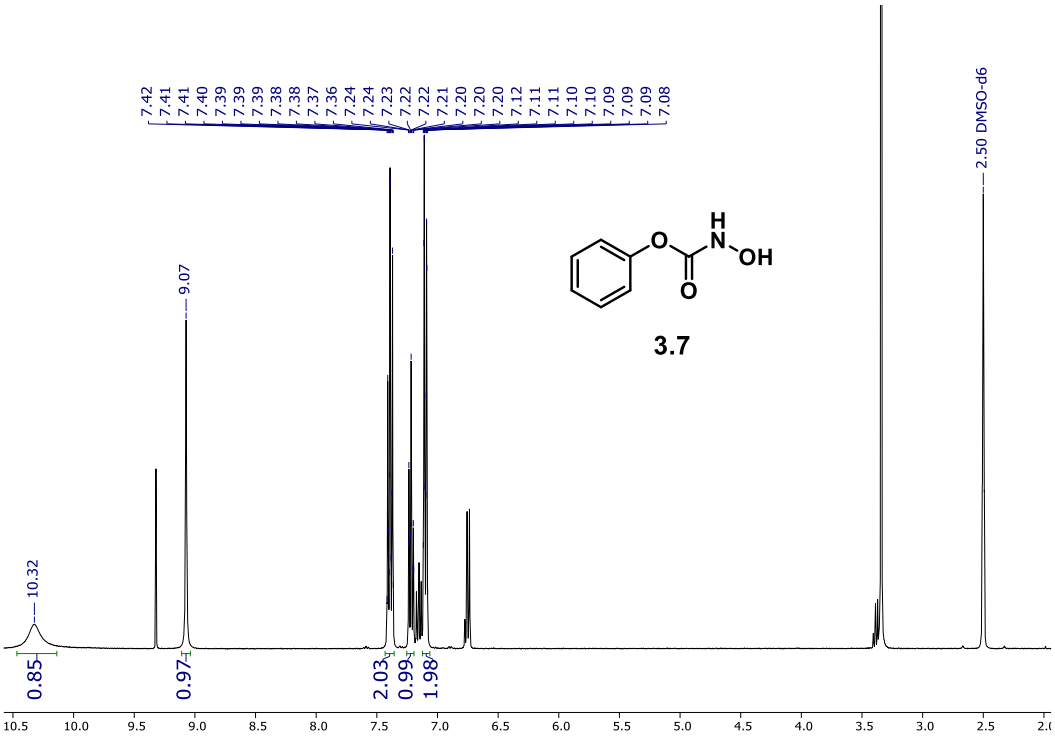

Figure 3.14 ^{1}H NMR spectrum of **3.7** in DMSO-d_6.

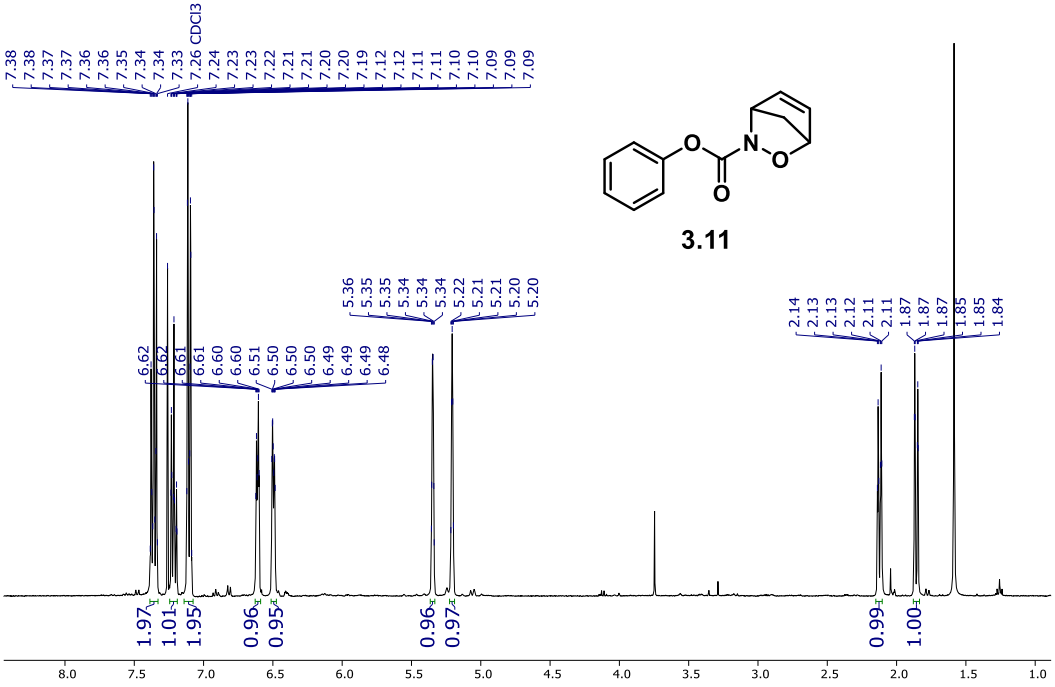

Figure 3.15 ^{1}H NMR spectrum of **3.11** in $CDCl_3$.

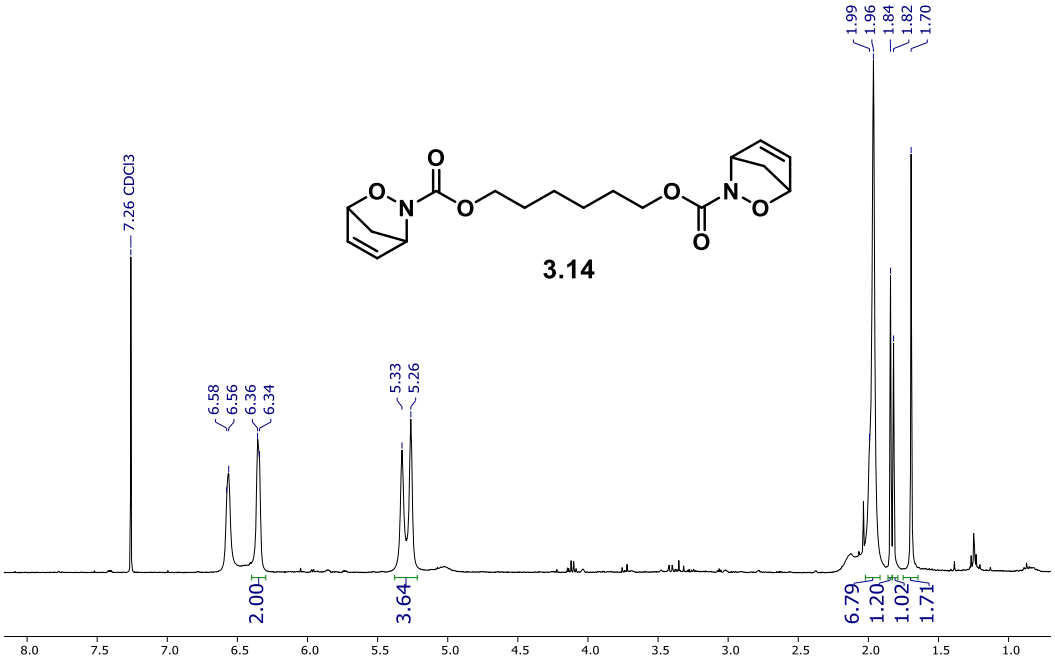

Figure 3.16 ^{1}H NMR spectrum of **3.14** in $CDCl_3$.

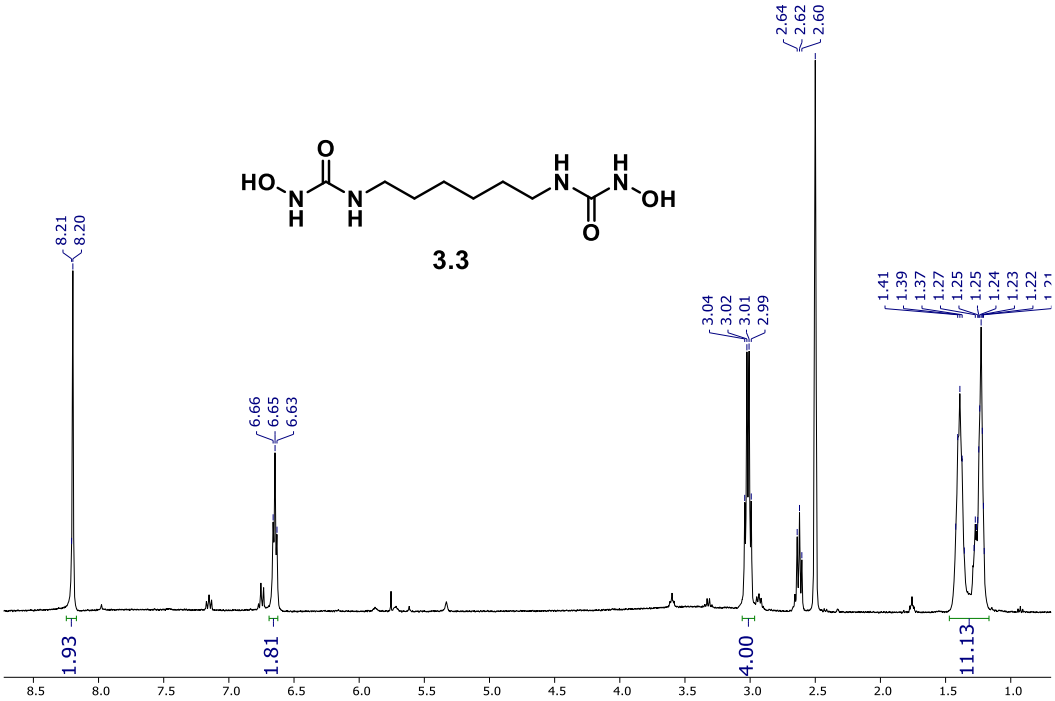

Figure 3.17 ^{1}H NMR spectrum of **3.3** in DMSO-d_6.

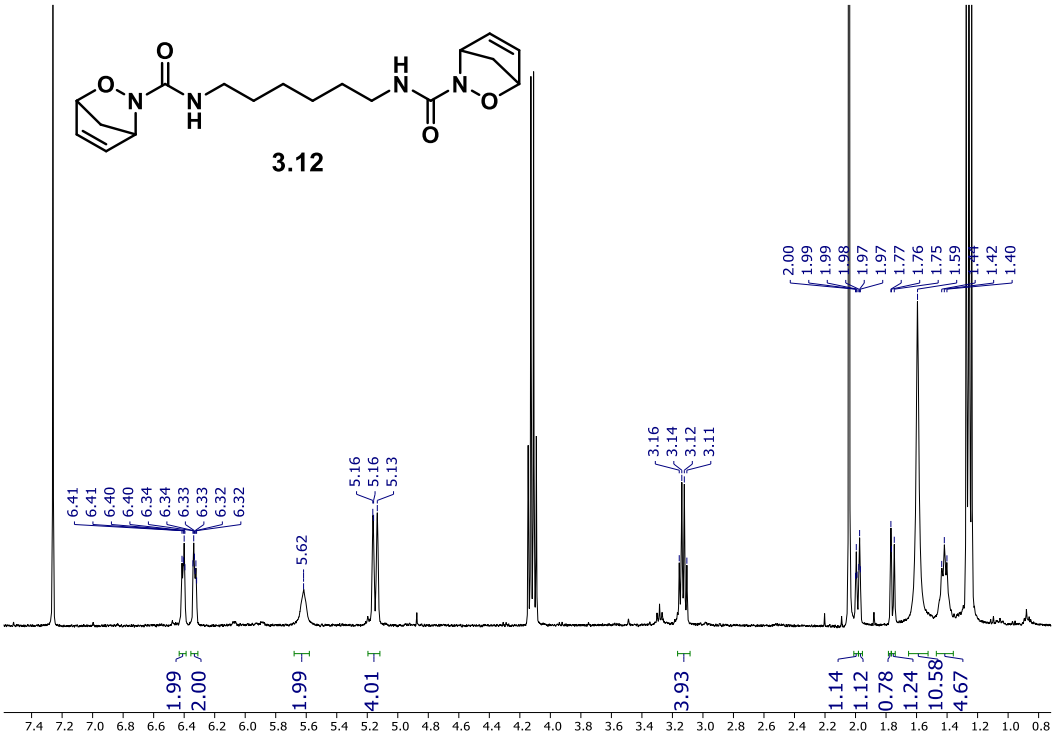

Figure 3.18 ^{1}H NMR spectrum of **3.12** in $CDCl_3$.

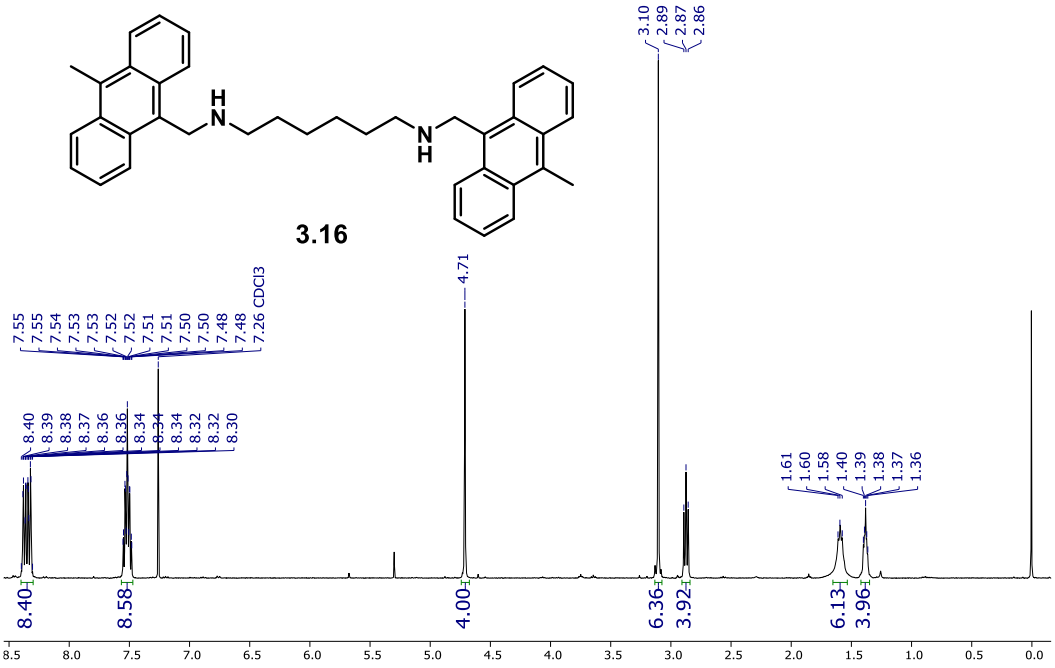

Figure 3.19 ^{1}H NMR spectrum of **3.16** in $CDCl_3$.

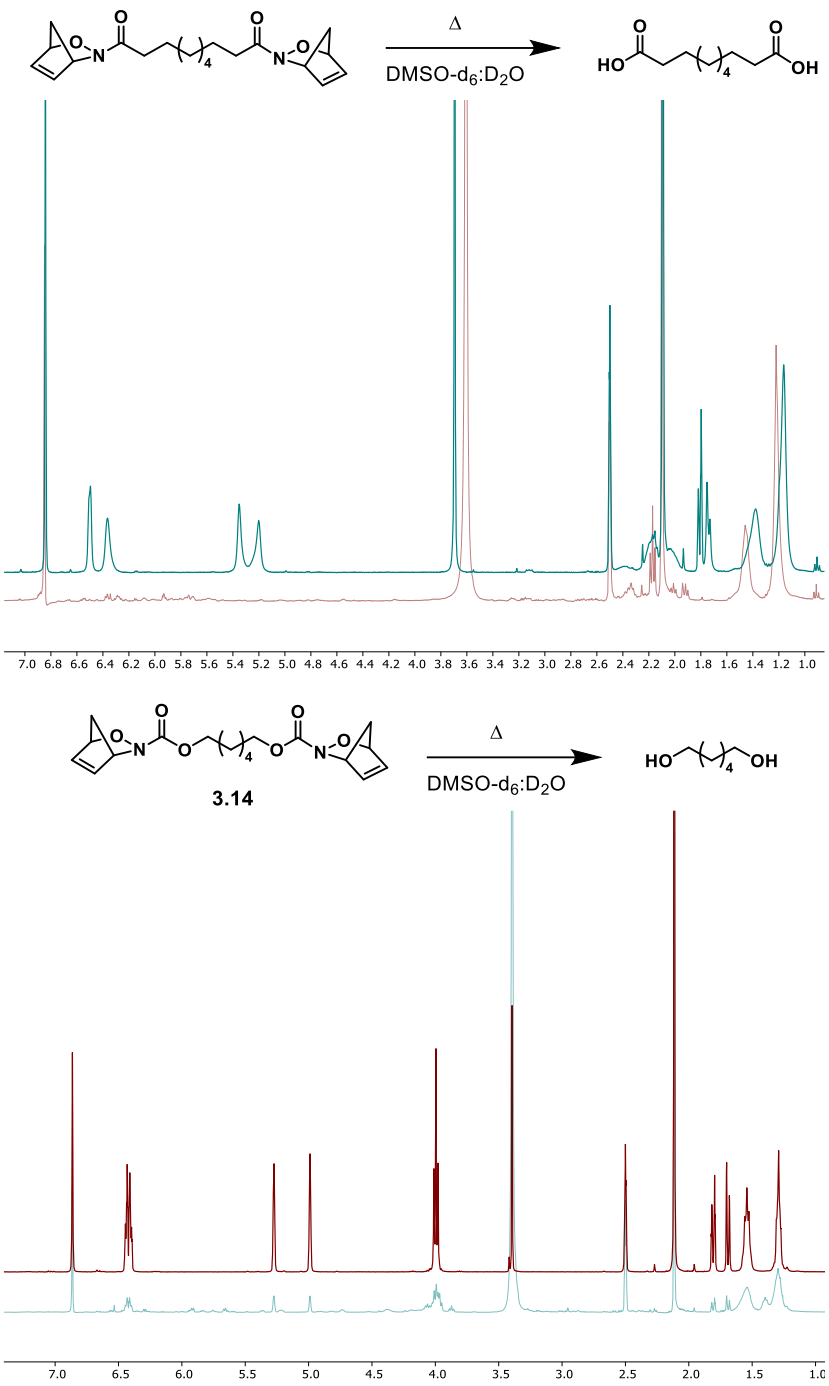

Figure 3.20 ^{1}H NMR spectrum of the decomposition of **3.13** (top) and **3.14** (bottom) in DMSO-d_6. In both experiments the top spectrum is t=0 and the bottom is t=24 hours.

(92) Khan, A.; Ahmed, N.; Rabnawaz, M. *Polymers (Basel).* **2020**, *12* (9), 2027.

(93) Hamad, K.; Kaseem, M.; Deri, F. *Polym. Degrad. Stab.* **2013**, *98* (12), 2801–2812.

(94) Sasse, F.; Emig, G. *Chem. Eng. Technol.* **1998**, *21* (10), 777–789.

(95) Scheutz, G. M.; Lessard, J. J.; Sims, M. B.; Sumerlin, B. S. *J. Am. Chem. Soc.* **2019**, *141* (41), 16181–16196.

(96) Chen, X.; Dam, M. A.; Ono, K.; Mal, A.; Shen, H.; Steven, R.; Sheran, K.; Wudl, F.; Science, S.; Series, N.; et al. *Science* **2002**, *295* (5560), 1698–1702.

(97) Mineo, P.; Barbera, V.; Romeo, G.; Ghezzo, F.; Scamporrino, E.; Spitaleri, F.; Chiacchio, U. *J. Appl. Polym. Sci* **2015**, *132*, 42314.

(98) Mayo, J. D.; Adronov, A. *J. Polym. Sci. Part A Polym. Chem.* **2013**, *51* (23), 5056–5066.

(99) Diaz, M. M.; Van Assche, G.; Maurer, F. H. J. J.; Van Mele, B. *Polym. (United Kingdom)* **2017**, *120*, 176–188.

(100) Inglis, A. J.; Nebhani, L.; Altintas, O.; Schmidt, F. G.; Barner-Kowollik, C. *Macromolecules* **2010**, *43* (13), 5515–5520.

(101) Schenzel, A. M.; Moszner, N.; Barner-Kowollik, C. *Polym. Chem.* **2017**, *8* (2), 414–420.

(102) Yoshie, N.; Saito, S.; Oya, N. *Polymer (Guildf).* **2011**, *52* (26), 6074–6079.

(103) Kensy, V. K.; Peterson, G. I.; Church, D. C.; Yakelis, N. A.; Boydston, A. J. *Org. Biomol. Chem.* **2016**, *14* (24), 5617–5621.

(104) Ahmad, M.; Hamer, J. *J. Org. Chem.* **1966**, *31* (9), 2831–2833.

(105) Horsewood, P.; Kirby, G. W.; Sharma, R. P.; Sweeny, J. G. *J. Chem. Soc. Perkin Trans. 1* **1981**, 1802–1806.

(106) Kirby, G. W.; Sweeny, J. G. *J. Chem. Soc., Perkin Trans. 1* **1981**, 3250–3254.

(107) Kirby, G. W.; Sweeny, J. G. *J. Chem. Soc. Chem. Commun.* **1973**, 19, 704–705.

(108) Xu, Y.; Alavanja, M.-M.; Johnson, V. L.; Yasaki, G.; King, S. B. *Tetrahedron Lett.* **2000**, *41*, 4265–4269.

(109) Keck, G. E.; Webb, R. R.; Yates, J. B. *Tetrahedron* **1981**, *37* (23), 4007–4016.

(110) Samoshin, A. V.; Hawker, C. J.; Read De Alaniz, J.; Alaniz, J. R. De. *ACS Macro Lett.* **2014**, *3* (8), 753–757.

(111) Fieser, L. F.; Jones, J. E. *J. Am. Chem. Soc.* **1942**, *64* (7), 1666–1669.

(112) Yousefinejad, S.; Honarasa, F.; Nekoeinia, M.; Zangene, F. *J. Solution Chem.* **2017**, *46* (2), 352–373.

(113) Chaiyaveij, D.; Batsanov, A. S.; Fox, M. A.; Marder, T. B.; Whiting, A. *J. Org. Chem.* **2015**, *80* (19), 9518–9534.

Chapter 4. Synthesis of a Dynamic Linear Step-Growth Polymer Using 1,2-oxazines

4.1 Abstract

We report work towards the synthesis of two AB monomers used in the step-growth polymerization of a linear poly(1,2-oxazine). Both targeted monomers consist of a hydroxyurea dienophile with either a 1,2,3,4,5-pentamethylcyclopentai-1,3-diene (CP*) or 9,10-dimethyl anthracene diene. For both monomers, the amine precursors to the hydroxyurea derivatives have been successfully synthesized.

4.2 Introduction

By 2025, the annual global production of plastic waste is expected to reach 2.3×10^8 tons.[114] Many plastics are currently recycled using mechanical recycling or mechanically breaking down plastics and purifying them for future use. Current methods of purification for mechanical recycling are inefficient making isolation of the pure polymer near impossible.[115,116] Chemical recycling, chemically reducing a polymer back to its monomers, can be used to overcome some issues related to mechanical recycling. To facilitate chemical recycling synthesizing plastics that containing reversible covalent bonds such as imines, alkenes, boronic esters, and products of cycloaddition reactions ([2+2] or [4+2]).[95] Cycloaddition reactions such as the Diels-Alder reaction offer significant promise because of their click chemistry characteristics while also being thermally and mechanochemically reversible.

Using reversible reactions with a step-growth polymerization allows for easier recycling as no post recycling steps are needed to allow the monomers to be repolymerized. When designing a polymer via a step-growth polymerization there are two different systems that can be used. The first being a two-monomer system (AABB), in which for synthesizing linear polymers the two monomers are used that each have two reactive functional groups. In a Diels-Alder system one

monomer contains the diene and the other the dienophile. The major advantage to this system is the ease of synthesis. Allowing each monomer to be synthesized on its own removes the need for protecting groups. Second, this method allows for more structural diversity amongst the polymer backbone, enabling a great amount of diversity in material properties.[30,33,117]

One major drawback for the AABB system is that the molecular weight of the resulting polymers is heavily dependent on the ratios of the monomers. The degree of polymerization ($\bar{X}_n$) of the polymer can be calculated using the following equation:

$$\bar{X}_n = \frac{1+r}{1+r-2rp} \tag{4.1}$$

where r is the stoichiometric ratio between monomers AA and BB such that $r \leq 1$, and p is the conversion for the polymerization. In the case the polymerization reaches 100% conversion or p = 1 then the equation can be simplified to:

$$\bar{X}_n = \frac{1+r}{1-r} \tag{4.2}$$

in a scenario where the polymerization reaches full conversion but r = 0.99 (1:1.01 AA:BB) the $\bar{X}_n = 200$, however as r decreases the impact on $\bar{X}$ becomes more prominent ($r = 0.95 \therefore \bar{X}_n = 39$).

The need for exact stoichiometry is removed in second system by using a single monomer that contains an equal number of the two reactive functional groups (AB). This allows for much better control over the molecular weight of the final polymers because the concentration of the two functional groups will always be equal. In these case $\bar{X}_n$ can thus be calculated by using the Carothers equation:

$$\bar{X}_n = \frac{1}{1\text{-}p} \tag{4.3}$$

However, using these AB type monomers can require more complex syntheses and can require the use of protecting groups limiting the usable functional groups within the polymer backbone.

Despite its prevalence within the literature for the synthesis of polymer networks there are very few examples using the Diels-Alder reaction to polymerize linear polymers.[117–121] The most prevalent Diels-Alder reaction in both the synthesis of linear polymers and polymer networks is between furan and maleimide.[122–125] For step-growth polymerizations both AABB and AB systems have been demonstrated with using furan-maleimide Diels-Alder (**Figure 4.1**). The forward reaction will occur at temperatures near 60 °C and is thermally reversable at temperatures greater

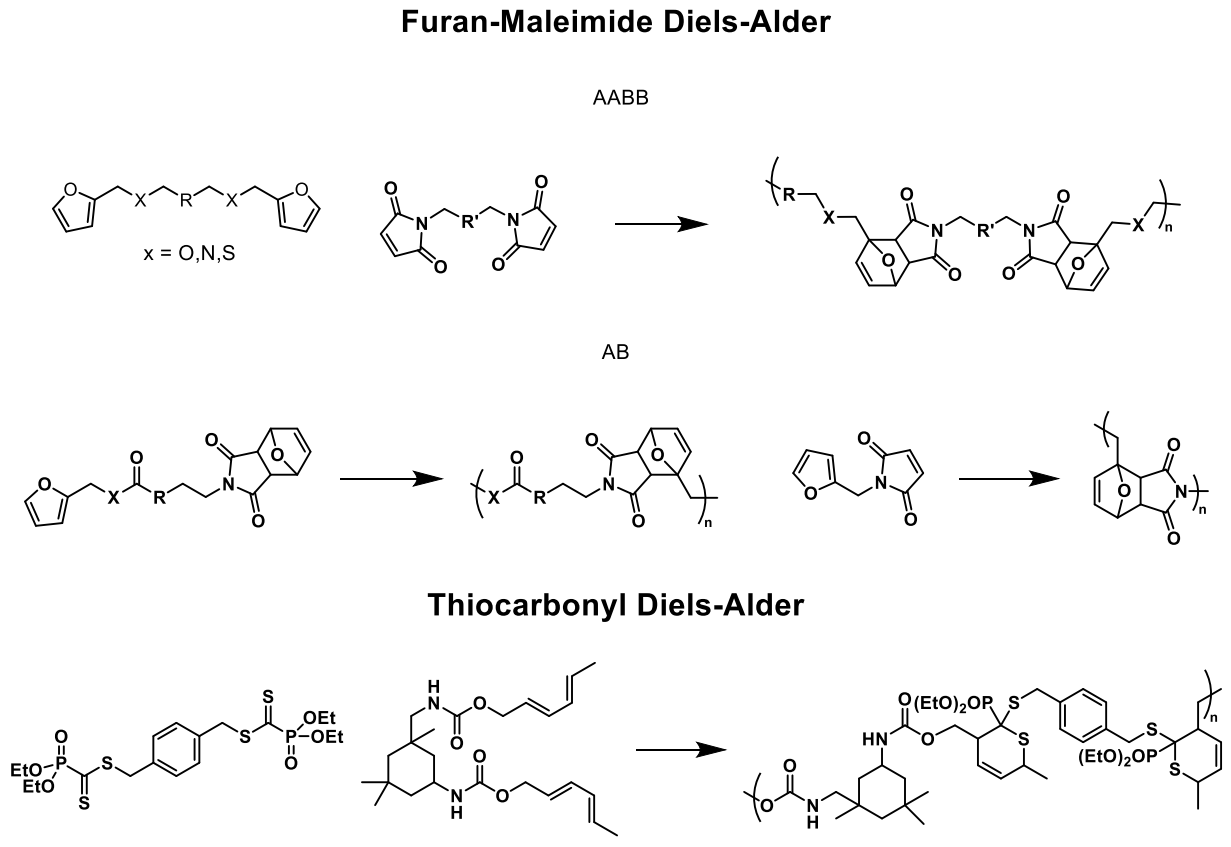

Figure 4.1 Examples of linear step-growth polymers synthesized using the Diels-Alder reaction.

than 90 °C, however when heated to above 200 °C the adduct will undergo dehydration and aromatization.[121,126] Using the furan-maleimide Diels-Alder pair, Vilela et al. demonstrated both AB and A_2B_2 systems using ϖ-undecenoic acid as a renewable cross-linker.[15,127] They were able to achieve an weight average molecular weight (M_w) of 16.5 kDa, with a dispersity (*Đ*) of 1.8 with their AB monomer. The final polymer exhibited a glass transition temperature (T_g) of -2 °C.[127] For the AABB system the authors synthesized polymers with much lower M_w (6.5 and 9.1 kDa), due to slight inequalities in the ratios of monomers. There was a dramatic decrease in the T_g for the polymers synthesized in the AABB system (-40 and -28 °C respectively).

A few other examples of AABB systems have been demonstrated for furan-maleimide Diels-Alder. This work included using several different functional group linkers including low molecular weight poly(ethylene glycol), saturated hydrocarbons, and terephthalates.[12] These systems have been used to synthesize polymers with number average molecular weights (M_n) that range from 2-30 kDa and were able change the conversion of the polymerization by cycling between 60 and 90 °C.[128]

The examples of reversible linear step-growth polymers are very limited outside of furan-maleimide Diels-Alder. To our knowledge, the only other example of an AB system for furan-maleimide Diels-Alder was demonstrated by Lacerda et. al.[29] They synthesized an AB monomer form furan and a furan protected maleimide separated by a single carbon linker. When heated to 110 °C the maleimide was be deprotected giving off gaseous furan, and when cooled to 60 °C the monomer was able to polymerize. The resulting polymer had a T_g of 90 °C, which is quickly followed by the onset of retro-Diels-Alder.

Another Diels-Alder reaction that has been used is between 1,3-dienes and thiocarbonyls, like the furan-maleimide the thiocarbonyl Diels-Alder has been used in the synthesis of crosslinked

polymer networks and in step-growth polymerizations.[100,129–135] In 2011 Zhou et al. used thioesters in the hetero-Diels-Alder reaction to synthesize linear polymers.[35] In their work they synthesized an AABB monomer system (**Figure 4.1**) using a bis-phosphonate dithioester with a bis-2,4-hexadiene. When polymerized the authors were able to synthesize polymers with peak molecular weights (M_p) of 9.6 kDa and showed that by changing solvents they were able to change the M_p of their resulting polymers. They also demonstrated that their polymer system like the furan-maleimide system required very high temperatures to become dynamic (>100 °C).

With the limited number of examples for reversible cycloadditions used to synthesize linear polymers, and those that do exist requiring a specific temperature range (80-110 °C) to be reversible a new covalent system is required. I believe this can be achieved by using 1,2-oxazines. 1,2-oxazines have been shown to be readily reversible at temperatures as low as 27 °C as well as temperatures greater than 80 °C.[103] This range is enabled by making slight alterations to the 1,3-diene and dienophile used to synthesize 1,2-oxazines.

King et. al. demonstrated that changes to the electronics and sterics around the nitroso carbamide dienophile can have a large impact rate of the retro-Diels-Alder reaction for 1,2-oxazines.[108] In their work they showed that by changing from a nitroso-urea to an N-phenyl-N'-nitrosocarbamide the half-life at 40 °C could be change from 2.6 hours to 0.26 hours. They also showed that by changing the electronics of the aryl substituent could further impact the half-life, however both *para*-OMe, and *para*-NO_2 substitutions decreased the rate of the retro-Diels-Alder reaction, suggesting that electronics alone were not the controlling the rate of the retro-Diels-Alder reaction.

The impact that the dienophile on the rate of the retro-Diels-Alder reaction was furthered studied in 2016 by the Boydston group.[103] In their work they compared how the identity of the

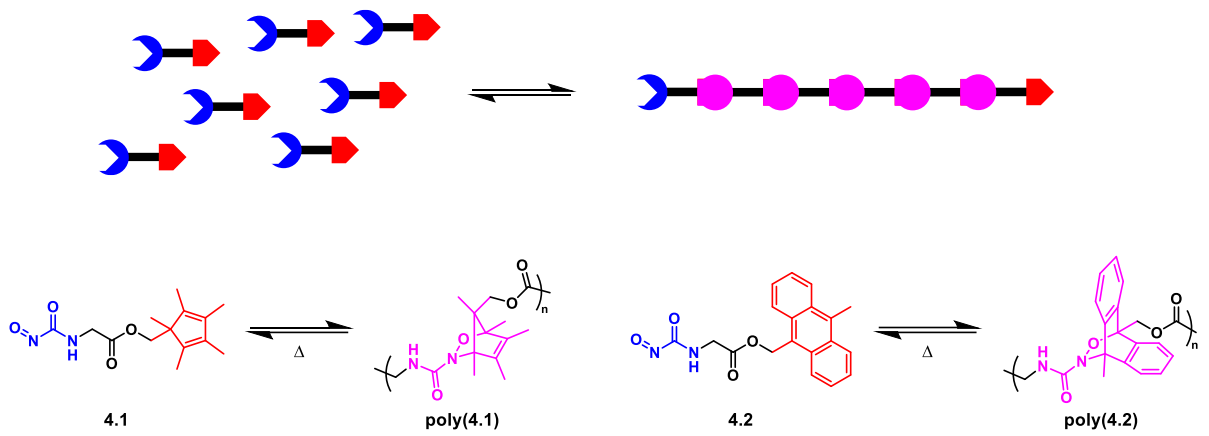

Figure 4.2 Cartoon depiction of a dynamic linear polymer synthesized via a step-growth polymerization (top). Monomers (**4.1** and **4.2**) used in the synthesis of the dynamic polymer (bottom).

nitrosocarbonyl affected the rate of the retro-Diels-Alder reaction by comparing the rates of isomerization of a carbamate, amide, and two carbamide dienophiles. No obvious trend based on electronics was observed, but there was a distinct change in the rates of isomerization for the different carbonyl derivatives. The slowest of dienophiles was the amide derivative, which showed consistent, but very little overall, isomerization at 37 °C for upwards of 11 days. While the unsubstituted carbamide derivative reached full equilibrium in less than 10 days. This rate difference was even more pronounced at 80 °C, where the unsubstituted carbamide reached full conversion within 3 hours and very little change was seen for the amide derivative.

Although no one study has looked at how the structure of the 1,3-dienes impact the rates of the retro-Diels-Alder reaction for 1,2-oxazines, studies have been published with showing the differences between small samples sizes of dienes. When comparing the stabilities of 1,2-oxazines synthesized from aryl-nitroso species and both 1,3-cyclopentadiene and 1,3-cyclohexadiene, the former could be isolated and stored at room temperature while the latter readily underwent the retro-Diels-Alder reaction at the same temperature.[104] Furthermore, there have been many examples in the literature of diene exchange reactions from 9,10-dimethyl anthracene based

oxazines with dienes that would form much more stable adducts like 1,3-cyclohexadinene, thebaine, *trans,trans*-1,4-phenyl-1,3-butadiene, cyclopentadiene, and 1,3-cyclohexadiene.[105109106110] This difference is potentially brought on by the differences in ring distortion from the 1,3-dienes to the 1,2-oxazines.[136]

Inspired by this work, we propose using 1,2-oxazines for the synthesis of dynamic linear step-growth polymers. To investigate the capabilities of this system, I proposed the synthesis of two AB type monomers, both monomers using a nitrosocarbamide as the dienophile to achieve reversibility at the lowest temperatures. While the 1,3-dienes will be either 1,2,3,4,5-pentamethyl cyclopentadiene (CP*), or 9,10-dimethylanthracene (**Figure 4.2**).

4.2 Results and Discussion

4.2.a Synthesis of CP-oxazine monomer*

The synthesis of the hydroxamic acid precursor (**4.6**) for monomer **4.1** was achieved in 4 steps from CP* (**Figure 4.3.A**). **4.3** was synthesized by adapting a previously reported

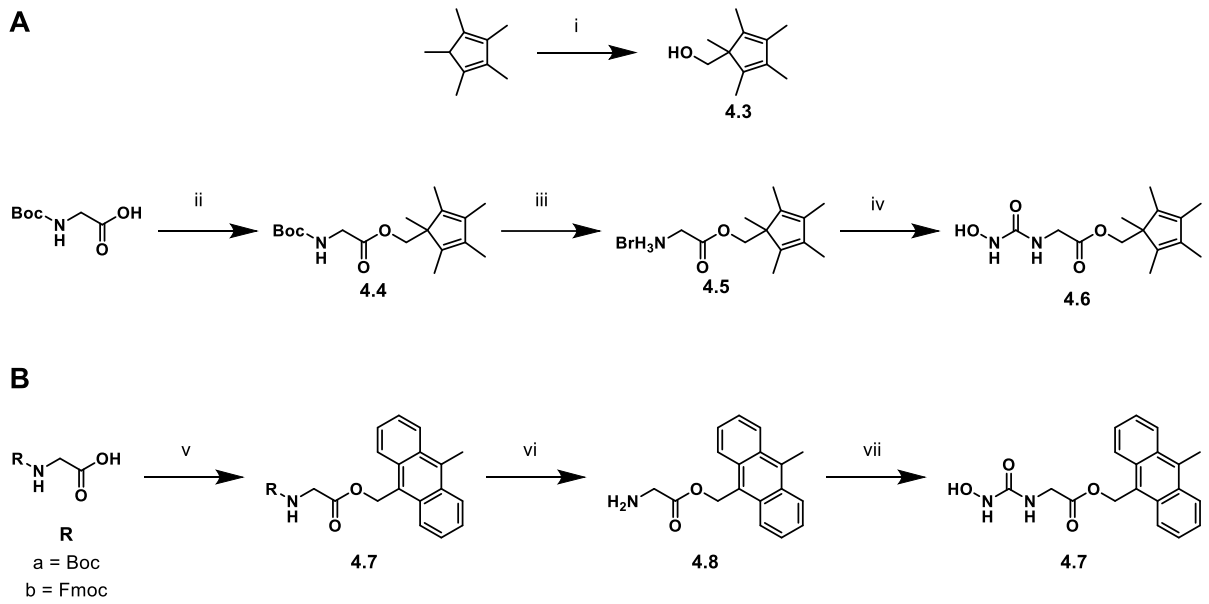

Figure 4.3. A) Synthesis for CP*-hydroxamic acid. i) *n*BuLi, paraformaldehyde. ii) **4.3**, CDI, DMAP. iii) AcBr, *i*PrOH. iv) **3.11**, Et_3N. B) Proposed synthesis for anthracene-hydroxamic acid. v) **3.6**, CDI, Gly-a/b. vi) a) AcBr, *i*PrOH. b) piperidine. vii) **3.11**, Et_3N.

procedure.[103] Briefly, CP* was deprotonated using *n*BuLi, before reacting with paraformaldehyde yielding **4.3**. The resulting alcohol was coupled with N-Boc-glycine to yield **4.4**. Purification of **4.4** was difficult due to the similarities in the polarities of **4.3** and **4.4**. As such, on larger scale reactions (>1 g) poor yields were achieved after column chromatography and as such the deprotection was carried out on a mixture **4.3** and **4.4**. The deprotection was performed using acetyl bromide (AcBr) and isopropanol to yield pure HBr salt **4.5**, after washing with Et_2O.

4.2.b. Synthesis of Anthracene-oxazine monomer

To demonstrate the diversity within 1,2-oxazines for the synthesis of AB step growth polymers I next targeted hydroxamic acid **4.7** (**Figure 4.3.B**). **3.6** was synthesized following the procedure outlined in Chapter 3. The carbonyl diimidazole (CDI) coupling was carried out using N-Boc-Gly to yield **4.7**. Like the CP* derivative the separation of **3.6** and **4.7** was difficult on larger scales, as such most of the initial work was carried out using a mixture of **3.6** and **4.7**.

We first attempt at the deprotection was done using AcBr and *i*PrOH, however due to solubility issues tetrahydrofuran was also used to help solubilize the **4.8**. The yields for this reaction were very low (< 5%), with the major product for the reaction being **3.6**. This is likely brought upon by the acid catalyzed hydrolysis of the anthracene with residual water or the transesterification with *i*PrOH. To avoid the elimination of the anthracene we next tried using trifluoracetic acid (TFA), which is a weaker acid than HBr. However, after trying different concentrations of TFA we were unable to prevent the decomposition of the ester (**Figure 4.4**).

To circumvent this issue going forward we changed to an fluorenylmethoxycarbonyl (Fmoc) protecting group. Fmoc is a base labile protecting group and can be removed using mild

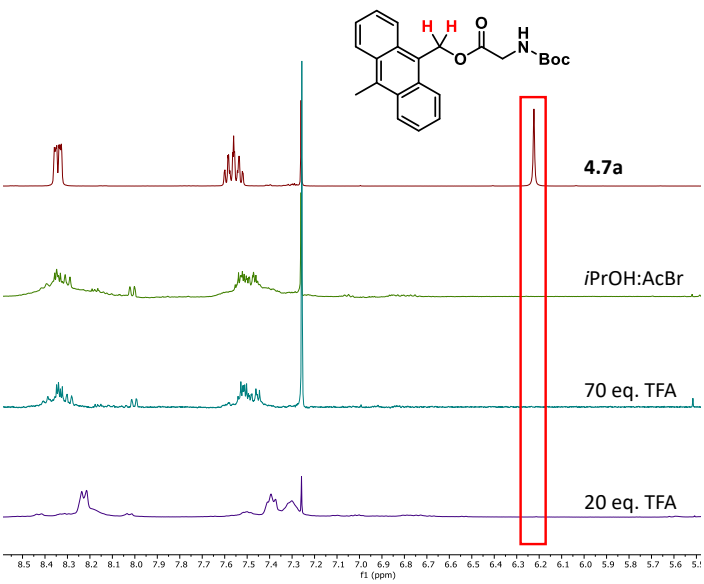

Figure 4.4 ^{1}H NMR spectra from the attempts at the Boc deprotection of **4.7a**. The ^{1}H signals for the benzylic ester (red) are no longer present in the crude reaction mixtures after the different deprotection attempts.

conditions.[137] Using the same CDI coupling as above **4.9** was obtained using Fmoc-Gly. The deprotection was caried out using piperidine (20% v/v) in methylene chloride. The deprotection was complete within 15 minutes, however when extended reactions times were used, we noticed an increase in the formation of **3.6**. Likely caused by either the polymerization of glycine or piperidine acting as a nucleophile and reacting with the electron poor ester to make the resulting amide. No work has been done yet to finalize the synthesis of hydroxamic acid **4.8**.

4.3 Conclusion

1,2-oxazines can greatly increase the chemical recyclability of step-growth polymers through their structural diversity. In this report we have made progress towards the synthesis of two precursors for the synthesis of 1,2-oxazine based polymers. The synthesis of the amine precursor for a 1,2,3,4,5-pentamethylcyclopentadiene hydroxamic acid was achieved. Instability of the anthracene containing ester to nucleophilic attack was demonstrate. Despite the stability issues of the anthracene ester the synthesis of the amine precursor for the anthracene hydroxamic acid was also achieved.

4.4 Future Work

The first step in this work is going to require investigation into the polymerization of these monomers and characterization of the resulting polymers. Some previous work has shown that there are several oxidants that can be used in the synthesis of the desired nitroso monomers such as air or hypervalent iodine.

Furthermore, the scope of dienes used should be expanded to include 1,3-cyclohexadiene derivatives and non-substituted cyclopentadiene derivatives. As well the monomers synthesized in this work only had a single carbon linker between the two oxazine components, expanding this to include longer linkages can allow the polymers to be moved into the bulk for the polymerization or have more interesting materials properties.

4.5 Experimental

4.5.a General considerations

^{1}H and ^{13}C NMR spectral data were recorded on Bruker Avance III 500 and Bruker Avance III 400 spectrometers. ^{1}H NMR chemical shifts for spectra collected in $CDCl_3$ or DMSO-d_6 are referenced to TMS (d = 0.00 ppm) or residual solvent peaks DMSO (d = 2.50 ppm), and $CDCl_3$ (d 7.26 ppm). ^{13}C NMR chemical shifts of spectra collected in $CDCl_3$ or DMSO-d_6 are referenced to the shifts of the carbon in $CDCl_3$ (d = 77.16 ppm) or DMSO-d_6 (d = 39.52 ppm). ^{1}H resonance data are reported as the following format: chemical shift in ppm [multiplicity, coupling constant(s) (J in Hz), and integration].

Reactions requiring anhydrous or air-free conditions were performed in the flame-dried glassware under nitrogen or argon atmosphere. Reported reaction temperatures are the temperature of the external heating bath. Triethylamine was distilled from CaH_2 and stored in a Schlenk flask.

Anhydrous solvents were collected from a solvent purification system prior to use. All other reagents were purchased from commercial sources and used as received unless otherwise specified.

4.5.b Synthetic procedures

(1,2,3,4,5-pentamethylcyclopenta-2,4-dien-1-yl)methanol (**4.3**)

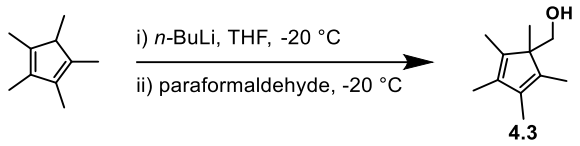

A flame-dried N_2 purged 100 mL 3-neck flask was charged with a magnetic stir bar, 1,2,3,4,5-pentamethylcyclopenta-1,3-diene (1.0 mL, 6.4 mmol, 1.0 eq.), THF (50 mL) before being cooled to -20 °C. Then n-butyllithium (2.3 mL, 2.5 M in hexanes, 0.92 eq.) was added slowly via syringe. The reaction mixture was stirred for 30 minutes before paraformaldehyde (0.38 g, 13 mmol, 2.0 eq.) was added under a cone of N_2. After 90 minutes the reaction was warmed to room temperature and carefully quenched with DI H_2O. The mixture was extracted with ethyl acetate (3x). The combined organic phase was washed with brine and dried over Na_2SO_4 and purified by column chromatography (10 to 20% ethyl acetate in hexanes), yielding **4.3** (0.17 g, 16%). ^{1}H NMR (400 MHz, $CDCl_3$) δ 3.50 (s, 2H), 1.82 – 1.78 (m, 6H), 1.74 (d, J = 1.0 Hz, 6H), 0.87 (s, 3H).

(1,2,3,4,5-pentamethylcyclopenta-2,4-dien-1-yl)methyl (tert-butoxycarbonyl)glycinate (**4.4**)

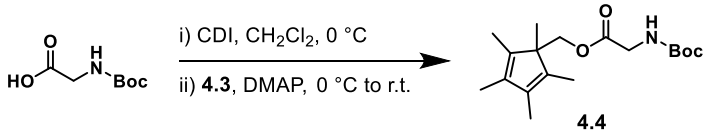

To a flame-dried N_2 purged 10 mL round bottom flask 1,1'-Carbonyldiimidazole (0.142 g, 0.881 mmol, 1.0 eq.) and CH_2Cl_2 (1 mL) was added. The mixture was then cooled to 0 °C after which (tert-butoxycarbonyl)glycine (0.154 g, 0.881 mmol, 1.0 eq.) was added. After 45 minutes 4-Dimethylaminopyridine (0.010 g, 0.088 mmol, 0.1 eq.) and **4.3** (0.1544 g, 0.881 mmol, 1.0 eq.) in CH_2Cl_2 (1 mL) was added and the reaction was removed from the ice bath. 18 hours later the

reaction was concentrated under reduced pressure and suspended in diethyl ether. The solution was washed with DI H_2O, sat. $NaHCO_3$, and brine and dried over Na_2SO_4. The material was purified by column chromatography (20% ethyl acetate in hexanes) to yield **4.4** (0.1600 g, 56%). ^{1}H NMR (400 MHz, $CDCl_3$) δ 4.92 (s, 1H), 4.00 (s, 2H), 3.83 (d, J = 5.5 Hz, 2H), 1.77 – 1.71 (m, 12H), 1.44 (s, 9H), 0.94 (s, 3H). ^{13}C NMR (101 MHz, $CDCl_3$) δ 170.22, 155.70, 138.47, 135.37, 80.03, 68.77, 55.48, 42.53, 28.46, 16.93, 11.20, 10.36.

(1,2,3,4,5-pentamethylcyclopenta-2,4-dien-1-yl)methyl 2-(bromo-l5-azaneyl)acetate (**4.5**)

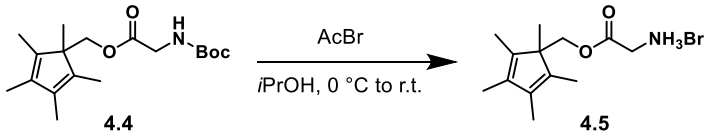

In a 7 mL vial isopropanol (0.25 mL) was cooled to 0 °C, then acetyl bromide (36 µL, 0.495 mmol, 1.0 eq.) was added. A second 7 mL vial was charged with a magnetic stir bar, **4.4** (0.1600 g, 0.495 mmol, 1.0 eq.), and isopropanol (0.25 mL). The second vial was cooled to 0 °C then the acetyl bromide and isopropanol mixture was added dropwise. The reaction was left to stir for 18 hours and the ice bath was allowed to expire after which diethyl ether was added. The slurry was filtered and washed with diethyl ether to yield **4.5** (0.062 g, 56%) as an off-white powder. ^{1}H NMR (400 MHz, DMSO) δ 8.11 (s, 3H), 4.03 (s, 2H), 3.74 (s, 2H), 1.73 (s, 12H).

(10-methylanthracen-9-yl)methyl (tert-butoxycarbonyl)glycinate (**4.7a**)

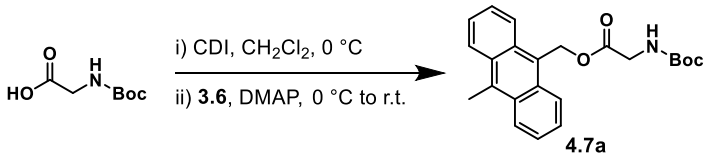

To a flame-dried N_2 purged 10 mL round bottom flask 1,1'-Carbonyldiimidazole (0.365 g, 2.25 mmol, 1.3 eq.) and CH_2Cl_2 (2.5 mL) was added. The mixture was then cooled to 0 °C after which (tert-butoxycarbonyl)glycine (0.303 g, 1.73 mmol, 1.0 eq.) was added. After 45 minutes 4-

dimethylaminopyridine (0.021 g, 0.173 mmol, 0.1 eq.), **3.6** (0.4552 g, 2.05 mmol, 1.18 eq.) and CH_2Cl_2 (2.5 mL) was added, and the reaction was removed from the ice bath. 18 hours later the reaction was further diluted with CH_2Cl_2. The solution was washed with DI H_2O, sat. $NaHCO_3$, and brine and dried over Na_2SO_4. The material was purified by column chromatography (20% ethyl acetate in hexanes) to yield **4.7a** (0.472 g, 72%). ^{1}H NMR (400 MHz, $CDCl_3$) δ 8.34 (dt, J = 8.3, 2.3 Hz, 4H), 7.62 – 7.49 (m, 4H), 6.22 (s, 2H), 5.03 (t, J = 6.6 Hz, 1H), 3.92 (d, J = 5.6 Hz, 2H), 3.12 (s, 3H), 1.43 (s, 9H). ^{13}C NMR (101 MHz, $CDCl_3$) δ 170.81, 155.79, 133.44, 130.86, 129.93, 126.40, 125.54, 125.16, 124.49, 123.96, 80.08, 60.05, 42.58, 28.41, 14.64.

(10-methylanthracen-9-yl)methyl 2-(bromo-l5-azaneyl)acetate (**4.8**)

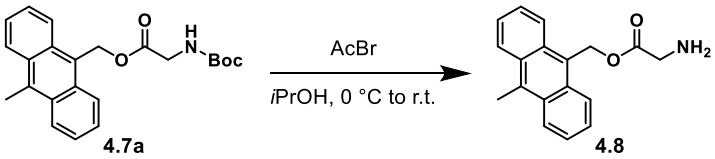

In a 7 mL vial isopropanol (10 mL) was cooled to 0 °C, then acetyl bromide (0.92 mL, 12.4 mmol, 10.0 eq.) was added. A second 7 mL vial was charged with a magnetic stir bar, **4.4** (0.472 g, 1.24 mmol, 1.0 eq.), and THF (10 mL). The second vial was cooled to 0 °C then the acetyl bromide and isopropanol mixture was added dropwise. The reaction was left to stir for 18 hours and the ice bath was allowed to expire after the reaction mixture was concentrated and suspended in CH_2Cl_2. The solution was then washed with sat. $NaHCO_3$ and brine and dried with Na_2SO_4. The material was purified via column chromatography (10% methanol in dichloromethane) to yield **4.8.** ^{1}H NMR (400 MHz, $CDCl_3$) δ 8.37 (dt, J = 8.3, 2.1 Hz, 4H), 7.63 – 7.52 (m, 5H), 6.24 (s, 2H), 3.44 (s, 2H), 3.15 (s, 3H).

(10-methylanthracen-9-yl)methyl (((9H-fluoren-9-yl)methoxy)carbonyl)glycinate (**4.7b**)

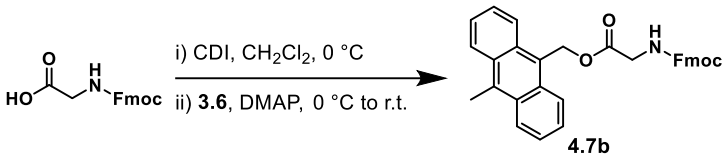

To a flame-dried N_2 purged 10 mL round bottom flask 1,1'-Carbonyldiimidazole (0.250 g, 1.50 mmol, 1.3 eq.) and CH_2Cl_2 (2.5 mL) was added. The mixture was then cooled to 0 °C after which (((9H-fluoren-9-yl)methoxy)carbonyl)glycine (0.310 g, 1.40 mmol, 1.0 eq.) was added. After 45 minutes 4-dimethylaminopyridine (0.014 g, 0.12 mmol, 0.1 eq.), **3.6** (0.3500 g, 1.4 mmol, 1.2 eq.) and CH_2Cl_2 (2.5 mL) was added, and the reaction was removed from the ice bath. 18 hours later the reaction was further diluted with CH_2Cl_2. The solution was washed with DI H_2O, sat. $NaHCO_3$, 1 M HCl, and brine and dried over Na_2SO_4. **4.7b** was used without further purification. ^{1}H NMR (400 MHz, $CDCl_3$) δ 8.33 (td, J = 9.1, 1.3 Hz, 4H), 7.75 (d, J = 7.7 Hz, 2H), 7.62 – 7.50 (m, 6H), 7.39 (t, J = 7.5 Hz, 2H), 7.29 – 7.24 (m, 2H), 6.25 (s, 2H), 4.35 (d, J = 7.2 Hz, 2H), 4.11 (t, 1H), 4.01 (d, J = 5.7 Hz, 2H), 3.10 (s, 3H).

(10-methylanthracen-9-yl)methyl 2-(bromo-l5-azaneyl)acetate (**4.8**)

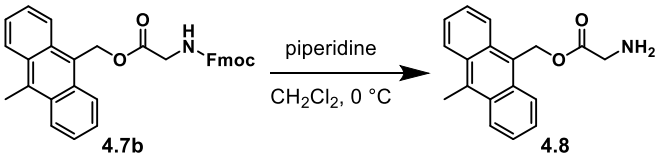

To a flame-dried N_2 purged 25 mL round bottom flask a stir bar, **4.7b** (0.150 g, 0.299 mmol, 1.0 eq.), and CH_2Cl_2 (5 mL) was added. The reaction mixture was cooled to 0 °C after which piperidine (2.5 mL) in CH_2Cl_2 (5 mL) was dropwise. Over the next 15 minutes all components became soluble in the CH_2Cl_2 after which the reaction was concentrated under reduced pressure. The material was purified by column chromatography (10% methanol in dichloromethane) to yield **4.8** (0.016 g, 20%)

4.5.c Spectral Data

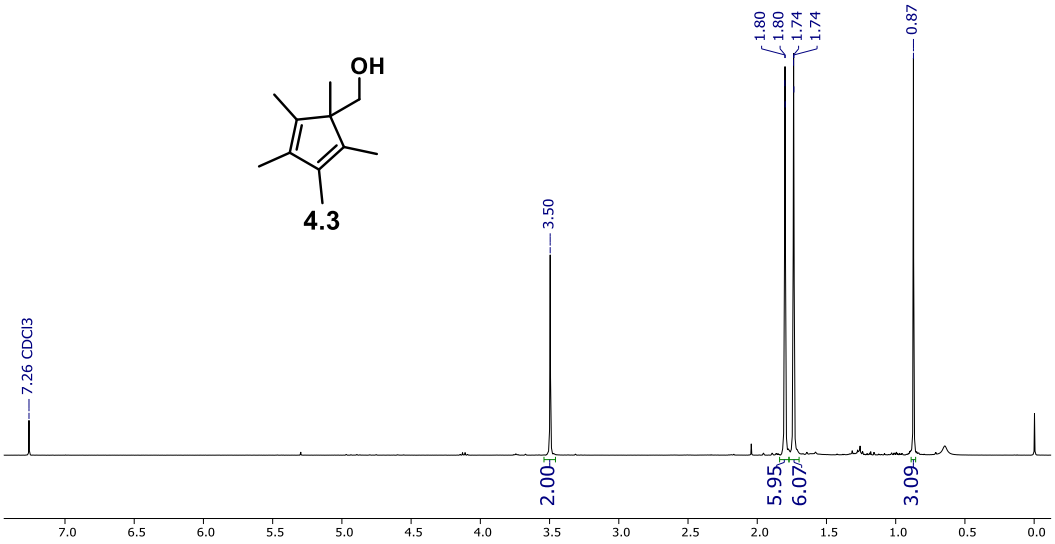

Figure 4.5 ^{1}H NMR spectrum of **4.3** in $CDCl_3$.

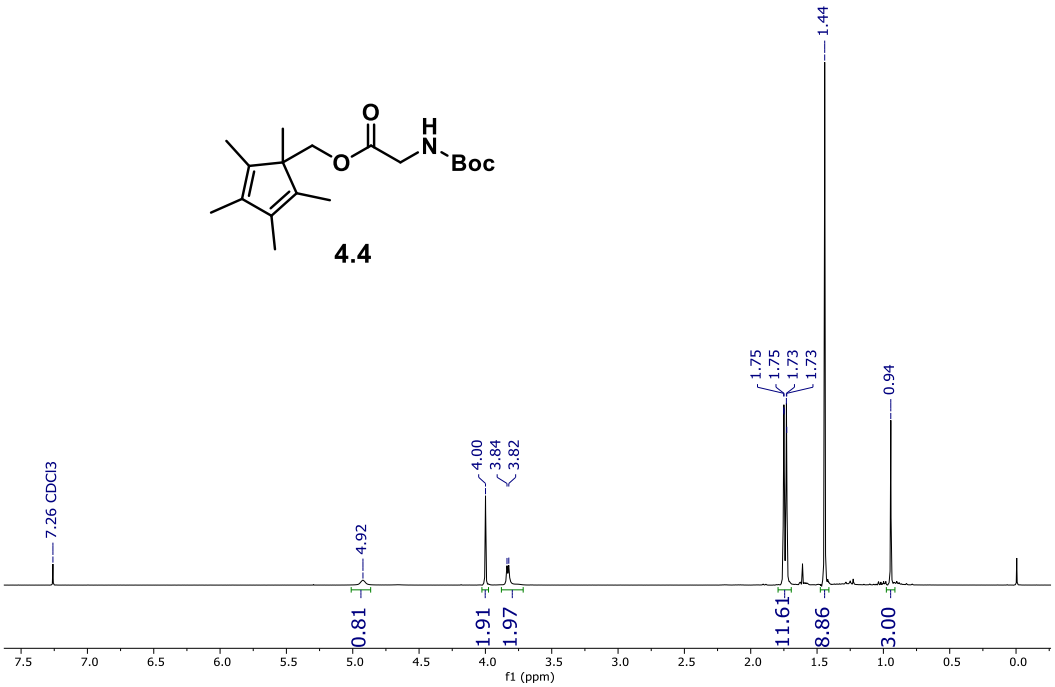

Figure 4.6 ^{1}H NMR spectrum of **4.4** in $CDCl_3$.

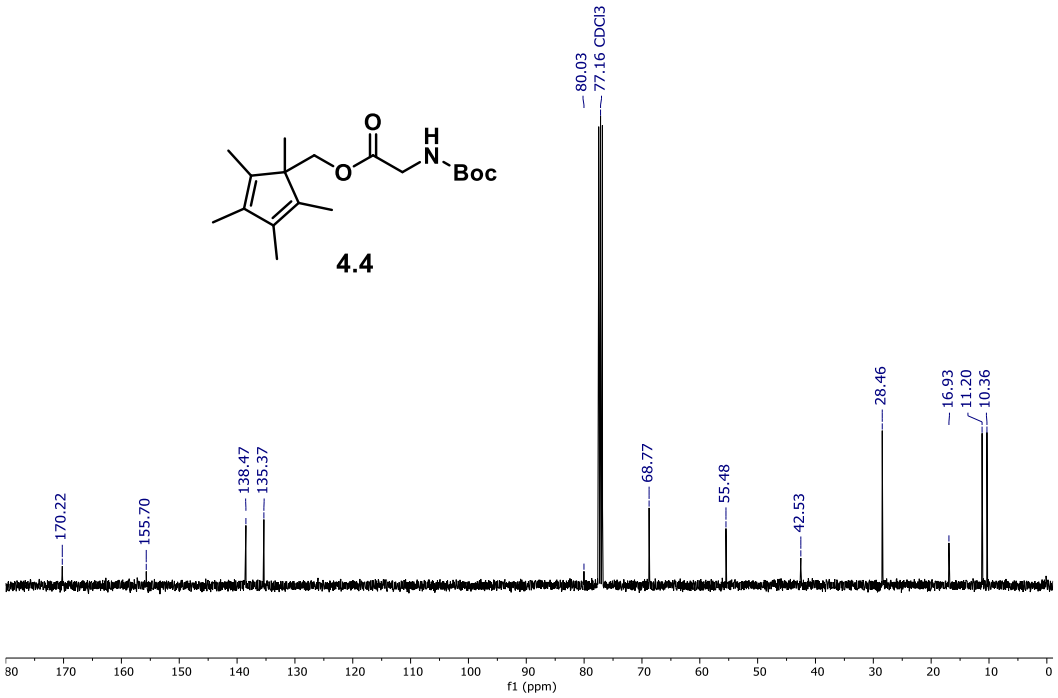

Figure 4.7 ^{13}C NMR spectrum of **4.4** in $CDCl_3$.

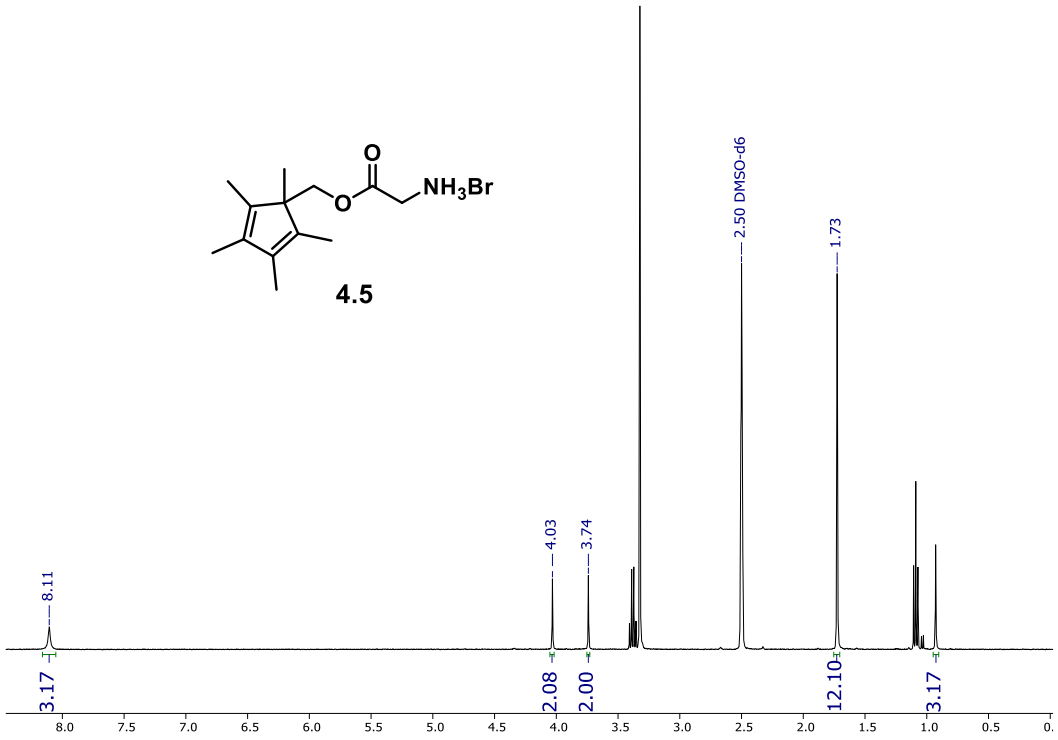

Figure 4.8 ^{1}H NMR spectrum of **4.5** in DMSO-d_6.

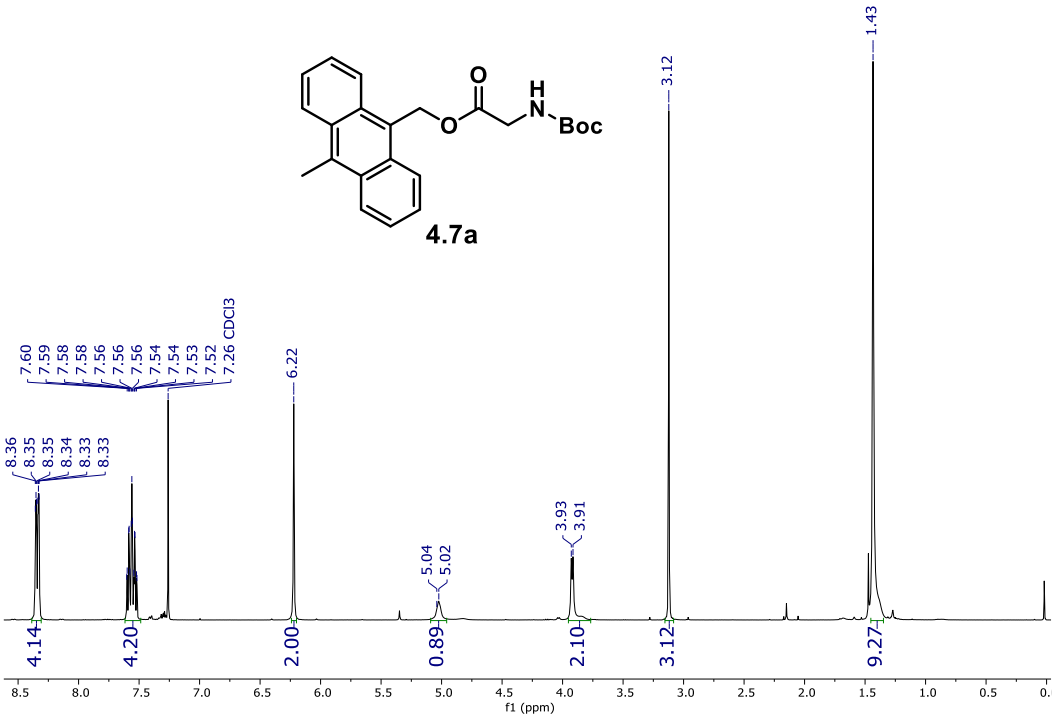

Figure 4.9 ^{1}H NMR spectrum of **4.7a** in $CDCl_3$.

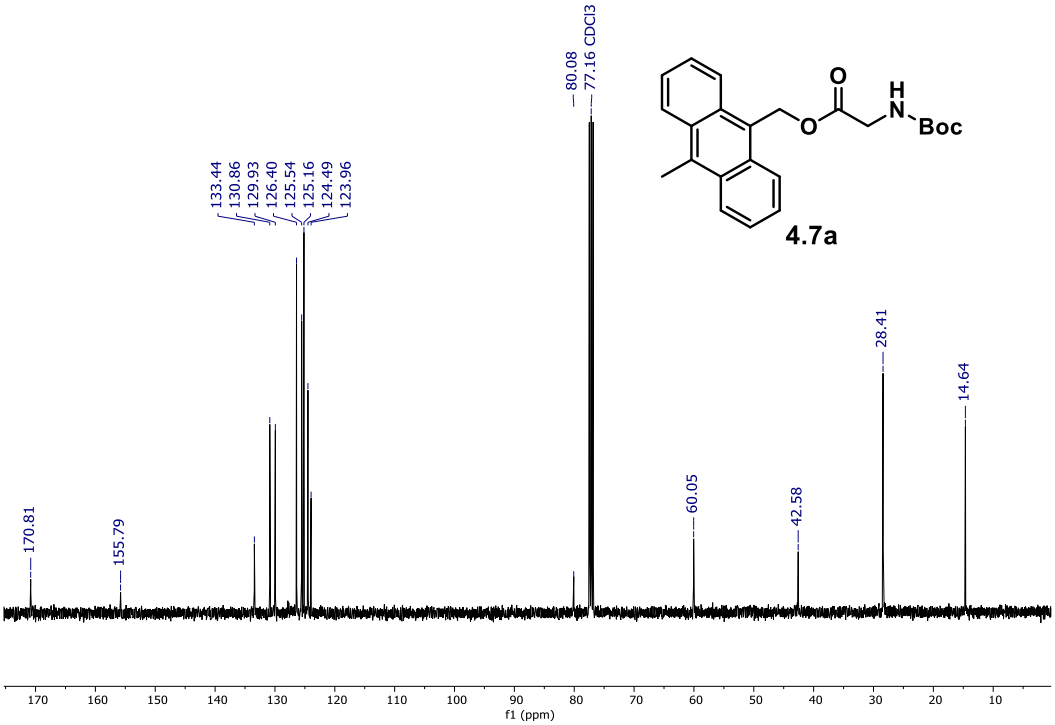

Figure 4.10 ^{13}C NMR spectrum of **4.7a** in $CDCl_3$.

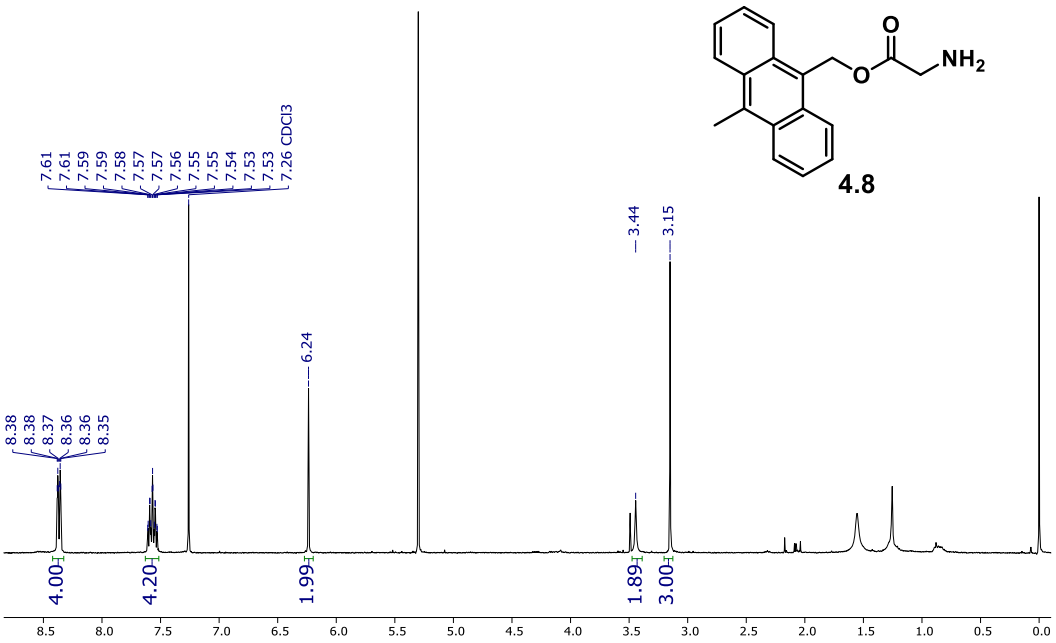

Figure 4.11 ^{1}H NMR spectrum of **4.8** in $CDCl_3$.

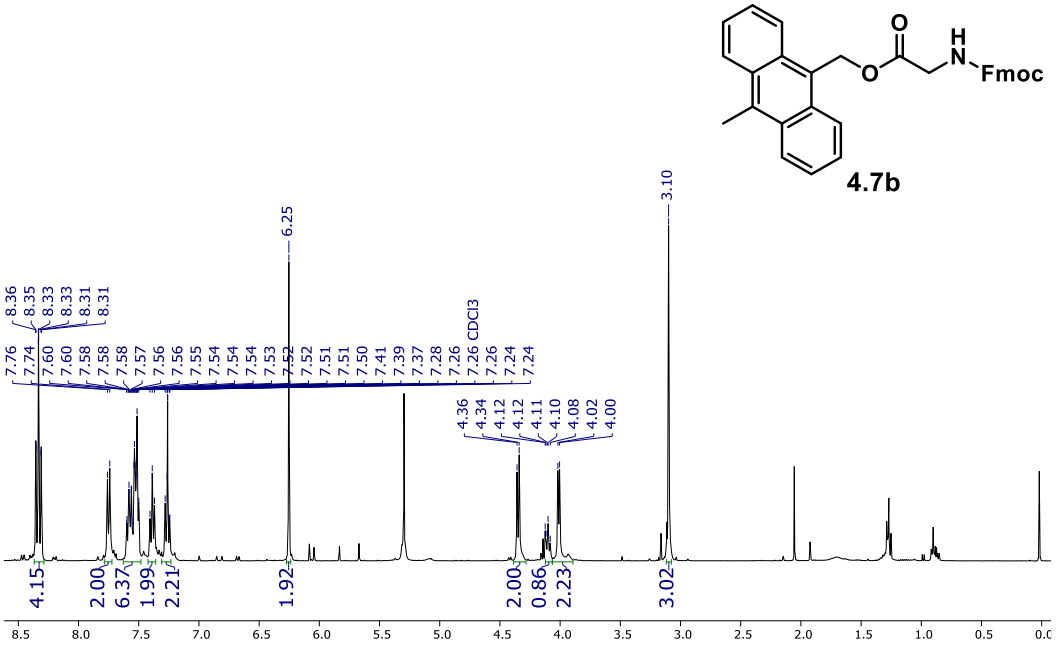

Figure 4.12 ^{1}H NMR spectrum of **4.7b** in $CDCl_3$.

Notes and References for Chapter 4

(114) Lebreton, L.; Andrady, A. *Palgrave Commun.* **2019**, *5* (1), 6.

(115) Al-Salem, S. M.; Lettieri, P.; Baeyens, J. *Waste Manag.* **2009**, *29* (10), 2625–2643.

(116) Shen, L.; Worrell, E. Plastic Recycling. In *Handbook of Recycling: State-of-the-art for Practitioners, Analysts, and Scientists*; 2014; pp 179–190.

(117) Ursache, O.; Gaina, C.; Gaina, V. *Express Polym. Lett.* **2017**, *11* (6), 467–478.

(118) Strachota, B.; Morand, A.; Dybal, J.; Matějka, L. *Polymers (Basel).* **2019**, *11* (6), 1–23.

(119) Vilela, C.; Silvestre, A. J. D.; Gandini, A. *J. Polym. Sci. Part A Polym. Chem.* **2013**, *51* (10), 2260–2270.

(120) Gheneim, R.; Perez-Berumen, C.; Gandini, A. *Macromolecules* **2002**, *35* (19), 7246–7253.

(121) Gandini, A.; Belgacem, M. N. *ACS Symp. Ser.* **2007**, *954*, 280–295.

(122) Maiti; Bidinger. *J. Chem. Inf. Model.* **1981**, *53* (9), 1689–1699.

(123) Diakoumakos, C. D.; Mikroyannidis, J. A. *J. Polym. Sci. Part A Polym. Chem.* **1992**, *30* (12), 2559–2567.

(124) Gaina, V.; Gaina, C. *Polym. - Plast. Technol. Eng.* **2002**, *41* (3), 523–540.

(125) Goussé, C.; Gandini, A. *Polym. Int.* **1999**, *48* (8), 723–731.

(126) Widstrom, A. L.; Lear, B. J. *Sci. Rep.* **2019**, *9* (1), 1–8.

(127) Vilela, C.; Cruciani, L.; Silvestre, A. J. D.; Gandini, A. *RSC Adv.* **2012**, *2* (7), 2966–2974.

(128) Kuramoto, N.; Hayashi, K.; Nagai, K. *J. Polym. Sci. Part A Polym. Chem.* **1994**, *32* (13), 2501–2504.

(129) Brandt, J.; Lenz, J.; Pahnke, K.; Schmidt, F. G.; Barner-Kowollik, C.; Lederer, A. *Polym. Chem.* **2017**, *8* (43), 6598–6605.

(130) Sinnwell, S.; Inglis, A. J.; Davis, T. P.; Stenzel, M. H.; Barner-Kowollik, C. *Chem. Commun.* **2008**, *2* (17), 2052–2054.

(131) Paulöhrl, T.; Inglis, A. J.; Barner-Kowollik, C. *Adv. Mater.* **2010**, *22* (25), 2788–2791.

(132) Kötteritzsch, J.; Bode, S.; Yildirim, I.; Weber, C.; Hager, M. D.; Schubert, U. S. *Des. Monomers Polym.* **2015**, *18* (7), 627–640.

(133) Inglis, A. J.; Sinnwell, S.; Davis, T. P.; Barner-Kowollik, C.; Stenzel, M. H. *Macromolecules* **2008**, *41* (12), 4120–4126.

(134) Nebhani, L.; Sinnwell, S.; Inglis, A. J.; Stenzel, M. H.; Barner-Kowollik, C.; Barner, L. *Macromol. Rapid Commun.* **2008**, *29* (17), 1431–1437.

(135) Glassner, M.; Blinco, J. P.; Barner-Kowollik, C. *Polym. Chem.* **2011**, *2* (1), 83–87.

(136) Levandowski, B. J.; Houk, K. N. *J. Org. Chem.* **2015**, *80* (7), 3530–3537.

(137) Ralhan, K.; KrishnaKumar, V. G.; Gupta, S. *RSC Adv.* **2015**, *5* (126), 104417–104425.

Chapter 5. Mechanochemical Reactivity of 1,2-Oxazine Hetero Diels-Alder Adducts

My work for this project was centered on the synthesis and characterization of the ATRP initiators. All work done for the sonication of the polymers and kinetic analysis was performed by Derek Church at the University of Washington.

5.1 Abstract

We have demonstrated the synthesis of 1,2-oxazine centered polymers using ATRP. Preliminary results suggest that these 1,2-oxazine containing polymers are mechanochemically reversible through the retro-Diels-Alder reaction. Trapping studies have shown that upon activation free 1,3-diene can be trapped using a pyrene hydroxamic acid and quantified using UV-vis spectroscopy. Future work needs to be done better understand the structure reactivity relationship of 1,2-oxazines by mechanochemical activation.

5.2 Introduction

Polymer mechanochemistry has become an established field in recent years with the overarching goal of obtaining new mechanoresponsive polymeric materials.[138–144] Self-healing materials, mechanoresponsive drug delivery platforms, and strain-sensing materials are just some of the purported applications that could arise from continued development in this area. The crux on which these potential applications rely upon is the utility of mechanically-sensitive moieties termed "mechanophores."[145] These mechanophores can undergo various strain-induced transformations such as homolytic scission,[146–152] ring-opening,[153–160] and cycloreversion reactions.[161–166] To ensure the continued growth of this field, new mechanosensitive moieties capable of triggering unique responses must be developed.

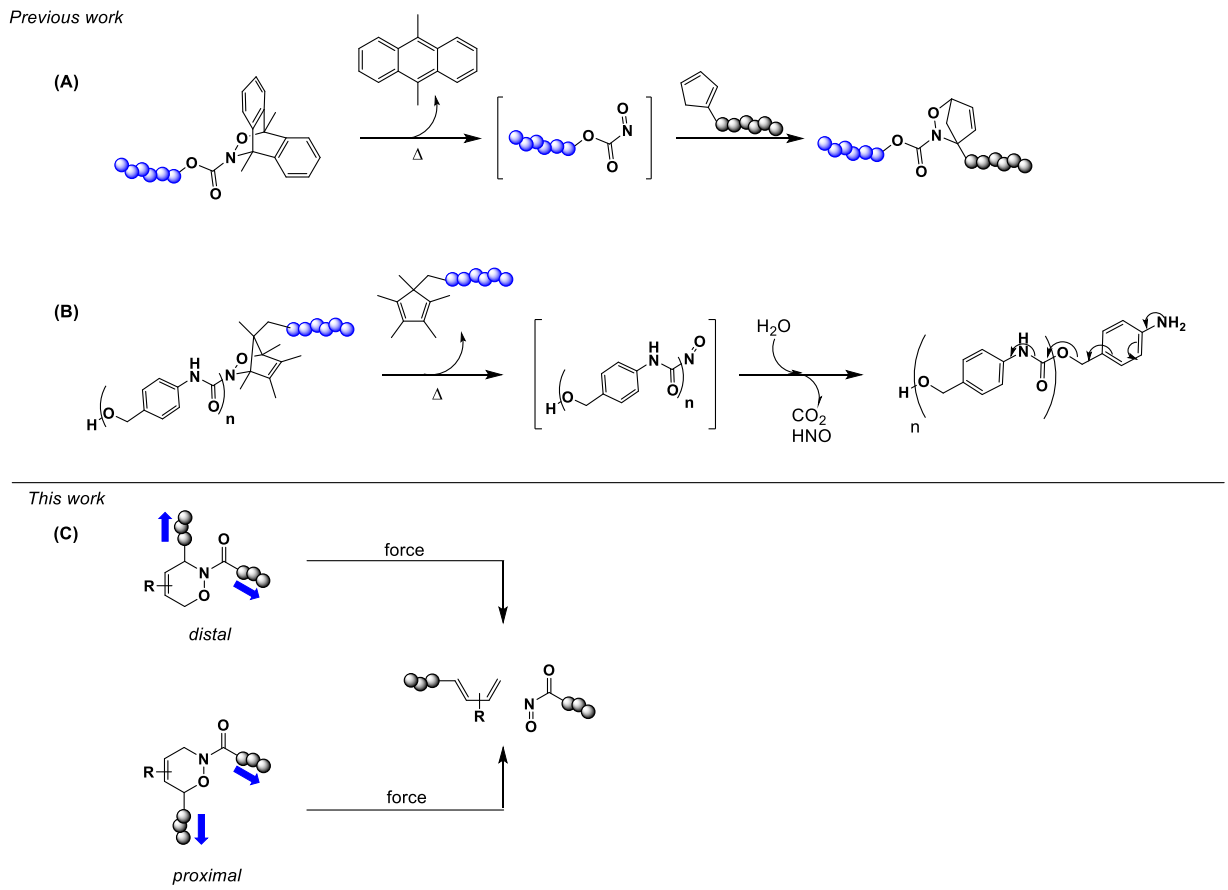

Figure 5.2 Precedence and current work on stimuli-responsive 1,2-oxazine-containing polymers.

Recently, our research has focused on the study of 1,2-oxazines for thermally responsive materials.[103,167,168] These moieties can undergo a thermally induced [4 + 2] cycloreversion at relatively moderate temperatures to release a diene and nitroso dienophile (**Figure 5.1**).[106,108,169–171] By tuning the diene and nitroso moiety, the thermal barrier for the retro Diels–Alder reaction can be attenuated and affords high modularity to this system. These moieties have already been demonstrated to have interesting capabilities in the context of polymer chemistry. For example, we have harnessed the unique breakdown pathway of N-carbonyl functionalized 1,2-oxazines to thermally trigger the depolymerization of a polycarbamate at physiological conditions **(Figure 5.2A)**.[168] Read de Alaniz has demonstrated that these moieties can be used towards polymer conjugation via a diene exchange at mild temperatures (**Figure 5.2B**).[172]

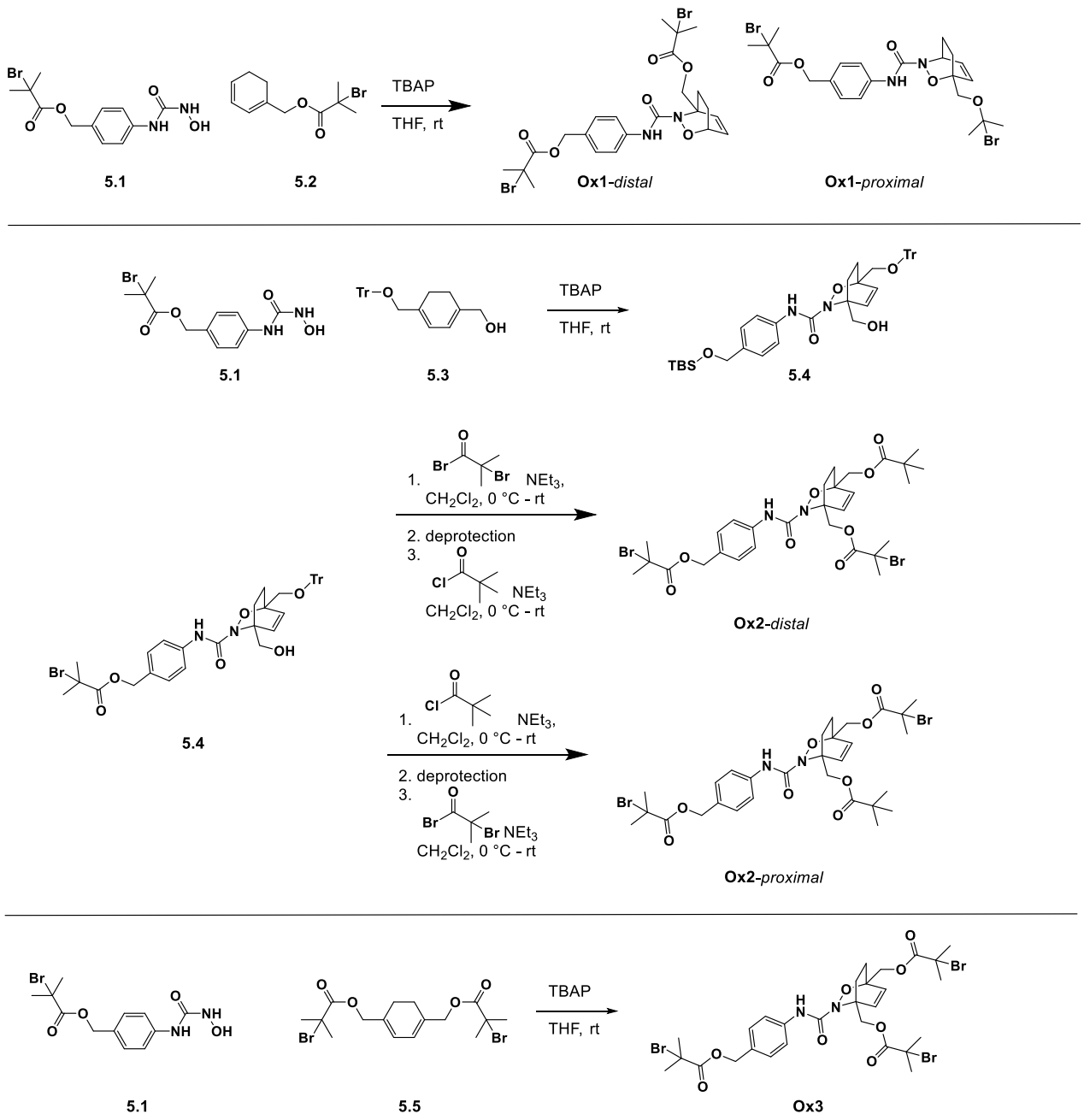

Figure 5.3 Synthesis of **Ox1**, **Ox2** and **Ox3**.

Inspired by the thermal activation of 1,2-oxazines at relatively moderate temperatures as well as the precedent for Diels–Alder adducts to undergo mechanochemically-induced [4 + 2] cycloreversion reactions,[173] we decided to examine the potential of 1,2-oxazines as a mechanophore. We find these Diels–Alder adducts particularly interesting due to the asymmetry

of the moiety compared to previously examined [4 + 2] adducts, such as the furan-maleimide adducts studied by Bo and coworkers. We suspect that the reactivity resulting from elongation of the *distal* isomer should differ from that of the *proximal* isomer (**Figure 5.2C**). The mechanochemical consequences of polymer attachment and elongation across a mechanophore has been previously explored, both experimentally and computationally, in a variety of different systems.[153,160,174–182] Our findings will further compliment the growing understanding of the structure-mechanochemical activity relationships that affect the mechanical activation of mechanophores. Furthermore, these 1,2-oxazine adducts are unique with respect to other

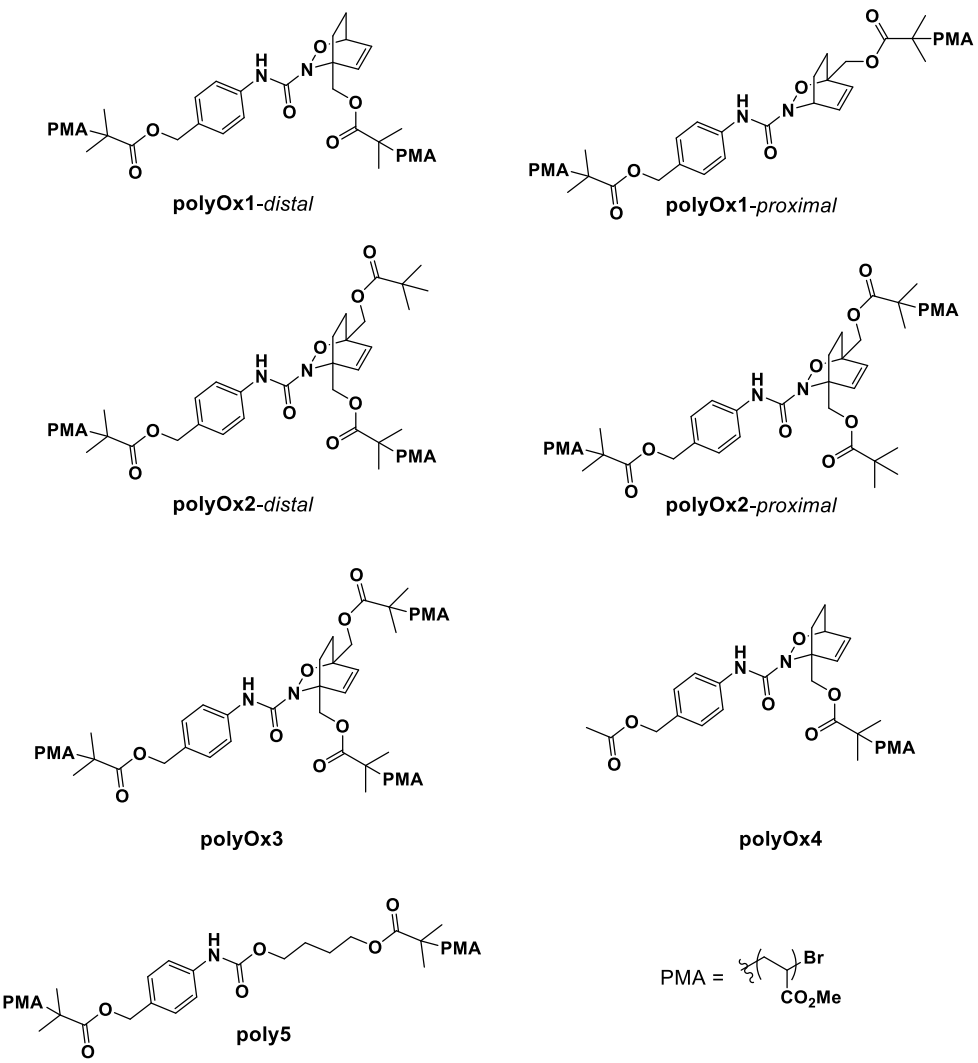

Figure 5.4 Structures of 1,2-oxazine containing polymers and control polymers.

mechanophores in their potential to trigger further downfield processes such as self-immolative polymer depolymerizations.[168]

5.3 Results and Discussion

Ox1, **Ox2**, **Ox3**, and **Ox4** were synthesized by the in-situ oxidation of the hydroxyurea component in the presence of the corresponding diene to form the Diels–Alder adduct (**Figure 5.3**). In the case of **Ox1**, the *distal* and *proximal* isomers were separated by straightforward column chromatography. For **Ox2**, a mono-protected 1,3-cyclohexadiene-1,4-diol using the bulky trityl-protecting group was used for the Diels–Alder reaction, which gave exclusively a single isomer. **Ox2-***distal* and **Ox2-***proximal* could then be obtained by alternating the order in which the polymerization initiator and pivaloyl chloride-capping moieties were installed.

PolyOx1-*distal*, **polyOx1**-*proximal*, **polyOx2**-*distal* and **polyOx2**-*proximal* were synthesized via atom transfer radical polymerization (ATRP) from their respective initiators producing polymers of ~60 kDa and narrow dispersity (**Table 5.2**). P**olyOx3** was similarly synthesized by ATRP, however, with a molecular weight of ~90 kDa. Previously we demonstrated that kinetic degradation comparisons of polymers with star and linear topologies must examine polymers with identical $M_{n,arm}$ as opposed to total molecular weight.[183,184] Control polymers **polyOx4** and **poly5** were also synthesized. In **polyOx4**, the oxazine should undergo no activation due to its terminal location on the polymer chain end and therefore should have a slower degradation kinetic profile than an oxazine-centered polymer. For **poly5** we wanted to verify that the carbamate-like linkage of the oxazine was not susceptible to preferential chain scission. **Figure 5.5** summarizes the structure of polymers studied.

Each polymer was sonicated in dry, N_2-purged THF at 13.8 W/cm^2 and its degradation was monitored by size exclusion chromatography (SEC) with in-line multi-angle light scattering

Table 5.1 Summary of k_{RI} for mechanochemical chain scission of control and oxazine-containing polymers.

Polymer	$M_{n,total}$ (kDa)	$M_{n,arm}$ (kDa)	k_{RI} ($\times 10^{-2}$ min^{-1})
polyOx1-proximal	59.2	29.6	0.99 ± 0.09
polyOx1-*distal*	59.3	29.6	1.06 ± 0.06
polyOx2-*proximal*			
polyOx2-*distal*			
polyOx3	90.7	30.2	1.35 ± 0.08
polyOx4	59.4	29.7	0.83 ± 0.06
poly5	57.8	28.9	0.83 ± 0.02

M_{total} (M_n values) determined by GPC analysis using multi-angle laser light scattering (MALS) to give M_w values from which M_n values were calculated. Rate constants were calculated from linear regression of the RI signal intensity at the M_p retention time of the virgin sample versus ultrasonication "on time" and are an average of three runs ± one standard deviation.

(MALS) and refractive index (RI) detector. The first-order rate constant for polymer degradation was determined by monitoring the depletion of the RI intensity corresponding to the P_{max} retention time of the parent polymer chromatogram as a function of sonication time.[185] The results obtained thus far are summarized in **Table 5.1**.

PolyOx4 in which the oxazine mechanophore is placed at the non-mechanochemically active polymer chain end and **poly5** in which no mechanophore is present at all, expectedly have identical chain scission rate constants of 0.83×10^{-2} min^{-1}. In the case of **poly5**, it is important to note that the presence of the centrally located carbamate linkage provides no preferential rate enhancement to chain scission.

Both **polyOx1** isomers displayed faster chain scission rate constants than the control polymers. Specifically, **polyOx1**-*proximal* had a rate constant of polymer breakdown of 0.99×10^{-2} min^{-1} while **polyOx1**-*distal* isomer had a slightly faster rate constant of 1.06×10^{-2} min^{-1}, in

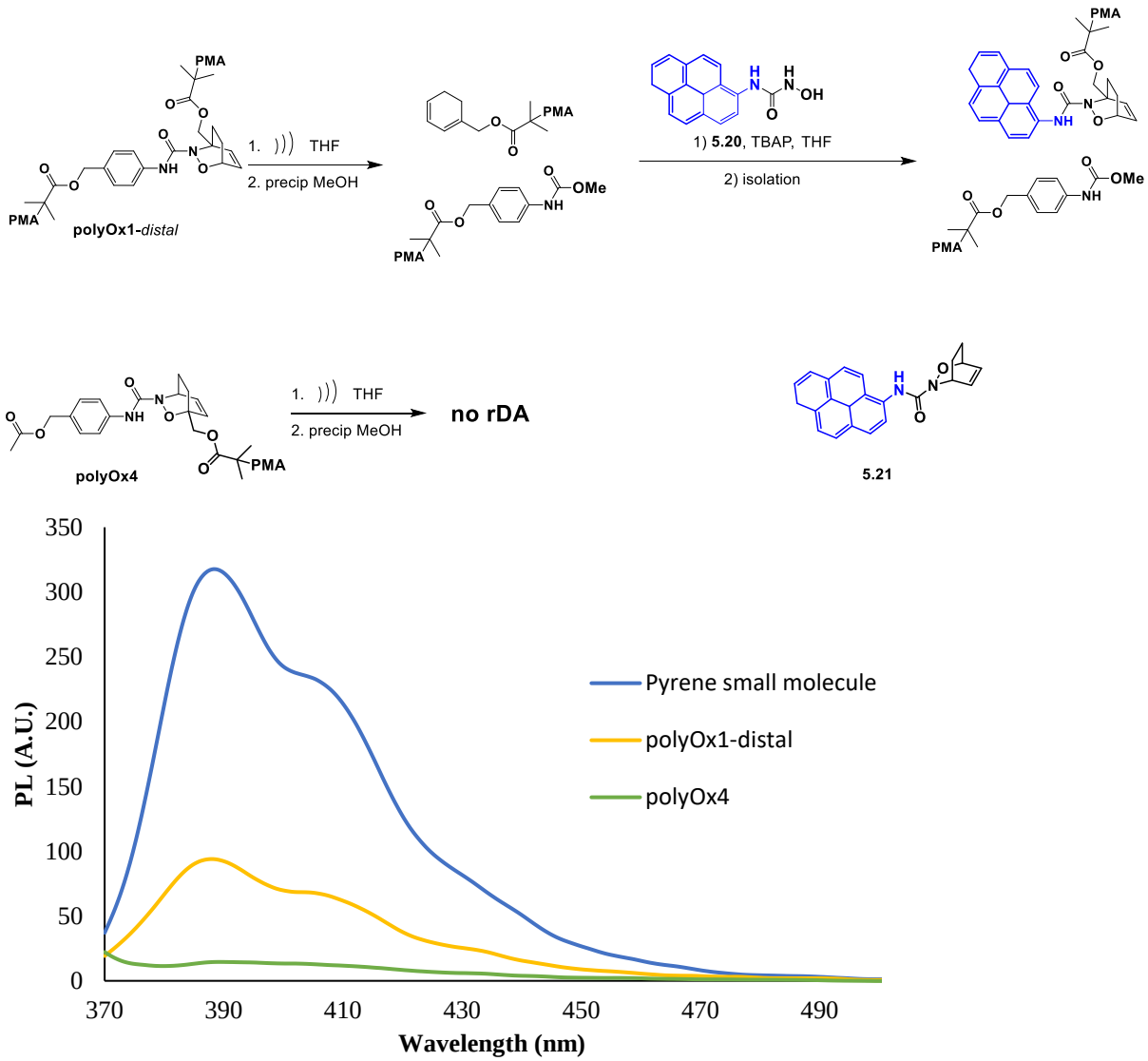

Figure 5.5 A) Reaction scheme for in situ oxidation and tagging of liberated diene with **5.20**.

B) Photoluminescent spectra of sonicated solutions of **polyOx1** and **polyOx4** in THF.

line with the relative cycloreversion activation barriers derived by CoGEF. The rate enhancement (~1.3 fold) of the latter relative to control polymers **polyOx4** and **poly5** is consistent with previous reports comparing polymer chain scission with and without a single chain-centered mechanophores under sonication conditions.[166,184] The similarities in rate constants of the **polyOx1** isomers, despite the large differences in activation energies to cycloreversion derived *in silico*, may be due to shortcomings of the CoGEF computational method.

PolyOx3 had an increased rate constant for polymer breakdown of 1.35×10^{-2} min^{-1}, a ~1.3 fold rate enhancement over **polyOx1** and ~1.6 fold enhancement over the control polymers. Analysis of polymer breakdown for **polyOx2** is necessary before any meaningful conclusions can be made about this result.

To confirm that the enhanced scission rate is due to oxazine cycloreversion, trapping studies were conducted via the in situ oxidation of **5.20** in the presence of sonicated solutions of **polyOx1**-*distal* and **polyOx4 (Figure 5.5A**). After subsequent purification of excess small molecule, photoluminescent measurements of the resulting polymer solutions clearly display a signal consistent with the pyrene fluorescent tag for the sonicated solution of **polyOx1**-*distal* while **polyOx4** displayed a complete absence of this signal (**Figure 5.5B**). This further corroborates the mechanochemically-induced cycloreversion of 1,2-oxazines as activation occurs only when the adduct is placed centrally within a polymer chain where the forces are greatest.

5.4 Conclusions

Preliminary evidence has been obtained that suggests the 1,2-oxazine moiety is mechanochemically active. Polymers that contain a chain-centered 1,2-oxazine degrade more rapidly under ultrasonic conditions than polymers in which this moiety is absent or at the chain end. Furthermore, trapping studies suggest that these enhancements in the rate of chain scission is due to cycloreversion of the 1,2-oxazine DA adduct. Full understanding of the structural properties that affect the mechanochemical activation of 1,2-oxazines will be vital for future applications of this mechanophore.

These adducts could make valuable contributions to the field of self-healing materials. Mechanical deformation of the material would mediate the cycloreversion process while spontaneous self-healing could occur under mild conditions once the mechanical load is removed.

Comparatively, the formation of the widely utilized furan-maleimide DA adduct requires temperatures near 70 °C for rapid adduct formation and material self-healing. Another unique characteristic of 1,2-oxazines is its ability to trigger self immolative polymer depolymerization upon cycloreversion and release of the nitrosocarbonyl dienophile. This property could be harnessed for a unique new class of mechanically degradable materials.

5.5 Experimental

5.5.a. General Considerations

Dry toluene, pyridine, and CH_2Cl_2 were obtained from a Glass Contour solvent purification system. Et_3N and methyl acrylate were distilled under N_2 after drying over CaH_2 overnight. All other reagents and solvents were used as obtained from commercial sources. Compounds **5.6**,[186] **5.7**,[187] **5.9**,[188,189] and **5.17**[190] were prepared according to literature procedure. ^1H and ^{13}C NMR spectra were recorded on a Bruker AVance 300 or 500 MHz spectrometer. Chemical shifts are reported in delta (δ) units, expressed in parts per million (ppm) downfield from tetramethyl silane using the residual protio-solvent as an internal standard ($CDCl_3$, ^1H: 7.26 ppm and ^{13}C: 77.2 ppm). LRMS was performed on a Bruker Esquire equipped with either an electrospray ionization (ESI) or IonSense SVP100 DART source. GPC setup consists of an Agilent 1260 Infinity II HPLC pump, three in-line MZ-Gel 10 μm size-exclusion columns (pore sizes = 10^3, 10^3, and 10^5 Å), miniDAWN-TREOS 3-angle multi-angle laser light scatter and OptiLab T-rEx refractive index detectors (each from Wyatt Technologies Corporation). The mobile phase consisted of HPLC grade THF. No calibration standards were used, and dn/dc values were obtained for each injection assuming 100% mass elution from the columns. Sonication experiments were done using a 20 kHz Sonics VSX series sonication probe (1.2 cm tip diameter) calibrated according to literature

procedures.[186] Fluorescence spectroscopy was conducted using a Perkin Elmer Luminescence Spectrometer LS 50 B.

5.5.b. Synthetic Procedures

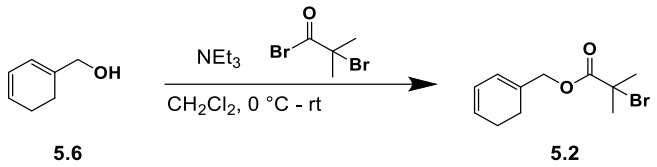

5.6 **5.2**

*Synthesis of **2***

Into a flame-dried round bottom flask, **5.6** (60 mg, 0.55 mmol, 1.0 equiv.), dry CH_2Cl_2 (1 mL) and a magnetic stir bar were added. The reaction mixture was placed in an ice bath. NEt_3 (85 µL, 0.61 mmol, 1.1 equiv.) was then added to the solution. A solution of α-bromoisobutyryl bromide (75 µL, 0.61 mmol, 1.1 equiv.) in dry CH_2Cl_2 (1 mL) was then added dropwise. The reaction mixture was stirred for 18 h, during which time the ice bath expired. The solvent was removed under reduced pressure. The crude residue was taken up in ether and washed successively with DI H_2O (2 × 10 mL), sat. $NaHCO_3$ (2 × 10 mL) and brine (1 × 10 mL). The organic layer was dried over Na_2SO_4, filtered through a thin pad of Celite, and concentrated under reduced pressure. The product was isolated via flash column chromatography (10% EtOAc/hexanes) to obtain a colorless transparent oil in 65% yield. ^{1}H NMR (500 MHz, $CDCl_3$) δ 6.09 – 5.72 (m, 2H), 4.66 (s, 2H), 2.20 (s, 4H), 1.95 (s, 6H). ^{13}C NMR (126 MHz, $CDCl_3$) Need spectra for both. δ LRMS (ESI): $[M+Na]^+$ calc for…

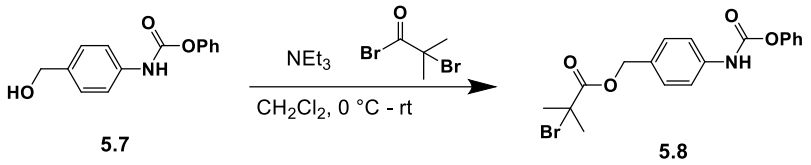

5.7 5.8

*Synthesis of **5.8***

Into a flame-dried round bottom flask, **5.7** (1.0 g, 4.11 mmol, 1.0 equiv.), dry CH_2Cl_2 (14 mL) and a magnetic stir bar were added. The reaction mixture was placed in an ice bath. NEt_3 (0.64 mL, 4.52 mmol, 1.1 equiv.) was then added to the solution. A solution of α-bromoisobutyryl bromide (0.56 mL, 4.52 mmol, 1.1 equiv.) in dry CH_2Cl_2 (4 mL) was then added dropwise. The reaction mixture was stirred for 18 h, during which time the ice bath expired. The solvent was removed under reduced pressure. The crude residue was taken up in diethyl ether and washed successively with DI H_2O (2 × 10 mL), sat. $NaHCO_3$ (2 × 10 mL) and brine (1 × 10 mL). The organic layer was dried over Na_2SO_4, filtered through a thin pad of Celite, and concentrated under reduced pressure. The product was isolated via flash column chromatography (20% EtOAc/hexanes) to obtain a yellow crystalline solid in 68% yield. ^{1}H NMR (500 MHz, $CDCl_3$) δ 7.66 – 7.04 (m, 9H), 5.20 (s, 2H), 1.98 (s, 6H). ^{13}C NMR (126 MHz, $CDCl_3$) δ 171.6, 151.8, 150.6, 137.7, 130.8, 129.5, 129.1, 125.8, 121.7, 118.9, 67.3, 55.8, 30.8. LRMS (ESI): $[M+NH_4]^+$ calcd for $C_{18}H_{22}BrN_2O_4$, 409.07, found 409.1.

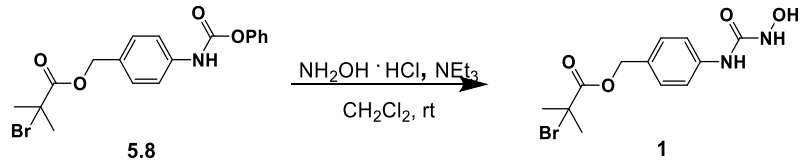

5.8 1

*Synthesis **5.1***

Into a flame-dried round bottom flask, **5.8** (2.37 g, 6.04 mmol, 1.0 equiv.), hydroxylamine hydrochloride (629 mg, 9.06 mmol, 1.5 eq.), dry CH_2Cl_2 (12 mL) and a magnetic stir bar were added. NEt_3 (2.55 mL, 18.12 mmol, 3 equiv.) was then added to the solution. The reaction mixture was stirred for 18 h at room temperature. The solvent was removed under reduced pressure. The crude residue was taken up in ethyl acetate and washed with brine (3 × 50 mL). The organic layer was dried over Na_2SO_4, filtered through a thin pad of Celite, and concentrated under reduced pressure. The residual solids were suspended in diethyl ether, filtered and washed with diethyl ether. The product was obtained as an off white solid in 44% yield. ^{1}H NMR (500 MHz, DMSO) δ 9.00 (s, 1H), 8.89 (d, J = 3.3 Hz, 2H), 7.64 (d, J = 8.3 Hz, 2H), 7.28 (d, J = 8.3 Hz, 2H), 5.12 (s, 2H), 1.90 (s, 6H). ^{13}C NMR (126 MHz, $CDCl_3$) δ 170.7, 158.6, 139.5, 129.0, 128.5, 119.1, 67.0, 57.3, 30.3. LRMS (ESI): $[M-1]^-$ calcd for $C_{12}H_{14}BrN_2O_4$, 329.01, found 328.8.

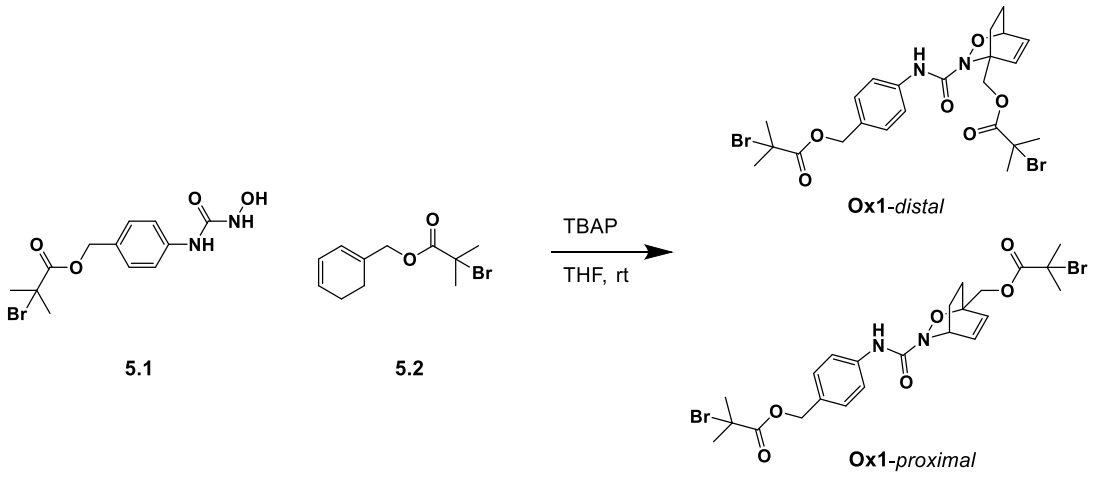

*Synthesis of **Ox1***

Into a round bottom flask, **5.1** (128 mg, 0.39, 1.1 eq.), **5.2** (95 mg, 0.36 mmol, 1.0 eq.), THF (2 mL) and a magnetic stir bar were added. Tetrabutylammonium periodate (169 mg, 0.39 mmol,

1.1 eq.) was then added. The reaction was allowed to stir at room temperature for 3 hours. Ethyl acetate (10 mL) was added, and the reaction mixture was washed with sat. sodium bisulfite (2 × 10 mL), sat. $NaHCO_3$ (1 × 10 mL0, 1 M HCl (1 × 10 mL) and diH_2O (1 × 10 mL). The organic layer was dried over Na_2SO_4, filtered through a thin pad of Celite, and concentrated under reduced pressure. Each isomer was isolated via flash column chromatography (gradient 20 - 40% EtOAc/hexanes) to obtain the proximal isomer (54% yield) and *distal* (6% yield) as yellow oils. *Proximal Isomer:* ^{1}H NMR (500 MHz, $CDCl_3$) δ 7.77 (s, 1H), 7.49 (d, J = 7.7 Hz, 2H), 7.30 (d, J = 7.9 Hz, 2H), 6.67 (t, J = 6.9 Hz, 1H), 6.44 (d, J = 8.4 Hz, 1H), 5.14 (s, 2H), 5.03 (s, 1H), 4.56 (d, J = 12.5 Hz, 1H), 4.42 (d, J = 12.5 Hz, 1H), 2.23 (t, J = 11.1 Hz, 1H), 2.06 (d, J = 14.9 Hz, 2H), 1.94 (d, J = 6.3 Hz, 6H), 1.92 (s, 6H), 1.67 (t, J = 12.3 Hz, 1H), 1.37 (t, J = 10.3 Hz, 1H). ^{13}C NMR (126 MHz, $CDCl_3$) δ 171.5, 171.4, 159.3, 137.8, 133.6, 130.5, 129.6, 129.0, 119.5, 78.0, 67.3, 66.5, 55.8, 55.2, 50.4, 30.8, 30.7, 30.7, 26.3, 20.5. LRMS (ESI): $[M+Na]^+$ calcd for $C_{23}H_{29}Br_2N_2O_6$, 587.04, found 587.9.

Distal Isomer: ^{1}H NMR (500 MHz, $CDCl_3$) δ 7.83 (s, 1H), 7.41 (d, J = 7.8 Hz, 2H), 7.30 (d, J = 8.0 Hz, 2H), 6.60 – 6.50 (m, 2H), 5.24 (d, J = 11.3 Hz, 1H), 5.13 (s, 2H), 5.01 – 4.81 (m, 2H), 2.29 (dd, J = 14.5, 7.0 Hz, 1H), 2.14 (t, J = 13.4 Hz, 1H), 1.95 (d, J = 4.4 Hz, 7H), 1.91 (s, 7H), 1.70 (t, J = 12.2 Hz, 1H), 1.44 (dt, J = 16.3, 8.2 Hz, 1H). ^{13}C NMR (126 MHz, $CDCl_3$) Spectra for ^{13}C δ LRMS (ESI): $[M+1]^+$ calcd for $C_{23}H_{29}Br_2N_2O_6$, 587.04, found 587.4.

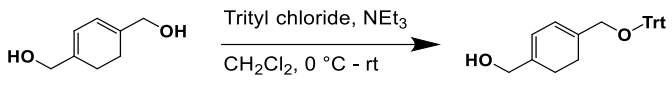

5.9 **5.3**

*Synthesis of **5.3***

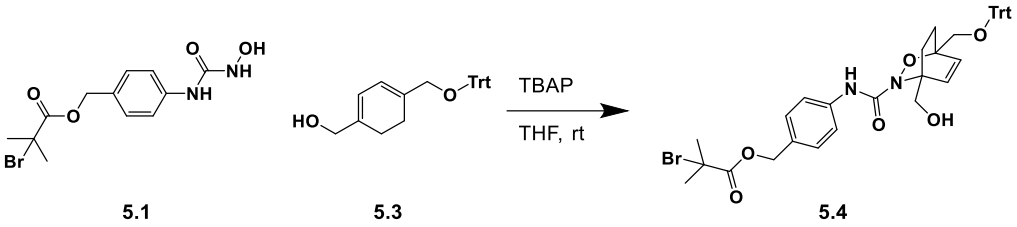

5.1 5.3 5.4

*Synthesis of **5.4***

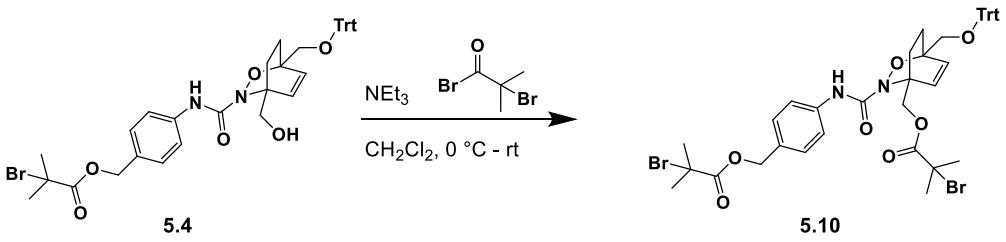

5.4 5.10

*Synthesis of **5.10***

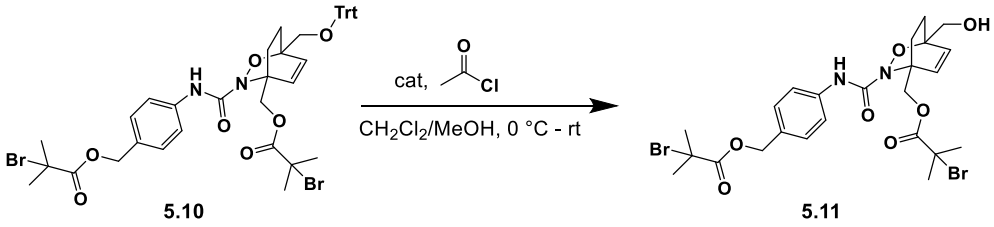

5.10 5.11

*Synthesis of **5.11***

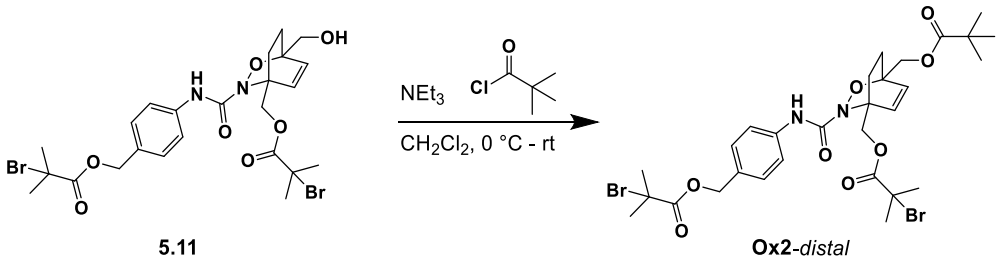

5.11 **Ox2**-*distal*

Synthesis of ***Ox2-distal***

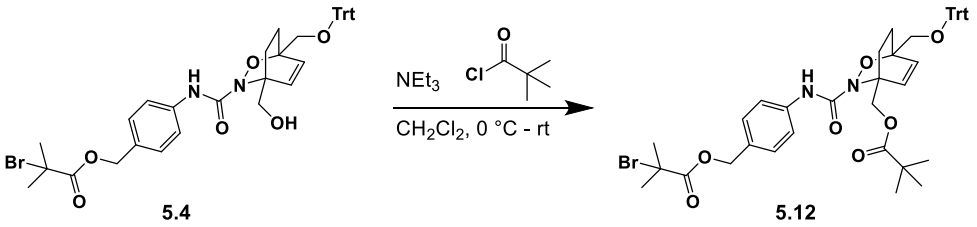

5.4 **5.12**

Synthesis of ***5.12***

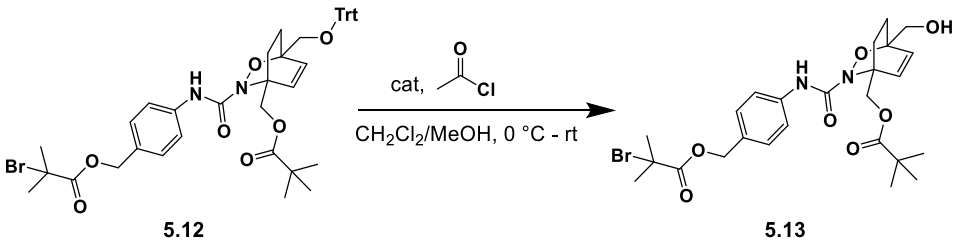

5.12 **5.13**

Synthesis of ***5.13***

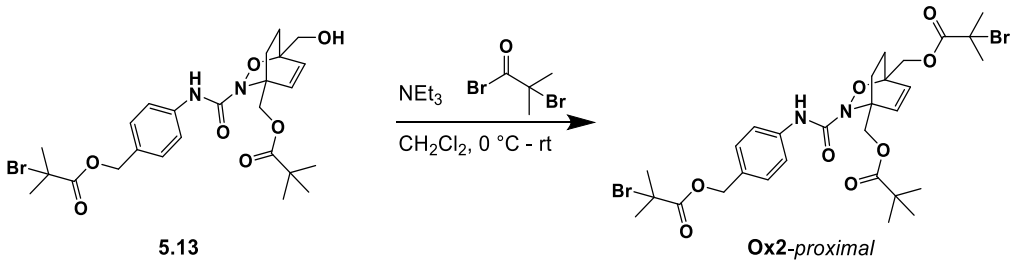

5.13 **Ox2**-*proximal*

Synthesis of ***Ox2****-proximal*

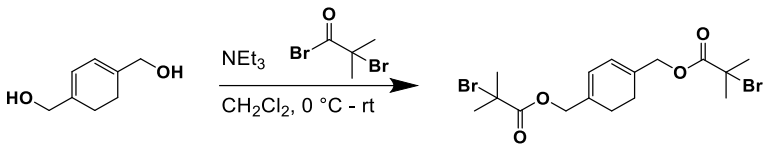

5.9 **5.5**

*Synthesis of **5.5***

Into a flame-dried round bottom flask, **5.9** (60 mg, 0.55 mmol, 1.0 equiv.), dry CH_2Cl_2 (1 mL) and a magnetic stir bar were added. The reaction mixture was placed in an ice bath. NEt_3 (85 µL, 0.61 mmol, 1.1 equiv.) was then added to the solution. A solution of α-bromoisobutyryl bromide (75 µL, 0.61 mmol, 1.1 equiv.) in dry CH_2Cl_2 (1 mL) was then added dropwise. The reaction mixture was stirred for 18 h, during which time the ice bath expired. The solvent was removed under reduced pressure. The crude residue was taken up in ether and washed successively with DI H_2O (2 × 10 mL), sat. $NaHCO_3$ (2 × 10 mL) and brine (1 × 10 mL). The organic layer was dried over Na_2SO_4, filtered through a thin pad of Celite, and concentrated under reduced pressure. The product was isolated via flash column chromatography (10% EtOAc/hexanes) to obtain a colorless transparent oil in 65% yield. ^1H NMR (500 MHz, $CDCl_3$) δ5.85 (s, 2H), 4.54 (s, 4H), 2.13 (s, 4H), 1.81 (s, 12H). ^{13}C NMR (126 MHz, $CDCl_3$) δ 170.8, 132.5, 121.6, 68.0, 55.6, 30.6, 23.6. $[M+NH_4]^+$ calcd for $C_{16}H_{26}Br_2NO_4$, 454.02, found 454.3.

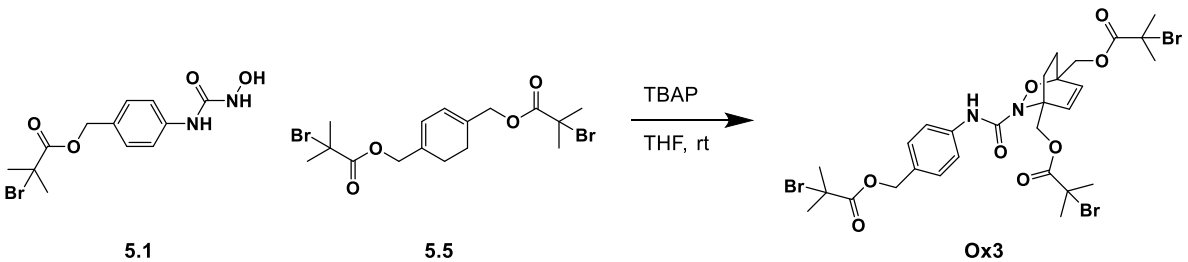

5.1 **5.5** **Ox3**

*Synthesis of **Ox3***

Into a round bottom flask, **1** (149 mg, 0.45, 1.3 eq.), **5** (152 mg, 0.35 mmol, 1.0 eq.), THF (3 mL) and a magnetic stir bar were added. Tetrabutylammonium periodate (195 mg, 0.45 mmol, 1.3 eq.) was then added. The reaction was allowed to stir at room temperature for 3 hours. Ethyl acetate (10 mL) was added, and the reaction mixture was washed with sat. sodium bisulfite (2 × 10 mL), sat. $NaHCO_3$ (1 × 10 mL0, 1 M HCl (1 × 10 mL) and diH_2O (1 × 10 mL). The organic layer was dried over Na_2SO_4, filtered through a thin pad of Celite, and concentrated under reduced pressure. The product was isolated via flash column chromatography (gradient 20 - 30% EtOAc/hexanes) to obtain a yellow oil in 38% yield. ^{1}H NMR (500 MHz, $CDCl_3$) δ 7.92 (s, 1H), 7.46 (d, J = 7.9 Hz, 2H), 7.29 (d, J = 7.9 Hz, 2H), 6.68 (d, J = 8.4 Hz, 1H), 6.45 (d, J = 8.4 Hz, 1H), 5.29 (d, J = 24.8 Hz, 1H), 5.13 (s, 2H), 4.90 (d, J = 11.3 Hz, 1H), 4.66 (d, J = 12.6 Hz, 1H), 4.41 (d, J = 12.7 Hz, 1H), 2.38 – 2.10 (m, 2H), 1.90 (dd, J = 26.5, 12.1 Hz, 18H), 1.79 (t, J = 12.0 Hz, 1H), 1.42 (t, J = 13.3 Hz, 1H). ^{13}C NMR (126 MHz, $CDCl_3$) δ 171.8, 171.5, 171.1, 159.7, 137.7, 135.8, 131.0, 129.1, 129.0, 120.2, 78.6, 67.9, 67.4, 66.2, 61.5, 55.9, 55.0, 30.9, 30.9, 30.8, 30.7, 28.5, 24.6. LRMS (ESI): $[M+NH_4]^+$ calcd for $C_{28}H_{39}Br_3N_3O_8$, 782.02, found 782.6.

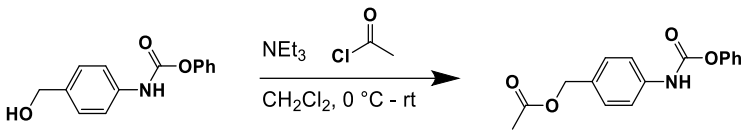

5.8 **5.14**

*Synthesis of **5.14***

Into a flame-dried round bottom flask, **5.8** (2.56g, 10.52 mmol, 1.0 equiv.), dry CH_2Cl_2 (50 mL) and a magnetic stir bar were added. The reaction mixture was placed in an ice bath. NEt_3 (1.62 mL, 11.57 mmol, 1.1 equiv.) was then added to the solution. A solution of acetyl chloride (0.83 mL, 11.57 mmol, 1.1 equiv.) in dry CH_2Cl_2 (12 mL) was then added dropwise. The reaction

mixture was stirred for 18 h, during which time the ice bath expired. The solvent was removed under reduced pressure. The crude residue was taken up in diethyl ether and washed successively with DI H_2O (2 × 10 mL), sat. $NaHCO_3$ (2 × 10 mL) and brine (1 × 10 mL). The organic layer was dried over Na_2SO_4, filtered through a thin pad of Celite, and concentrated under reduced pressure. Clean product obtained as an off-white crystalline solid in 93% yield. ^{1}H NMR (500 MHz, $CDCl_3$) δ 7.57 – 7.12 (m, 9H), 5.10 (s, 2H), 2.14 (s, 3H). ^{13}C NMR (126 MHz, $CDCl_3$) δ 171.0, 151.8, 150.6, 137.7, 131.3, 129.4, 129.3, 125.7, 121.6, 119.0, 65.9, 21.0. LRMS (ESI): $[M+Na]^+$ calcd for $NaC_{16}H_{15}NO_4$, 308.09, found 308.1.

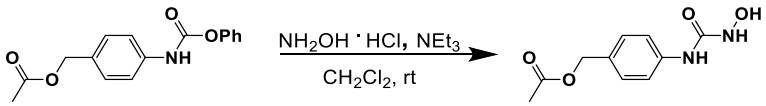

5.14 **5.15**

*Synthesis of **5.15***

Into a flame-dried round bottom flask, **5.14** (2.57 g, 9.01 mmol, 1.0 equiv.), hydroxylamine hydrochloride (939 mg, 13.52 mmol, 1.5 eq.), dry CH_2Cl_2 (18 mL) and a magnetic stir bar were added. NEt_3 (3.80 mL, 27.03 mmol, 3 equiv.) was then added to the solution. The reaction mixture was stirred for 18 h at room temperature. The solvent was removed under reduced pressure. The crude residue was taken up in ethyl acetate and washed with brine (3 × 50 mL). The organic layer was dried over Na_2SO_4, filtered through a thin pad of Celite, and concentrated under reduced pressure. The residual solids were suspended in diethyl ether, filtered and washed with diethyl ether. The product was obtained as a off white solid in 75% yield. ^{1}H NMR (500 MHz, DMSO) δ 9.00 (s, 1H), 8.87 (d, J = 9.0 Hz, 2H), 7.63 (d, J = 7.8 Hz, 2H), 7.25 (d, J = 7.9 Hz, 2H),

4.98 (s, 2H), 2.03 (s, 3H). ^{13}C NMR (126 MHz, DMSO) δ 170.4, 158.6, 139.4, 129.7, 128.8, 119.1, 65.5, 20.8. LRMS (ESI): $[M - 1]^-$ calcd for $C_{10}H_{11}N_2O_4$, 223.07, found 223.4.

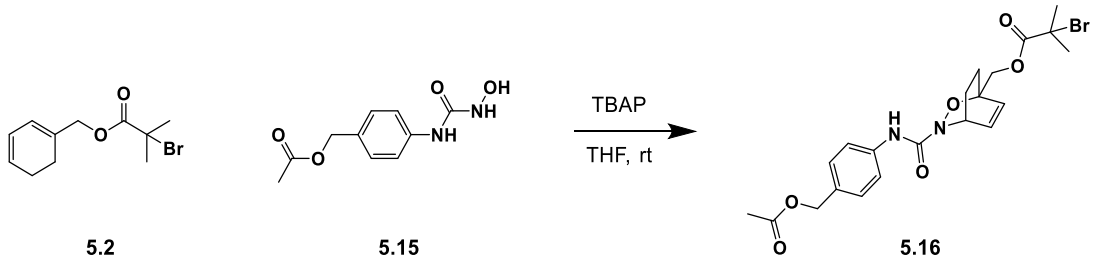

5.2 **5.15** **5.16**

*Synthesis of **5.16***

Into a round bottom flask, **5.2** (138 mg, 0.53 mmol, 1.0 eq.), **5.15** (130 mg, 0.58, 1.1 eq.), THF (3 mL) and a magnetic stir bar were added. Tetrabutylammonium periodate (251 mg, 0.58 mmol, 1.1 eq.) was then added. The reaction was allowed to stir at room temperature for 3 hours. Ethyl acetate (10 mL) was added and the reaction mixture was washed with sat. sodium bisulfite (2 × 10 mL), sat. $NaHCO_3$ (1 × 10 mL0, 1 M HCl (1 × 10 mL) and diH_2O (1 × 10 mL). The organic layer was dried over Na_2SO_4, filtered through a thin pad of Celite, and concentrated under reduced pressure. The *proximal* isomer was isolated via flash column chromatography (30% EtOAc/hexanes) to obtain a yellow oil in 23% yield. ^{1}H NMR (500 MHz, $CDCl_3$) δ 7.73 (s, 1H), 7.48 (d, J = 8.5 Hz, 2H), 7.29 (d, J = 8.1 Hz, 2H), 6.76 – 6.61 (m, 1H), 6.44 (d, J = 8.4 Hz, 1H), 5.04 (s, 3H), 4.57 (d, J = 12.5 Hz, 1H), 4.41 (d, J = 12.5 Hz, 1H), 2.25 (t, J = 6.6 Hz, 1H), 2.07 (q, J = 4.6 Hz, 4H), 1.95 (d, J = 3.4 Hz, 6H), 1.73 – 1.61 (m, 1H), 1.38 (td, J = 11.8, 4.0 Hz, 1H). ^{13}C NMR (126 MHz, $CDCl_3$) 171.7, 171.1, 159.4, 137.8, 133.7, 131.2, 129.6, 129.3, 119.6, 78.0, 66.6, 66.1, 55.2, 50.4, 30.8, 26.4, 21.2, 20.6. Better spectra for both. LRMS (ESI):

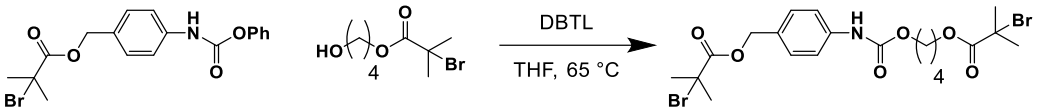

5.8 **5.17** **5.18**

*Synthesis of **5.18***

Into a flame-dried, N_2-purged round bottom flask, **5.8** (400 mg, 1.02 mmol, 1.0 eq.), **5.17** (268 mg, 1.12, 1.1 eq.), dry THF (2 mL) and a magnetic stir bar were added. Dibutyltin dilaurate (30 µL, 0.051 mmol, 0.05 eq.) was added and the reaction mixture was placed in a pre-heated oil bath. After 24 hours, ether was added and the organic layer was washed with 1 M NaOH (2 × 5 mL) and brine (1 × 5 mL). The organic layer was dried over Na_2SO_4, filtered through a thin pad of Celite, and concentrated under reduced pressure. The product was isolated via flash column chromatography (20% EtOAc/hexanes) to obtain a colorless oil in 60% yield ^{1}H NMR (500 MHz, $CDCl_3$) δ 7.39 (d, 2H), 7.32 (d, J = 8.1 Hz, 2H), 6.80 (s, 1H), 4.23 (s, 4H), 1.93 (s, 12H), 1.80 (s, 4H). ^{13}C NMR (126 MHz, $CDCl_3$) δ 171.9, 171.6, 129.3, 118.7, 67.4, 65.5, 64.9, 56.0, 55.9, 30.8, 25.5, 25.3. Better spectra for both. LRMS (ESI): $[M+Na]^+$ calcd for $NaC_{20}H_{27}Br_2NO_6$, 558.01, found 558.3.

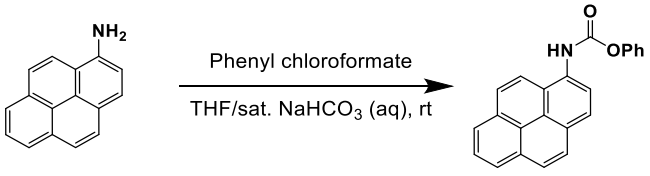

5.19

*Synthesis of **5.19***

Into a round bottom flask, 1-aminopyrene (300.0 mg, 1.38 mmol, 1.0 eq.) was dissolved in a mixture of THF (1.4 mL), sat. $NaHCO_3$ aq. (1.4 mL) and diH_2O (0.7 mL). Phenyl chloroformate (0.19 mL, 1.52 mmol, 1.1 eq.) was then added dropwise to the reaction mixture while stirring. Tan solids immediately precipitated out of solution upon addition. After 1.5 hours, the solids were filtered and washed subsequently with diH_2O, THF and diethyl ether. Solids were then dried under reduced pressure to give 325 mg (75% yield) of a tan solid. Product was used in the next step without any further purification. Limited solubility precluded the acquisition of adequate ^1H and ^{13}C NMR spectra. LRMS (ESI): $[M+1]^+$ calcd for $C_{23}H_{16}NO_2$, 338.12, found 338.0.

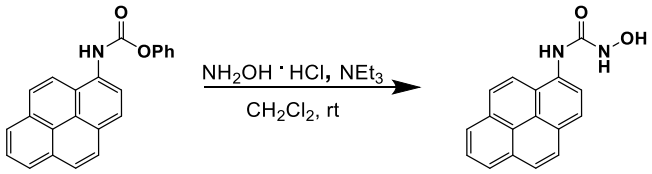

5.19 **5.20**

*Synthesis of **5.20***

Into a round bottom flask, **5.19** (309.0 mg, 0.99 mmol, 1.0 eq.), hydroxylamine hydrochloride (342 mg, 4.93 mmol, 5.0 eq.), dry CH_2Cl_2 (5.0 mL) and a magnetic stir bar were added. NEt_3 (1.4 mL, 9.86 mmol, 10.0 equiv.) was then added to the solution. The suspended solids gradually changed color from tan to pale yellow. The solids were filtered and copiously washed with CH_2Cl_2. The product was obtained as a pale yellow solid 196 mg (70% yield). ^1H NMR (500 MHz, DMSO) δ ^{13}C NMR (126 MHz, $CDCl_3$) δ LRMS (ESI): $[M-1]^-$ calcd for $C_{17}H_{11}N_2O_2$, 275.08, found 275.2.

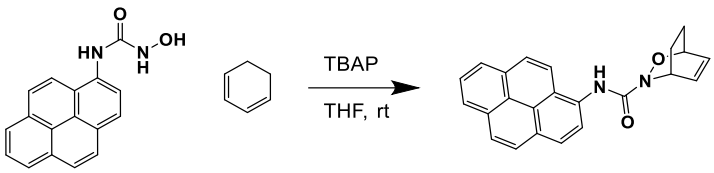

5.20 **5.21**

*Synthesis of **5.21***

Into a round bottom flask, **5.20** (50.0 mg, 0.18 mmol, 1.0 eq.), 1,3-cyclohexadiene (22.0 µL, 0.23 mmol, 1.3 eq.), THF (4 mL) and a magnetic stir bar were added. Tetrabutylammonium periodate (78.0 mg, 0.18 mmol, 1.0 eq.) was then added to the reaction mixture. Reaction mixture was stirred for 4 hours. Ethyl acetate (10 mL) was added and the reaction mixture was washed with sat. sodium bisulfite (2 × 10 mL), sat. $NaHCO_3$ (1 × 10 mL0, 1 M HCl (1 × 10 mL) and diH_2O (1 × 10 mL). The organic layer was dried over Na_2SO_4, filtered through a thin pad of Celite, and concentrated under reduced pressure. The product was isolated via flash column chromatography (30% EtOAc/hexanes) to obtain a yellow oil (55 mg, 86% yield). ^{1}H NMR (500 MHz, $CDCl_3$) δ ^{13}C NMR (126 MHz, $CDCl_3$) Spectra for both. LRMS (ESI):

Representative Polymerization Procedure

In a nitrogen-filled dry box, initiator **Ox1**-*distal* (20.7 mg, 0.035 mmol, 1.0 equiv.), methyl acrylate (3.17 mL, 35 mmol, 1000 equiv.), dry DMF (5.6 mL) and a magnetic stir bar were added into a scintillation vial. A solution of CuBr (5.0 mg, 0.035 mmol, 1.0 equiv.) and PMDETA (7.3 µL, 0.035 mmol, 1.0 equiv.) in DMF (0.6 mL) was then added to reaction mixture. The vial was sealed with a Teflon-lined screw cap and the reaction solution was stirred at room temperature for 18 h. The viscous solution was then added dropwise into an excess of MeOH causing the polymer to precipitate from solution. The solvent was decanted and the resulting polymer residue was rinsed with MeOH (3 × 20 mL). The polymer was dissolved in CH_2Cl_2 (10 mL) and filtered

through a plug of neutral alumina to remove residual copper. The solvent was removed under reduced pressure and the resulting polymeric residue was further dried under reduced pressure. General structures are shown in Figure 7.4, and data from GPC analysis is given in Table 7.3.

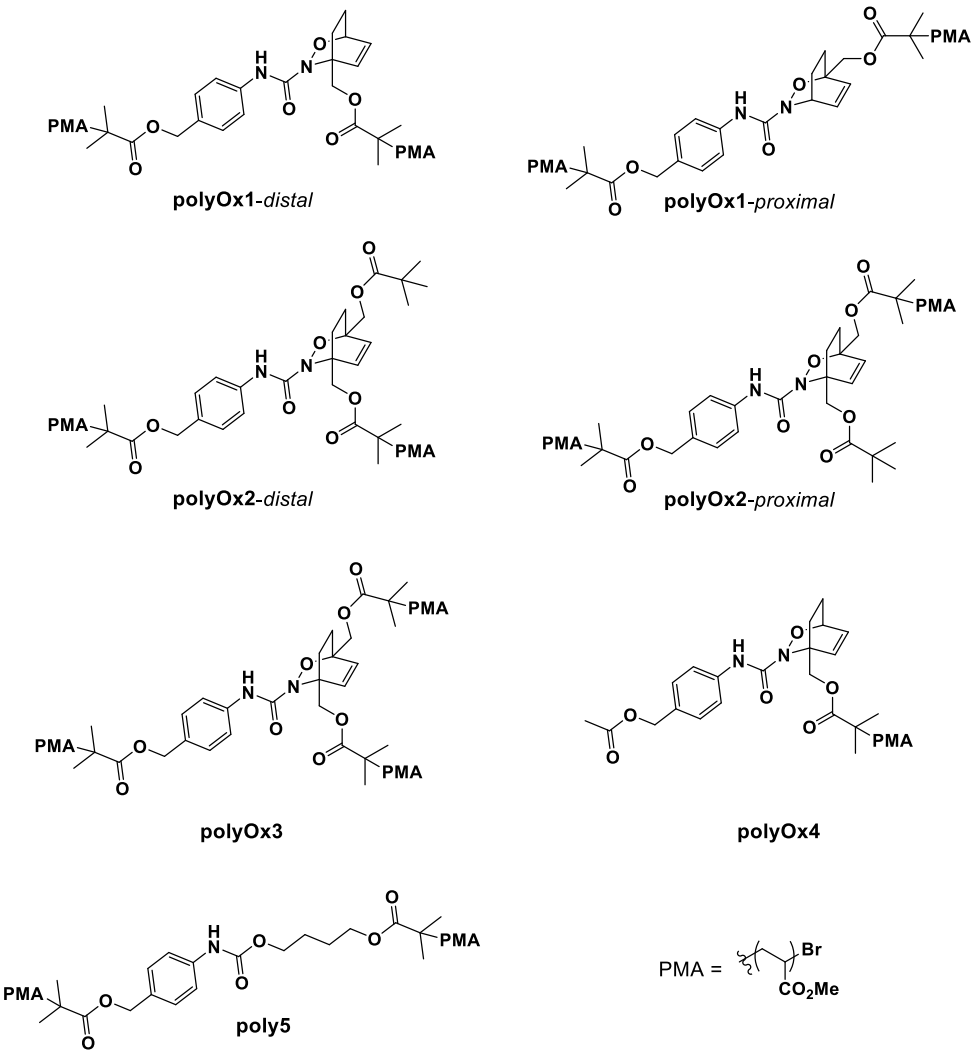

Figure 5.6. Structure of polymers investigated in this study.

Table 5.2. Polymer molecular weights and dispersity.

Polymer	M_n (kDa)	Đ
polyOx1-proximal	59.2	1.07

polyOx1-*distal*	59.3	1.05
polyOx3	90.7	1.04
polyOx4	59.4	1.06
Poly5	57.8	1.08

Sonication Procedure

Sonication experiments were done in a flame-dried, N_2-purged Suslick flask, with the sonication horn (1 cm diameter) already attached to Suslick flask. Each arm of the Suslick flask was fitted with a rubber septum. In a separate flame-dried round bottom flask, the polymer sample was dissolved in dry THF at a concentration of 5 mg/ml. The polymer solution was then transferred to the Suslick flask under dry N_2 via syringe. The entire apparatus (sonication horn + Suslick flask) was then transferred to a cold room (4 °C) for the duration of sonication experiment. Polymer solutions were sonicated at 13.8 W/cm^2 for a pulse of 1s on, 9s off. Aliquots of 0.5 mL were withdrawn from the reaction periodically and analyzed by GPC.

Procedure for Tagging and Isolation of Mechanochemically Liberated Diene

A **polyOx1**-*distal* solution in dry THF (5 mg/mL, 12 mL) was sonicated for 220 minutes of total on time consisting of the following time points: 20, 40, 60, 80, 100, 120, 140, 180, and 220 minutes. The sonicated solution was carefully poured into a round bottom flask and MeOH (12 mL) was then added to the solution mixture to quench any residual acyl nitroso end groups. The solution was then concentrated (~100 mg/mL) under reduced pressure and precipitated into MeOH

(10 mL). The supernatant was removed and the residual polymer was washed with diethyl ether and dried, providing 50 mg of polymer. The polymer was dissolved in 3 mL of THF. **PyrHU** (13 mg, 0.05 mmol) and tetrabutylammonium periodate (20.4 mg, 0.05 mmol) were then added and the reaction mixture was allowed to stir for 5 hours at room temperature. The tagged polymer was then isolated from the small molecule reaction mixture via size exclusion chromatography (see GPC setup under *General Considerations*) and collection of the waste stream corresponding to the polymer retention times (17 – 27 minutes). The photoluminescence emission spectrum of the resulting polymer solution was collected from 370 to 600 nm using an excitation wavelength of 360 nm.

5.5.c ^{1}H and ^{13}C NMR spectra

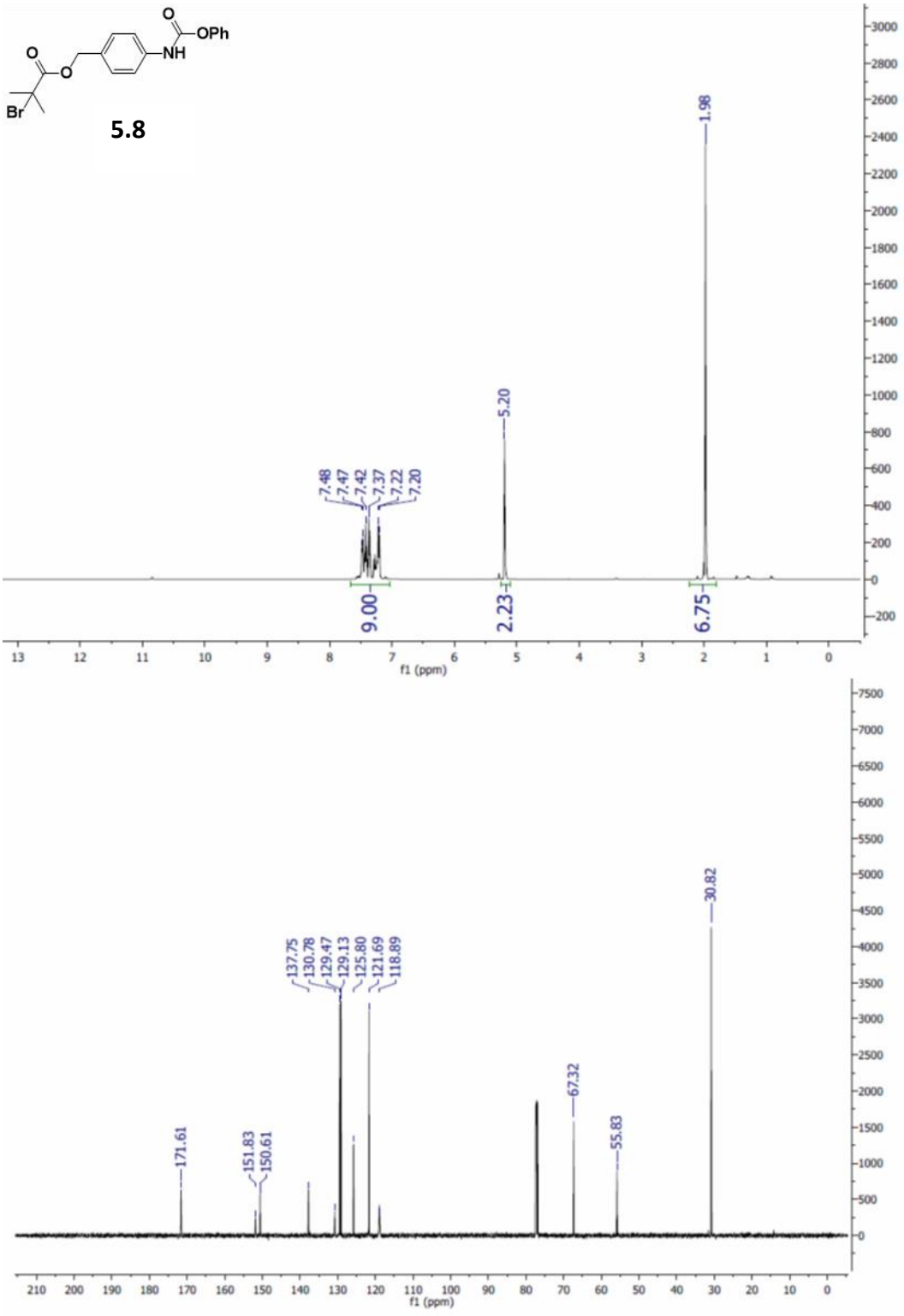

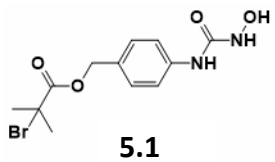
O
OH
NH
NH
O
O
Br

5.1

9.00
8.89
8.88
7.65
7.63
7.29
7.27
5.12
1.90
0.87
1.94
1.67
1.71
2.04
6.00
f1 (ppm)

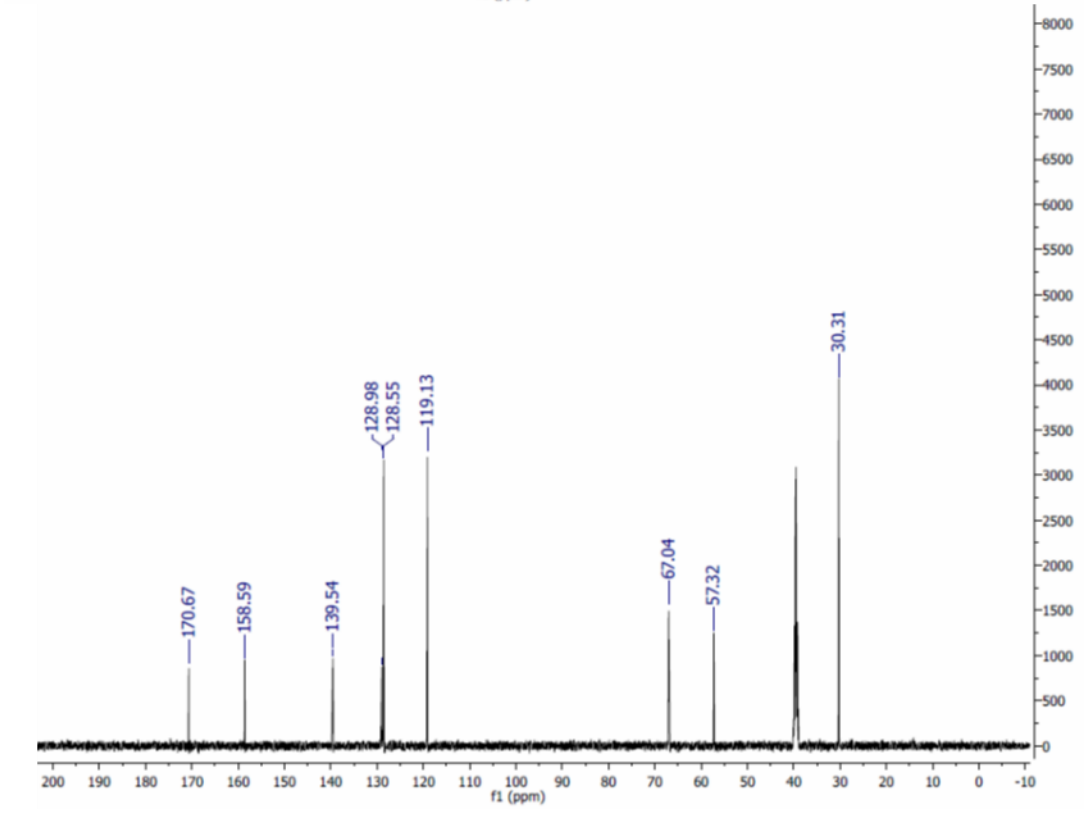
170.67
158.59
139.54
128.98
128.55
119.13
67.04
57.32
30.31
f1 (ppm)

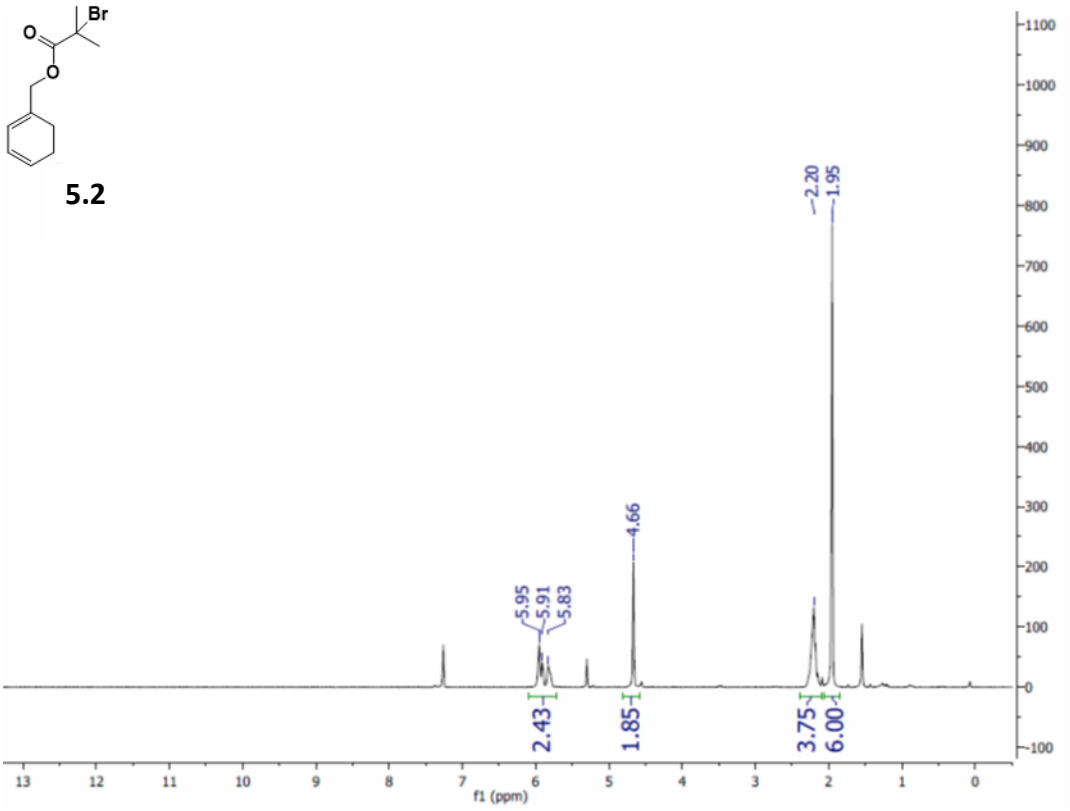
Br
O
O
5.2
2.20
1.95
4.66
5.95
5.91
5.83
2.43
1.85
3.75
6.00
f1 (ppm)

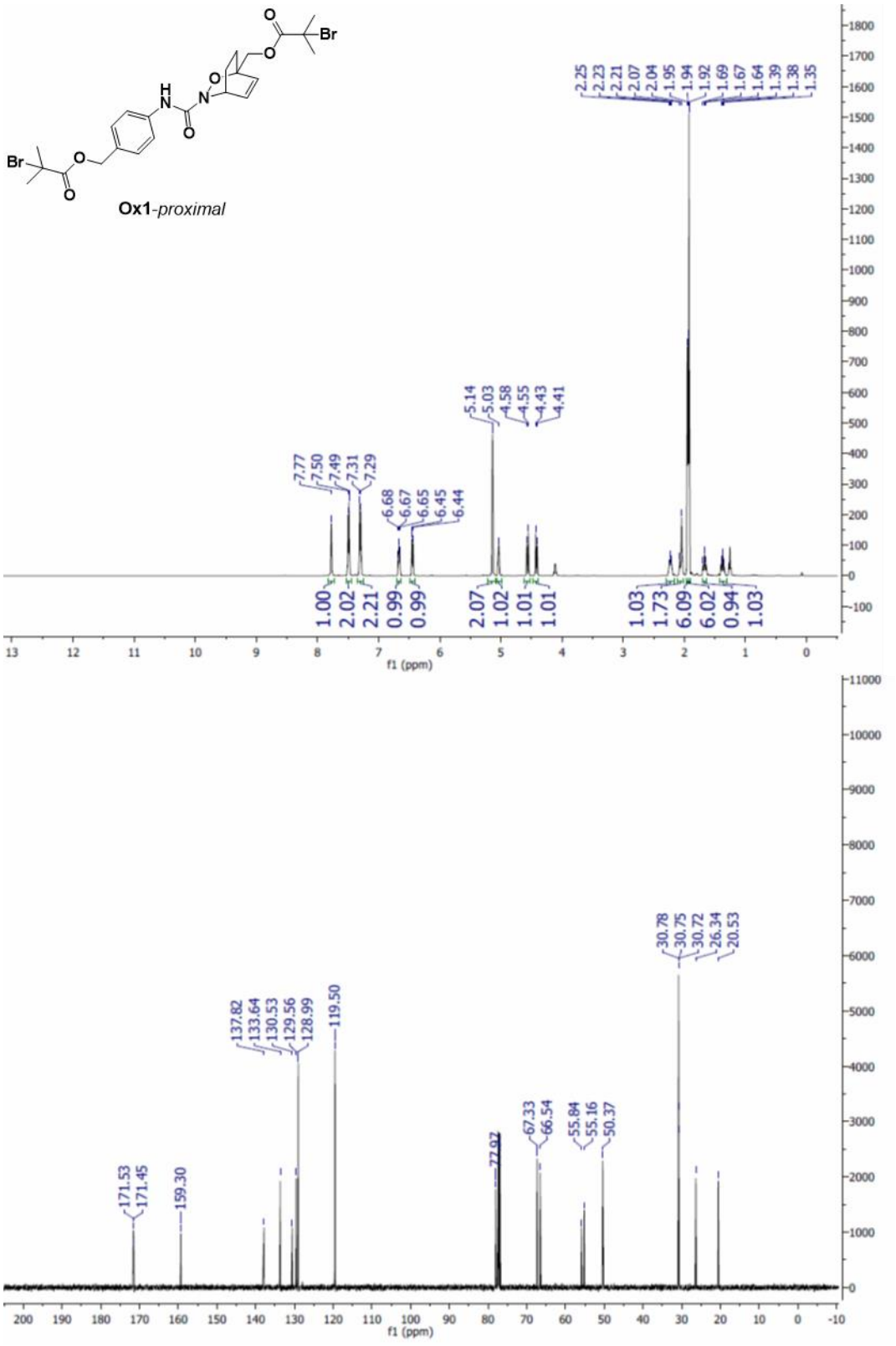
Ox1-proximal
f1 (ppm)
f1 (ppm)

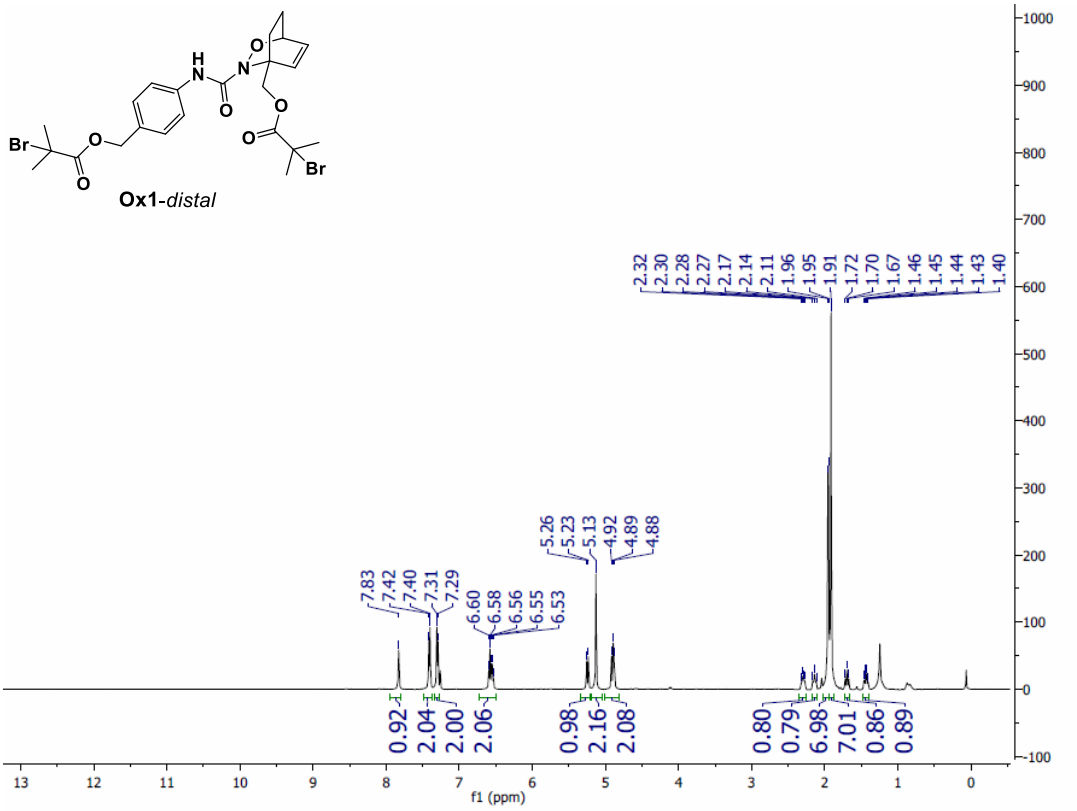
Br
O
O
H
N
O
N
O
O
O
Br
Ox1-distal
7.83
7.42
7.40
7.31
7.29
6.60
6.58
6.56
6.55
6.53
5.26
5.23
5.13
4.92
4.89
4.88
2.32
2.30
2.28
2.27
2.17
2.14
2.11
1.96
1.95
1.91
1.72
1.70
1.67
1.46
1.45
1.44
1.43
1.40
0.92
2.04
2.00
2.06
0.98
2.16
2.08
0.80
0.79
6.98
7.01
0.86
0.89
f1 (ppm)

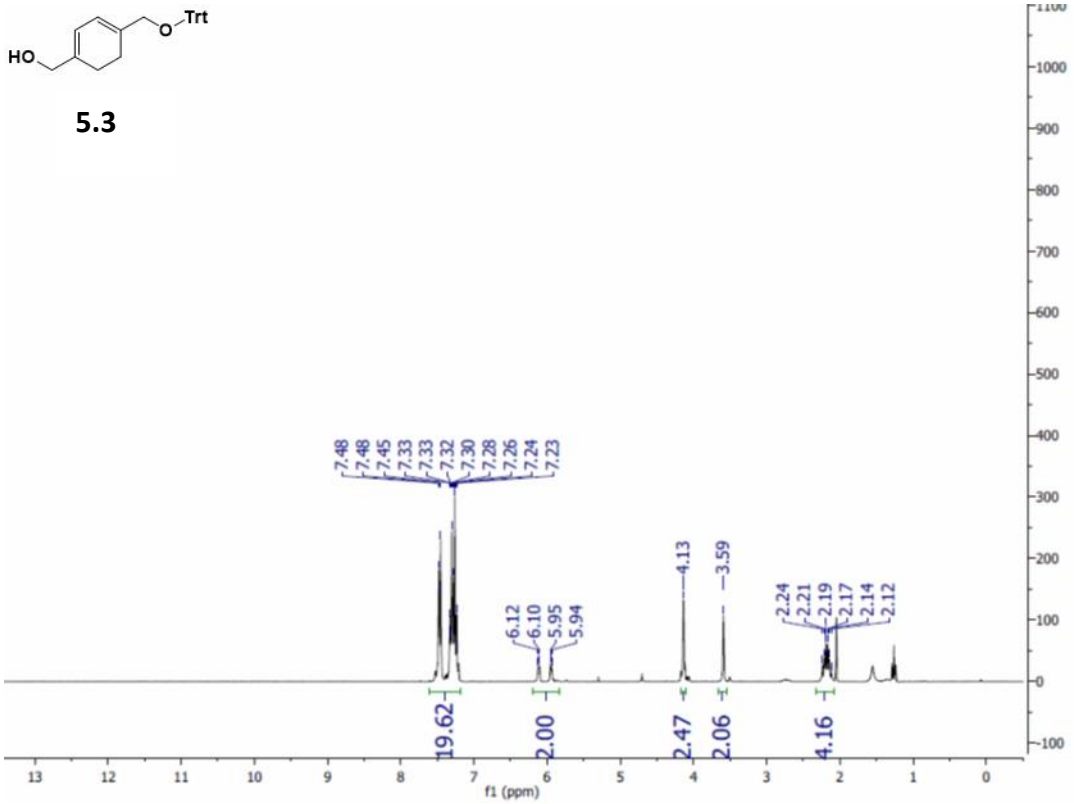
HO
O
Trt
5.3
7.48
7.48
7.45
7.33
7.33
7.32
7.30
7.28
7.26
7.24
7.23
6.12
6.10
5.95
5.94
4.13
3.59
2.24
2.21
2.19
2.17
2.14
2.12
19.62
2.00
2.47
2.06
4.16
f1 (ppm)

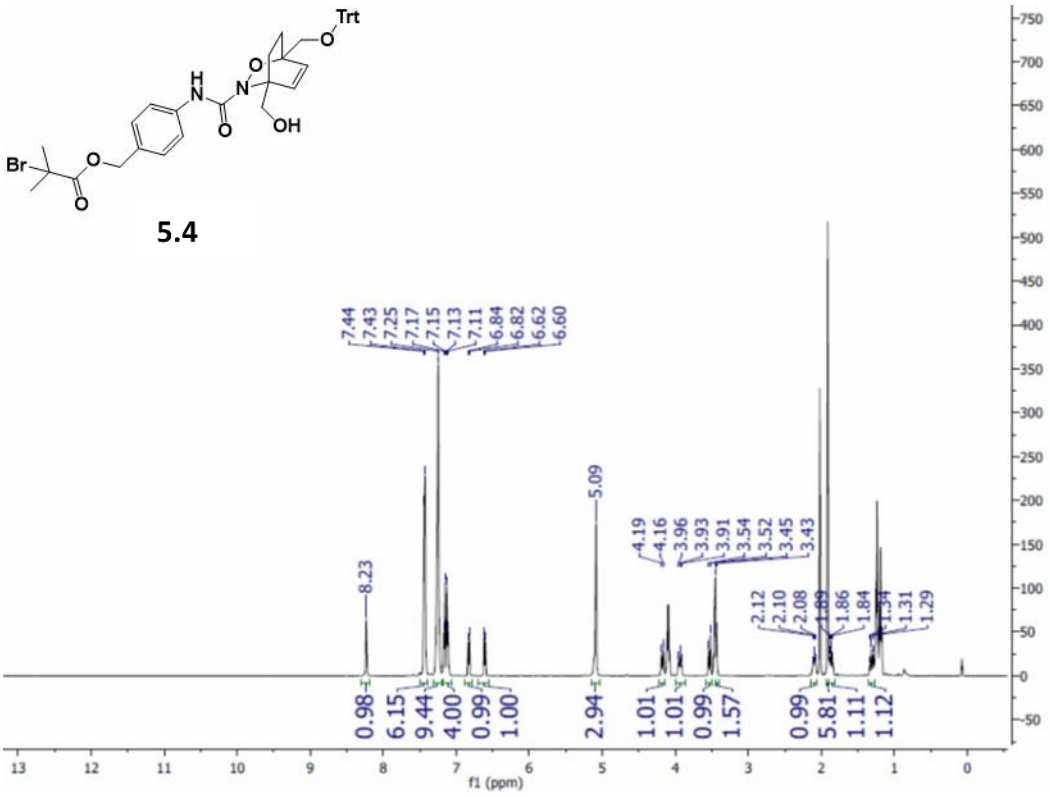
Trt
O
H
N
O
N
O
OH
Br
O
O
5.4
7.44
7.43
7.25
7.17
7.15
7.13
7.11
6.84
6.82
6.62
6.60
8.23
5.09
4.19
4.16
3.96
3.93
3.91
3.54
3.52
3.45
3.43
2.12
2.10
2.08
1.89
1.86
1.84
1.34
1.31
1.29
0.98
6.15
9.44
4.00
0.99
1.00
2.94
1.01
1.01
0.99
1.57
0.99
5.81
1.11
1.12
f1 (ppm)

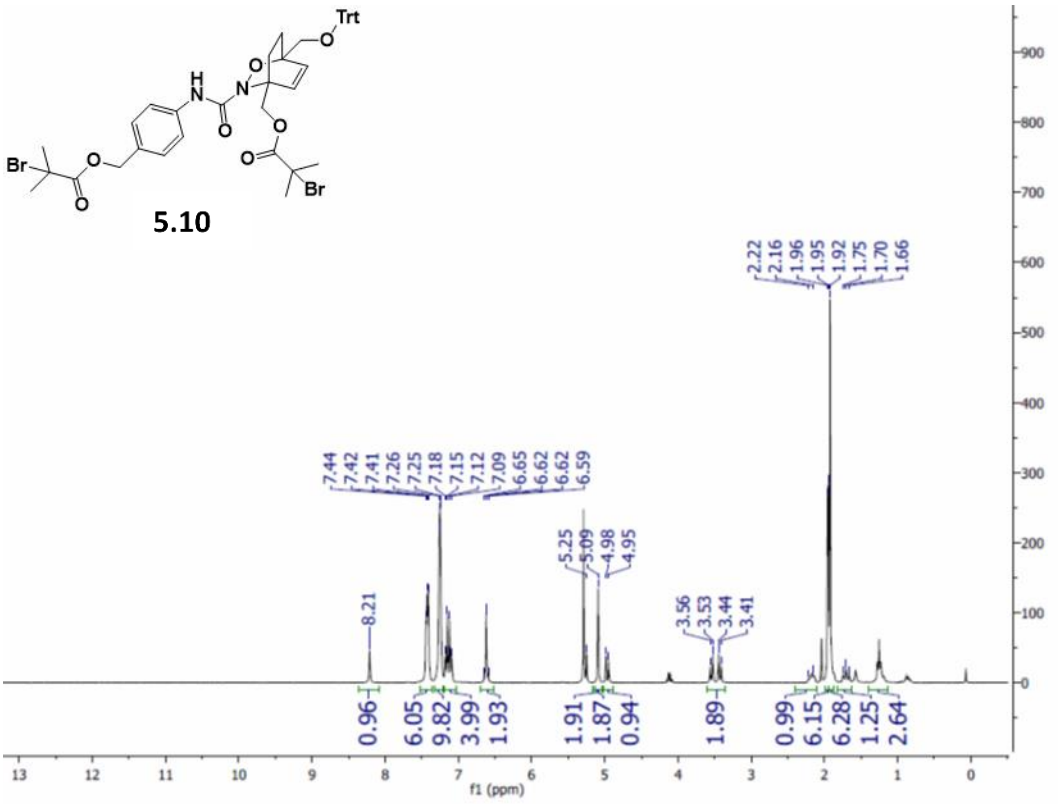
Trt
Br
Br
5.10
7.44
7.42
7.41
7.26
7.25
7.18
7.15
7.12
7.09
6.65
6.62
6.62
6.59
8.21
5.25
5.09
4.98
4.95
3.56
3.53
3.44
3.41
2.22
2.16
1.96
1.95
1.92
1.75
1.70
1.66
0.96
6.05
9.82
3.99
1.93
1.91
1.87
0.94
1.89
0.99
6.15
6.28
1.25
2.64
f1 (ppm)

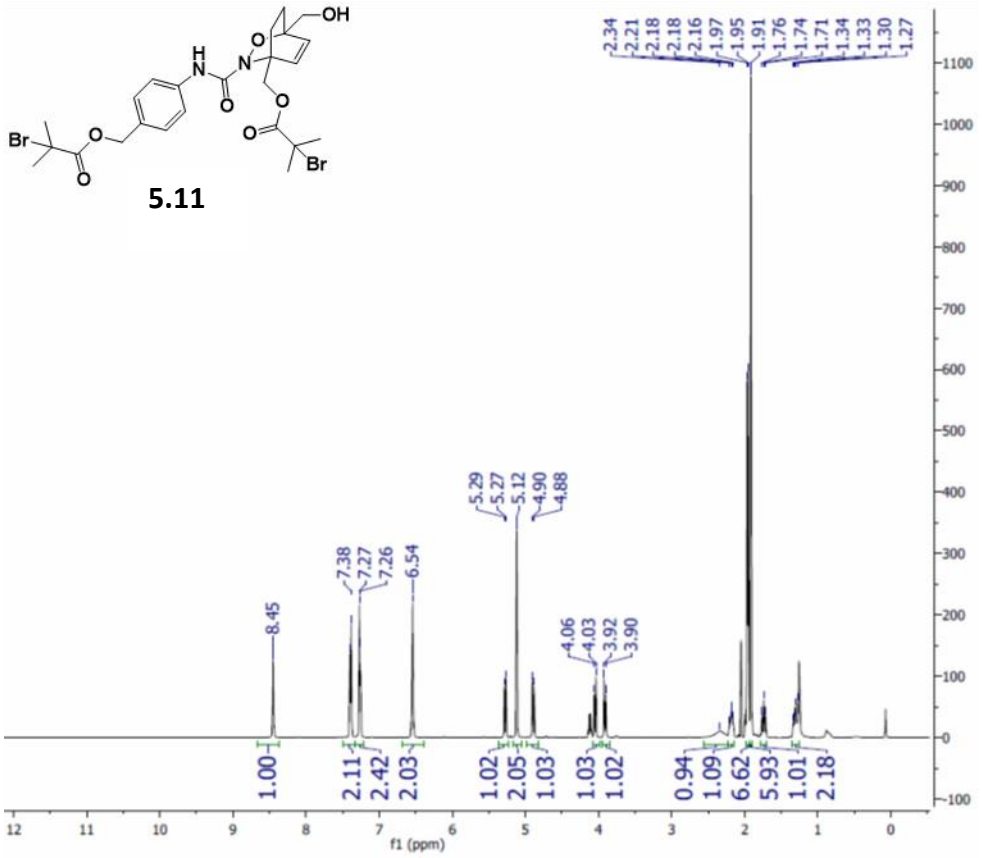
OH
H
N
O
N
O
O
Br
O
O
O
Br
5.11
2.34
2.21
2.18
2.18
2.16
1.97
1.95
1.91
1.76
1.74
1.71
1.34
1.33
1.30
1.27
5.29
5.27
5.12
4.90
4.88
7.38
7.27
7.26
6.54
8.45
4.06
4.03
3.92
3.90
1.00
2.11
2.42
2.03
1.02
2.05
1.03
1.03
1.02
0.94
1.09
6.62
5.93
1.01
2.18
f1 (ppm)

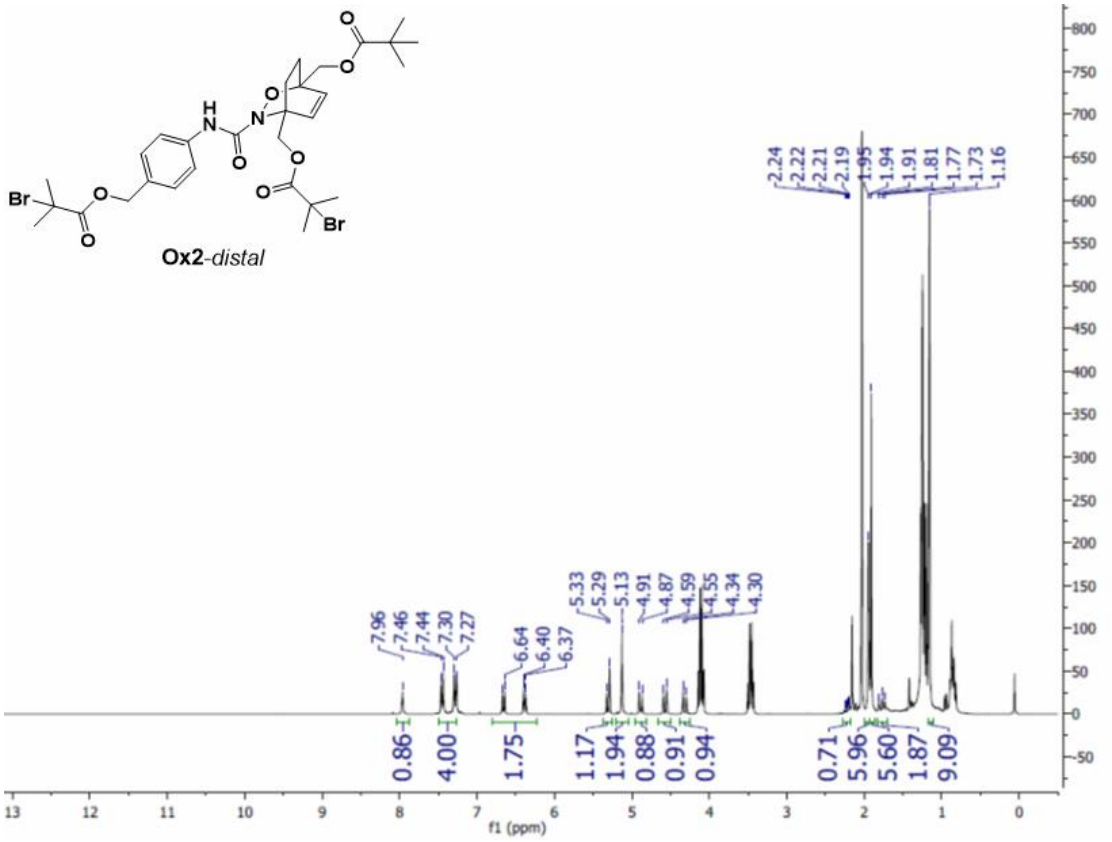
Br
O
O
H
N
N
O
O
O
O
O
O
Br
Ox2-distal
7.96
7.46
7.44
7.30
7.27
6.64
6.40
6.37
5.33
5.29
5.13
4.91
4.87
4.59
4.55
4.34
4.30
2.24
2.22
2.21
2.19
1.95
1.94
1.91
1.81
1.77
1.73
1.16
0.86
4.00
1.75
1.17
1.94
0.88
0.91
0.94
0.71
5.96
5.60
1.87
9.09
f1 (ppm)

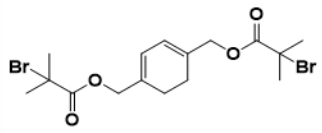
Br
O
O
O
O
Br

5.5

5.85
4.54
2.13
1.81
1.80
4.00
3.86
12.62
f1 (ppm)

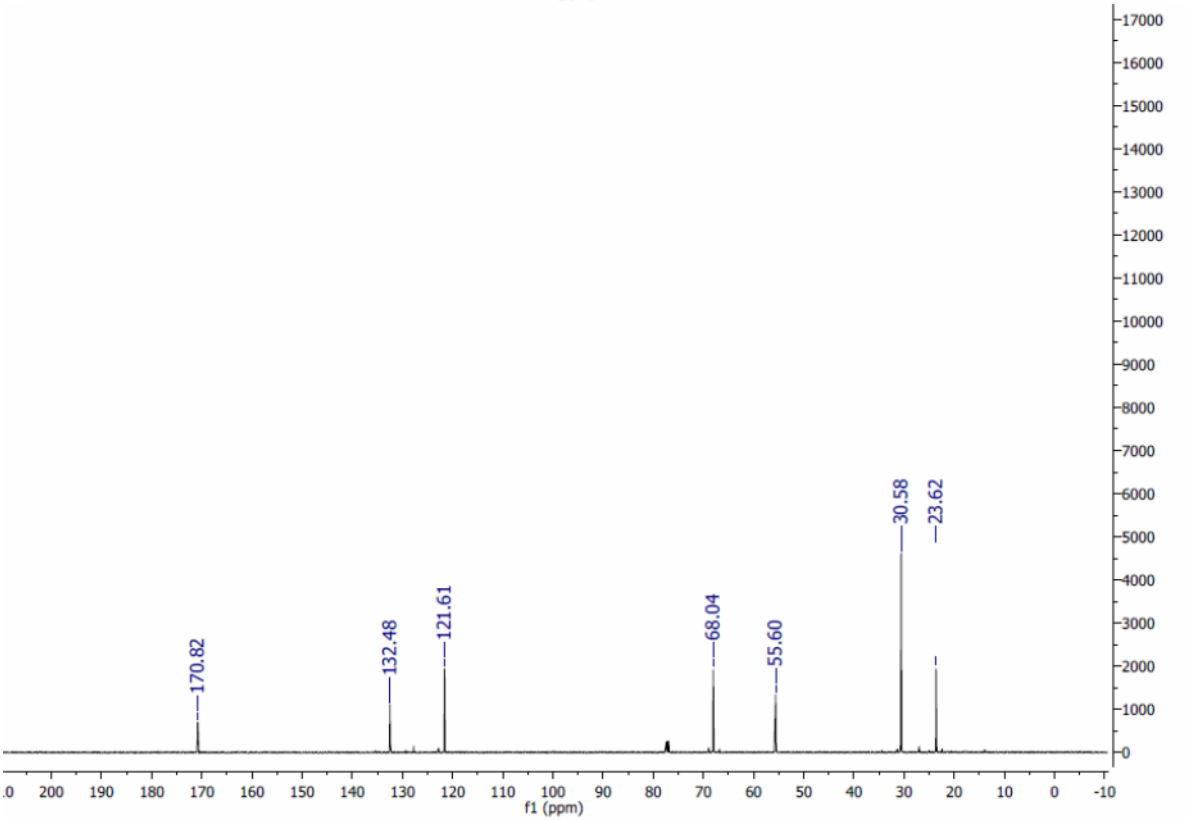
170.82
132.48
121.61
68.04
55.60
30.58
23.62
f1 (ppm)

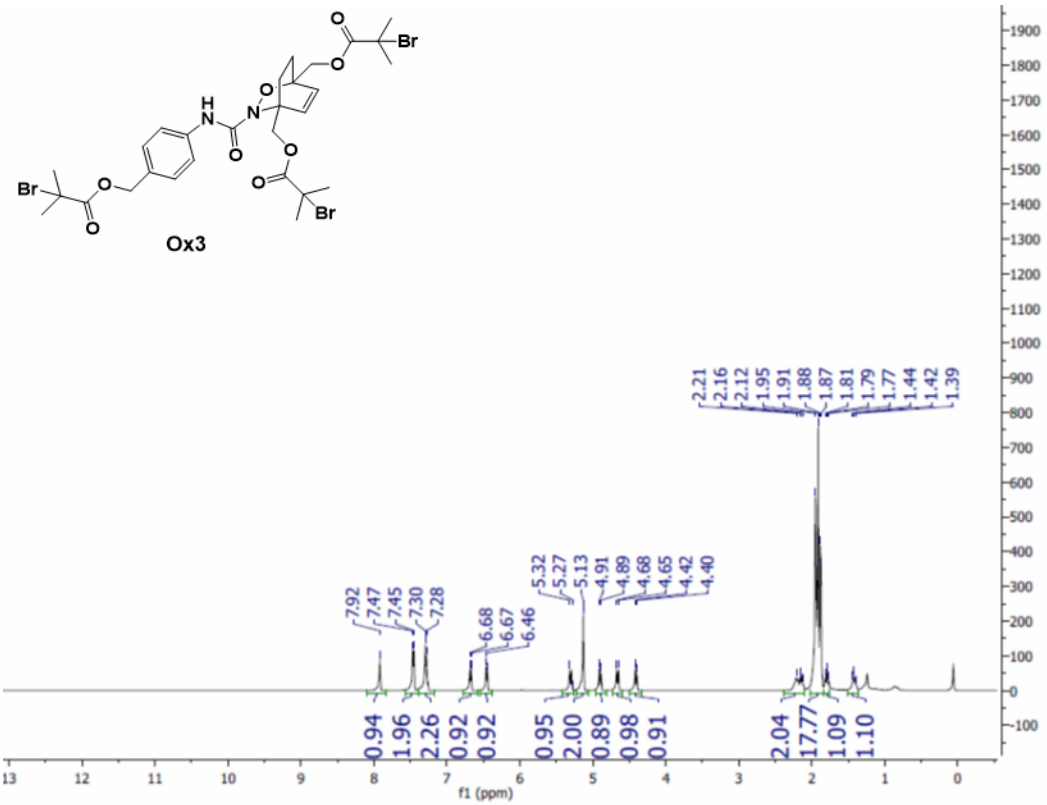
Br
O
O
H
N
O
N
O
O
O
Br
Br
O
O
Ox3
7.92
7.47
7.45
7.30
7.28
6.68
6.67
6.46
5.32
5.27
5.13
4.91
4.89
4.68
4.65
4.42
4.40
2.21
2.16
2.12
1.95
1.91
1.88
1.87
1.81
1.79
1.77
1.44
1.42
1.39
0.94
1.96
2.26
0.92
0.92
0.95
2.00
0.89
0.98
0.91
2.04
17.77
1.09
1.10
f1 (ppm)

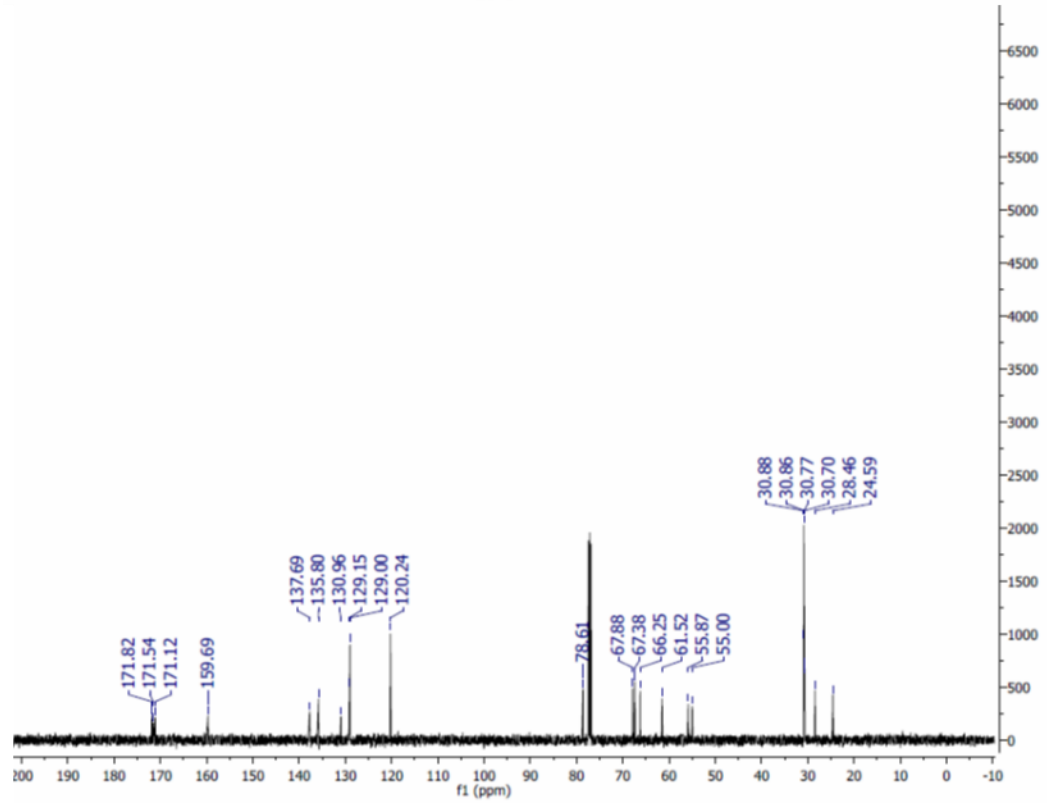
171.82
171.54
171.12
159.69
137.69
135.80
130.96
129.15
129.00
120.24
78.61
67.88
67.38
66.25
61.52
55.87
55.00
30.88
30.86
30.77
30.70
28.46
24.59
f1 (ppm)

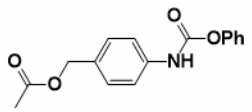
O
OPh
NH
O
O

5.14

7.48
7.47
7.44
7.42
7.41
7.39
7.35
7.33
7.29
7.28
7.26
7.22
7.21
5.10
2.14
9.00
2.25
2.60
f1 (ppm)
137.70
131.31
129.40
129.26
125.69
121.65
118.97
171.04
151.85
150.64
65.95
20.99
f1 (ppm)

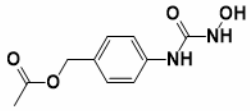
O
OH
NH
NH
O
O

5.15

9.00
8.88
8.86
7.63
7.62
7.25
7.24
4.98
2.03
1.00
2.13
1.82
1.85
2.19
2.70
f1 (ppm)

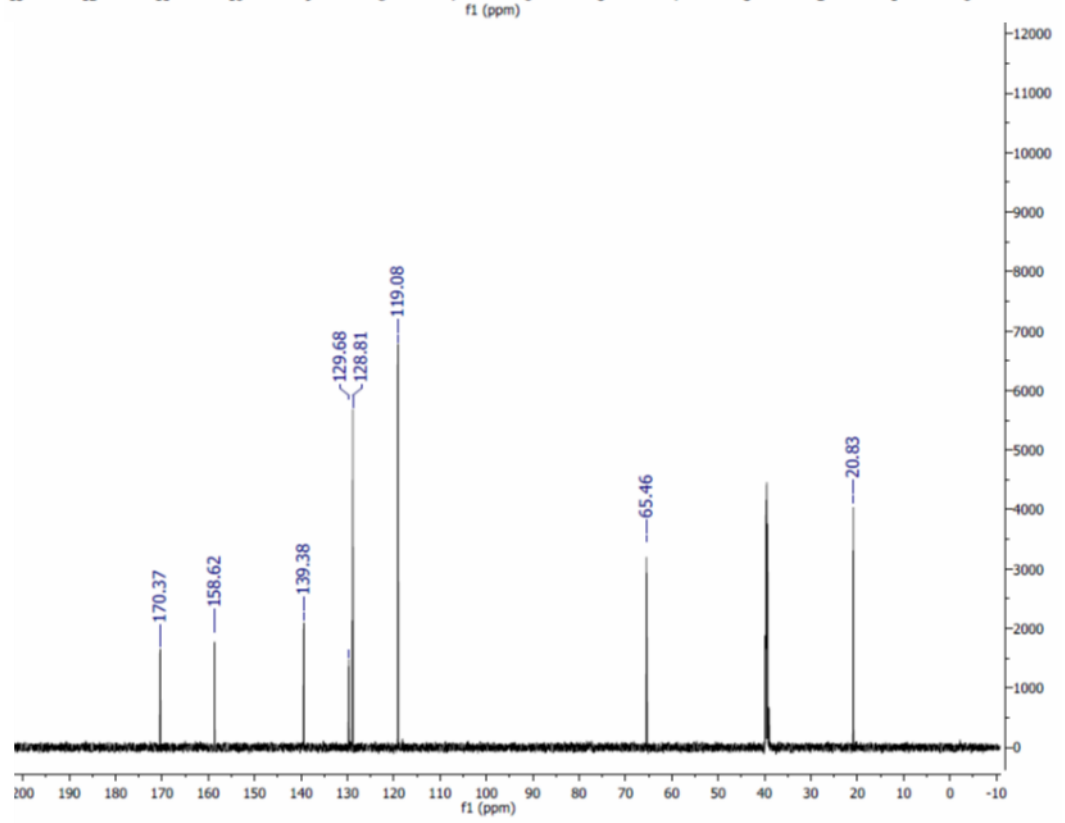
170.37
158.62
139.38
129.68
128.81
119.08
65.46
20.83
f1 (ppm)

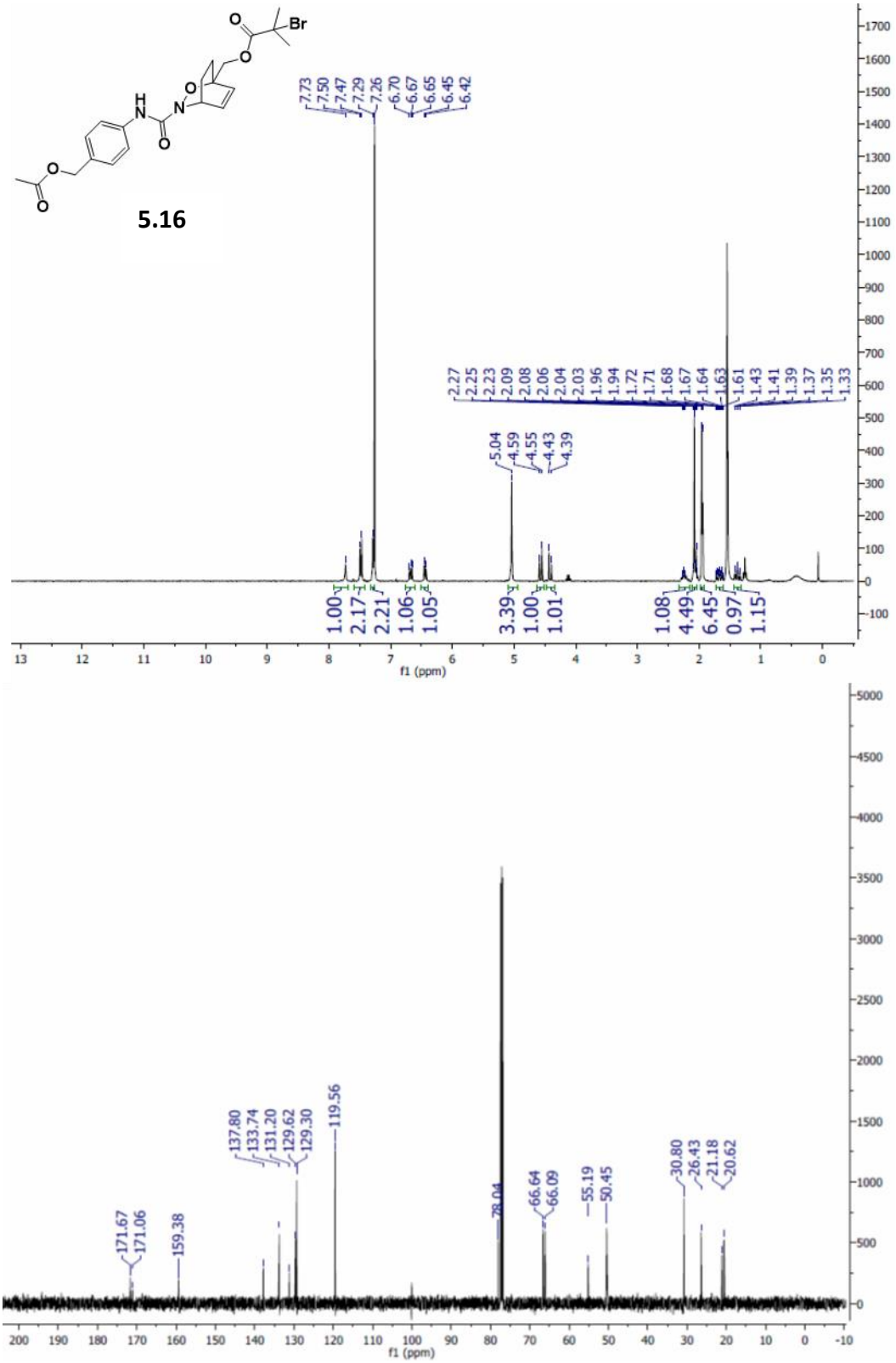
5.16
7.73
7.50
7.47
7.29
7.26
6.70
6.67
6.65
6.45
6.42
5.04
4.59
4.55
4.43
4.39
2.27
2.25
2.23
2.09
2.08
2.06
2.04
2.03
1.96
1.94
1.72
1.71
1.68
1.67
1.64
1.63
1.61
1.43
1.41
1.39
1.37
1.35
1.33
1.00
2.17
2.21
1.06
1.05
3.39
1.00
1.01
1.08
4.49
6.45
0.97
1.15
f1 (ppm)
171.67
171.06
159.38
137.80
133.74
131.20
129.62
129.30
119.56
78.04
66.64
66.09
55.19
50.45
30.80
26.43
21.18
20.62
f1 (ppm)

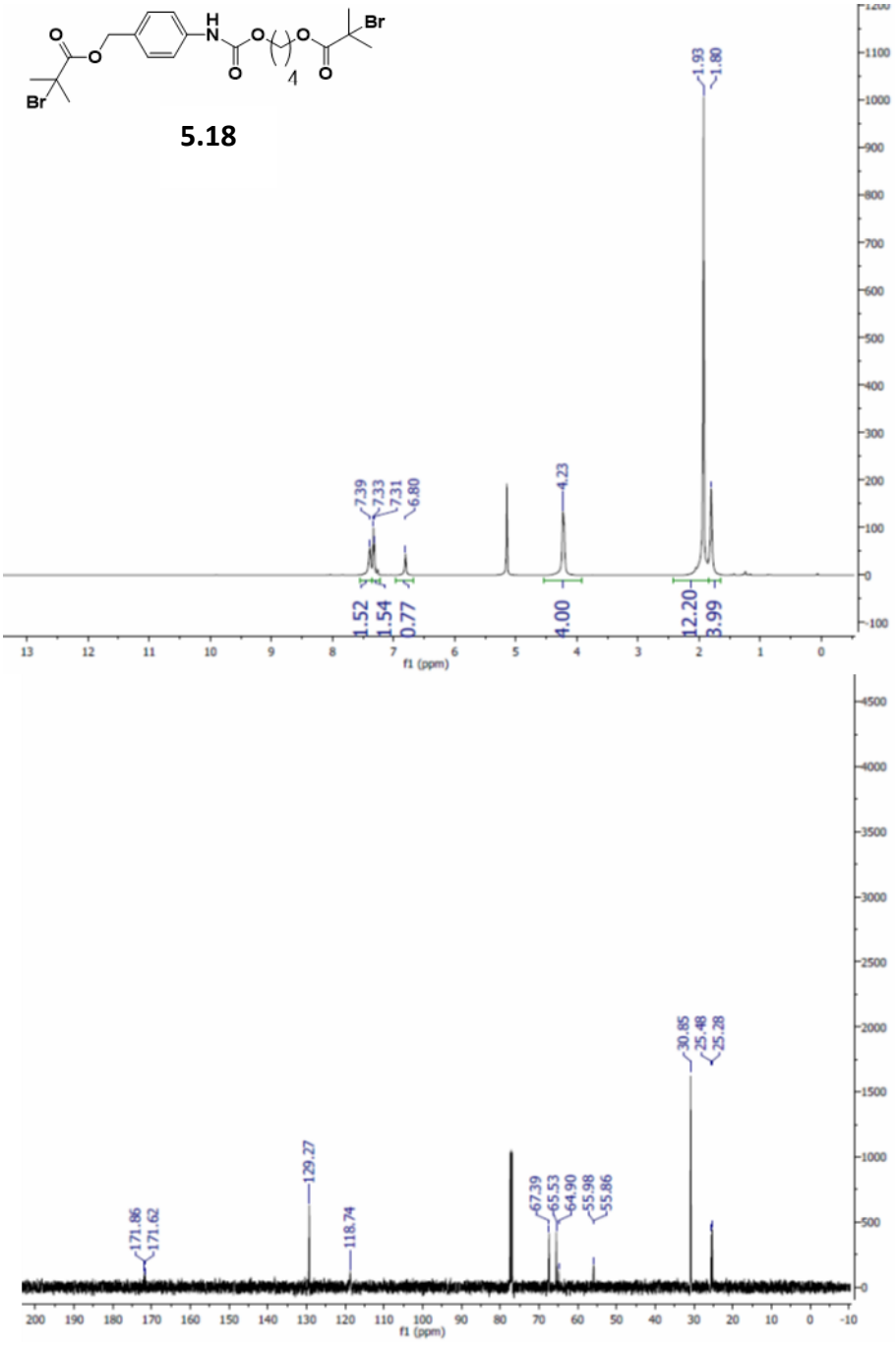
Br
H
N
O
O
O
O
O
O
Br
1
5.18
7.39
7.33
7.31
6.80
4.23
1.93
1.80
1.52
1.54
0.77
4.00
12.20
3.99
f1 (ppm)
171.86
171.62
129.27
118.74
67.39
65.53
64.90
55.98
55.86
30.85
25.48
25.28
f1 (ppm)

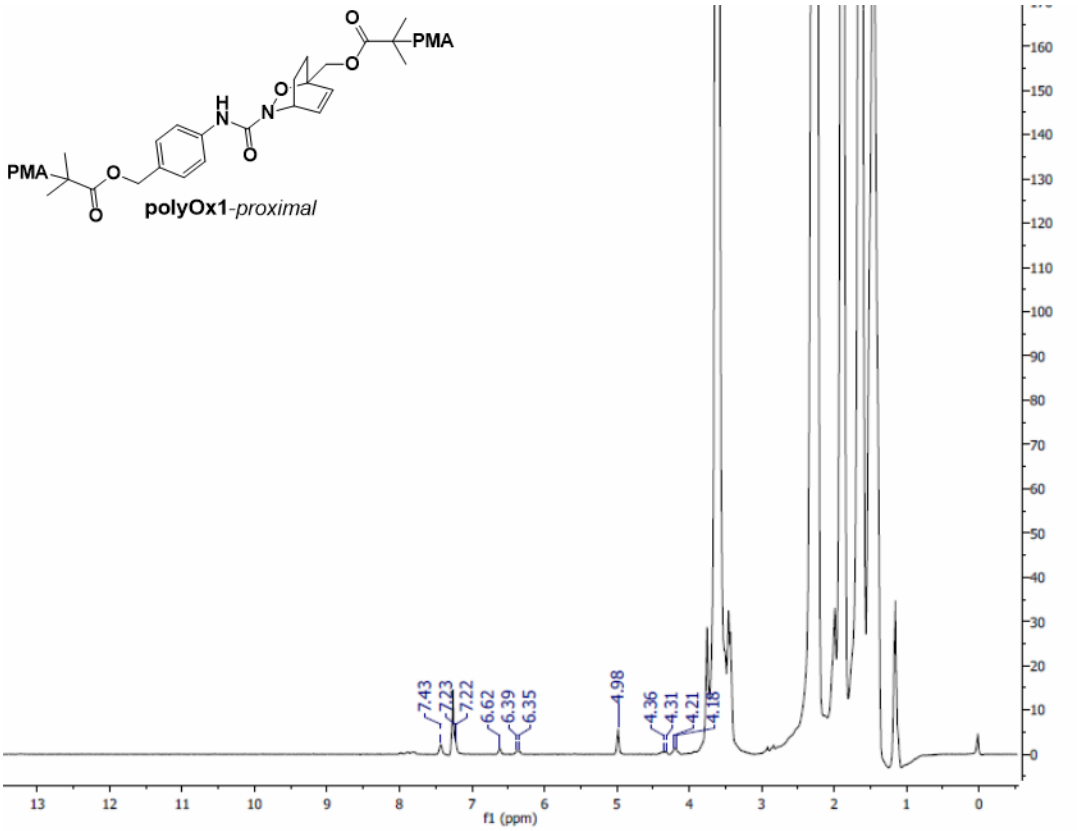
PMA
PMA
polyOx1-proximal
7.43
7.23
7.22
6.62
6.39
6.35
4.98
4.36
4.31
4.21
4.18
f1 (ppm)

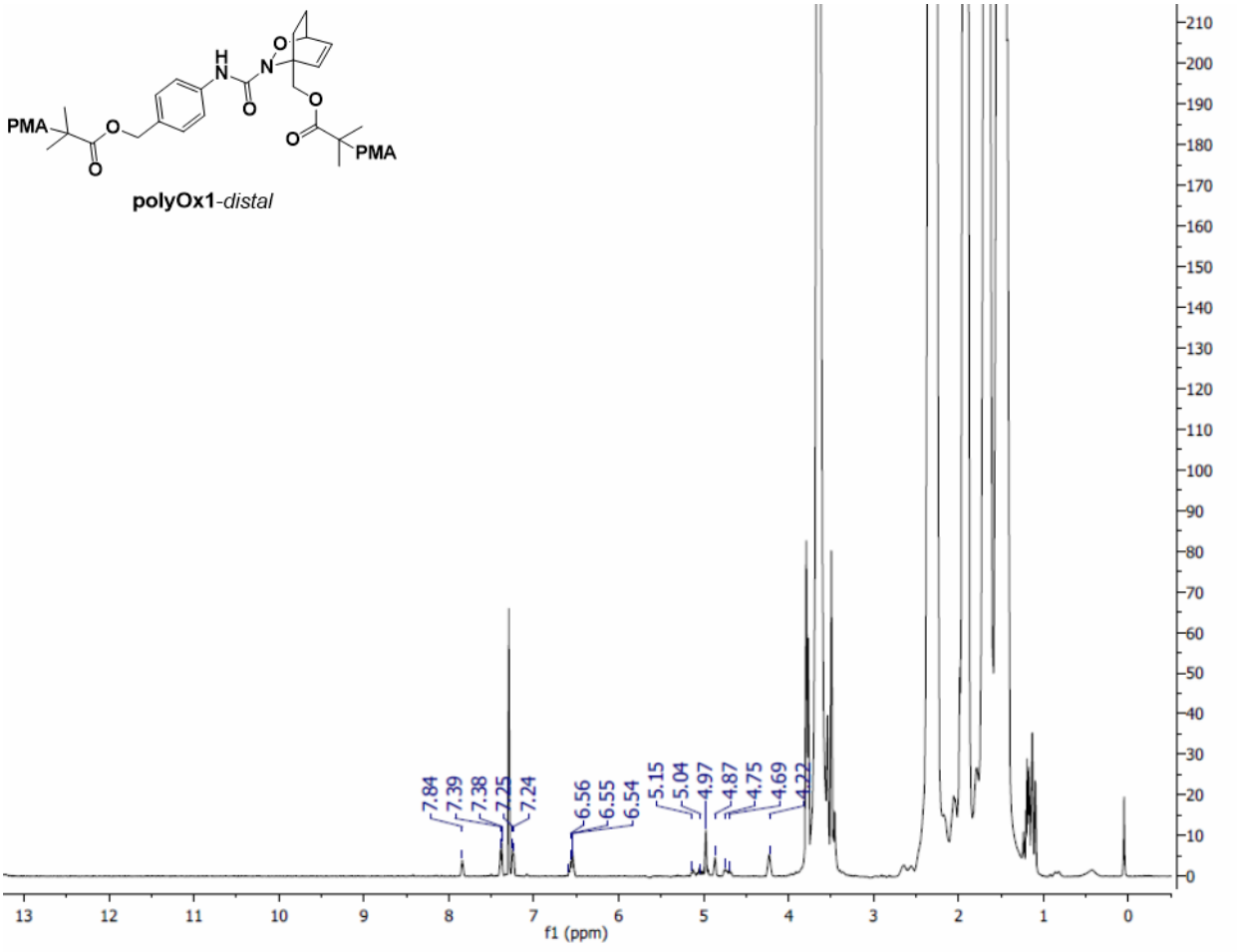
PMA
PMA
polyOx1-distal
7.84
7.39
7.38
7.25
7.24
6.56
6.55
6.54
5.15
5.04
4.97
4.87
4.75
4.69
4.22
f1 (ppm)

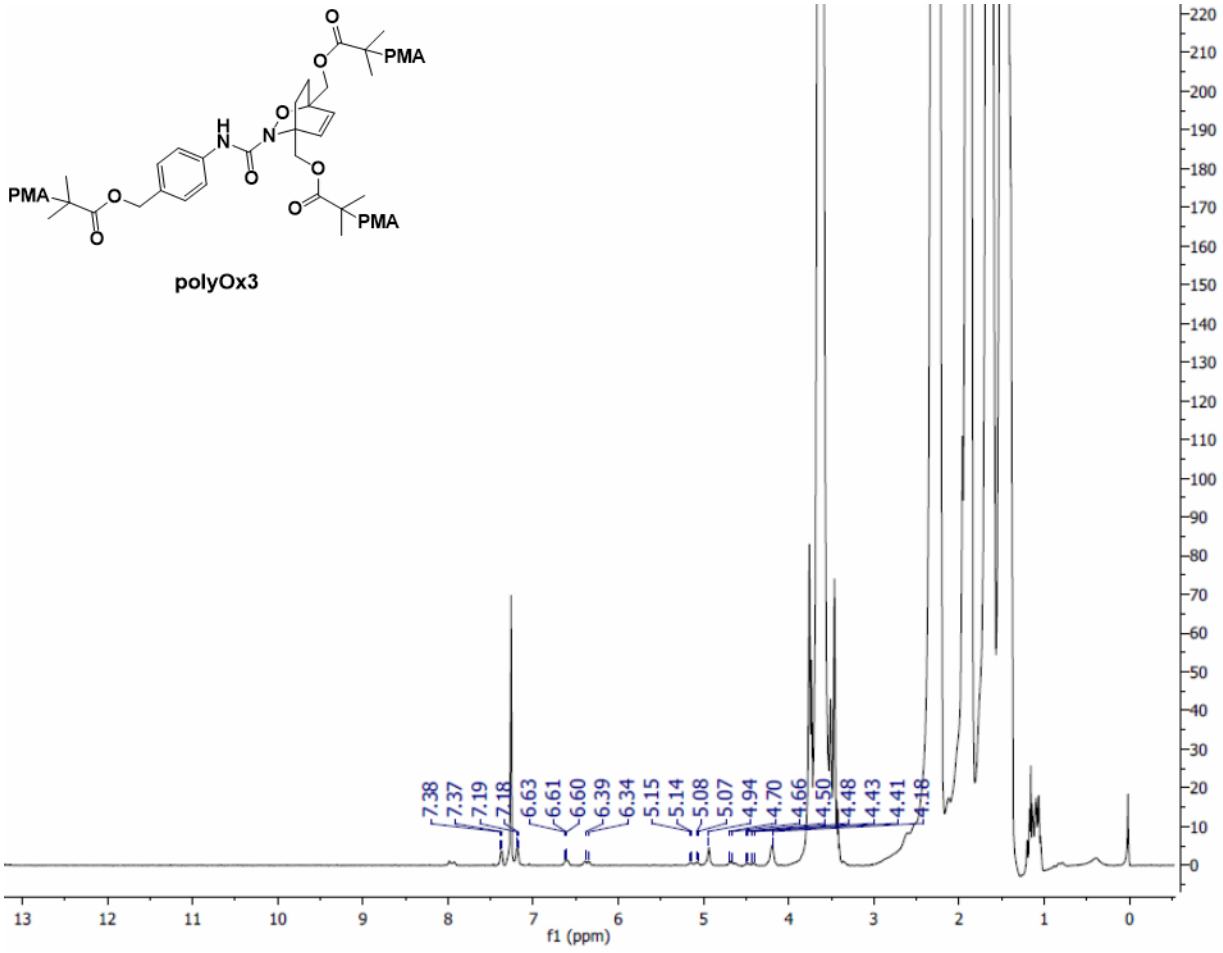
PMA
PMA
PMA
polyOx3
7.38
7.37
7.19
7.18
6.63
6.61
6.60
6.39
6.34
5.15
5.14
5.08
5.07
4.94
4.70
4.66
4.50
4.48
4.43
4.41
4.18
f1 (ppm)

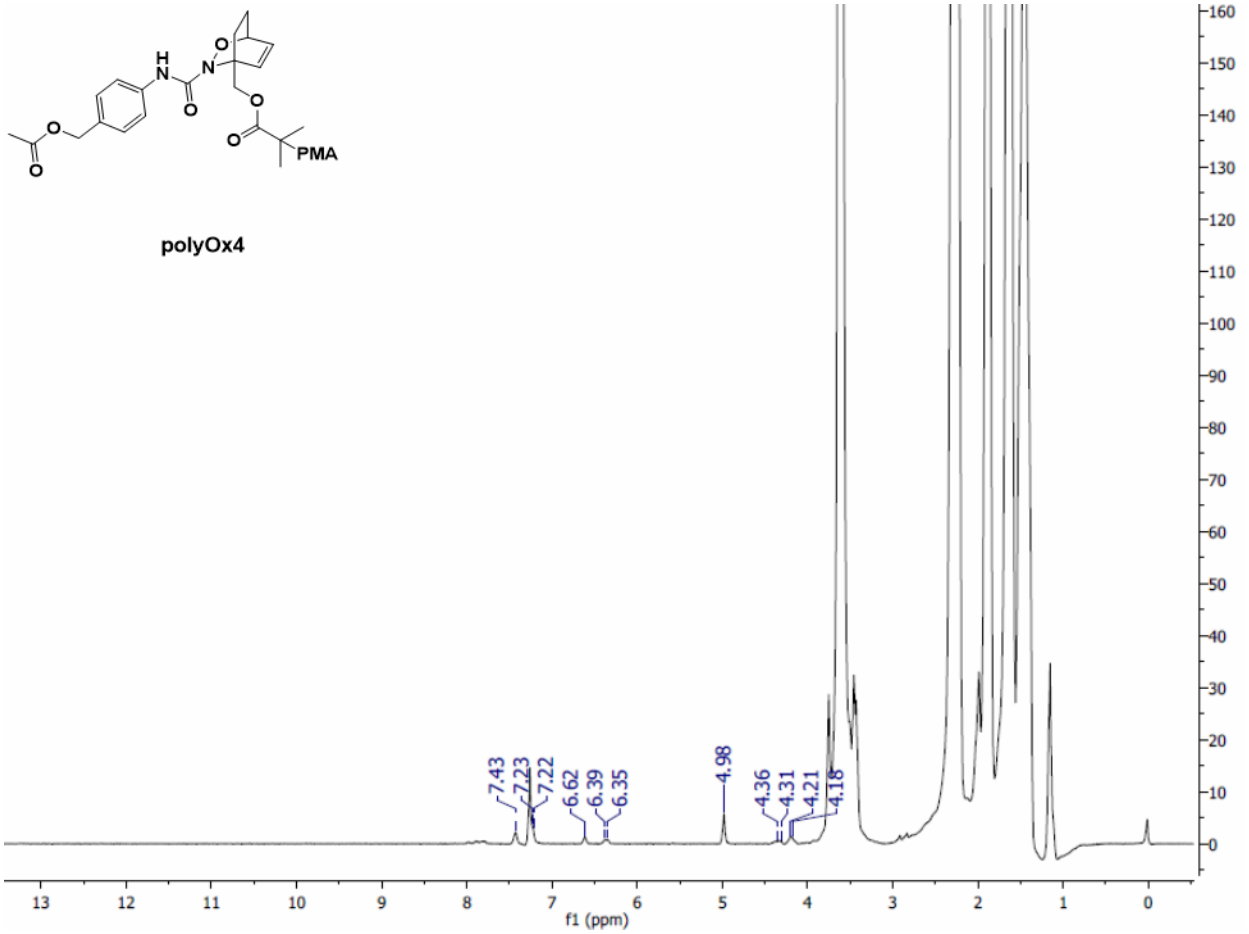
PMA
polyOx4
7.43
7.23
7.22
6.62
6.39
6.35
4.98
4.36
4.31
4.21
4.18
f1 (ppm)

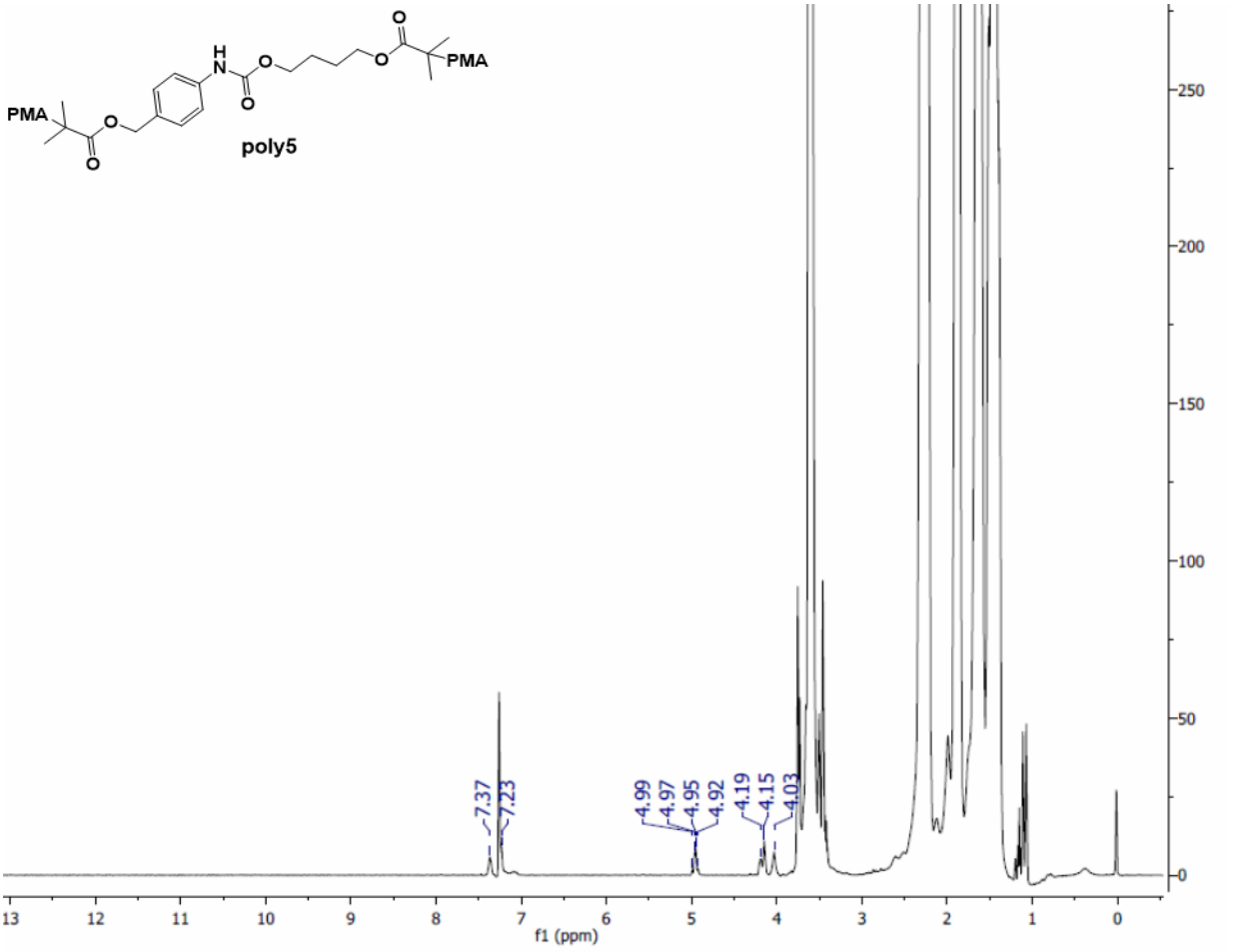

Notes and References for Chapter 5

(138) Larsen, M. B.; Boydston, A. J. *Macromol. Chem. Phys.* **2016**, *217* (3), 354–364.

(139) Brantley, J. N.; Bailey, C. B.; Wiggins, K. M.; Keatinge-Clay, A. T.; Bielawski, C. W. *Polym. Chem.* **2013**, *4* (14), 3916–3928.

(140) Sottos, N. R. *Nat. Chem.* **2014**, *6* (5), 381–383.

(141) May, P. A.; Moore, J. S. *Chem. Soc. Rev.* **2013**, *42* (18), 7497–7506.

(142) Ghanem, M. A. M. A.; Basu, A.; Behrou, R.; Boechler, N.; Boydston, A. J. A. J.; Craig, S. L. S. L.; Lin, Y.; Lynde, B. E. B. E.; Nelson, A.; Shen, H.; et al. *Nat. Rev. Mater.* **2021**, *6* (1), 84–98.

(143) Groote, R.; Jakobs, R. T. M.; Sijbesma, R. P. *Polym. Chem.* **2013**, *4* (18), 4846–4859.

(144) Ariga, K.; Mori, T.; Hill, J. P. *Adv. Mater.* **2012**, *24* (2), 158–176.

(145) Li, J.; Nagamani, C.; Moore, J. S. *Acc. Chem. Res.* **2015**, *48* (8), 2181–2190.

(146) Imato, K.; Irie, A.; Kosuge, T.; Ohishi, T.; Nishihara, M.; Takahara, A.; Otsuka, H. *Angew. Chem. Int. Ed* **2015**, *54* (21), 6168–6172.

(147) Verstraeten, F.; Göstl, R.; Sijbesma, R. P. *Chem. Commun.* **2016**, *52* (55), 8608–8611.

(148) Poly, A.; Berkowski, K. L.; Potisek, S. L.; Hickenboth, C. R.; Moore, J. S. *Macromolecules* **2005**, *38* (22), 8975–8978.

(149) Sheiko, S. S.; Sun, F. C.; Randall, A.; Shirvanyants, D.; Rubinstein, M.; Lee, H. Il; Matyjaszewski, K. *Nature* **2006**, *440* (7081), 191–194.

(150) Li, Y.; Nese, A.; Lebedeva, N. V.; Davis, T.; Matyjaszewski, K.; Sheiko, S. S. *J. Am. Chem. Soc.* **2011**, *133* (43), 17479–17484.

(151) Imato, K.; Kanehara, T.; Ohishi, T.; Nishihara, M.; Yajima, H.; Ito, M.; Takahara, A.; Otsuka, H. *ACS Macro Lett.* **2015**, *4* (11), 1307–1311.

(152) Encina, M. V.; Lissi, E.; Sarasúa, M.; Gargallo, L.; Radic, D. *J. Polym. Sci. Polym. Lett. Ed.* **1980**, *18* (12), 757–760.

(153) Robb, M. J.; Kim, T. A.; Halmes, A. J.; White, S. R.; Sottos, N. R.; Moore, J. S. *J. Am. Chem. Soc.* **2016**, *138* (38), 12328–12331.

(154) Zhang, H.; Gao, F.; Cao, X.; Li, Y.; Xu, Y.; Weng, W.; Boulatov, R. *Angew. Chem. Int. Ed* **2016**, *55* (9), 3040–3044.

(155) Wang, Z.; Ma, Z.; Wang, Y.; Xu, Z.; Luo, Y.; Wei, Y.; Jia, X. *Adv. Mater.* **2015**, *27* (41), 6469–6474.

(156) Diesendruck, C. E.; Steinberg, B. D.; Sugai, N.; Silberstein, M. N.; Sottos, N. R.; White,

S. R.; Braun, P. V.; Moore, J. S.; Moore, S. *J. Am. Chem. Soc.* **2012**, *134* (30), 12446–12449.

(157) Lenhardt, J. M.; Black, A. L.; Craig, S. L. *J. Am. Chem. Soc.* **2009**, *131* (31), 10818–10819.

(158) Klukovich, H. M.; Kean, Z. S.; Ramirez, A. L. B. B.; Lenhardt, J. M.; Lin, J.; Hu, X.; Craig, S. L. *J. Am. Chem. Soc.* **2012**, *134* (23), 9577–9580.

(159) Davis, D. A.; Hamilton, A.; Yang, J.; Cremar, L. D.; Van Gough, D.; Potisek, S. L.; Ong, M. T.; Braun, P. V.; Martínez, T. J.; White, S. R.; et al. *Nature* **2009**, *459* (7243), 68–72.

(160) Hickenboth, C. R.; Moore, J. S.; White, S. R.; Sottos, N. R.; Baudry, J.; Wilson, S. R. *Nature* **2007**, *446* (7134), 423–427.

(161) Gossweiler, G. R.; Hewage, G. B.; Soriano, G.; Wang, Q.; Welshofer, G. W.; Zhao, X.; Craig, S. L. *ACS Macro Lett.* **2014**, *3* (3), 216–219.

(162) Larsen, M. B.; Boydston, A. J. *J. Am. Chem. Soc.* **2013**, *135* (22), 8189–8192.

(163) Chen, Y.; Spiering, A. J. H. H.; Karthikeyan, S.; Peters, G. W. M. M.; Meijer, E. W.; Sijbesma, R. P. *Nat. Chem.* **2012**, *4* (7), 559–562.

(164) Kean, Z. S.; Black Ramirez, A. L.; Yan, Y.; Craig, S. L. *J. Am. Chem. Soc.* **2012**, *134* (31), 12939–12942.

(165) Klukovich, H. M.; Kean, Z. S.; Iacono, S. T.; Craig, S. L. *J. Am. Chem. Soc.* **2011**, *133* (44), 17882–17888.

(166) Kryger, M. J.; Ong, M. T.; Odom, S. A.; Sottos, N. R.; White, S. R.; Martinez, T. J.; Moore, J. S. *J. Am. Chem. Soc.* **2010**, *132* (13), 4558–4559.

(167) Church, D. C.; Nourian, S.; Lee, C.-U. U.; Yakelis, N. A.; Toscano, J. P.; Boydston, A. J. *ACS Macro Lett.* **2017**, *6* (1), 46–49.

(168) Peterson, G. I.; Church, D. C.; Yakelis, N. A.; Boydston, A. J. *Polymer (Guildf).* **2014**, *55* (23), 5980–5985.

(169) Christie, C. C.; Kirby, G. W.; McGuigan, H.; Mackinnon, J. W. M. *J. Chem. Soc. Perkin Trans. 1* **1985**, No. 6, 2469–2473.

(170) Atkinson, R. N.; Storey, B. M.; King, S. B. *Tetrahedron Lett.* **1996**, *37* (52), 9287–9290.

(171) Kirby, G. W.; Mcguigan, H.; Mackinnon, J. W. M.; Mclean, D.; Sharma, R. P. *J. CHEM. SOC. PERKIN TRANS. I* **1985**, No. 3, 1437–1442.

(172) Samoshin, A. V.; Hawker, C. J.; Read De Alaniz, J. *ACS Macro Lett.* **2014**, *3* (8), 753–757.

(173) Stevenson, R.; De Bo, G. *J. Am. Chem. Soc.* **2017**, *139* (46), 16768–16771.

(174) Groote, R.; Szyja, B. M.; Leibfarth, F. A.; Hawker, C. J.; Doltsinis, N. L.; Sijbesma, R. P. *Macromolecules* **2014**, *47* (3), 1187–1192.

(175) Kryger, M. J.; Munaretto, A. M.; Moore, J. S. *J. Am. Chem. Soc.* **2011**, *133* (46), 18992–18998.

(176) Kean, Z. S.; Niu, Z.; Hewage, G. B.; Rheingold, A. L.; Craig, S. L. *J. Am. Chem. Soc.* **2013**, *135* (36), 13598–13604.

(177) Wang, J.; Kouznetsova, T. B.; Niu, Z.; Ong, M. T.; Klukovich, H. M.; Rheingold, A. L.; Martinez, T. J.; Craig, S. L. *Nat. Chem.* **2015**, *7* (4), 323–327.

(178) Dopieralski, P.; Ribas-Arino, J.; Marx, D. *Angew. Chem. Int. Ed* **2011**, *50* (31), 7105–7108.

(179) Gossweiler, G. R.; Kouznetsova, T. B.; Craig, S. L. *J. Am. Chem. Soc.* **2015**, *137* (19), 6148–6151.

(180) Smalø, H. S.; Uggerud, E. *Chem. Commun.* **2012**, *48* (84), 10443–10445.

(181) Jacobs, M. J.; Schneider, G.; Blank, K. G. *Angew. Chem. Int. Ed* **2016**, *55* (8), 2899–2902.

(182) Konda, S. S. M.; Brantley, J. N.; Varghese, B. T.; Wiggins, K. M.; Bielawski, C. W.; Makarov, D. E. *J. Am. Chem. Soc.* **2013**, *135* (34), 12722–12729.

(183) Striegel, A. M. *J. Biochem. Biophys. Methods* **2003**, *56* (1–3), 117–139.

(184) Church, D. C.; Peterson, G. I.; Boydston, A. J. *ACS Macro Lett.* **2014**, *3* (7), 648–651.

(185) Florea, M. *J. Appl. Polym. Sci.* **1993**, *50* (12), 2039–2045.

(186) Holtz, H.; Stock, L. *J . Am. Chem. Soc.* **1964**, *86*, 5183–5188.

(187) Sagi, A.; Weinstain, R.; Karton, N.; Shabat, D. *J . Am. Chem. Soc.* **2008**, *8*, 5434–5435.

(188) Spangler, C.; Hennis, R. *J. Org. Chem* **1971**, *36* (7), 917–920.

(189) Chu, Y.; Lynch, V.; Iverson, B. L. *Tetrahedron* **2006**, *62* (23), 5536–5548.

(190) Bernaerts, K. V.; Schacht, E. H.; Goethals, E. J.; Du Prez, F. E. *J. Polym. Sci. Part A Polym. Chem.* **2003**, *41* (21), 3206–3217.

Chapter 6. Using Amphiphilic Block Co-Polymers for Moisture Resistant Ultra Gas-Barriers

My work for this project focused on the synthesis and characterization of the amphiphilic block copolymers. The LBL and thin film characterization was performed by Thomas Kolibaba at Texas A&M University.

6.1 Abstract

We have synthesized two amphiphilic block copolymers for use in the LbL assembly of polyelectrolyte gas barriers. The polymers consisted of a poly(styrene-block-acrylic acid) (PS-b-PAA) and a poly(styrene-block-2-dimethylaminoethyl methacrylate) (PS-b-PDMAEMA) that will function as a polyanion and polycation respectively. High and low molecular weight PS-b-PAA copolymers were synthesized using ARGET-ATRP, while high and low molecular weight PS-b-PDMAEMA were synthesized using RAFT and ATRP respectively. Characterization of the PS-b-PDMAEMA has proven difficult due to the nature of the polyamine. LbL assembly of the high molecular weight polymers showed a linear correlation between number of bilayers and film thickness.

6.2 Introduction

There is currently a need for optically transparent and flexible materials that act as moisture and oxygen barriers for use in food packaging and wearable electronics.[191] Entirely polymer based systems have been shown to act as either very efficient oxygen or moisture barriers or when assembled in a layer-by-layer (LbL) fashion.[192–194] When deposited on polyethylene terephthalate (PET) film, an entirely polymer coating can even completely inhibit the transmission of oxygen passing through a thin film (< 0.005 cm^3 m^{-2} day^{-1} atm^{-1}) while adding only 1 μm of thickness.

The LbL assembly of these materials involves applying thin films of oppositely charged polymer species in an alternating pattern to allow the formation of polyelectrolyte complexes

(PEC) through an entropically-driven process.[195,196] When using weak polyelectrolytes such as polyethyleneimine and poly(acrylic acid) these materials grow in an exponential fashion suggesting that the polymers not only add to the outer layer but also penetrate previously deposited layers.[192,197] Furthermore, by controlling the charge density through changing the solution pH of the polyelectrolyte solutions, the thickness, density, and composition of the films can be altered.[198–201]

Because of their ionic nature, PECs have favorable interactions with water. As a consequence of this, water acts as a plasticizer and can weaken the strength of the ionic bonds of the polymer species.[202] In moderate humidity the water can even improve the capabilities of the PEC as gas barriers because the water can fill the free volume within the material, preventing gasses from penetrating.[203–205] However, when the materials are in high humidity environments swelling can occur, increasing the free volume within the PEC film and increasing the rate at which oxygen and other gasses can pass.[192,202] In their seminal report for entirely polymer based gas barriers Grunlan et.al. attempt to prevent this swelling from occurring crosslinking the polyethyleneimine with glutaraldehyde after the LbL assembly. The crosslinking did help maintain some of the barrier's function, but they still saw an increase from no detectable oxygen transmission to 0.07-0.09 $cm^3\ m^{-2}\ day^{-1}\ atm^{-1}$.

LbL assembly of water vapor barriers has been demonstrated using a combination of a PEC and a single hydrophobic polymer (Nafion) layer.[194] By incorporating this hydrophobic layer Madras et.al. were able to limit the rate of water vapor transmission to $8 \times 10^{-6}\ g\ m^{-2}\ day^{-1}$. Inspired by this work and the work done in block copolymer lithography in building highly ordered polymer structures we propose using the LBL assembly of amphiphilic block copolymers for the synthesis of highly ordered thin films that will act as efficient gas barriers while also have several

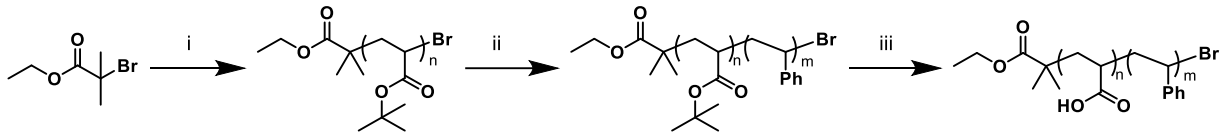

Figure 6.1 Synthetic scheme for poly(styrene-*block*-acrylic acid). i) *tert*-butyl acrylate, $CuBr_2$, Me_6Tren, Ascorbic acid, DMF. ii) styrene, $CuBr_2$, Me_6Tren, Ascorbic acid, anisole. iii) conc. HCl, 1,4-dioxane.

hydrophobic layers inhibiting the swelling of the films in high humidity.[206] To that end we propose using poly(styrene-*block*-acrylic acid) (PS-b-PAA) as a hydrophobic-block-anion copolymer and poly(styrene-*block*-2-dimethylaminoethyl methacrylate) (PS-b-PDMAEMA) as a hydrophobic-block-cationic copolymer. These block copolymers are known to self-assemble, and the polyelectrolytes are similar in structure to those already used in the field of PEC gas barriers.[207,208]

6.3. Results and Discussion

6.3.a. Anionic Block Co-Polymer Synthesis and Characterization

The controlled polymerization of acidic monomers is difficult, as such we chose to synthesize poly(tert-butyl acrylate) (P*t*BA) instead of poly(acrylic acid) (PAA), as it can be easily deprotected to yield PAA in the final block copolymer (**Figure 6.1**).[209–212] To accomplish this polymerization we chose to use ARGET-ATRP or Activator ReGenerated by Electron Transfer atom transfer radical polymerization for its ease of setup.

The synthesis of the P*t*BA was carried out using Cu(II)Br_2/Me_6Tren with ascorbic acid as the reducing reagent at 60 °C. Monomer conversion was determined using ^{1}H NMR spectroscopy, while molecular weight analysis was determined using gel permeation chromatography (GPC). Initial attempts at the polymerization were conducted in dimethyl formamide (DMF) using an initial monomer to initiator ratio of 220:1 with 10 mol% ascorbic acid. The polymerization reached near full conversion within 1 hour. The resulting polymer was monomodal by GPC suggestion no chain coupling occurred and had M_n of 36 kDa with a molecular weight dispersity (*Đ*) of 1.3 (**Figure 6.2**).

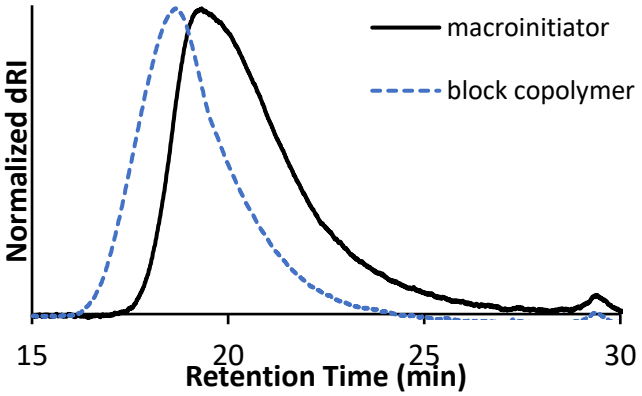

Figure 6.2 GPC trace for the P*t*BA macroinitiator (solid black line) and the product of the chain extension(blue dash).

Attempts at the chain extension with styrene using the same conditions were unsuccessful, no conversion could be seen by ^{1}H NMR spectroscopy even after 72 hours with an initial monomer to macroinitiator ratio of 1000:1. When the amount of ascorbic acid and $CuBr_2$/Me_6Tren was doubled relative to macroinitiator the chain extension was successful. The polymerization was monitored by ^{1}H NMR spectroscopy and was stopped when near equal degrees of polymerization for both blocks was reached. This ratio can be determined by comparing the integration of the phenyl protons of the styrene to the entire aliphatic region using the following equation.

$$\frac{PS}{PtBA} = \frac{I_p - I_m}{I_a - 1.5(I_p - I_m)} \tag{6.1}$$

where I_p is the integration for the phenyl protons of the polymer, I_m is the integration of the overlapping styrene monomer peaks and I_a is the integration for the aliphatic protons for the two

blocks. The M_n of the resulting polymer was 70 kDa with a *Đ* of 1.2, the increase in molecular weight is consistent with the ratio of repeat units between the poly(*t*-Butyl acylate) and PS blocks (290 and 310 respectively) (**Figure 6.2**).

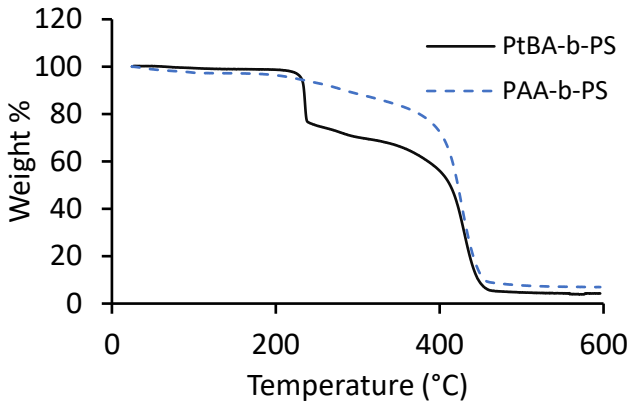

Figure 6.3 Comparison of the TGA for P*t*BA-b-PS (solid black) and PAA-b-PS (blue dash).

We next attempted to perform the deprotection of the *t*-butyl group to synthesize the PS-b-PAA. We were unsuccessful in doing the deprotection using trifluoro acidic acid in DCM. After 6 hours no carboxylic acid could be found by attenuated total reflectance Fourier transformed inferred spectroscopy (ATR-FTIR) (**Figure 6.14**). We next attempted using conc. HCl in 1,4-dioxaine and after 16 hours carboxylic acid was fully present by ATR-FTIR. This was confirmed by ^{1}H NMR spectroscopy as evident by the disappearance of the *t*-butyl group signal.

As a final confirmation we characterized the PAA-b-PS by thermogravimetric analysis (TGA) (**Figure 6.3**). The P*t*BA-b-PS showed an initial decomposition temperature at 220 °C, which is consistent with the thermal deprotection of P*t*BA, before reaching the decomposition temperature (T_d) of 382 °C.[212] After the deprotection a T_d of 394 °C was observed but the peak at 230 °C was no longer present. There was an observable mass loss starting at 210 °C likely due to the loss of water as the acrylic acid repeat units form anhydrides.[213]

The resulting polymers however were too high of a molecular weight to be soluble in solutions with more than 20% water in tetrahydrofuran (THF). As such using these same

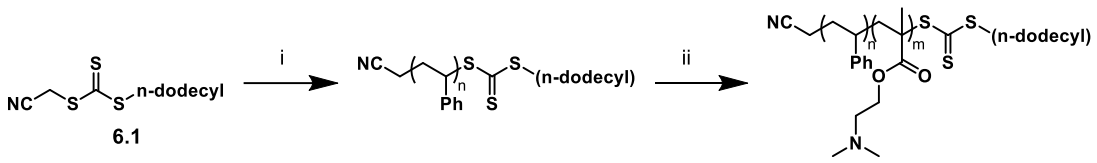

Figure 6.4 Synthetic scheme for poly(styrene-*block*-2-dimethylaminoethyl methacrylate). i) styrene, V-501. ii) 2-dimethylaminoethyl methacrylate, AIBN, toluene.

conditions, we were able to synthesize a block co-polymer with a final molecular weight before deprotection of 20 kDa.

6.3.b. Cationic Block Co-Polymer Synthesis

For the polycation we chose to use methyl acrylate over an acylate based polymer because of the lower rate of self-catalyzed hydrolysis of the methyl acrylate vs the acrylate to acrylic acid.[214] For the synthesis of PDMAEMA-b-PS we chose initially chose to use reversable addition fragmentation chain-transfer polymerization (RAFT) over ATRP to avoid using amine containing polymers with a Cu catalyst (**Figure 6.4**).

It has been shown that PDMAEMA can undergo irreversible termination of as such even though it is a much faster polymerization, as such we chose to first synthesize the PS block. Using CTA **6.1** with V-501 as the radical source we were able to synthesize PS, during the polymerization conversion was again monitored by ^{1}H NMR spectroscopy. The M_n for the purified polymer was 21 kDa with a $Đ$ of 1.09. Chain extension was performed using the PS macroinitiator with AIBN as the radical source. The polymerization was monitored by ^{1}H NMR spectroscopy until the ratio of PS

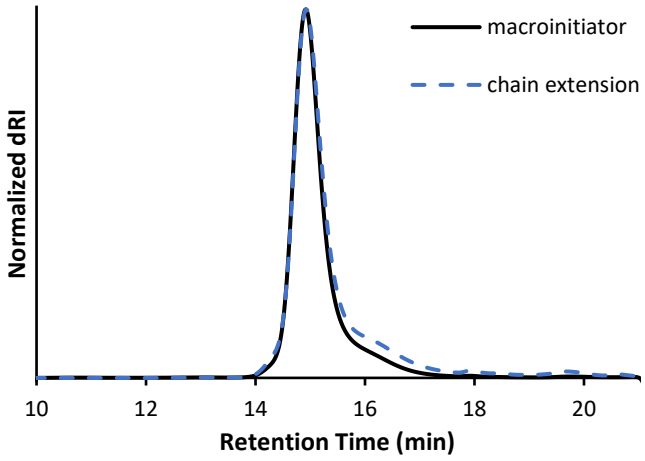

Figure 6.5 Attempted chain extension of PS (solid black) via RAFT (blue dash).

to P*t*BA were equal by comparing the integration of the phenyl protons of PS to the ester protons of the PDMAEMA. At this point we were unable to obtain data about the molecular weight of the resulting polymer using GPC, likely caused by interactions between the columns and the polyamine.

Similar to above we also targeted a lower molecular weight PS-b-PDMAEMA, however when the same conditions were used in the synthesis of the lower molecular weight polymer, we were unable to achieve chain extension. Both AIBN and V-501 showed conversion of 2-dimethylaminoethyl methacrylate by ^{1}H NMR spectroscopy. However, in these trials we saw no change in retention time by GPC of the resulting polymer (**Figure 6.5**). This led us to believe that chain extension was not occurring but that the radical initiator was initiating the homo-polymerization of the 2-dimethylaminoethyl methacrylate. To investigate this, we triturated the

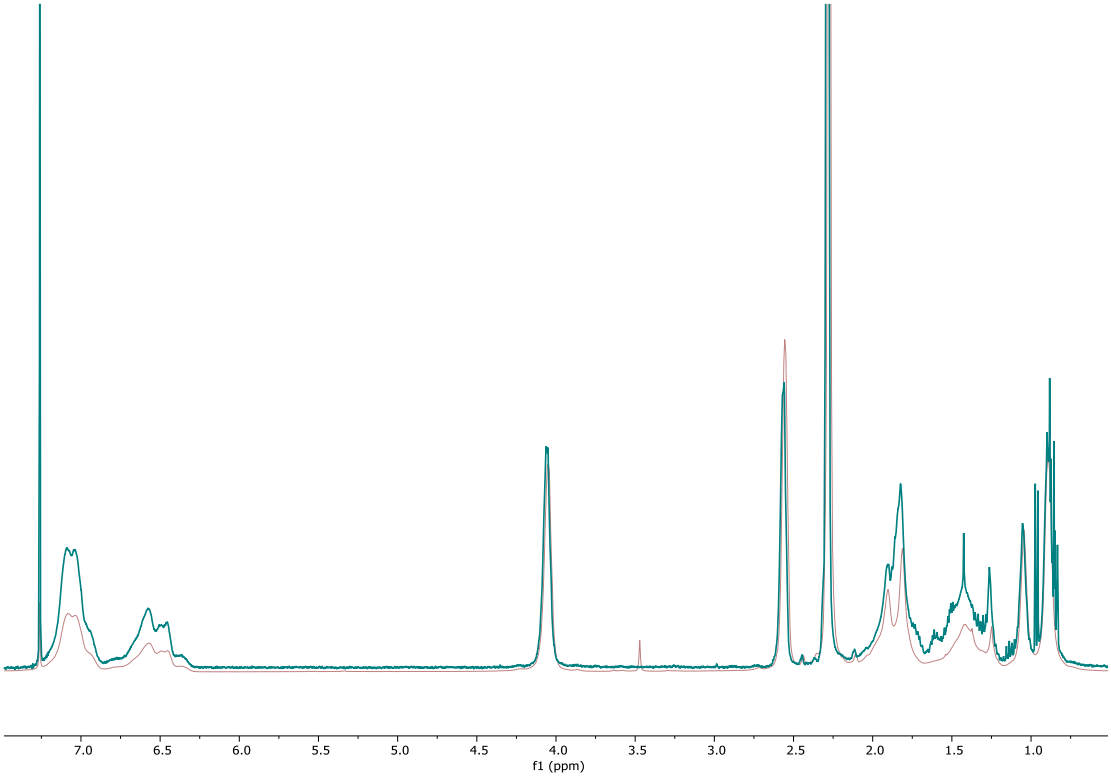

Figure 6.6 ^{1}H NMR spectrum comparing PS-b-PDMAEMA that was not triturated with methanol (blue) and one that was triturated with methanol.

PS-b-PDMAEMA in methanol so selectively dissolve any polymer containing PDMAEMA. After filtering off the residual solids the ^{1}H NMR spectrum for the solute showed a drastic decrease in the amount of PS (**Figure 6.6**). We were unable to remove all the PS using this method suggesting that we were seeing initiation but the initiation efficiency for the reaction was very low.

We next tried to synthesize the PS-b-PDMAEMA using ARGET-ATRP. To help prevent with the poor initiation we synthesized a PDMAEMA macro-initiator using the similar conditions to those used for the synthesis of the P*t*BA, to prevent the irreversible termination that can occur with these polymers we stopped the polymerization at 40% conversion. We were unable to get M_n data for the resulting polymers due to interactions between the polymer and the columns used on our system, nor were we able to use ^{1}H NMR spectroscopy to determine the molecular weight.

Without the molecular weight data, we moved forward to the chain extension relying on ^{1}H NMR spectroscopy to determine when to stop the polymerization. Using the same conditions as above for the chain extension of the P*t*BA-b-PS we were unable to get the chain extension to proceed. We hypothesize that this is due to the similarities between the structure of the polymer and the chosen ligand. We were able to solve this issue using traditional ATRP, likely because of the higher concentration of Cu in solution. The chain extension was monitored using ^{1}H NMR spectroscopy and was stopped once the ratio of PS was equal to that of PDMAEMA. Current work is focused on characterization of the final polymer.

6.3.c. LbL assembly of block copolymers

Using the higher molecular weight polymers initial attempts were made to grow the thin films on PET in THF and 3:1 THF:water. Results for these experiments can be seen in **Figure 6.15**. The films demonstrated linear increase in thickness as the number of bilayers increased

reaching converging at ~700 nm at 50 bilayers. After soaking the materials in both THF and water for 12 no change in the materials was detected, suggesting the successful formation of the PEC.

6.4. Conclusions

Using amphiphilic block copolymers have to potential prevent humid environments impede PEC gas barriers. We have demonstrated the synthesis of both high and low molecular weight (80 kDa and 20 kDa respectively) PAA-b-PS using ARGET-ATRP. The synthesis of PDMAEMA-b-PS was demonstrated using RAFT for a high molecular weight polymer and a combination of ARGET-ATRP and traditional ATRP for what should be a medium molecular weight polymer. Characterization of the amine containing polymer has thus far been difficult and future work is needed to fully characterize the lower molecular weight PDMAEMA-b-PS. The higher molecular weight block copolymers showed linear growth from the LbL deposition and successfully formed a PEC.

6.5 Future Directions

Further characterization of PDMAEMA-b-PS needs to be at the forefront of research for this project. Possible methods for this are investigating new mobile phases for GPC including THF with 1% triethyl amine or using DMF. Another possibility for characterizing the copolymer can using MALDI-TOF/MS. Using quantitative MALDI-TOF/MS can be used to gain information about the $Đ$, M_n, and M_w for polymers and could give us great insight into the materials synthesized. Followed by investigating the capabilities for these polymers to form gas barriers and investigating their response to humid environments.

Next steps for this would then move into applying novel polymer blocks that can be ionized in both acidic and basic solutions allowing for a simplification of the synthesis of the materials and yielding more uniform materials.

6.6 Experimental

6.6.a General Considerations

^{1}H and ^{13}C NMR spectral data were recorded on Bruker Avance III 500 and Bruker Avance III 400 spectrometers. ^{1}H NMR chemical shifts for spectra collected in $CDCl_3$ or DMSO-d_6 are referenced to TMS (d = 0.00 ppm) or DMSO residual peak (d = 2.50 ppm), respectively. ^{13}C NMR chemical shifts of spectra collected in $CDCl_3$ or DMSO-d_6 are referenced to the shifts of the carbon in $CDCl_3$ (d = 77.16 ppm) or DMSO-d_6 (d = 39.52 ppm). ^{1}H resonance data are reported as the following format: chemical shift in ppm [multiplicity, coupling constant(s) (J in Hz), and integration].

Reactions requiring anhydrous or air-free conditions were performed in the flame-dried glassware under nitrogen or argon atmosphere. Reported reaction temperatures are the temperature of the external heating bath. Triethylamine was distilled from CaH_2 and stored in a Schlenk flask. Anhydrous solvents were collected from a solvent purification system prior to use. All other reagents were purchased from commercial sources and used as received unless otherwise specified.

Gel permeation chromatography (GPC) was performed using the following setup: an Agilent Technologies Infinity Series II pump, either 2 or 3 inline columns, and Wyatt Technology mini-DAWN light scattering (LS) and Optilab T-rEX refractive index (RI) detectors using THF as the mobile phase with a flow rate of 1 mL/min. The absolute weight-average molecular weights were determined using multi-angle light scattering. Thermogravimetric analysis (TGA) was performed on a TA TGA Q50 under nitrogen from room temperature to 600 °C at 10 °C/min. Differential Scanning Calorimetry (DSC) was performed on a TA DSC Q250 calorimeter under nitrogen atmosphere at a heating rate of 10 °C/min and cooling rate of 5 °C/min.

Layer-by-layer growth was performed following previously reported procedures.[192]

6.6.b. Polymer Synthesis

Poly(tert-butyl acrylate) macroinitiator

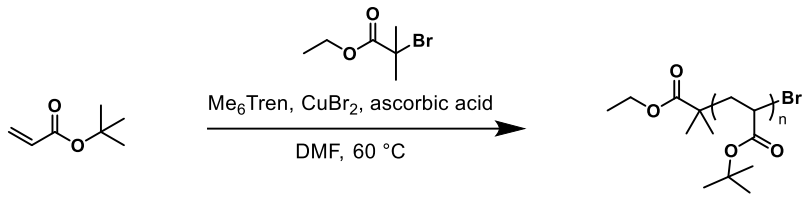

A 7 mL vial was charged with $CuBr_2$ (5 mg, 0.02 mmol, 1 eq.), Me_6Tren (60 µL, 0.2 mmol, 10 eq.), and DMF (1 mL). To a flame-dried N_2 purged 25 ml Schlenk tube a stir bar, *tert*-butyl acrylate (3.0 mL, 20.48 mmol, 30 eq.), ethyl α-bromoisobutyrate (100 µL, 0.678 mmol, 1 eq.), 0.3 mL of the CuB_2 solution, and DMF (1.27 mL). The solution was sparged with N_2 for one hour. Ascorbic acid (0.012 g, 0.0678 mmol, 0.1 eq.) was then added and the reaction was placed in a 60 °C oil bath. Aliquots were taken at 30 minutes intervals and conversion was monitored by ^1H NMR spectroscopy. When the desired conversion was reached the polymerization was quenched by opening to air. The reaction mixture was taken into tetrahydrofuran (10 mL) and precipitated from a 1:1 methanol : water mixture. The resulting solids were filtered and dried under reduced pressure to yield poly(*tert*-butyl acrylate).

Poly(tert-butyl acrylate-block-styrene)

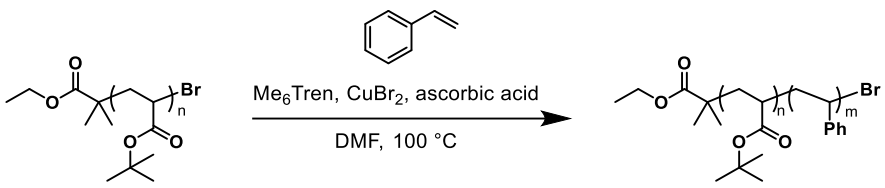

A 7 mL vial was charged with $CuBr_2$ (5 mg, 0.02 mmol, 1 eq.), Me_6Tren (60 µL, 0.2 mmol, 10 eq.), and DMF (1 mL). To a flame-dried N_2 purged 25 ml Schlenk tube a stir bar, styrene (0.53 mL, 4.6 mmol, 60 eq.), Poly(*tert*-butyl acrylate) macroinitiator (0.600 g, 0.09 mmol, 1 eq.), 0.3 mL of the CuB_2 solution, and anisole (0.6 mL). The solution was sparged with N_2 for one hour.

Ascorbic acid (0.012 g, 0.0678 mmol, 0.1 eq.) was then added and the reaction was placed in a 90 °C oil bath. Aliquots were taken at 30 minutes intervals and conversion was monitored by ^{1}H NMR spectroscopy. When the desired conversion was reached the polymerization was quenched by opening to air. The reaction mixture was taken into tetrahydrofuran (10 mL) and precipitated from excess methanol. The resulting solids were filtered and dried under reduced pressure to yield poly(*tert*-butyl acrylate-block-styrene).

Poly(acrylic acid-block-styrene)

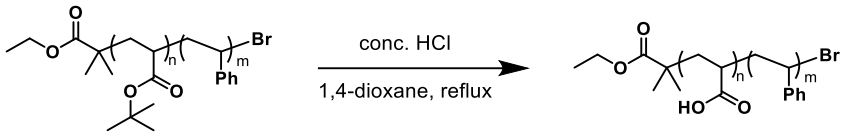

To a 10 mL vial a magnetic stir bar poly(*tert*-butyl acrylate)-block-poly(styrene) (0.40 g, 0.02 mmol, 1 eq.), and 1,4-dioxane (1 mL) were added. The flask was equipped with a reflux condenser, and conc. HCl (0.29 mL, 9.6 mmol, 500 eq.) was added. The flask was placed in placed in a preheated oil bath. The reaction was refluxed for 18 hours before being concentrated under reduced pressure. The resulting mixture was diluted with tetrahydrofuran and precipitated from cold hexenes. The resulting solids were dried under reduced pressure to yield poly(acrylic acid-block-styrene).

Poly(polystyrene) macroinitiator via RAFT

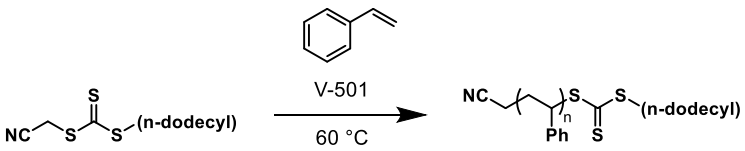

A flame-dried N_2 purged 25 mL Schlenk flask was charged with a magnetic stir bar, V-501 (0.0088 g, 0.0315 mmol, 0.1 eq.), CTA (0.100 g, 0.315 mmol, 1.0 eq.), and styrene (7.2 mL, 62.97 mmol, 200 eq.). The flask was sealed and degassed by 4 freeze-pump-thaw cycles before being submerged in a 60 °C oil bath. Aliquots were removed every 12 hours to monitor molecular weight

by GPC and to determine conversion by ^{1}H NMR spectroscopy. When the desired molecular weight was reached that flask was cooled in an ice bath and opened to air. The polymer solution was diluted with THF and precipitated form excess methanol to yield poly(styrene) as a yellow solid.

Poly(2-dimethylaminoethyl methacrylate-block-styrene) via RAFT

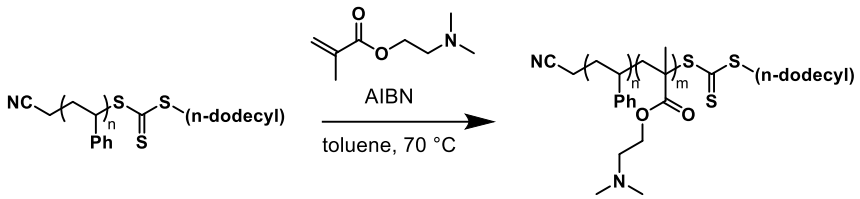

A flame-dried N_2 purged 25 mL Schlenk flask was charged with a magnetic stir bar, AIBN (0.0028 g, 0.0171 mmol, 0.2 eq.), macroinitiator (0.600 g, 0.085 mmol, 1.0 eq.), 2-dimethylaminoethyl methacrylate (1.01 mL, 6.0 mmol, 70 eq.), and toluene (0.5 mL). The flask was sealed and degassed by 4 freeze-pump-thaw cycles before being submerged in a 70 °C oil bath. Aliquots were removed every 12 hours to monitor molecular weight by GPC and to determine conversion by ^{1}H NMR spectroscopy. When the desired molecular weight was reached that flask was cooled in an ice bath and opened to air. The polymer solution was diluted with THF and precipitated form excess hexanes to yield poly(2-dimethylaminoethyl methacrylate-block-styrene) as a yellow solid.

Poly(2-dimethylaminoethyl methacrylate) macroinitiator via ARGET-ATRP

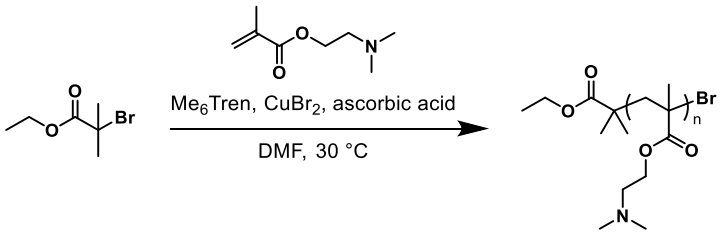

A 7 mL vial was charged with $CuBr_2$ (5 mg, 0.02 mmol, 2 eq.), Me_6Tren (60 µL, 0.2 mmol, 20 eq.), and DMF (1 mL). To a flame-dried N_2 purged 25 ml Schlenk tube a stir bar, 2-

dimethylaminoethyl methacrylate (5.7 mL, 34.0 mmol, 100 eq.), ethyl α-bromoisobutyrate (50 µL, 0.34 mmol, 1 eq.), 0.15 mL of the CuB_2 solution, and DMF (1.27 mL). The solution was sparged with N_2 for one hour. Ascorbic acid (0.006 g, 0.034 mmol, 0.1 eq.) was then added and the reaction was placed in a 30 °C oil bath. Aliquots were taken at 30 minutes intervals and conversion was monitored by ^{1}H NMR spectroscopy. When the desired conversion was reached the polymerization was quenched by opening to air. The reaction mixture was taken into tetrahydrofuran (10 mL) and precipitated from hexanes. The resulting solids were filtered and dried under reduced pressure to yield poly(2-dimethylaminoethyl methacrylate).

Poly(2-dimethylaminoethyl methacrylate-block-styrene) via ATRP

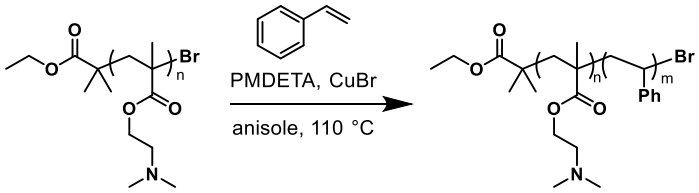

To a flame-dried, N_2 purged 25 ml Schlenk tube a stir bar, styrene (0.57 mL, 5.1 mmol, 80 eq.), macroinitiator (0.50 g, 0.064 mmol, 1 eq.), and anisole (0.25 mL) was added and placed in a 110 °C oil bath until the polymer dissolved. The solution was then cooled to room temperature and to that solution CuBr (0.009 g, 0.064 mmol, 1 eq.) and PMDETA (13 µL, 0.064 mmol, 1 eq) in anisole (0.25 mL) were added. The mixture was then degassed by 5 freeze-pump-thaw cycles before be submerged into a 110 °C oil bath. Aliquots were taken every 30 minutes to monitor the conversion of the polymerization by ^{1}H NMR spectroscopy. When the desired ratio of poly(styrene) and poly(2-dimethylaminoethyl methacrylate) was reached the reaction was opened to air and removed from the oil bath. The resulting mixture was diluted with THF and passed through a neutral alumina plug and precipitated from excess hexanes. The resulting solids were

filtered and dried under reduced pressure to yield poly(2-dimethylaminoethyl methacrylate-block-styrene).

6.6.c. Polymer Characterization Data

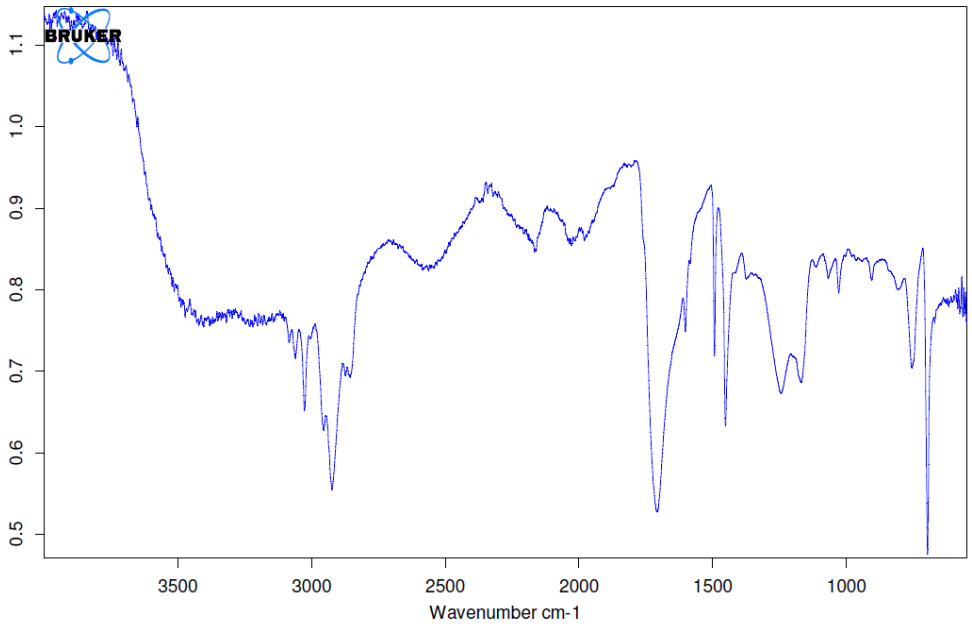

Figure 6.7 ATR-FTIR spectrum of PAA-b-PS.

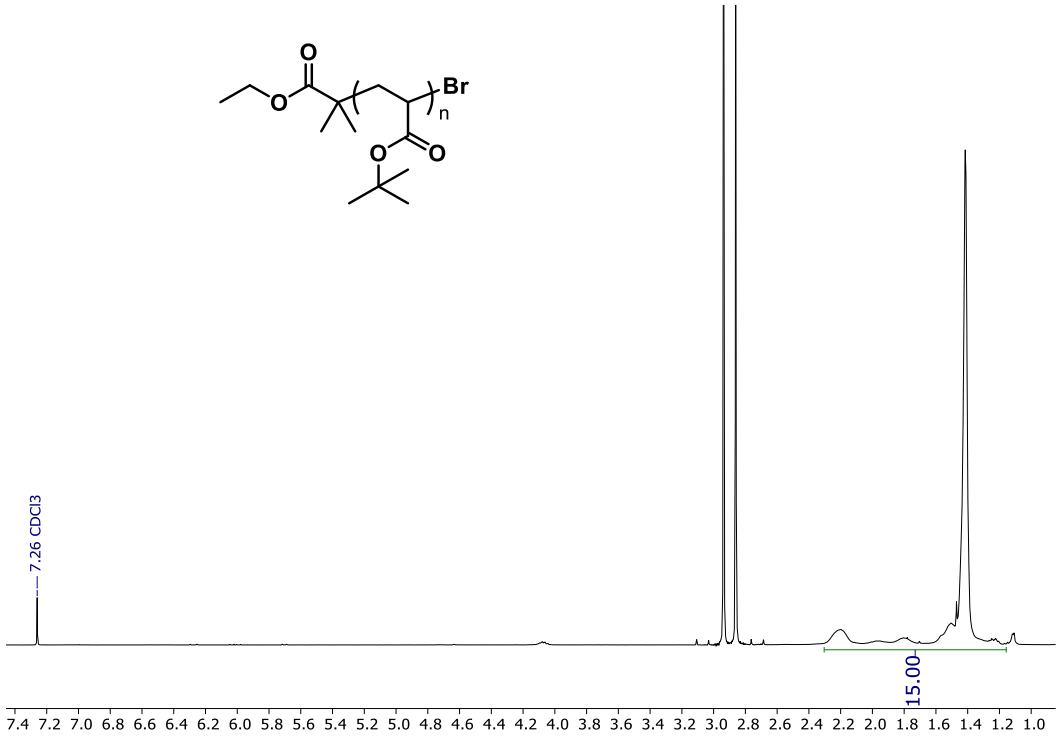

Figure 6.8 [1]H NMR spectrum of P*t*BA macroinitiator.

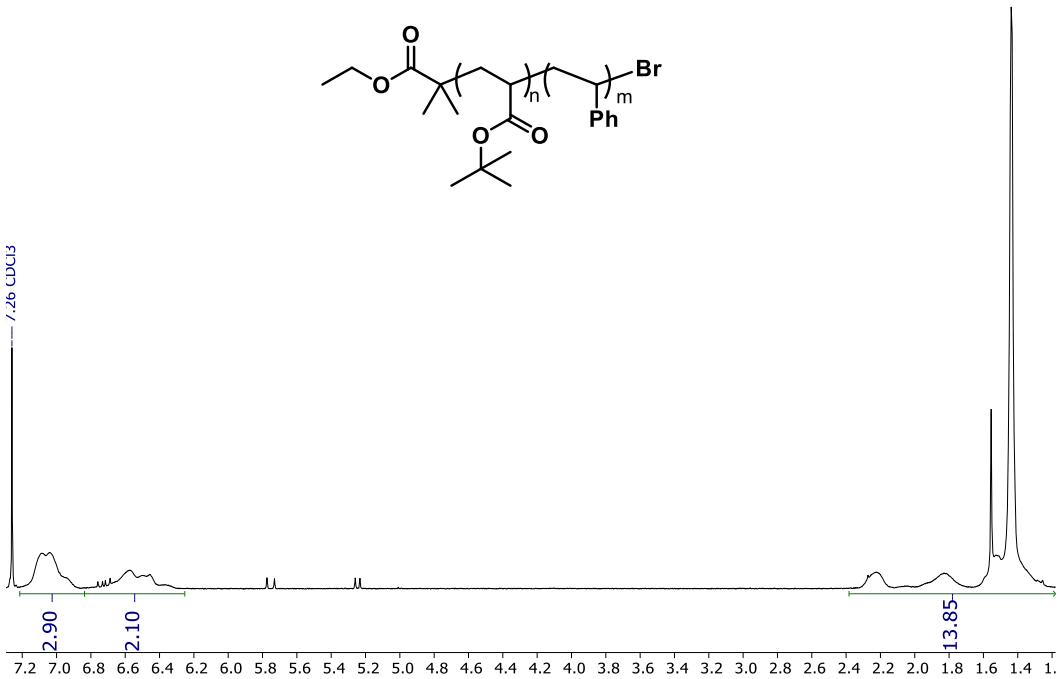

Figure 6.9 [1]H NMR spectrum of PS-b-P*t*BA.

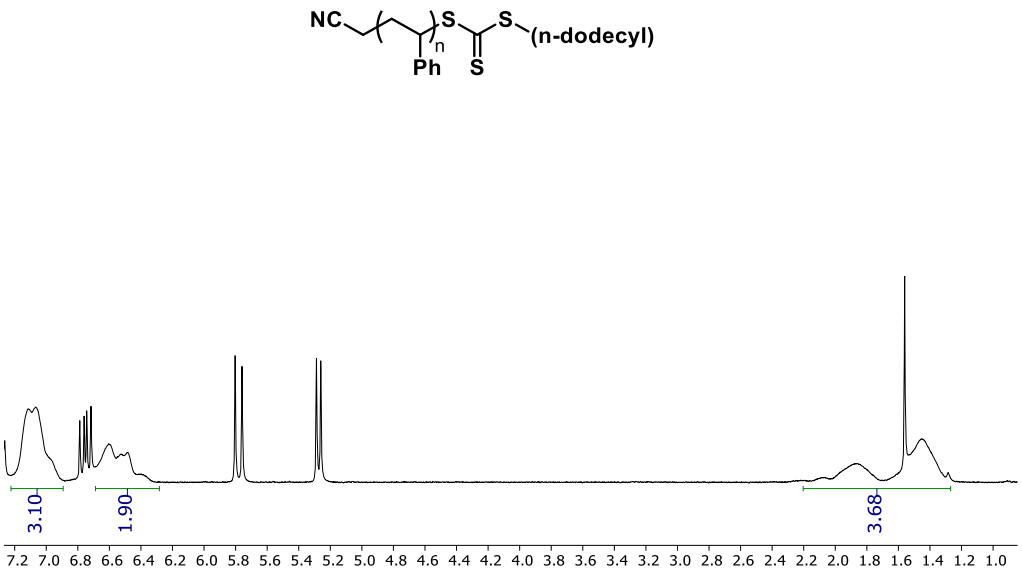

Figure 6.10 [1]H NMR spectrum of PS macroinitiator.

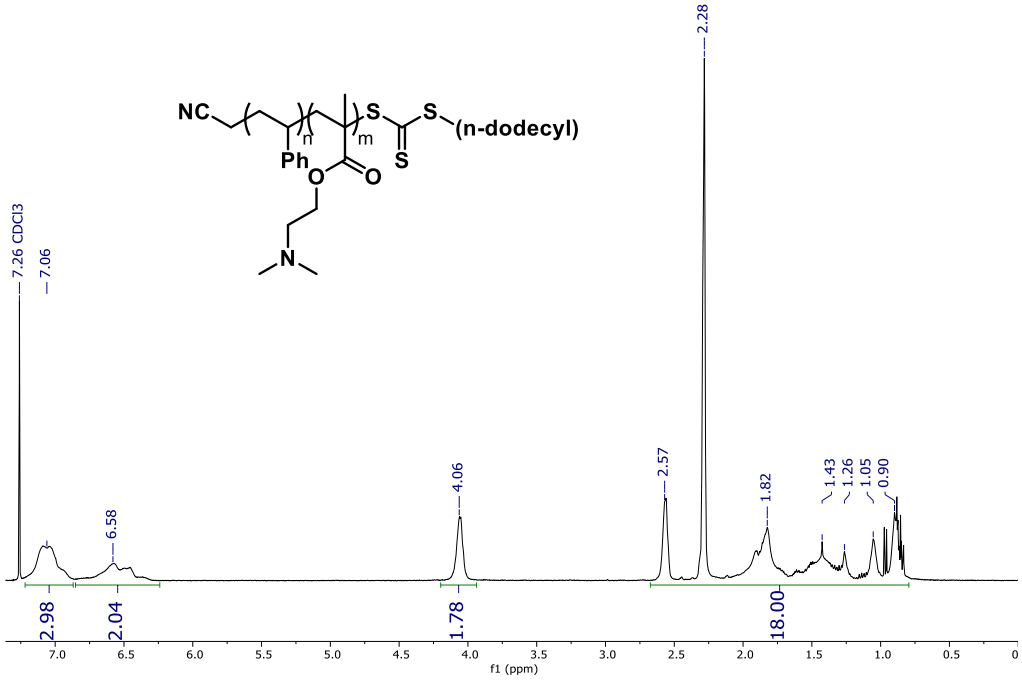

Figure 6.11 [1]H NMR spectrum of PS-b-PDMAEMA.

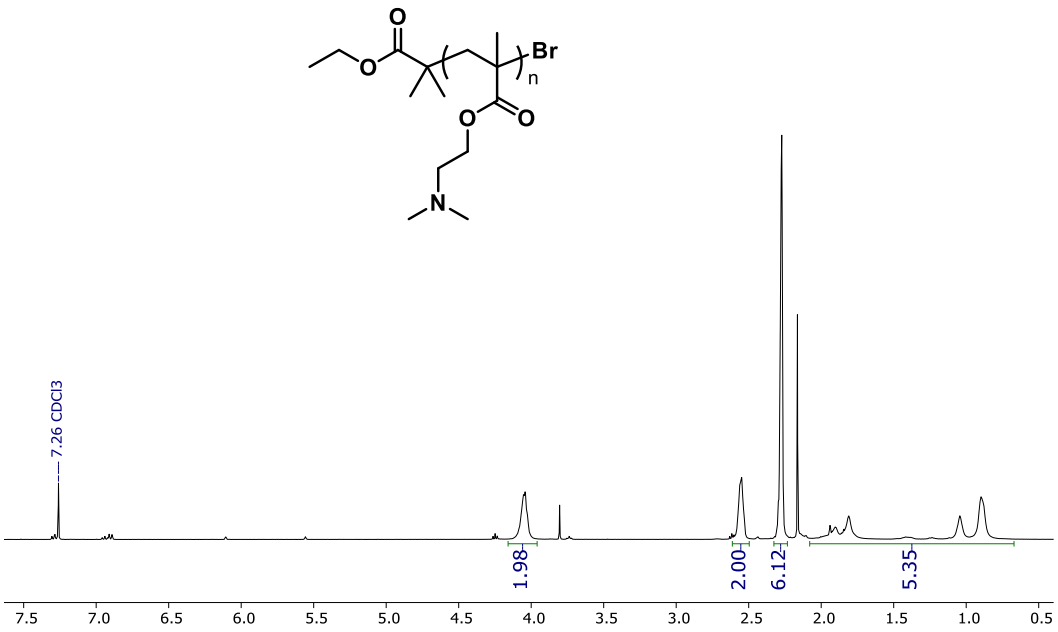

Figure 6.12 [1]H NMR spectrum of PDMAEMA macroinitiator.

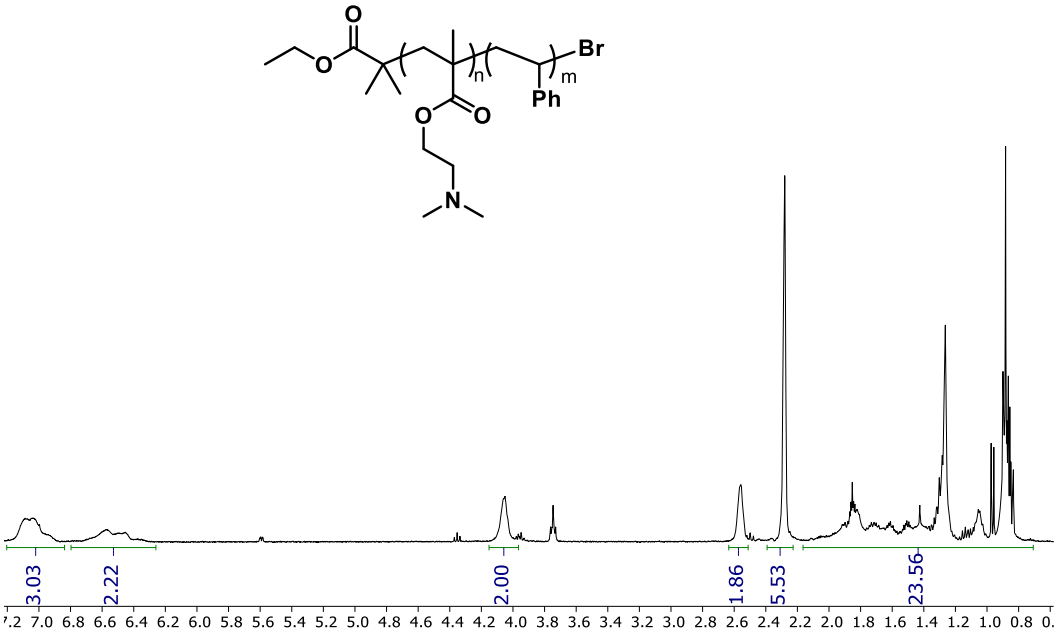

Figure 6.13 [1]H NMR spectrum of PDMAEMA-b-PS.

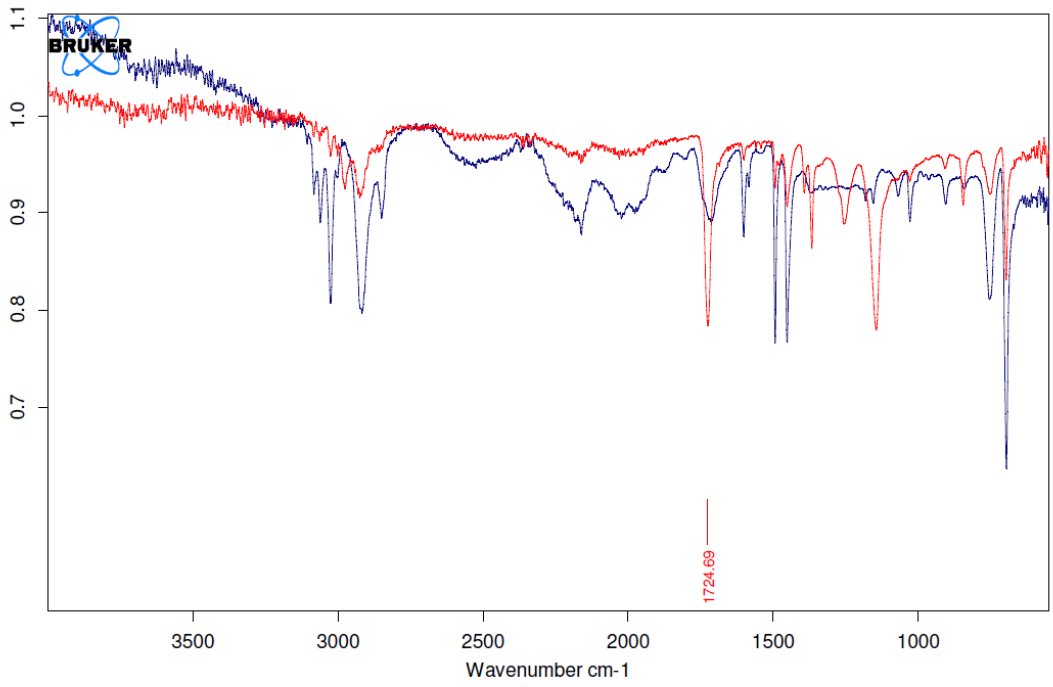

Figure 6.14 ATR-FTIR of failed deprotection of P*t*BA-b-PS. Red spectrum is the starting polymer and the blue spectrum is the polymer post deprotection.

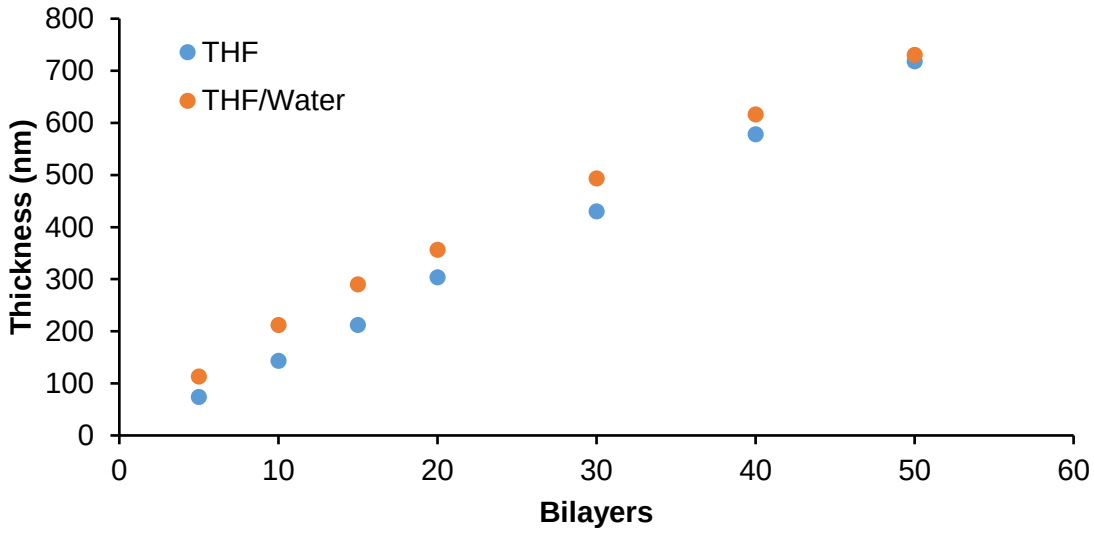

Figure 6.15 Results for the LbL deposition of PS-b-PAA and PS-b-PDMAEMA using THF (Blue) and 3:1 THF:H_2O (orange).

Notes and References for Chapter 6

(191) Kumar, R. S.; Auch, M.; Ou, E.; Ewald, G.; Jin, C. S. *Thin Solid Films* **2002**, *417* (1–2),

120–126.

(192) Yang, Y. H.; Haile, M.; Park, Y. T.; Malek, F. A.; Grunlan, J. C. *Macromolecules* **2011**, *44* (6), 1450–1459.

(193) Smith, R. J.; Long, C. T.; Grunlan, J. C. *Langmuir* **2018**, *34* (37), 11086–11091.

(194) Cho, E. S.; Evans, C. M.; Davidson, E. C.; Hoarfrost, M. L.; Modestino, M. A.; Segalman, R. A.; Urban, J. J. *ACS Macro Lett.* **2015**, *4* (1), 70–74.

(195) Sukhishvili, S. A.; Kharlampieva, E.; Izumrudov, V. *Macromolecules* **2006**, *39* (26), 8873–8881.

(196) Cini, N.; Tulun, T.; Blanck, C.; Toniazzo, V.; Ruch, D.; Decher, G.; Ball, V. *Phys. Chem. Chem. Phys.* **2012**, *14* (9), 3048–3056.

(197) Podsiadlo, P.; Michel, M.; Lee, J.; Verploegen, E.; Kam, N. W. S.; Ball, V.; Lee, J.; Qi, Y.; Hart, A. J.; Hammond, P. T.; et al. *Nano Lett.* **2008**, *8* (6), 1762–1770.

(198) Choi, J.; Rubner, M. F. *Macromolecules* **2005**, *38* (1), 116–124.

(199) Mendelsohn, J. D.; Barrett, J. C.; Chan, V. V.; Pal, A. J.; Mayers, A. M.; Rubner, M. F. *Langmuir* **2005**, *16*, 5017–5023.

(200) Shiratori, S. S.; Rubner, M. F. *Macromolecules* **2000**, *33* (11), 4213–4219.

(201) Yoo, D.; Shiratori, S. S.; Rubner, M. F. *Macromolecules* **1998**, *31* (13), 4309–4318.

(202) Fares, H. M.; Wang, Q.; Yang, M.; Schlenoff, J. B. *Macromolecules* **2019**, *52* (2), 610–619.

(203) Muramatsu, M.; Okura, M.; Kuboyama, K.; Ougizawa, T.; Yamamoto, T.; Nishihara, Y.; Saito, Y.; Ito, K.; Hirata, K.; Kobayashi, Y. *Radiat. Phys. Chem.* **2003**, *68* (3–4), 561–564.

(204) Zhang, Z.; Britt, I. J.; Tung, M. A. *J. Appl. Polym. Sci.* **2001**, *82* (8), 1866–1872.

(205) Grunlan, J. C.; Grigorian, A.; Hamilton, C. B.; Mehrabi, A. R. *J. Appl. Polym. Sci.* **2004**,

93 (3), 1102–1109.

(206) Boyd, D. A. *New Futur. Dev. Catal. Catal. by Nanoparticles* **2013**, 305–332.

(207) Zhu, Y. J.; Tan, Y. B.; Du, X. *Express Polym. Lett.* **2008**, *2* (3), 214–225.

(208) Man, Y.; Li, X.; Li, S.; Yang, Z.; Lee, Y. I.; Liu, H. G. *Colloids Surfaces A Physicochem. Eng. Asp.* **2019**, *580* (July), 123684.

(209) Mori, H.; Müller, A. H. E. *Prog. Polym. Sci.* **2003**, *28* (10), 1403–1439.

(210) Fantin, M.; Isse, A. A.; Gennaro, A.; Matyjaszewski, K. *Macromolecules* **2015**, *48* (19), 6862–6875.

(211) Wang, X. S.; Jackson, R. A.; Armes, S. P. *Macromolecules* **2000**, *33* (2), 255–257.

(212) Treat, N. D.; Ayres, N.; Boyes, S. G.; Brittain, W. J. *Macromolecules* **2006**, *39* (1), 26–29.

(213) Maurer, J. J.; Eustace, D. J.; Ratcliffe, C. T. *Macromolecules* **1987**, *20*, 196–202.

(214) Ros, S.; Wang, J.; Burke, N. A. D.; Stöver, H. D. H. *Macromolecules* **2020**, *53* (9), 3514–3523.